NUMERICAL APPROXIMATION OF (x,t)-DEPENDENT INTEGRAL-TRANSPORT EQUATIONS

by

John R. Essig

Course 22 February 1966

NUMERICAL APPROXIMATIONS FOR (x,t)-DEPENDENT INTEGRAL-TRANSPORT EQUATIONS

by

JOHN R. ESSIG

B.Ch.E., Villanova University

(1957)

SUBMITTED IN PARTIAL FULFILLMENT
OF THE REQUIREMENTS FOR THE
DEGREE OF DOCTOR OF
PHILOSOPHY

at the

MASSACHUSETTS INSTITUTE OF TECHNOLOGY

February, 1966

Signature of Author. . . . . .
Department of Nuclear Engineering
February 7, 1966

Certified by . . . . . .
Thesis Supervisor

Accepted by. . . . . .
Chairman, Departmental Committee
on Graduate Students

Bibliography

Produced Wednesday, April 13, 2011 at 8:23 AM

NUMERICAL APPROXIMATIONS FOR (x,t)-DEPENDENT INTEGRAL-TRANSPORT EQUATIONS

by

JOHN R. ESSIG

Submitted to the Department of Nuclear Engineering on February 7, 1966 in partial fulfillment of the requirements for the degree of Doctor of Philosophy.

ABSTRACT

Numerical models based on (x,t)-dependent integral-transport equations, in lieu of the usual integro-differential equations, have been developed for computing (x,t)-dependent neutron birth rate distributions in line and slab geometries. For a system of width W subdivided into N regions, the models express the birth rate in region I at time t as a sum of weighted birth rates in the N regions J at discrete times $t-\tau(I,J)$, plus the external source rate in region I at time t. Each weighting factor, or transfer coefficient, depends on the approximation made for the spatial distribution of the birth rate in region J at $t-\tau(I,J)$; for a particular model the spatial distribution in J is either assumed fixed or approximated by a modal expansion in low-order polynomials with $(J,t-\tau(I,J))$-dependent modal coefficients. The delay time $\tau(I,J)$ is given by the mean time-of-flight between birth and collision of neutrons from an assumed source distribution in J that collide in I.

The models were tested on relatively simple problems for which computed solutions could be checked by analytical methods, by comparison with published results of other methods, or by the degree of convergence with solutions obtained for larger N. From model comparisons based on accuracy and computing time, we found that a variable-distribution model in which the birth rate distribution in J is approximated by superimposing flat and slope-correction modes is the most effective of our models. As regards accuracy, this model is competitive with existing methods for a broad class of problems.

The slab models were extended to treat time-independent problems for infinite systems of repeated unit cells. An efficient computer code, SLBCEL, is included in the thesis.

Suggestions are made for extending the method to a wider class of problems.

Thesis Supervisor: Elias P. Gyftopoulos
Title: Professor of Nuclear Engineering

ACKNOWLEDGEMENTS

The author wishes to thank Professor Elias P. Gyftopoulos for his constructive criticism and encouragment during the course of this work and in the preparation of the final manuscript. Professors I. Kaplan and K. Hansen read earlier drafts of the thesis, and their comments were very helpful.

The author appreciates the opportunity to study at M.I.T. that was provided by the United States Navy. In addition, the encouragement and interest of fellow-officers stationed at M.I.T. is deeply appreciated.

All computer work associated with this thesis was accomplished using the facilities of the M.I.T. Computation Center.

The secretarial assistance of Mrs. Janice Foulke in preparing an earlier draft and her strenuous efforts in the production of the final product are gratefully acknowledged. In addition, the author wishes to thank fellow-student Larry Foulke for help in proofreading the thesis and for constructive comments on content.

Above all, the author wishes to thank his wife, Maryanne, for her steadfast patience and encouragement, for secretarial assistance, and for lovingly holding down the domestic fort while the author labored into the wee hours to complete this work.

TABLE OF CONTENTS

TABLE OF CONTENTS (cont'd)

TABLE OF CONTENTS (cont'd)

TABLE OF CONTENTS (cont'd)

LIST OF FIGURES

LIST OF FIGURES (cont'd)

LIST OF TABLES

LIST OF TABLES (cont'd)

CHAPTER 1

INTRODUCTION

In this thesis we develop, test and evaluate numerical models for computing approximate solutions of integral-transport equations for one-dimensional line and slab geometries. Our primary purpose is to develop techniques to solve for neutron distributions in time-dependent problems by numerically integrating time-dependent integral-transport equations in lieu of the usual time-dependent integro-differential equations. A secondary purpose is to develop improved techniques for treating spatial dependence in integral approximations, leading to more accurate, more efficient numerical models than obtainable with the techniques currently used. Results for both time-dependent and steady-state problems demonstrate the realization of this secondary objective.

1A. INTEGRAL-TRANSPORT EQUATIONS FOR WHICH NUMERICAL MODELS ARE DEVELOPED

The most general integral transport equation for which numerical models are developed in this thesis is the equation for slab geometry:

$$b(x,t) = c(x,t)\sum(x)\int_0^1 d\mu \int_0^W \frac{dx'}{\mu}\,\frac{1}{2}\,b\left(x',t-\frac{|x-x'|}{\mu v}\right)\cdot$$

$$\cdot\exp\left\{-\frac{[x-x']}{|x-x'|}\int_{x'}^{x}\frac{dx''}{\mu}\sum(x'')\right\} + s(x,t)\ , \qquad (1A.1)^*$$

---

*Note: In Appendix D, Eq. (1A.1) is derived from an integral-transport equation more generally applicable to nuclear reactor systems. The following simplifications are incorporated in the derivation of Eq. (1A.1):

a) Delayed neutrons are not treated explicitly.

b) The system is isolated from its surroundings; i.e., no neutrons enter the system across the boundary planes at x=0 and x=W.

c) The neutrons are treated as monoenergetic.

d) The medium is isotropic; i.e., the nuclear properties $\sum$ and c are independent of the direction of incident neutrons.

e) The directional distribution of births is isotropic with respect to a laboratory frame of reference; i.e., neutrons emitted by external sources and secondary neutrons emitted at collision sites are emitted with a spherically symmetric distribution. Note that this simplification does not constrain the flux distribution to be directionally isotropic.

f) The collision cross section, $\sum$, is constant with respect to time.

g) The nuclear properties, source rate density and birth rate density are constants with respect to the coordinates y and z in a Cartesian frame of reference (x,y,z). The system has an infinite extent in the (y,z) plane.

The practical significance of each of these simplifications, as regards restricting the class of nuclear reactor systems to which an equation incorporating the simplification is applicable, is discussed in standard textbooks on reactor physics. Some notes pertaining to the effects of these simplifications in reducing the number of computing operations in integral-equation-based numerical models are included in Appendix D.

where

b(x,t) is the birth rate density, $cm^{-3}sec^{-1}$, at the spatial coordinate x at time t

s(x,t) is the contribution to b(x,t) from an external source located at (x,t)

v is the neutron speed, $cm\ sec^{-1}$

Σ is the macroscopic collision cross section, cm^{-1}

c is the secondary emission coefficient, i.e., the mean number of secondaries per collision

W is the width of the system, cm

μ corresponds to the cosine of the acute angle between the x-axis and the straight-line track between the birth site of a neutron and its collision site; μ serves as a dummy variable in Eq. (1A.1).

The birth rate density is related to the neutron flux, ϕ, by

$$b(x,t) = c(x,t)\Sigma(x)\phi(x,t) + s(x,t) = b^{o}(x,t) + s(x,t), \quad (1A.2)$$

where the expression $\Sigma\phi$ is the collision rate density of "parent" neutrons and b^{o} is the secondary neutron birth rate density, or "progeny birth rate density." Identifying the terms in Eq. (1A.2) with those in Eq. (1A.1), one can see that the flux at (x,t) is expressed in Eq. (1A.1) in terms of the past history of the birth rate densities at all locations x' in the system. Numerical approximations for Eq. (1A.1) are studied in Chapter 3.

In Chapter 2, we study numerical models for a simpler integral-transport equation, the equation for line geometry:

$$b(x,t) = c(x,t)\sum(x)\int_0^W dx' \frac{1}{2} b(x',t-\frac{|x-x'|}{v})\cdot$$

$$\cdot\exp\left\{-\frac{[x-x']}{|x-x'|}\int_{x'}^{x} dx''\sum(x'')\right\} + s(x,t) , \qquad (1A.3)$$

where b and s are assigned the units $cm^{-1}sec^{-1}$. Eq. (1A.3) differs from Eq. (1A.1) in that neutrons are treated as if emitted in only the two discrete directions ($\mu = 1$) parallel to the x-axis, rather than with a spherically-symmetric distribution. Although Eq. (1A.3) has little or no practical value as regards applicability to real nuclear reactor systems, the equation incorporates the basic assumption of neutron transport theory that neutrons travel in straight lines at constant speeds between their birth sites and collision sites. For our purposes, the simplicity of Eq. (1A.3) and of the hypothetical class of systems it describes makes the equation a useful subject for evaluating alternative approaches for formulating integral-type numerical models. Those approaches which yield satisfactory numerical models for Eq. (1A.3) in Chapter 2 are applied to the more complex Eq. (1A.1) in Chapter 3.

The time-independent version of Eq. (1A.1) is studied in Chapter 4. Numerical models are developed both for treating systems of finite width W and for treating infinite systems in which the nuclear properties and external source distribution are periodic functions of x.

1B. THE FINITE-INTEGRAL APPROXIMATION

1B.1 Formulation of Models

In formulating numerical models for Eqs. (1A.1) and (1A.3), the system of width W is subdivided into N regions, each having the width $\Delta x = W/N$. The nuclear properties are treated as homogeneous within a given region, but may have different values in different regions. Both sides of Eq. (1A.1 or 1A.3) are multiplied by dx and integrated formally over the interval Δx corresponding to a particular "receiver" region I, where $1 \leq I \leq N$. The integral on the left-hand side defines B(I,t), the birth rate in region I at time t. Since parent neutrons colliding in region I at time t were born at various points within the system at previous times, we wish to express the progeny birth rate component of B(I,t) as a sum of weighted contributions from the birth rates in the N "source" regions J, each birth rate taken at an appropriate earlier time. To do this, the integral over x' between the limits 0 and W on the right-hand side of the integral equation is reexpressed as a sum of N integrals, each taken over the interval Δx corresponding to a different source region J. Then, focusing attention on the integral describing the contribution to B(I,t) from parent neutrons born in a particular region J, we approximate the space-time dependence of the birth rate density in region J by a relation having the form:

$$b(x',t-\frac{|x-x'|}{[u]v}) = B(J,t-\tau(I,J))u_o(x') + [C_1(J,t-\tau(I,J))u_1(x') + C_2(J,t-\tau(I,J))u_2(x')] , \quad (1B.1)$$

for x in region I, x' in region J, and $0 < \mu \leq 1$; where the terms enclosed within square brackets are not included for all models, and where

$u_o(x')$ is a function to be specified later which describes the assumed spatial distribution, or a modal component of the spatial distribution, of the birth rate in region J and may differ from model to model.* Those models for which only the term Bu_o is used on the right-hand side are called "fixed-distribution models." Where more than one term is used, the model is called a "variable-distribution model" and $u_o(x')$ describes the "unit flat mode", a uniform distribution in region J. For each model, $u_o(x')$ is defined such that its integral over the interval Δx corresponding to region J is equal to unity.

$u_1(x')$ describes the "unit slope-correction mode", a distribution varying linearly with x' in region J. Its integral over region J is equal to zero.

---

*Note: Since the integral expression containing $u_i(x')$, where i=1, 2 or 3, is integrated only over x' in the interval Δx corresponding to region J, we need to define $u_i(x')$ only for x' in region J. If we define $u_i(x')=0$ for all x' outside of region J, the integral may be assigned broader (e.g., infinite) limits.

$u_2(x')$ describes the "unit curvature-correction mode", a parabolic distribution in region J. Its integral over region J is equal to zero.

$\tau(I,J)$ is the mean delay time between births in region J and their collisions in region I. The expression from which $\tau(I,J)$ is computed for a given model describes the mean flight-time of those neutrons from an assumed source distribution (e.g., $u_0(x')$) in region J which collide in region I with either an assumed or a rigorously-derived spatial distribution.

$C_1(J,t-\tau(I,J))$ and $C_2(J,t-\tau(I,J))$ are modal coefficients for the unit slope- and curvature-correction modes, respectively. The modal coefficients are computed from simple expressions which are linear in the birth rates at time $t-\tau(I,J)$ in region J and in neighboring regions. These expressions will be derived later.

We shall refer to the approximation of the space-time dependence of the birth rate distribution in source region J by the spatial dependence at the discrete time $t-\tau(I,J)$ as the "discrete-delay-time approximation."*

After the substitution indicated by Eq. (1B.1) has been made in each of the N integrands in the integral equation for B(I,t), the

---

*Note: In Chapter 3, a multiple-delay-time model is formulated for slab geometry by taking the additional step reexpressing the integral over μ in Eq. (1A.1) as a sum of N_μ integrals, each taken over a different angular interval. The discrete-delay-time models, which have been programmed and tested, correspond to the case where $N_\mu = 1$.

integral equation may be reduced in a straight-forward manner to the following relation:

$$B(I,t) = c(I,t) \sum_{J=1}^{N} \Big\{ G(I,J)B(J,t-\tau(I,J)) + \Big[G_{slp}(I,J)C_1(J,t-\tau(I,J)) + G_{crv}(I,J)C_2(J,t-\tau(I,J)) \Big] \Big\} + S(I,t) \,, \qquad (1B.2)$$

where the terms enclosed within the square brackets may be identified with the corresponding terms in Eq. (1B.1) and where

$S(I,t)$ is the external source rate in region I at time t, $\int_{(\Delta x)_I} dx\, s(x,t)$

$c(I,t)$ is the secondary emission coefficient in region I at time t

$G(I,J)$ is the number of collisions in region I of neutrons born in region J with the distribution $u_o(x')$

$G_{slp}(I,J)$ is the number of collisions in region I of neutrons born in region J with the distribution $u_1(x')$

$G_{crv}(I,J)$ is the number of collisions in region I of neutrons born in region J with the distribution $u_2(x')$

The transfer coefficients G, G_{slp} and G_{crv} are computed from closed-form expressions which are linear in known functions and which are derived by performing the indicated integrations over x', x and, for slabs, μ on the right-hand side of the integral equation for B(I,t). Since the integral-transport equations approximated by Eq. (1B.2) have time-independent collision cross-sections, the transfer coefficients are time-independent and need be computed only once for a given problem or for the class of problems having the same set of N optical region widths, $\Sigma(I)\Delta x$.

The final step in formulating the numerical model is to specify the unit time step, Δt, between successive computations of the set of N regional birth rates and between stored values in the birth rate memory. In order that the numerical equations will be explicit,* the unit time step is chosen to be less than, or equal to, the smallest of the $\tau(I,I)$. For a typical problem with $v = 2 \times 10^5$ cm/sec and $\Delta x = 1$cm, the unit time step is on the order of 10^{-6} sec.

1B.2 Outline of Models Developed

Note that the basic approximation given by Eq. (1B.1) allows considerable freedom of choice in the number of terms to be used on the right-hand side and in the expressions used to define some of the individual terms. One of the objectives of this thesis is to evaluate various options, basing comparisons on the accuracy of computed solutions and on computational efficiency. In the next few paragraphs we outline some of the models to be developed and tested in subsequent chapters.

Three representative fixed-distribution models and one variable-distribution model are developed for line geometry in Chapter 2. Among the fixed-distribution models are Model M, the "midpoint approximation", in which neutrons born in region J are assumed to have been emitted from the midpoint of region J, and Model F, the "flat approximation", in which neutrons are assumed to have been born with

*Note: All quantities on the right-hand side are known before the quantity on the left-hand side is to be computed. $B(J,t-\tau(I,J))$ is computed by linear interpolation between stored values when $\tau(I,J)/\Delta t$ is not an integer.

a uniform distribution in region J. In the variable-distribution model, Model FS, the spatial dependence of the birth rate density in region J at time $t-\tau(I,J)$ is approximated by superimposing weighted flat and slope-correction modes. The computer code OVRR4, written for Models F and FS, is described in Appendix A.

Three models are developed for slab geometry in Chapter 3. These models, designated Model F, Model FS and Model FSC, are characterized by the use of the first term, the first two terms or all three terms, respectively, on the right-hand side of Eq. (1B.1). The expressions for the delay times are based on the flat approximation. The applicable computer code, TOVSR, is described in Appendix B.

The three slab models are applied in Chapter 4 to solve for time-independent birth rate distributions in sub-critical systems in which the neutron populations are supported by external sources. The method used to extend the applicability of the slab models to infinite systems in which properties, external source distributions and birth rate densities are periodic functions of x, i.e., infinite systems of repeated unit cells, is described in Chapter 4. The finite-integral approximation, Eq. (1B.2), is simplified considerably for time-independent problems; from the set of N simplified equations, the birth rate distribution is computed using a non-iterative reduction procedure in lieu of time-consuming iteration. The applicable computer code, SLBCEL, is described in Appendix D.

Some suggestions for improving our line and slab models, based on evaluation of test results, are included in the summaries of Chapters 2 and 3, respectively. Some recommendations for further work in extending the basic methodology developed in this thesis to treat higher-dimensional problems are given in Chapter 5.

1B.3 Testing and Evaluation of Models

As will be evident in the subsequent chapters, each model is initially tested on relatively simple problems for which computed solutions may be checked either analytically or by comparison with results reported in the literature for other methods. Convergence properties of the model are checked by repeatedly solving the same problem using different values of N. Results of these convergence calculations also give an indication of the accuracy of the solution obtained with a particular N. Although the simple test problems do not exploit the full capacility of the model for generating space-time transients, they prove to be useful tools for evaluating the various approximations that are made in formulating the model.

The following factors affect the accuracy of the computed solutions and will be studied in some detail:

a) Deviation of the assumed spatial distribution of the birth rate in source region J from the actual distribution.

b) Growth rate of the birth rate in source region J for problems in which $B(J,t-\tau)$ has varied smoothly with $(t-\tau)$.

c) Discontinuities in $B(J,t-\tau)$ caused by discontinuities in the time-dependence of external source rates or secondary emission coefficients.

d) Optical width of region J, $\Sigma(J)\Delta x$, in mean free paths.

To compare directly one model with another, each model is used to solve the same problem, in some cases for several values of N. The more satisfactory model for the particular problem is the one which yields a more accurate solution using less computing time.

1C. RELATION WITH PREVIOUS WORK

With this section we conclude our introduction by comparing some of the characteristics of our models with those of models developed previously by other workers, and by pointing out areas where our efforts contribute to the sate of the art.

1C.1 Finite-Integral Models

In recent years, numerical models based on time-independent integral-transport equations have been developed by a number of workers. Numerical models for computing neutron distributions in infinite slab systems of repeated unit cells have been developed by Honeck[1-3], Judge[4-5], and Church[6]. Honeck's slab model* includes a multigroup treatment of energy-dependence and allows for linearly

*Note: Honeck has also developed a cylindrical cell model and a true two-dimensional model for rod lattices with isotropic emission. In the two-dimensional model, neutrons born in a given region are assumed to be emitted from the midpoint of the region.

anisotropic scattering.* The models of Judge and Church treat neutrons as monoenergetic. In all of these models, neutrons are assumed to be born with a uniform spatial distribution (flat approximation) in source region J, and the set of numerical equations is solved by an iteration scheme.

Comparative results presented in Chapter 4 demonstrate that, for equivalent accuracy, a net savings in computing operations can be obtained by using a variable-distribution model in lieu of the flat approximation for slab cells greater than one mean free path thick. The advantage grows with cell thickness. Additional savings are obtained through the use of a non-iterative reduction scheme for solving the set of numerical equations. It should be mentioned here that the use of a variable-distribution model for treating the spatial dependence is not incompatible with either a multigroup formulation or the inclusion of linearly-anisotropic scattering in the numerical model.

As regards previous work in which finite-integral models have been developed to study systems with time-varying neutron fluxes, Judge and Daitch[7] have developed finite-integral models having $N \leq 3$ to solve for the inverse periods associated with stationary (space-time separable) solutions of time-dependent integral-transport equations. The slab equation approximated by Judge and Daitch is equivalent to Eq. (1A.1) as modified by first dropping the external

*Note: Accounting for linearly-anisotropic scattering in slab geometry requires twice the number of discrete variables needed for a model which accounts for only isotropic emission but is otherwise equivalent.

source term and the x- and (x,t)-dependence of the nuclear properties, and then recasting the equation into stationary form by introducing the restriction of space-time separability on the solution. The resulting stationary equation is time-independent. The finite-integral model is then formulated by treating the flux as spatially uniform within a given region (flat approximation). These few-region models are effective tools for calculating inverse periods in very sub-critical, optically-thin slabs.

The author has found no evidence of previous attempts to develop numerical models which are formulated from time-dependent integral-transport equations in the manner outlined in Section 1B. Given the system parameters and the past history of the birth rate distribution, these models are capable of generating space-time transient solutions directly.

1C.2 Finite-Difference Models

Existing methods for computing time-dependent transport solutions in slab geometry have been based, for the most part, on spherical-harmonics and discrete-ordinates approximations, e.g., the well-known P_L and S_L approximations*, for the angular dependence of the angular flux in an integro-differential transport equation such as that equivalent to Eq. (1A.1). These methods are discussed in

---

*Note: The integro-differential equation is replaced by L+1 linked differential equations in L+1 unknown functions of x and t. Numerical models are normally formulated by replacing partial derivatives by finite-difference expressions.[8,11,12]

standard textbooks.[8-11] Here we shall point out only some general differences between finite-integral models for Eq. (1A.1) and finite-difference models for the integro-differential equation equivalent to Eq. (1A.1):

a) For equivalent numbers of spatial intervals, the number of discrete variables which must be computed at each time step is given by N for the finite-integral model and by LN+N for the finite-difference model. This apparent advantage of the finite-integral model is offset, however, by the fact that the algorithm for computing one of the LN+N variables in the finite-difference model contains only a few terms[8,11], whereas the number of terms on the right-hand side of Eq. (1B.2) is an integer times N.* For a multiple-delay-time model, the number of terms on the right-hand side of Eq. (1B.2) is multiplied by the factor N_μ, the number of angular intervals.

b) The finite-integral model is a past-history formulation requiring storage of the N birth rates at several previous times to have available the data needed to compute the birth rates at time t. The finite-difference model is an initial-value formulation requiring storage, in the usual case, of the values of

---

*Note: For large (optically-thick) systems, the number of terms in Eq. (1B.2) can be reduced since only a negligible fraction of the neutrons born in region J survive the flight to region I when regions I and J are separated by several mean free paths.

the LN+N discrete variables at the previous time step only. Additional storage requirements to permit computing several time steps before transferring results from the computer core to output tapes are considerably less for the finite-integral model with its fewer discrete variables.

c) The major disadvantage of our method relative to finite-difference approximations is the requirement for storage of the two-dimensional arrays G, G_{slp}, G_{crv} and τ.* These parameters are stored because the expressions from which they are computed are fairly complex and it is therefore not desirable to recompute them each time they are used. Coupling coefficients in the finite-difference models, on the other hand, are easily computed from "local" properties which are given by one-dimensional arrays of length L or N at most.

Considering the differences pointed out in the preceding discussion, one might justifiably question our interest in expending further effort to develop and program finite-integral models. Recall, however, that the comparisons were based on the assumed equivalence of the number of spatial intervals used with each type model. If we change the basis for comparison to be equivalent accuracy of the solutions for a given problem, we will find that the number N needed with a typical finite-integral model is usually

---

*Note: For systems in which Σ is independent of x, the magnitudes of the transfer parameters are functions of |I-J| only; therefore, storage is needed only for one-dimensional arrays having N elements.

much smaller than the number N needed with a finite-difference model. For example, we might point to the previously-mentioned work of Judge and Daitch[7], who obtained excellent results in calculating the fundamental stationary solutions (asymptotic solutions) for the flux in very thin, very subcritical slabs using N=1 or 3. Since the spatial distribution of the asymptotic flux is known to be fairly uniform in one of these systems, the use of a single flat mode or three flat regional modes is an excellent approximation. Finite-difference models developed from P_L or S_L approximations to the equivalent stationary integro-differential equation would require a much larger number of spatial mesh points in addition to large L. Other examples illustrating the smaller values of N needed with finite-integral models are given in Chapters 2 and 3.

The number of angular intervals N_μ needed to obtain accurate solutions with a finite-integral model for Eq. (1A.1) depends on the rates of growth of the birth rates in the various source regions J. We shall first examine the limiting case of time-independent problems. For time-independent problems, in which the birth rates do not vary with time, no additional accuracy can be obtained by using $N_\mu > 1$; for these problems, the use of $N_\mu=1$ in the finite-integral model is equivalent in a sense to the use of $L\to\infty$ in finite-difference models based on P_L or S_L approximations to the equivalent integro-differntial equation.* Although this equivalence is not true for time-dependent problems, it is reasonable to expect that discrete-

*Note: In Chapters 3 and 4 several comparisons are made between finite-integral results and published, high-order S_L and P_L results.

delay-time (N_μ=1) models for Eq. (1A.1) will yield satisfactory solutions for time-dependent problems in which the birth rates in the various source regions do not change too rapidly with time. The growth rate limits indicated by the test results in Chapter 3 are broad enough to include reasonably fast space-time transients, e.g., a transient having local growth rates equivalent to doubling times of 200 microseconds or more in a system with $v=2\times10^5$ cm/sec and Σ=1 cm^{-1}. To accurately compute very fast transients, e.g., system responses to localized initial sources, one would need to use a multiple-delay-time model with suitably large N_μ. For this reason, we include in Chapter 3 a method for formulating multiple-delay-time models. Although we have not coded the multiple-delay-time models, we expect that the accuracy of fast-transient solutions computed for slab systems thicker than one mean-free-path using a high-order multiple-delay-time model would be similar to the accuracy of fast-transient solutions to Eq. (1A.3) computed using the corresponding discrete-delay-time model for line geometry.

CHAPTER 2

LINE GEOMETRY

Introduction to Chapter 2

In this chapter we develop, test and evaluate numerical models for Eq. (1A.3), the simplified integral-transport equation for line geometry. In the hypothetical line reactor, there are only two discrete directions of particle motion; with the simplifications of isotropy, half of the particles born are emitted towards the left and half are emitted towards the right, the direction of increasing x. Wing[13] used line geometry (his "rod model") to illustrate effectively some of the physical and mathematical characteristics of integro-differential and invariant-imbedding formulations.* Here we use line geometry to illustrate basic methodology associated with finite-integral models and to evaluate some alternative approaches for formulating finite-integral models.

The physical interpretation of Eq. (1A.3) and the relation between the integral-transport equation and the finite-integral approximation are discussed in Section 2A. Three representative fixed-distribution models are described in Section 2B. A variable-distribution model with superimposed flat and slope-correction modes is developed in Section 2C. Computational characteristics of the corresponding numerical equations, such as convergence, explicitness,

*Note: The set of two coupled differential equations equivalent to Eq. (1A.3) is given in Appendix E. In addition a finite-difference model is formulated and an analytical constraint for testing some of our computed solutions is derived. We shall refer to these again in Section 2E.

memory requirements and computing times, are discussed. Some brief remarks concerning the computer programs written to test the line models are included in Section 2D.

Computed asymptotic solutions for source-free systems with time-independent properties are reported and analyzed in Section 2E. These problems are particularly convenient for evaluating the various models because the solutions can be checked analytically. In addition, errors due to the discrete-delay-time approximation and the population growth rate can be substantially isolated from errors due to the approximation for the space-dependence by solving an auxiliary problem.* Computed space-time transient responses to short-lived, localized external sources are studied in Section 2F. These solutions illustrate the effects of discontinuities in the time-dependence of the parent birth rates. A procedure for computing importance distributions is described in Section 2G; an example distribution for a small, slightly supercritical system is reported. Finally, examples of problems with time-varying external sources and time-varying secondary emission coefficients are given in Sections 2H and 2I, respectively.

2A. INTERPRETATION OF INTEGRAL-TRANSPORT EQUATION AND RELATION WITH FINITE-INTEGRAL APPROXIMATION

Let us multiply Eq. (1A.3) by the element dx and, for convenient referencing, rewrite the equation:

*Note: The "auxiliary problem" is defined in Subsection 2E.4.

$$b(x,t)dx = \frac{c(x,t)\Sigma(x)dx}{2} \int_0^W dx' b(x', t - \frac{|x-x'|}{v}) \cdot$$

$$\cdot \exp\left\{ - \frac{[x-x']}{|x-x'|} \int_{x'}^{x} dx'' \Sigma(x'') \right\} + s(x,t)dx. \qquad (2A.1)$$

Eq. (2A.1) has a simple physical interpretation. Consider the infinitesimal source element dx' about x'; $b(x',t-|x-x'|/v)dx'$ is the birth rate in dx' at a time which is earlier than t by an interval equal to the flight-time required for a particle to travel from x' to x. One-half of the particles born are emitted towards the receiver element dx. The fraction of these that reach dx is given by the exponential term. The fraction of those reaching dx that collide in dx is given by the factor $\Sigma(x)dx$. The product of the four factors gives the contribution to the collision rate in dx at t from particles born in dx'. The integral over all source elements in the system then gives the collision rate in dx. The progeny birth rate is equal to the product of the secondary emission coefficient and the collision rate. Adding the external source rate, one obtains the birth rate.

Figure 2A.1 shows the relation between a receiver point (x,t) and the contributing source points (x',t') in the space of the coordinates x and t.

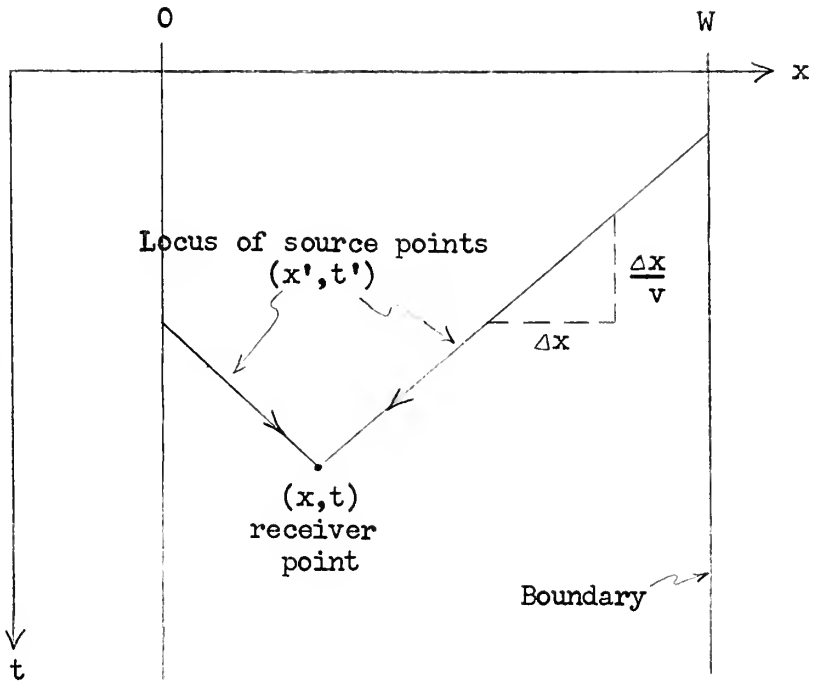

Figure 2A.1 Relation between Receiver and Source Points in (x,t)-Space

Equation (2A.1) relates the birth rate in the infinitesimal receiver element dx with the parent birth rates in an infinite number of infinitesimal source elements dx'. For numerical purposes we want to approximate Eq. (2A.1) by a model relating the birth rate in a finite receiver region I with the birth rates in a finite number of finite source regions J. Figure 2A.2 shows the relation between the integral-transport equation and the finite-integral model.

As described in Chapter 1, we subdivided the system of length W into N regions, each having the length $\Delta x=W/N$, and treat the nuclear properties as homogeneous within each region. Then, splitting the integral over x' in Eq. (2A.1) into N distinct

integrals, and integrating both sides of the equation over the interval Δx corresponding to region I, we obtain:

$$B(I,t) = \int_{(\Delta x)_I} b(x,t)dx$$

$$= c(I,t) \sum_{J=1}^{N} \left\{ \int_{(\Delta x)_I} dx \frac{\Sigma(I)}{2} \int_{(\Delta x)_J} dx' b(x', t - \frac{|x-x'|}{v}) \cdot \right.$$

$$\left. \cdot \exp\left\{ - \frac{[x-x']}{|x-x'|} \int_{x'}^{x} dx'' \Sigma(x'') \right\} \right\} + S(I,t), \qquad (2A.2)$$

where the sum over J gives the collision rate in region I. With the exception of the terms in the summation, Eq. (2A.2) is identical to Eq. (1B.2), the finite-integral approximation.

We now focus our attention on the integral expression which gives the contribution to the collision rate in region I from neutrons born in region J:

$$\int_{(\Delta x)_I} dx \frac{\Sigma(I)}{2} \int_{(\Delta x)_J} dx' \, b(x', t - \frac{|x-x'|}{v}) \exp\left\{ - \frac{[x-x']}{|x-x'|} \int_{x'}^{x} dx'' \Sigma(x'') \right\}. \qquad (2A.3)$$

By analogy with Fig. 2A.1 , the hatched area in Fig. 2A.3 contains all possible birth positions in (x,t)-space of parent neutrons which were born in J and which collide in I at time t. With the discrete-delay-time approximation, $b(x', t-|x-x'|/v)$ is replaced by $b(x', t-\tau(I,J))$. The nature of this approximation is fairly obvious from Fig. 2A.3 .

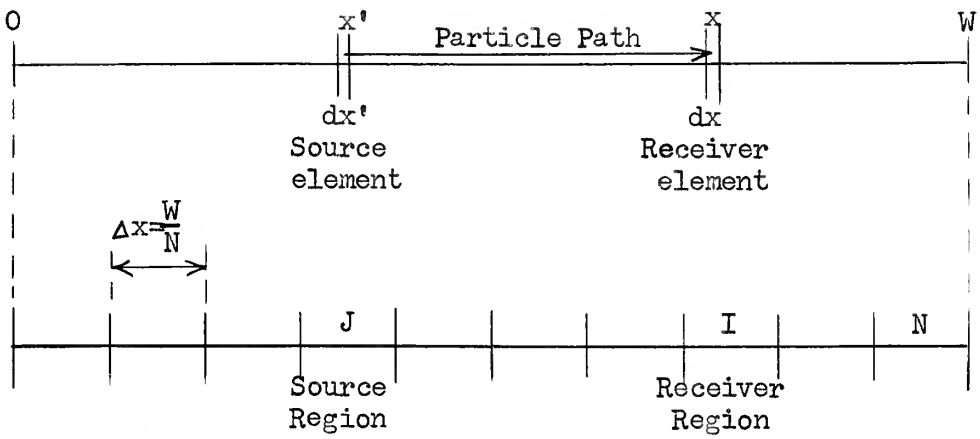

Figure 2A.2 Relation between the Integral Equation and the Finite Approximation

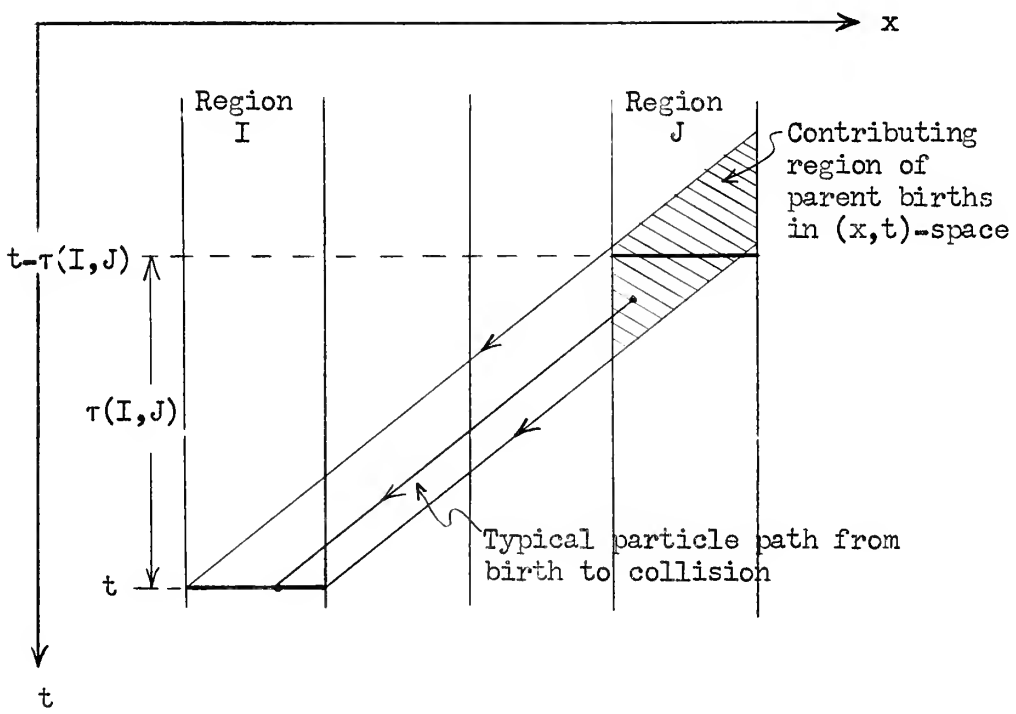

Figure 2A.3 Schematic Diagram of Discrete Delay-time Approximation

In the next two sections, specific models are formulated by approximating the x'-dependence in $b(x',t-\tau(I,J))$ as indicated by Eq. (1B.1), where the various functions retained in Eq. (1B.1) are defined explicitly. Expressions for the $\tau(I,J)$ are derived independently.

2B. FIXED-DISTRIBUTION MODELS

In this section we develop three fixed-distribution models. For these models, Eq. (1B.1) reduces to

$$b(x',t-\frac{|x-x'|}{v}) = B(J,t-\tau(I,J))u_o(x') \ . \qquad (2B.1)$$

Similarly, Eq. (1B.2) reduces to

$$B(I,t) = c(I,t) \sum_{J=1}^{N} [G(I,J)B(J,t-\tau(I,J))] + S(I,t). \qquad (2B.2)$$

The models to be developed are designated Model I, Model M and Model F, respectively. A detailed description of each model follows.

2B.1 Model I: Simple Nodal Approximation of the Integral Equation

For Model I, we focus attention of the N discrete points x_i which are the midpoints of their respective regions, I. We assume that the birth rate density at the midpoint of each region is equal to the mean birth rate density in the region and that particles which were born at x_j and which collide at x_i at time t represent, in the mean, all particles which were born in region J and which collide in region I at time t. Model I can then be formulated directly from Eq. (2A.2) simply by substituting x_i for x and x_j for x', performing the trivial integrations

$$\int_{(\Delta x)_I} dx = \int_{(\Delta x)_J} dx' = \Delta x,$$

and identifying terms.*

The transfer coefficients are given by

$$G(I,J) = \frac{\Sigma(I)\Delta x}{2} \exp\left\{ - \frac{[x_i - x_j]}{|x_i - x_j|} \int_{x_j}^{x_i} dx''\Sigma(x'') \right\} .$$

For $I \neq J$,

$$G(I,J) = \frac{P(I)}{2} e^{-[P(J)/2+P(I)/2+P_b(I,J)]} , \qquad (2B.3a)$$

where $P(I)$ is the optical width (in mean free paths) of region I and $P_b(I,J)$ is the sum of the optical widths of all regions lying between regions I and J; for $I = J$,

$$G(I,I) = \frac{\Sigma(I)\Delta x}{2} = \frac{P(I)}{2} \qquad (2B.3b)$$

The delay times for $I \neq J$ are given by

$$\tau(I,J) = \frac{|x_i - x_j|}{v} = |I-J| \frac{\Delta x}{v} . \qquad (2B.4a)$$

Special attention need only be given to approximating $\tau(I,I)$ by a realistic, non-zero expression. We assume that the mean distance

---

*Note: Model I differs from all other models developed in that it is essentially a midpoint-to-midpoint formulation rather than a midpoint-to-region formulation, as is Model M, or a region-to-region formulation, as is Model F. We have, in effect, arbitrarily specified the collision distribution in region I. For this reason, the method used above to present Model I is considered preferable to adapting the general approach outlined previously.

travelled by particles born at x_i and colliding in region I is $\Delta x/4$, or half of the distance to the edge of the region. In this case,

$$\tau(I,I) = \frac{\Delta x}{4v} . \qquad (2B.4b)$$

The convergence of the Model I formulation to the integral equation (2A.1) in the limit as $N \to \infty$ and $\Delta x \to 0$ is fairly obvious. For systems with optically-wide regions, however, it can be shown that Model I violates the principle of conservation of particles. Consider for example, a homogeneous system subdivided into thirty regions, each of which is 0.5 mean freepath wide. Since the systems extends at least seven mean free paths on each side of region 15, only a minute fraction of particles born in region 15 will leak from the system; the sum over all I of the G(I,15) should therefore be slightly less than unity. We find, however, that the partial sum over regions 6 to 24 is equal to 1.012. Model I predicts more collisions, and subsequent births, than conservation permits. Because of this excess production, birth rates computed with Model I tend to grow too fast.

2B.2 Model M: Midpoint Approximation

For Model M, we treat all particles born in region J as if emitted from the midpoint x_j. The expression for G(I,J), the fraction colliding in region I, is then derived rigorously. Model M is therefore consistent with the conservation of particles. Assuming an arbitrary distribution for the parent particles, however, is equivalent to repositioning particles at the time of their births and therefore violates the conservation of importance.

With the midpoint approximation, the function $u_o(x')$ in Eq. (2B.1) is given by the Dirac delta function; i.e.,

$$u_o(x') = \delta(x'-x_j) \ . \qquad (2B.5)$$

Substituting Eqs. (2B.1) and (2B.5) into Expression (2A.3), and factoring $B(J,t-\tau(I,J))$ out of the integral expression, the integral expression reduces to

$$G(I,J) = \int_{(\Delta x)_I} dx \frac{\Sigma(I)}{2} \exp\left\{ - \frac{[x-x_j]}{|x-x_j|} \int_{x_j}^{x} dx''\Sigma(x'') \right\} ,$$

from which

$$G(I,J) = \frac{1}{2} [1-e^{-P(I)}]e^{-[P(J)/2+P_b(I,J)]} \qquad (2B.6a)$$

for $I \neq J$, and

$$G(I,I) = 1 - e^{-P(I)/2} \ . \qquad (2B.6b)$$

For very small P(I), it can be shown that Eqs. (2B.6) reduce to Eqs. (2B.3). The delay times used with Model M are the same as those used for Model I, given by Eqs. (2B.4).

The following two characteristic errors of Model M will be apparent in the results of test problems reported in Section 2E. First, in comparison with models which treat the distribution of births in region J as a smoothly-varying function, Model M overestimates G(J,J) and therefore underestimates the net leakage from region J of particles born in region J. For large P(J), parent particles and their progeny tend to be trapped in region J. Second, the midpoint-to-

midpoint delay times, $\tau(I,J)$, are overestimated. Consider a uniform source distribution in region J. For non-zero P(J), most of the particles which escape from region J in the direction of region I were born in that half of region J which is closer to region I. Similarly, most of the particles which collide in region I collide in that half of region I which is closer to region J. The mean delay time between births in J and collisions in I is clearly less than $|x_i - x_j|/v$. Due to the overestimated $\tau(I,J)$, population growth or decay rates predicted by Model M tend to be smaller than the correct values.

2B.3 Model F: Flat Approximation

For Model F, we assume that the birth rate in source region J is distributed uniformly over region J such that

$$u_o(x') = \frac{1}{\Delta x} . \qquad (2B.7)$$

Substituting Eqs. (2B.1) and (2B.7) into Expression (2A.3), and factoring $B(J,t-\tau(I,J))$ out of the integral expression, we obtain

$$G(I,J) = \int_{(\Delta x)_I} dx \frac{\Sigma(I)}{2} \int_{(\Delta x)_J} dx' \frac{1}{\Delta x} \exp\left\{ - \frac{[x-x']}{|x-x'|} \int_{x'}^{x} dx'' \Sigma(x'') \right\},$$

from which

$$G(I,J) = \frac{1}{2P(J)} [1 - e^{-P(J)}][e^{-P_b(I,J)}][1 - e^{-P(I)}] \qquad (2B.8a)$$

for $I \neq J$, and

$$G(I,I) = 1 - \frac{1}{P(I)}\left[1 - e^{-P(I)}\right] . \qquad (2B.8b)$$

In Eq. (2B.8a), the expression

$$\frac{1}{2P(J)}\left[1 - e^{-P(J)}\right]$$

gives the fraction of the particles born in J that leak past each boundary of region J; the expression in the second set of brackets gives the probability that a particle will not collide along the flight path between regions I and J; the expression in the third set of brackets gives the probability that a particle entering region I will collide in region I.

To obtain the delay times, we assume a uniform source distribution, $1/\Delta x$, in region J and derive the expression for the mean distance travelled by source particles that collide in region I. Dividing this expression by v, we obtain the mean delay time between births in J and collisions in I. Thus,

$$\tau(I,J) = \frac{1}{vG(I,J)} \int_{(\Delta x)_I} dx \frac{\Sigma(I)}{2} \int_{(\Delta x)_J} dx' \frac{|x-x'|}{\Delta x} \exp\left\{ - \frac{[x-x']}{|x-x'|} \int_{x'}^{x} dx''\Sigma(x'') \right\} ,$$

from which

$$\tau(I,J) = \left\{ \left[\frac{1}{P(J)} - \frac{e^{-P(J)}}{[1 - e^{-P(J)}]} \right] + \left[|I-J| - 1 \right] + \left[\frac{1}{P(I)} - \frac{e^{-P(I)}}{[1-e^{-P(I)}]} \right] \right\} \frac{\Delta x}{v} \qquad (2B.9a)$$

for $I \neq J$, and

$$\tau(I,I) = \left\{ \frac{P(J) - 2 + [2 + P(J)]\, e^{-P(J)}}{P(J)[P(J) - 1 + e^{-P(J)}]} \right\} \frac{\Delta x}{v} \quad . \qquad (2B.9b)$$

The three dimensionless expressions denoted by the brackets in Eq. (2B.9a) give the mean distances, in subregion lengths, travelled in region J, in the regions between I and J, and in region I, respectively, by particles which are born in J and collide in I.

In Table 2B.1 we list some characteristic values of the transfer parameters computed with Models I, M and F. These numbers illustrate the differences between the various models.

2B.4 Some Computational Characteristics of the Finite Approximation

In applying Eq. (2B.2) for numerical computations, the birth rates are computed only at discrete times and then stored. The unit time step, Δt, is set equal to the smallest of the $\tau(I,I)$ in order that the resulting numerical equation will be explicit; at time t, then, all birth rates needed on the right-hand side of Eq. (2B.2) are either known or can be obtained by simple interpolation between known values. The birth rate in region I at time step K, where K is an integer, is given by

$$B(I,K) = c(I,K) \sum_{J=1}^{N} [G(I,J)B(J,K-\tau_k(I,J))] + S(I,K), \qquad (2B.10)$$

where

$$\tau_k(I,J) = \frac{\tau(I,J)}{\Delta t} \quad . \qquad (2B.11)$$

Table 2B.1

Selected Values of Transfer Parameters Computed with Models, I, M and F.

Optical Width of Region I, P(I)	G(I,I)			$\tau(I,I)v/\Delta x$		Contribution of Mean Track Length in Region I to $\tau(I,J)v/\Delta x$	
	Model I	Model M	Model F	Models I,M	Model F	Models I,M	Model F
.02	.01	.0100	.0100	0.25	.3322	0.5	.4983
.1	.05	.0488	.0484		.3278		.4917
.4	.20	.1812	.1758		.3117		.4668
1.0	.50	.3934	.3678		.2817		.4180
5.0	2.50	.9180	.8014		.1521		.1932
10.0	5.00	.9933	.9000		.0889		.1000

In Models I and M, the $\tau_k(I,J)$ are integers; in Model F, they are non-integers and $B(J,K-\tau_k(I,J))$ is obtained by linear interpolation between stored values. The number of time steps of memory required is given by the largest of the $\tau_k(I,J)$, $\tau_k(1,N)$, for Models I and M and by the integer just larger than $\tau_k(1,N)$ for Model F.*

Since $\tau_k(1,N)$ is nearly proportional to N, the storage capacity required for the birth rate memory, as well as for the transfer-parameter arrays G and τ, is proportional to N^2. In the computing algorithms, the argument K is dropped from c and S in Eq. (2B.10); at time steps when changes are scheduled to be made, the c(I) and S(I) are appropriately altered. Storage is not required for the past history of these parameters.

From Eq. (2B.10), it is clear that the number of computing operations required to compute all B(I,K) at time step K is approximately proportional to N^2. The computing time for our IBM-7094 codes can therefore by estimated be the relation

$$T_{comp.} = \alpha_t N^2 \text{ seconds per time step,} \qquad (2B.12)$$

where α_t is equal to .0002 for Models I and M and .0005 for Model F.** If we allow twenty seconds for reading in the program and problem data and computing the transfer parameters, approximately one minute is required for a 200 time-step, twenty region, Model F calculation.

---

*Note: For optically-thick systems, in which contributions to B(I,t) from source regions optically-distant from region I may be neglected, the required number of time steps of memory is reduced.

**Note: The values of α_t have been determined experimentally from the computing times for several problems.

From Table 2B.1, $\tau(I,I)v/\Delta x$ does not vary greatly from 0.3 for $P(I)<2$. Since $\Delta x = W/N$, $\tau(I,I)Nv/W$ is nearly constant. For a given system, then, the unit time step Δt is approximately inversely proportional to the number of regions into which the system is subdivided. In order to compute a transient having a given time duration, then, the required number of time steps is approximately proportional to N; the total computing time is therefore approximately proportional to N^3.

For a typical problem with $v = 2 \times 10^5$ cm/sec and $\Delta x = 1$ cm, the unit time step is approximately 1.5 microseconds. To compute a transient lasting 1.5 milliseconds requires that we compute the birth rates at 1000 time steps. If Model F is used with N = 20, the total computing time is [(1000) (.0005) (400) + 20] sec, or 220 sec. From this, it is clear that computing time sets a practical limit on the time duration of transients which can be studied using the finite-integral method.

The strong dependence of both storage requirements and computing efficiency on N justifies the development of more sophisticated models. When comparing two models for computing a given transient, the better model is the one that yields a more accurate solution with a smaller value of the parameter $\alpha_t N^3$.

2C. MODEL FS: VARIABLE DISTRIBUTION MODEL WITH SUPERIMPOSED FLAT AND SLOPE-CORRECTION MODES

In this section we develop a variable-distribution model, Model FS, in which the birth rate distribution in source region J, $b(x',t-\tau(I,J))$, is approximated by a sum of a flat mode and a linearly-varying slope-correction mode:

$$b(x',t-\tau(I,J)) = B(J,t-\tau(I,J))\frac{1}{\Delta x} + C_1(J,t-\tau(I,J))u_1(x') \quad . \qquad (2C.1)$$

Since the integral of $b(x',t-\tau(I,J))$ over region J is, by definition, equal to $B(J,t-\tau(I,J))$, the slope-correction mode must be antisymmetric with respect to the midpoint of region J in order that its integral over region J be equal to zero. Therefore

$$u_1(x') = A[x' - x_j] \qquad (2C.2)$$

and $C_1(J,t-\tau(I,J))/A$ is the computed slope of the birth rate distribution in region J.

To get an expression for the slope C_1/A, we take advantage of the continuity of the flux distribution from one region to the next. The nuclear properties c and Σ may be different in each region of the system; for convenience, however, they are assumed to be independent of time.* We assume that the gross slope of the flux distribution in an interior region J at time $t-\tau$ is given approximately by the expression

$$\frac{\phi(J+1,t-\tau)/\Delta x - \phi(J-1,t-\tau)/\Delta x}{2\Delta x} \quad ,$$

*Note: For the variable-distribution models developed for slab geometry in Chapter 3, c and Σ must be homogeneous across groups of three successive regions, but c may vary with time.

where $\underline{\phi}(J+1,t-\tau)$ is the integral of the flux in region J+1 and $\underline{\phi}(J+1,t-\tau)/\Delta x$ is the mean flux in region J+1.* From Eq. (1A.2),

$$b(x,t-\tau) = c(x')\Sigma(x')\phi(x',t-\tau) + s(x',t-\tau)$$

$$= \Sigma_p(x')\phi(x',t-\tau) + s(x',t-\tau)$$

$$= b^o(x',t-\tau) + s(x',t-\tau) \ , \qquad (2C.3)$$

where Σ_p is the production cross section and b^o is the progeny birth rate density. The gross slope of the progeny birth rate distribution in region J is thus given by the product of $\Sigma_p(J)$ and the slope of the flux distribution. We assume that the external source rate $S(J,t-\tau)$ is distributed uniformly over region J; the slope of the birth rate distribution is then equal to the slope of the progeny birth rate distribution.

Noting that the integral of $b^o(x,t-\tau)$ over region J+1 is

$$B^o(J+1,t-\tau) = \Sigma_p(J+1)\underline{\phi}(J+1,t-\tau), \qquad (2C.4)$$

we may write

$$C_1(J,t-\tau(I,J)) = \Sigma_p(J)[B^o(J+1,t-\tau(I,J))/\Sigma_p(J+1) -$$

$$B^o(J-1,t-\tau(I,J))/\Sigma_p(J-1)] \ , \qquad (2C.5)$$

for $2 \leq J \leq [N - 1]$, and

$$u_1(x') = \frac{x'-x_j}{2[\Delta x]^2} \qquad (2C.6)$$

---

*Note: In future sections we adopt the notation $\phi(I,t)$ to indicate the mean flux in region I at time t.

The unit flat and slope-correction modes are shown in Fig. 2C.1 .

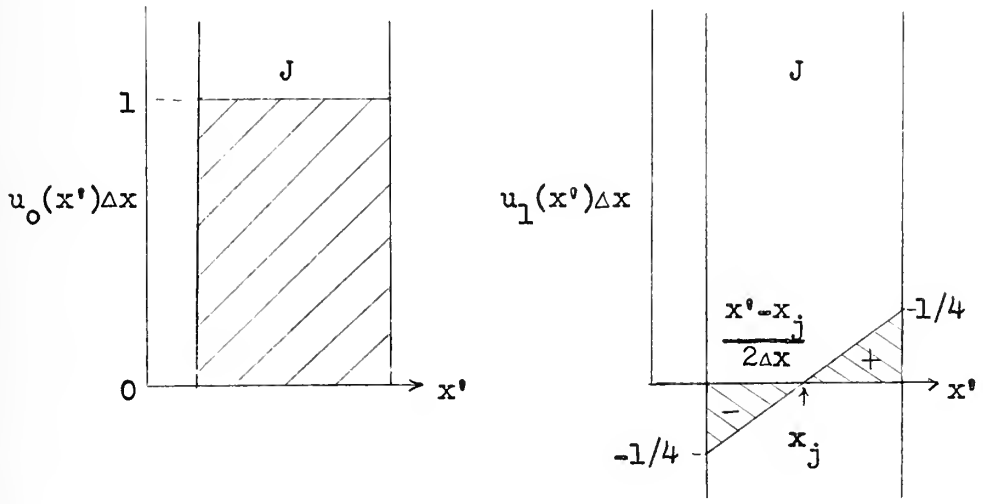

a) Unit flat mode

b) Unit slope-correction mode vs. x.

Figure 2C.1 Unit Modes for Model FS

The modal coefficient for region 1 is computed using the progeny birth rates in regions 1 and 2:

$$C_1(1,t-\tau(I,1)) = 2\left[\frac{\sum_p(1)}{\sum_p(2)} B^o(2,t-\tau(I,1)) - B^o(1,t-\tau(I,1))\right] . \quad (2C.7a)$$

Similarly,

$$C_1(N,t-\tau(I,N)) = 2\left[B^o(N,t-\tau(I,N) - \frac{\sum_p(N)}{\sum_p(N-1)} B^o(N-1,t-\tau(I,N))\right] . \quad (2C.7b)$$

Substituting Eqs. (2C.1) and (2C.6) in Eq. (2A.2) as modified by the discrete-delay-time approximation, subtrating S(I,t) from each side, expressing $B(J,t-\tau(I,J))$ as a sum of $B^o(J,t-\tau(I,J))$ and $S(J,t-\tau(I,J))$,

and identifying terms, we obtain the finite integral equation for Model FS:

$$B^{o}(I,t) = c(I) \sum_{J=1}^{N} \Big\{ G(I,J) \Big[B^{o}(J,t-\tau(I,J)) + S(J,t-\tau(I,J)) \Big] + G_{slp}(I,J) C_1(J,t-\tau(I,J)) \Big\} , \qquad (2C.8)$$

where the $G(I,J)$ and $\tau(I,J)$ are the Model F values, given by Eqs. (2B.8) and (2B.9). The numerical model is obtained by replacing the arguments t and $\tau(I,J)$ in Eqs. (2C.5,7,8) by K and $\tau_k(I,J)$ respectively. Memory is provided for both the progeny birth rate and the external source rate; the coefficient C_1, however, is computed each time it is needed, using Eqs. (2C.5,7a, or 7b). The transfer coefficient $G_{slp}(I,J)$ is given by

$$G_{slp}(I,J) = \int_{(\Delta x)_I} dx \frac{\Sigma(I)}{2} \int_{(\Delta x)_J} dx' \frac{[x'-x_j]}{2[\Delta x]^2} \exp\left\{ - \frac{[x-x']}{|x-x'|} \int_{x'}^{x} dx'' \Sigma(x'') \right\} , \qquad (2C.9)$$

from which

$$G_{slp}(I,J) = \frac{[I-J]}{|I-J|} \frac{1}{8P(J)} \left[1 + e^{-P(J)} - \frac{2}{P(J)} \left[1 - e^{-P(J)} \right] \right] \cdot \left[e^{-P_b(I,J)} \right] \left[1 - e^{-P(I)} \right] \qquad (2C.10a)$$

for $I \neq J$, and

$$G_{slp}(I,I) = 0 . \qquad (2C.10b)$$

With Model F, the computed leakage from region J of particles born in region J is the same in both directions. By adding the slope

correction in Model FS, we redistribute the leakage, increasing the fraction leaking from region J in the direction of increasing birth rate density and decreasing by an equal amount the fraction leaking in the opposite direction. The importance of the slope correction increases both with the deviation of the flux distribution from a uniform distribution, as reflected in the value of $C_1(J,t-\tau)$, and with the optical thickness of region J, as indicated by the ratios $|G_{slp}(I,J)|/G(I,J)$ given in Table (2C.1).

The IBM-7094 computing time for Model FS is given by

$$T_{comp} = 0.0009\ N^2 \text{ seconds/time step.} \qquad (2C.11)$$

Table 2C.1

The Ratio $|G_{slp}(I,J)|/G(I,J)$ for Selected Values of P(J)

Optical Width of Region J, P(J)	$\frac{\lvert G_{slp}(I,J)\rvert}{G(I,J)}$
0	0
0.02	.0008
0.06	.0025
0.10	.0042
0.40	.0166
1.0	.0410
2.0	.0783
5.0	.153
∞	.250

2D. COMPUTER PROGRAMS FOR THE LINE MODELS

The computer programs developed for testing the line models are written in FORTRAN II language [14,15] for the IBM-7094 computer. The program OVRR4, for use with Models F and FS, handles up to thirty regions; nuclear properties may be assigned independently for each region. OVRR4 is described in Appendix A. Included are an input form, definitions of the input and output variables, a FORTRAN listing of the program liberally annotated by comment statements, and the printed output from a simple example problem.

The problems have been designed for flexibility, both in the types of problems which can be solved and in selective rewriting for special purposes. In OVRR4, for example, the values of 21 different integer control variables, which must be specified in the input, regulate the logical flow of the program and the printed output for a specific problem. Some options for simple types of changes in sources and properties with time are already incorporated into the program. In addition, user-written subroutines SOURCE and TDEP may be called at various points in the program to change the source and property distributions in any desired manner consistent with the model being used. In order to facilitate selective reprogramming of any of the subroutines, all important variables, as well as some additional dummy control variables and arrays, are included in COMMON storage. The structure of the computer program for slab models is similar to OVRR4.

2E. TESTS OF ASYMPTOTIC SOLUTIONS

Perhaps the most convenient class of solutions for testing and comparing the various models are the asymptotic ($t\to\infty$) solutions for isolated, source-free systems with time-independent properties. An asymptotic solution, which describes the fundamental natural mode for the particular system, conforms to the following simple relation:

$$b(x,t+\tau) = b(x,t)e^{\lambda\tau} , \qquad (2E.1)$$

where λ is the asymptotic inverse period, $\sec^{-1}$. The relative x-dependence (shape) of the asymptotic birth rate distribution is independent of time.

2E.1 Computational Procedure for Generating Asymptotic Solutions

The asymptotic solutions are obtained by setting up an arbitrary initial memory distribution in the array B(I,K), setting the elements of array S(I) equal to zero, and performing the computations specified by Eq. (2B.10) or Eq. (2C.8) for all regions $1 \leq I \leq N$ and for as many time steps as required for higher modes to decay substantially. We test for asymptoticity at each time step K using the following procedure. Three regions (I_1=1, I_2=N/2, and I_3=N-3) are arbitrarily selected for testing purposes. The following ratios are computed:

$$R_1(K) = B(I_1,K)/B(I_1,K-1); \qquad (2E.2a)$$

$$R_2(K) = B(I_2,K)/B(I_2,K-1); \qquad (2E.2b)$$

$$R_3(K) = B(I_3,K)/B(I_3,K-1). \qquad (2E.2c)$$

As the higher modes decay, the values of $R_1(K)$,R_2,(K) and $R_3(K)$ tend to become equal and not to change from one time step to the next. We therefore compute the value of Y, where

$$Y = |R_2(K) - R_1(K)| + |R_3(K) - R_1(K)| + |R_1(K) - R_1(K-1)| +$$

$$+ |R_2(K) - R_2(K-1)| + |R_3(K) - R_3(K-1)| , \qquad (2E.3)$$

and compare it with the convergence criterion γ, a number read into the computer with the problem data. Values used for γ ranged from 10^{-6} to 10^{-7}. If $Y > \gamma$ the program proceeds to the next time step. If $Y \leq \gamma$, the asymptotic inverse period is computed according to the relation,

$$\lambda = \frac{\ln(R_2(K))}{\Delta t} \quad ; \qquad (2E.4)$$

and is printed out along with the normalized asymptotic birth rate and flux distributions.

2E.2 Small, Nearly Critical, Homogeneous System

For systems which are nearly critical, the ratio $R_2(K)$ is very close to unity. Over an interval of several time steps, the population level changes only slightly. Consequently, slight errors in the $\tau(I,J)$ and errors due to the discrete delay-time approximation have negligible effect on the computed solutions. These systems are therefore particularly useful for evaluating the relative performance of the approximations made for the x'-dependence of $b(x',t-\tau(I,J))$ in the various models.

In Table 2E.1 are given the inverse asymptotic periods computed for a 6.375 cm. homogeneous line reactor with $\Sigma = 0.5$ cm^{-1}, c=1.4, and v=2x10^5 cm/sec. Although the data available for this particular system is somewhat sparse, the results illustrate some of the model characteristics which were discussed previously in Sections 2B and 2C. We would expect the more sophisticated Model FS to yield the most accurate results. The close agreement of the two Model FS results supports confidence in their accuracy. In the following paragraphs, the directions of the errors in the Model F and Model M results are explained.

Table 2E.1

Inverse Periods Computed for
6.375 cm Reactor

Model	N	λ, sec^{-1}
M	10	143
F	20	19
FS	13	70
FS	20	71

The asymptotic birth rate distribution has a cosine shape, symmetric with respect to the midpoint of the reactor.* Consider the distribution of births in any source region J which lies off-center. The fraction escaping from region J in the direction of the midpoint of

*Note: The possible functional forms of asymptotic solutions for homogeneous systems are derived in Appendix E. Results of shape analyses of some distributions computed with the finite-integral models are given in later subsections. The normalized asymptotic flux distribution, $\phi_o(I)$, computed by Model FS with N = 13 is given in Table 2G.1.

the reactor is greater than the fraction escaping in the opposite direction. Model F, however, equates the two fractions and thereby overestimates the net leakage from the reactor. This accounts for the smaller growth rate predicted by Model F.

Model M also equates the two escape fractions. As noted previously, however, Model M overestimates G(J,J) and thus underestimates 1-G(J,J), the total fraction escaping from region J. The trapping error more than offsets the error due to the equality of the two escape fractions, thus underestimating the net leakage from the system and resulting in the larger growth rate predicted by Model M.

From the data given in Table 2B.1, Model I would predict a still higher growth rate.

While the percentage differences in the various values of λ might seem to indicate that Models M and F are unsatisfactory, this is not so. The point is that in a very small system, λ is extremely sensitive to factors that affect the fraction of particles born that escape from the system. Here we have exploited this sensitivity to illustrate errors in the midpoint and flat approximations. In Subsection 2E.5 we study a system which is identical to the system studied here except that the width is 10 cm. For the 10 cm. system, $\lambda = 21140 \text{ sec}^{-1}$. Compared with the 300-fold increase in λ for a 57 percent increase in system width, the one-fold increase in λ due to the Model M errors indicates that the Model M calculation is reasonably good.

In later subsections we report results obtained for highly supercritical systems, for which errors in the approximations involving time dependence have a noticeable effect on the numerical solutions. In the next two subsections, methods for testing the accuracy of the computed inverse periods are described.

2E.3 Theoretical Constraint Relating the Asymptotic Inverse Period and the Spatial Distribution in a Homogeneous System

In Appendix E, the functional forms of asymptotic solutions for homogeneous line reactors are derived. Of the three possible forms, the following one is of interest to us in this chapter:

$$b(x,t) = A \cos(\alpha[x - W/2])e^{\lambda t} , \qquad (2E.5)$$

where A is a constant depending on the initial population level (arbitrary, for our purposes), and $\alpha[cm^{-1}]$ and $\lambda[sec^{-1}]$ are constants for a particular system. In the rigorous asymptotic solution of the transport equations, α and λ are related by

$$\alpha^2 = \Sigma^2[c - 1] + \frac{\lambda}{v}\Sigma[c - 2] - [\frac{\lambda}{v}]^2 . \qquad (2E.6)$$

Eq. (2E.6) is a useful tool for testing the accuracy of asymptotic solutions computed using our line models. In Subsection (2E.5), the method for analyzing the N normalized asymptotic birth rates $B_o(I)$, which are printed out by the program, to obtain the corresponding value of α is described and illustrated by an example. We ask the question: "Is this value of α consistant with the value of λ printed out by the program?" To answer this question, we assume for the moment that the value of α is correct for the system studied and

calculate the equivalent value of λ, λ_s, using the relation

$$\lambda_s = v\left[\frac{\Sigma[c-2]}{2} \pm \sqrt{\frac{\Sigma^2 c^2}{4} - \alpha^2}\right] , \qquad (2E.7)$$

which follows from Eq. (2E.6) by straightforward algebra.† The closeness of λ_s to the computed value of λ is a measure of the accuracy of the computed asymptotic solution. Results in Subsection 2E.5 show that the values of λ_s and λ converge with increasing N, illustrating the convergence with increasing N of the computed asymptotic solutions to the rigorous asymptotic solution of the transport equations.

2E.4 Solution of Auxiliary Problems--A Method for Isolating Errors Due to the Discrete-Delay-Time Approximation

In this subsection, we develop a method for isolating errors due to the combination of a fast-growing population and the approximations involving time-dependence that are included in our models.

Let us rewrite Eq. (2E.1) in a somewhat different form:

$$\begin{aligned} b(x',t-\tau) &= b(x',t)e^{-\lambda\tau} \\ &= b(x',t)e^{-\lambda_{est}\tau}\, e^{-\lambda^*\tau} \end{aligned} \qquad (2E.8)$$

where λ is the true value of the asymptotic inverse period, λ_{est} is an estimated value, and $\lambda^* = \lambda - \lambda_{est}$. Substituting Eq. (2E.8) into Eq. (1A.3), as modified for source-free systems with time-independent properties, we obtain

† Note: Only one of the two values given by Eq. (2E.7) is admissible. For the systems studied in this chapter, the value obtained using the positive value of the square root is applicable.

$$b(x,t) = c(x)\Sigma(x) \int_0^W dx' \frac{b(x',t)}{2} \exp\left\{-\frac{\lambda^*}{v}|x-x'|\right\} \cdot$$

$$\cdot \exp\left\{-\frac{\lambda_{est}}{v}|x-x'| - \frac{[x-x']}{|x-x'|}\int_{x'}^{x} dx''\,\Sigma(x'')\right\} \qquad (2E.9)$$

Combining the two terms in the second exponent,

$$b(x,t) = c(x)\Sigma(x) \int_0^W dx' \frac{b(x',t)}{2} \exp\left\{-\frac{\lambda^*}{v}|x-x'|\right\} \cdot$$

$$\cdot \exp\left\{-\frac{[x-x']}{|x-x'|}\int_{x'}^{x} dx''\,\left[\Sigma(x'') + \frac{\lambda_{est}}{v}\right]\right\} . \qquad (2E.10)$$

We now define

$$\Sigma^*(x) = \Sigma(x)\left[1 + \frac{\lambda_{est}}{v\Sigma(x)}\right] , \qquad (2E.11a)$$

and

$$c^*(x) = \frac{c(x)}{\left[1 + \frac{\lambda_{est}}{v\Sigma(x)}\right]} . \qquad (2E.11b)$$

Substituting Eqs. (2E.11) into (2E.10), we obtain

$$b(x,t) = c^*(x)\Sigma^*(x) \int_0^W dx' \frac{b(x',t)}{2} \exp\left\{-\frac{\lambda^*}{v}|x-x'|\right\} \cdot$$

$$\cdot \exp\left\{-\frac{[x-x']}{|x-x'|}\int_{x'}^{x} dx''\,\Sigma^*(x'')\right\} \qquad (2E.12)$$

Equation (2E.12) describes the asymptotic brith rate distribution in both the reference system with properties $\Sigma(x)$, $c(x)$ and λ and the auxiliary system with properties $\Sigma^*(x)$, $c^*(x)$ and λ^*, where W and v are the same for both systems. The distribution shapes are the same. Note that if λ_{est} were equal to λ, the system with properties $\Sigma^*(x)$ and $c^*(x)$ would be a critical reactor, i.e., a steady state system. In any case, the inverse period of the auxiliary system is λ^*.

This suggests the following procedure. Estimating the inverse period of the reference system from the results of a run, we compute the properties $\Sigma^*(x)$ and $c^*(x)$ using Eqs. (2E.11). A run is then made to find the asymptotic solution of the auxiliary system. The predicted asymptotic inverse period is a close approximation of λ^*. If the auxiliary systems is nearly critical, errors due to neglect of population growth rate in formulating the model are negligible. An improved value of λ for the reference system is obtained by adding λ_{est} and the predicted λ^*. Furthermore, the shape of the auxiliary system solution better represents the true shape for the reference system.

Thus, we have a procedure which is useful in three ways: to evaluate the errors incurred by the neglect of population growth rate; to improve the predicted asymptotic solution for a system with a rapidly growing or decaying population by solving just one auxiliary problem; and to test both the consistency of the method and accuracy of the program, since the properties of the auxiliary system differ from those of the reference system.

We verify that the asymptotic inverse period for the 10 cm system studied in the next subsection is 21140 sec^{-1} by solving one auxiliary problem. It is easy to show that this same basic procedure is also applicable for slab systems. In Chapter 3, the procedure is used extensively in the evaluation of the discrete-delay-time approximation.

2E.5 Small, Very Supercritical, Homogeneous System

In this subsection we report the results obtained for an isolated homogeneous system with W=10 cm, $\Sigma = 0.5\ cm^{-1}$, c=1.4, and $v = 2 \times 10^5$ cm/sec. This system is classified as "small" because it is only five mean free paths wide. The nuclear properties are identical to those of the nearly critical 6.375 cm system discussed in Subsection 2E.2.

Figure 2E.1 shows the N-dependence of the asymptotic inverse periods computed with Models D, I and M.* The unit time step used with Model D was set equal to $\Delta x/4v$, consistent with that used with Models I and M. Figure 2E.2 shows the results obtained with Models M, F and FS. Note the reduced range and expanded scale of the ordinate. The broken curves in each figure are plots of λ_s versus N.

Each of the runs yielded an asymptotic distribution which conforms very closely to a cosine shape, cos αy, where y=x-W/2. The data in Table 2E.2 illustrate the shape analysis of the 16-region

---

* Note: Model D is based on an implicit, first-order, finite-difference approximation to the differential equations for line geometry. It is described in Appendix E.

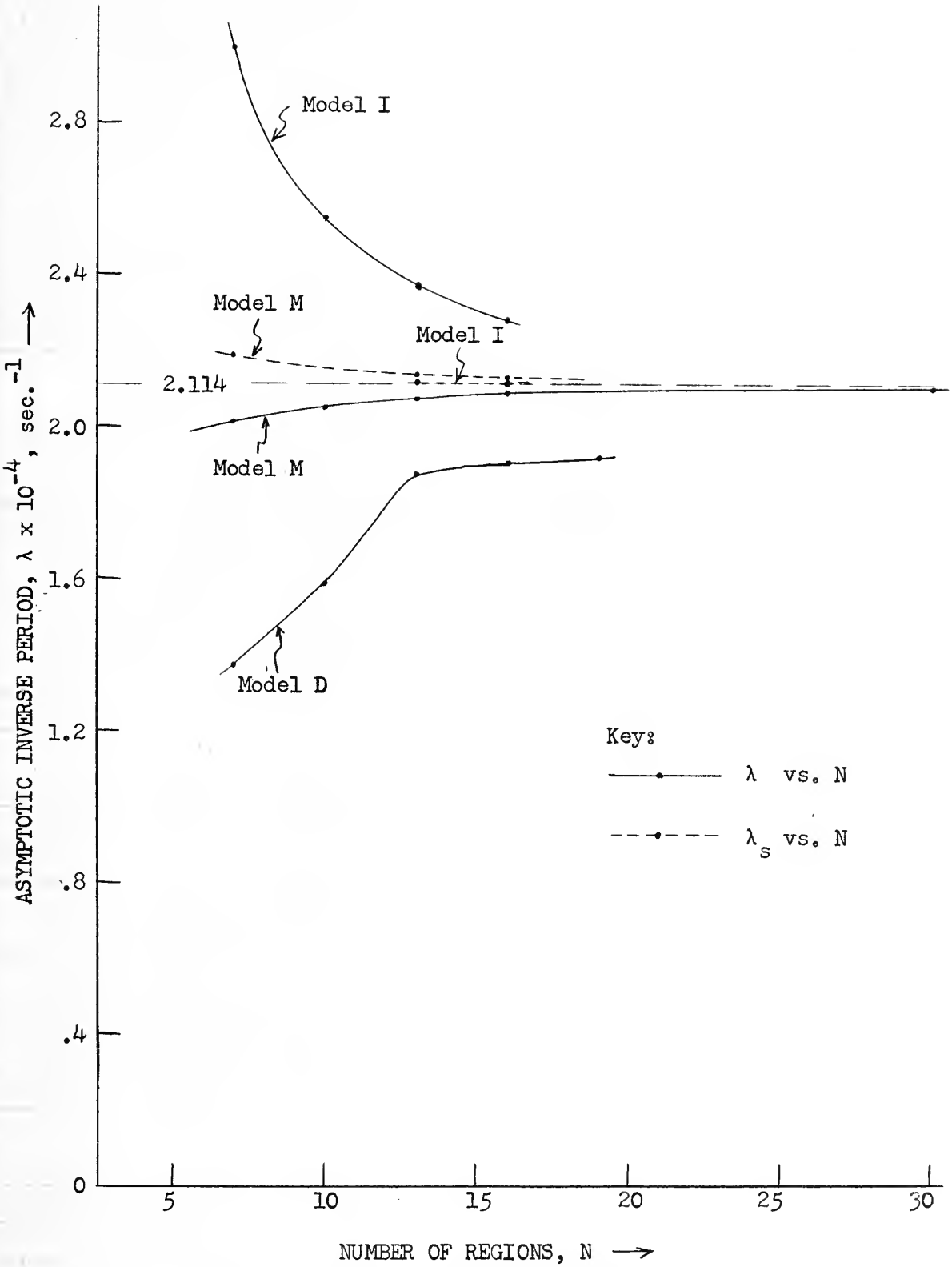

Figure 2E.1 Asymptotic Inverse Period vs. N for 10 cm. Homogeneous System. Models D, I and M.

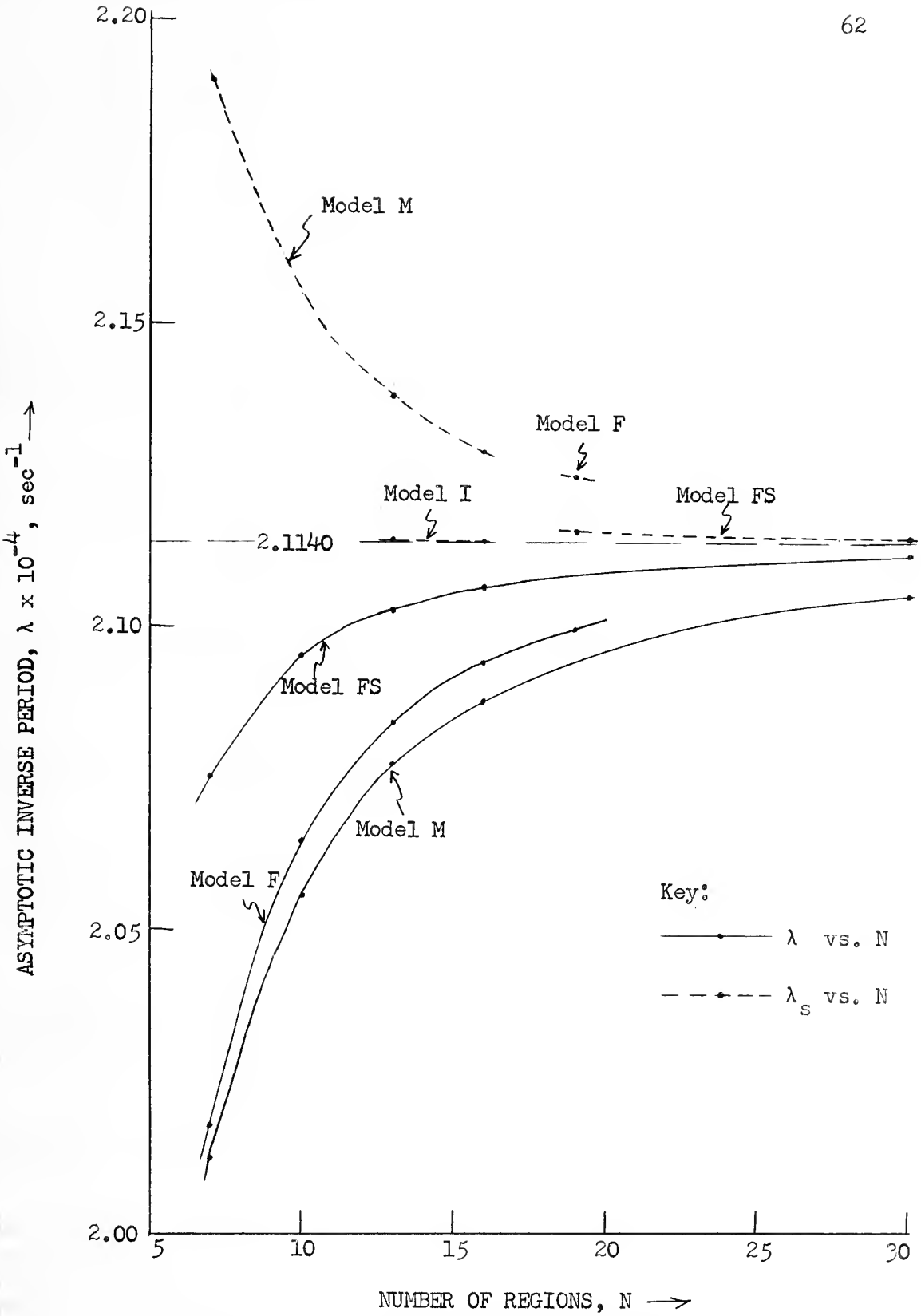

Figure 2E.2 Asymptotic Inverse Period vs. N for 10 cm. Homogeneous System. Models M, F and FS.

distribution computed with Model I. The normalized asymptotic birth rate, $B_o(I)$, is assumed equal to the birth rate density, $[\Delta x]^{-1}$ sec^{-1}, at the midpoint of region I. It is necessary to estimate the birth rate density at the midpoint of the system, i.e., at y=0. Note the consistency of the computed values of α, particularly for regions near the edge.

Using α=.238985 cm^{-1} in Eq. (2E.7), we obtain λ_s=~~22142~~ 21142 sec^{-1}. A similar analysis on the thirteen-region distribution computed with Model I yielded λ_s=21145 sec^{-1}. Since λ_s, as well as λ, must converge with increasing N, the closeness of the two values indicates that they are not far from the correct value of the asymptotic inverse period.

Table 2E.2

Example of Shape Analysis. Model I, N=16

I	$B_o(I)$, $[\Delta x]^{-1}$ sec^{-1}	$Cos(\alpha y_i)$= $B_o(I)/B_o(8.5)$	αy_i	y_i, cm.	α, cm^{-1}
8.5	(est.) 1.283410	1		0	
9	1.279836	.997215	.074651	.3125	.23888
10	1.251335	.975008	.224038	.9375	.238974
11	1.194969	.931089	.373409	1.5625	.238981
12	1.111993	.866436	.522776	2.1875	.238983
13	1.004254	.782489	.672143	2.8125	.238984
14	.874151	.681116	.821510	3.4375	.238985
15	.724583	.564576	.970877	4.0625	.238985
16	.558878	.435464	1.120243	4.6875	.238985

The most accurate computation, Model FS with N=30, yielded λ=21119 and λ_s=21148 sec^{-1}. Based on the apparent accuracy of

Model FS for the nearly critical 6.375 cm system in Subsection 2E.2, we postulate that the small errors in λ and λ_s are largely due to our having neglected the growth rate in formulating Model FS. In order to pin down the correct solution for the 10 cm system, then, an auxiliary system is defined for λ_{est}=21130 sec^{-1}. From Eqs. (2E.11), Σ^*=.60565 cm^{-1} and c^*=1.15578. A thirty-region Model FS solution of the auxiliary system yielded λ^* = 9.8 sec^{-1}, from which the inverse period of the reference system is 21130 + 9.8 = 21140 sec^{-1}. Shape analysis of the asymptotic distribution computed for the auxiliary system yielded α = .23899 cm^{-1}, from which λ_s = 21140 sec^{-1}. The asymptotic solution of the reference system is therefore given by

$$b(x,t) = A \cos(.23899[x - 5])e^{21140t} ,$$

where x is measured in centimeters and t, in seconds.

Having established the correct solution, we can now analyze the results presented in Figs. (2E.1) and (2E.2). Note that all λ and λ_s computed with the integral models converge smoothly, with increasing N, towards the correct solution.

Whereas Model M overestimated the inverse period of the nearly critical 6.375 cm system, it underestimates λ in this very supercritical system. The errors due to the trapping effect and to the overestimated $\tau(I,J)$ act in opposite directions for supercritical systems and tend to cancel in this particular case. Model M thus appears to be a more effective approximation than it actually is.

The excess production due to non-conservation of particles in Model I is clearly evident in the λ vs N curve for Model I. Considering the partial cancellation of errors due to the overestimated $\tau(I,J)$ and the equivalence with Model M as regards storage requirements and computing times, we conclude that Model I merits no further attention for one-dimensional geometries. Although the accuracy of the λ_s results for Model I may have some significance, the large deviation of λ from λ_s does not promote confidence in the use of Model I for computing space-time transients. Furthermore, Model I shows no significant improvement over Model D, which is approximately twice as fast ($\alpha_t \approx$ .0001 sec) as Model I.

The marked improvement of the results obtained with Models M, F and FS over those obtained with Model D is a second example supporting the point made in Chapter 1 concerning the smaller N usually needed with finite-integral models. The greater speed of the Model D program for a given N is attributed in part to the fact that the program was designed to solve a restricted class of problems, permitting shortcuts, and in part to the fact that the program for Model D does not have to compute or search for the argument $\tau_k(I,J)$ for each $J \rightarrow I$ computation. From Fig. 2E.1 , we see that the Model M result for N = 7 is considerably more accurate than the Model D result for N = 13; comparing computing times per time step, $\alpha_t N^2$, we obtain .010 sec for Model M and .017 sec for Model D. Although somewhat larger unit time steps may be used with Model D and the performance

of Model D for different values of $v\Delta t/\Delta x$ is a suitable area for investigation, no further Model D calculations were made.*

The reason that the λ computed with Model F are less than those computed with Model FS was discussed in Subsection 2E.2. A second characteristic of the flat approximation, also due to underestimating the fraction escaping from region J in the direction of increasing birth rate density, is the generation of distributions which are flatter than the correct solutions. For the system studied here, Model F underestimates α, and therefore overestimates λ_s, as is evident in Fig. 2E.2.

As regards the more accurate Model FS, all sources of error which we have uncovered act in the same direction for this system. From the accuracy of the solution for the auxiliary system described previously, it is clear that most of the error in the inverse period computed with Model FS is a consequence of our having neglected the growth rate in formulating the model. From Fig. 2A.3 one can see that if the birth rate increases with time, and if the birth rate density in region J is spatially uniform at any given time, the birth density in J of particles which can collide in region I at time t is largest at the edge of region J which is closer to region I and decreases with distance. If we had accounted for this non-uniform

---

* Note: Many options are available for formulating finite-difference models.[8,11,12] For example, explicit, first-order approximations will be faster than Model D for a given N and do not require a matrix inversion. Further studies comparing efficient finite-difference models with the finite-integral models, as regards accuracy per unit of computing time, are recommended.

source distribution, the $\tau(I,J)$ would be smaller or the contribution $G_{slp}(I,J)C_1(J,t-\tau(I,J))$ would be more positive. Either correction would result in larger values of λ than were obtained with Model FS. A third source of error is due to the neglect of the curvature of the birth rate distribution in region J. Since the distribution is convex, addition of a curvature-correction mode would reduce the fraction of particles escaping from region J and, by analogy with Model M, result in a larger value of λ. The curvature correction is studied in the next two chapters in connection with slab geometry.

Considering the rapid growth rate, the Model FS solutions are quite good. The error of the inverse period computed using only 10 regions [P(I)=0.5] is less than 0.5 percent. For equivalent accuracy, 16 regions are required with Model F and 20 with Model M. The corresponding values of the model evaluation parameter, $\alpha_t N^3$, are 0.9 for Model FS, 2.0 for Model F, and 1.6 for Model M. For this problem then, the superiority of Model FS with respect to computational efficiency is established.

2E.6 Large, Supercritical, Homogeneous System

In this subsection we study a homogeneous system with W = 100 cm, $\Sigma = 0.5$ cm^{-1}, c = 1.1 and v = 2×10^5 cm/sec. The optical widths of the regions range from 2.5 mean free paths for N=20 to 7.143 for N=7. The inverse periods computed with Models M, F and FS are plotted vs N in Fig. 2E.3. Four points are worth making here.

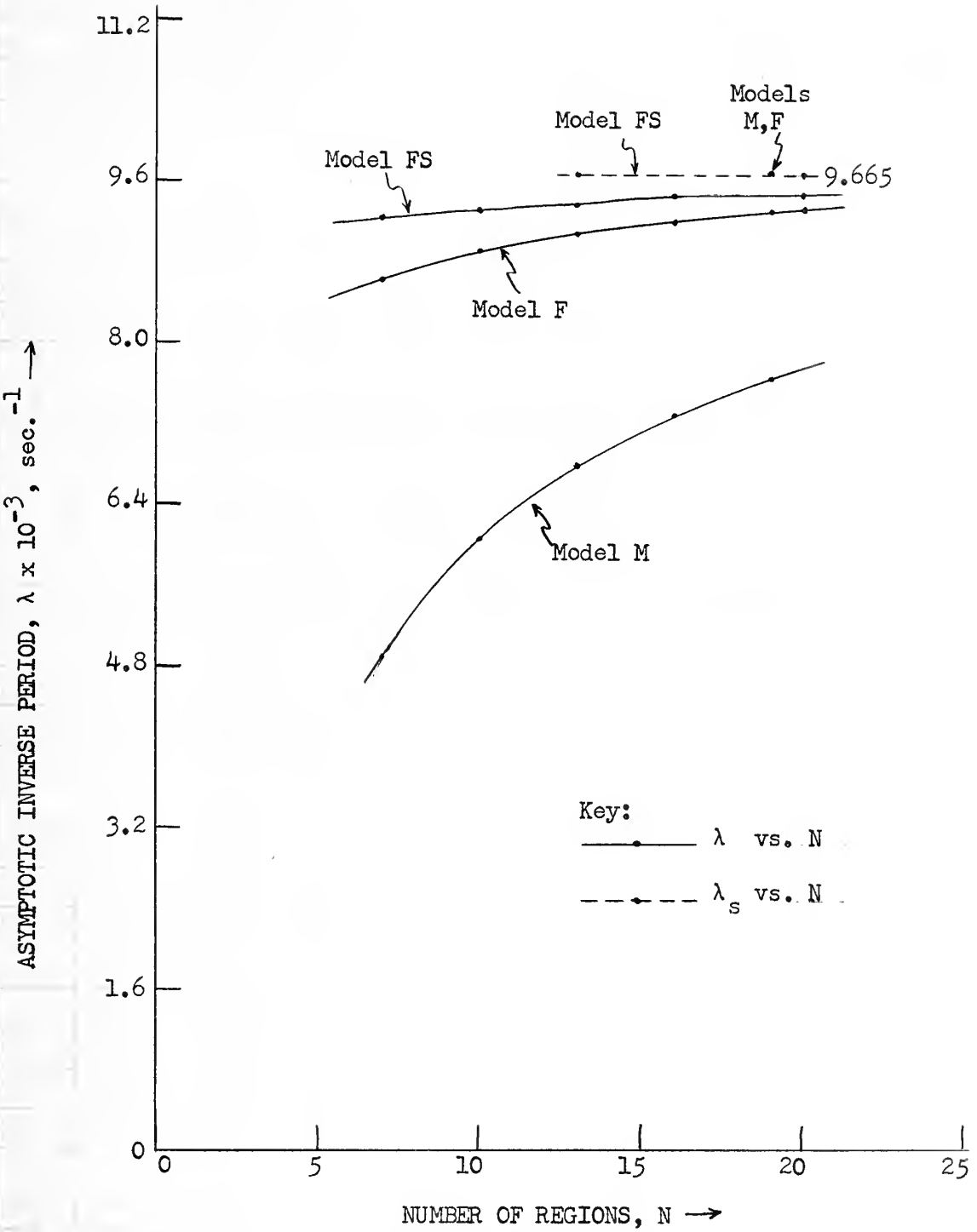

Figure 2E.3 Asymptotic Inverse Period vs. N for 100 cm. Homogeneous System. Models M, F and FS.

First, the results obtained with Model M are particularly poor due to the large region widths. From Table 2B.1, the errors in the Model M delay-times grow rapidly with P(I) and P(J).

Second, the computed distribution shapes are quite consistent. Shape analyses on the Model FS results for both N=13 and N=20 yielded $\lambda_s = 9665 \text{ sec}^{-1}$. Based on this, we conclude that the asymptotic solution is very closely approximated by

$$b(x,t) = A \cos(.03028[x - 50])e^{9665t} .$$

Third, the error of the Model FS results, as well as that of the other models, is much larger for the 100 cm system than for the 10 cm system. This is due to the greater effect in the larger system with $P(J) \geq 2.5$, of the neglect of curvature and growth rate in the expressions for the transfer parameters. Although the inverse period is less than half that of the 10 cm reactor, the growth rate effect is more important here because the ratio R_2 of Subsection 2E.1 is much larger ($R_2 = 1.053357$ for the 20-region Model FS run), the number of time steps required for a particle to cross one region is somewhat greater, and the relative importance of the slope correction increases with P(J). In the summary of this chapter, we suggest a simple modification of Model FS to account for the growth rate in region J.

Fourth, the accuracy of the 10-region Model FS result is equivalent to the accuracy of the 20-region Model F result. The advantage of Model FS is greater here than for the 10 cm system of the previous subsection.

2E.7 Inhomogeneous System

The systems studied thus far have been homogeneous. In this subsection we report the asymptotic solutions obtained for an inhomogeneous system with W = 10 cm and v = 2×10^5 cm/sec. The collision cross section is 0.5 cm^{-1} over the entire system. In the interval $0 < x < 5$ cm, c = 1.4; in the interval $5 < x < 10$ cm, c = 0.9.

Runs were made using Model FS with 10 and 20 regions. From the 10-region run we obtained $\lambda = 506$ sec^{-1}; from the 20-region run, $\lambda = 533$ sec^{-1}. The normalized asymptotic flux and birth rate distributions are plotted in Fig. 2E.4 . The curves are drawn through the N = 20 data. The discontinuity of the birth rate density is a consequence of the discontinuity of c. The apparent continuity of the flux derivative at the interface is a consequence of the homogeneity of the collision cross section. The closeness of the two solutions is consistent with the results obtained for the homogeneous systems and indicates a high degree of accuracy for the N = 20 solution.

Summary

From the results presented in this section, it is clear that Model FS is preferable for problems in which the flux varies smoothly with x and t. In those cases where model comparisons have been made, Model FS has yielded more accurate solutions for less computing time. As regards the other models, we have already discarded Models I and D. Based on the Model M results for the 100 cm system, the applicability of Model M is restricted to systems with small P(J), say $P(J) < 0.5$.

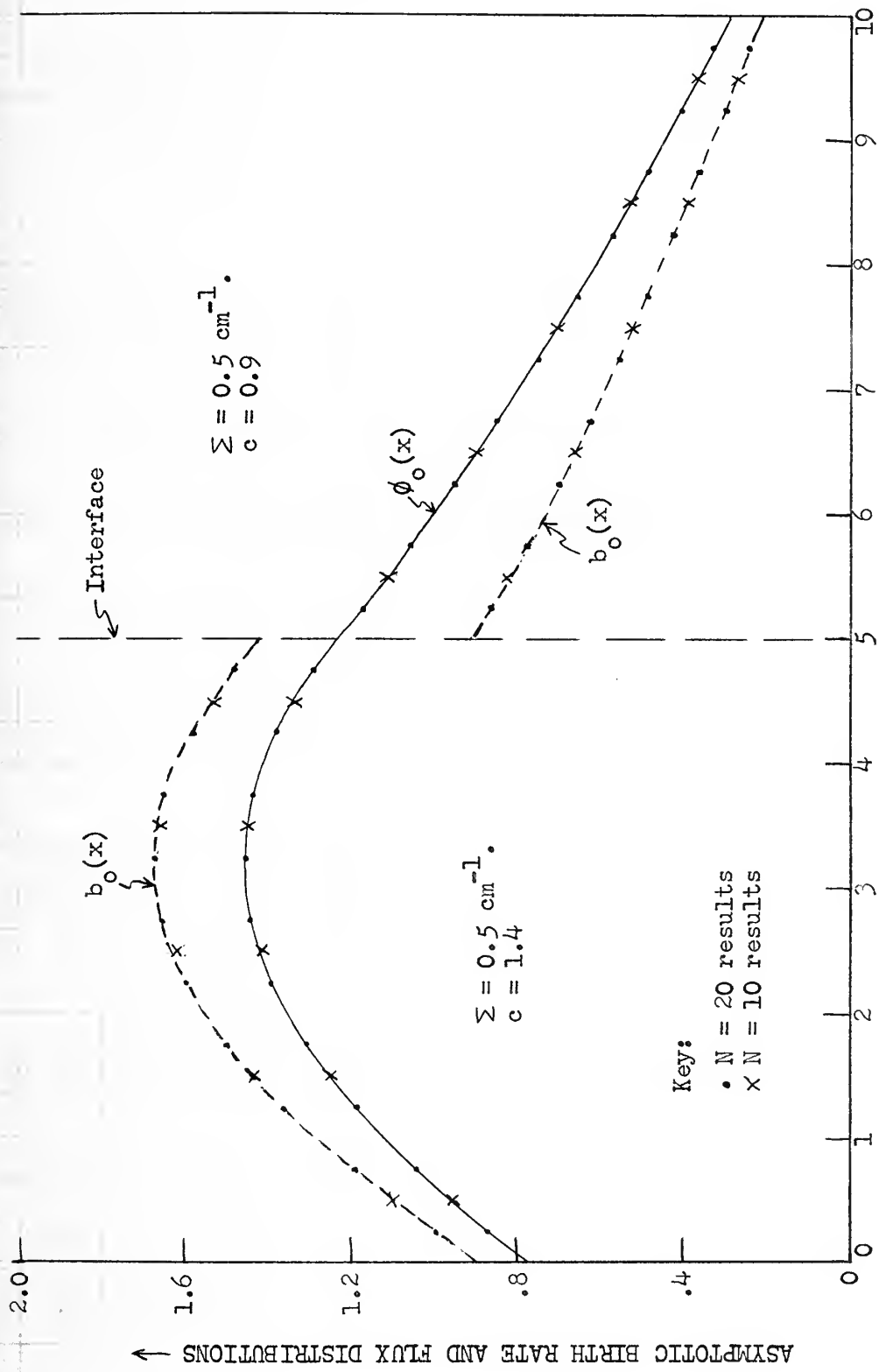

Figure 2E.4 Asymptotic Distributions for 10 cm. Inhomogeneous System.

2F. TEST OF TRANSIENT RESPONSES TO LOCALIZED INITIAL SOURCES

In the previous section we tested the finite-integral models on the simplest, least demanding class of time-dependent problems--the generation of asymptotic solutions. In this section we study a more interesting class of solutions--the space-time transient responses to short-lived external sources localized to a small section of the system.

The transient responses are generated by reading an external source distribution and its duration in seconds, or number of time steps, into the computer and setting the initial memory distribution equal to zero. The birth rate distribution is then computed for a specified number of time steps.

2F.1 Restrictions on External Source Localization in Space and Time

Figure 2F.1 shows the computed variation of the birth rate with time in region 6 of the 10 region, 6.375 cm system treated in Subsection 2E.2.2. Model M was used for these computations.* For each run a unit external source rate was placed in region 3.

The dashed-line curve shows the predicted response for the case in which the unit source rate persisted for only one time step, .797 μ-sec. The oscillations are a consequence of our attempt to treat a source localized to a smaller region of (x,t)-space than is compatible with the approximations inherent in Model M. Referring

---

* Note: Models F and FS have the same basic characteristics as those shown for Model M in this subsection. Because the $\tau(I,J)$ are non-integer, however, numerical oscillations are damped out faster.

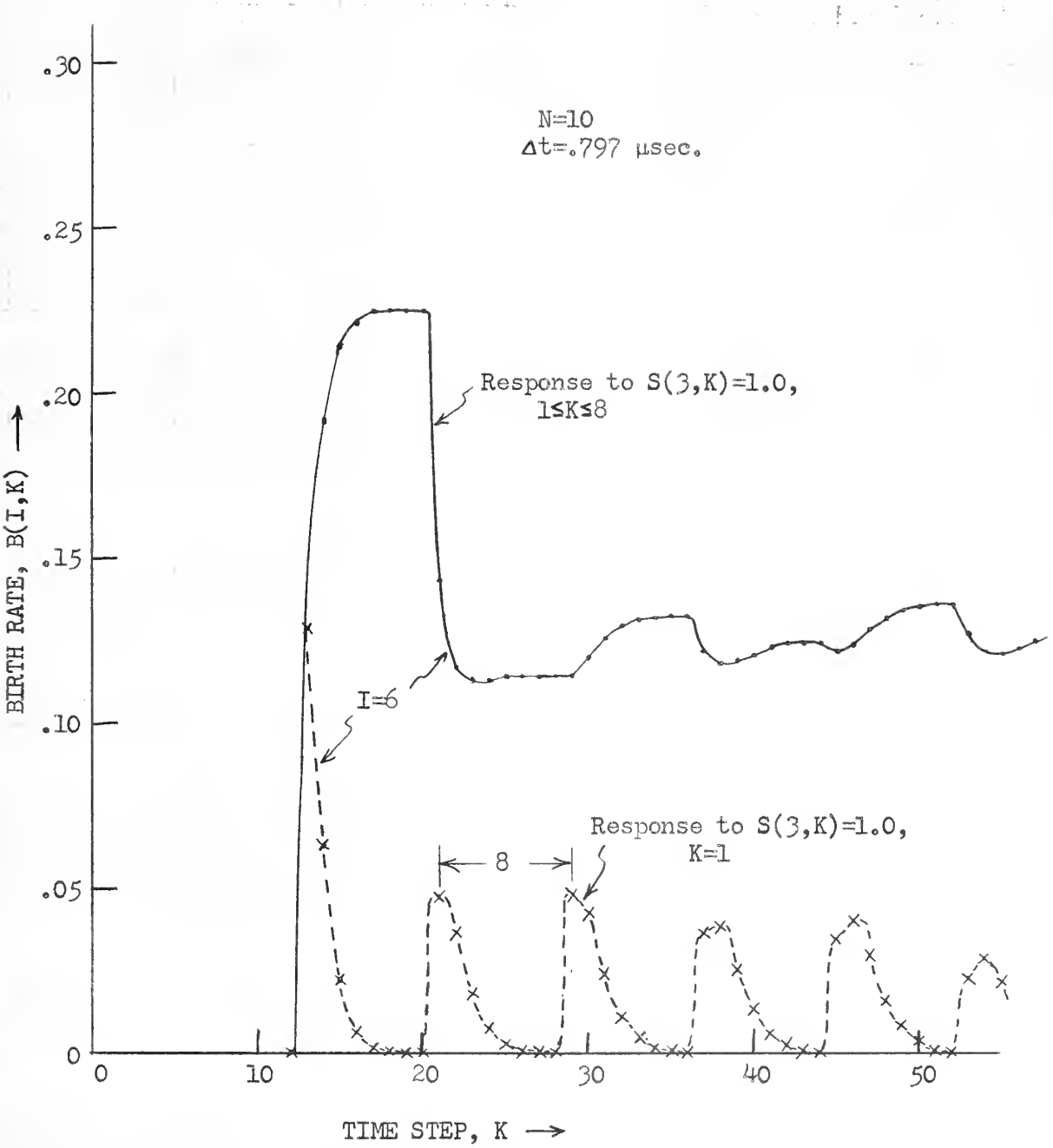

Figure 2F.1 Model M Transient Response to Localized Source in 6.375 cm. System. B(6,K) vs. K.

to Fig. 2A.3 , the birth rate B(I,K) receives contributions from parents which were born in region J over a time interval equal to the time required for a particle to cross two regions. With the discrete-delay-time approximation, we assume that the birth rate in region J during the contributing time interval is nearly constant and is satisfactorily sampled by the birth rate at the discrete time corresponding to $K-\tau_k(I,J)$. Since $\Delta x/v=4\Delta t$ for Model M, Model M treats all external source particles colliding in region 6 as colliding at time step $4(6-3)+1=13$, rather than over the range of time steps extending from 11 to 15 for a discrete source in the center of region 3, or from 9 to 17 for a uniformly distributed source. The birth rates at time steps 14 to 20 are the progeny of the births at time step 13 resulting from successive collisions within region 6. Note that the peak-to-peak separation is eight time steps. The peak at time step 21 consists of second and higher generation births due both to collisions of first-generation parents born in regions 2 and 7 and to higher-generation parents born in regions 3 to 5, the latter characterized by reversals of direction in adjacent regions of two successive generations, for example, $3 \rightarrow 5 \rightarrow 6 \rightarrow 5 \rightarrow 6$. The third peak includes contributions from first generation births in regions 1 and 8. The fourth peak includes contributions from first generation births in region 9; the decrease in magnitude is due to the leakage from the system of those external source neutrons emitted toward the left, prior to time step $37-\tau_k(6,1) = 17$. Similarly,

the decrease in magnitude of the sixth peak, as compared with the fifth peak, is due to the leakage of external source neutrons out of the right side of the system.

Understanding the limitations imposed by the discrete-delay-time approximation, we can generate physically meaningful solutions. The solid curve in Fig. 2F.1 shows the response for a run in which the external source was maintained for eight time steps. The major peak and the decreases at time steps 37 and 51 are physically meaningful for the reasons stated above. The dips in the response near time steps 29 and 47 are non-physical, later generation consequences of "chopping off the edges" of the major peaks in the various regions by starting their buildup too late and stopping it too early. Note that the solution for the problem with the eight time-step source duration could also be obtained by superimposing the dashed-line curve with seven others just like it, but successively displaced one time step to the right.

It is obvious that additional numerical oscillations would be superimposed on the solid curve of Fig. 2F.1 if the external source rate were maintained for nine or ten time steps. Such numerical oscillations are characteristic of all line models for systems having regions small enough that the great majority of particles born in a region escape from the region. For an external source localized to one region or spread out over several adjacent regions, we have found that numerical oscillations are minimized when the following two relations are satisfied:

$$\frac{\left[\begin{array}{c}\text{Source duration,}\\ \text{number of time steps}\end{array}\right]\left[\begin{array}{c}\text{Source width,}\\ \text{number of regions}\end{array}\right]}{2\left[\frac{\Delta x}{v\Delta t}\right]} \approx \text{Integer;} \qquad \text{(2F.1a)}$$

$$\left[\begin{array}{c}\text{Source duration,}\\ \text{number of time steps}\end{array}\right] \geq \frac{\Delta x}{v\Delta t} \ . \qquad \text{(2F.1b)}$$

2F.2 Transient Response in Small System

In this subsection we report the transient responses computed with Models F and FS for the 6.375 cm homogeneous system of Subsection 2E.2. The system is subdivided into 20 regions. An external source is maintained in regions 5 and 6 for three time steps. Since $\Delta x/[v\Delta t]=3.08$, the external source localization in (x,t)-space is nearly compatible with the relations (2F.1).

Figure 2F.2 shows the time dependence of the progeny birth rates $B^{o}(I,K)$ for regions 2, 6, 12 and 18. The points marked by dots represent the Model F results; the points marked by "x" give the Model FS results. Only a representative few of the Model FS data are plotted since their differences from the Model F results are negligible; both models treat the external source rate as part of the flat mode and the ratio $|G_{slp}(I,J)|/G(I,J)$ is very small for P(J) = .1594. Note that numerical oscillations are relatively small.

The major peaks include all first-generation progeny of the external source particles. Upon emission, half of the source particles travel to the left and half to the right. The two groups of directed particles, or waves, separate and move across the system in opposite directions at speed v. The major peaks show this motion and the

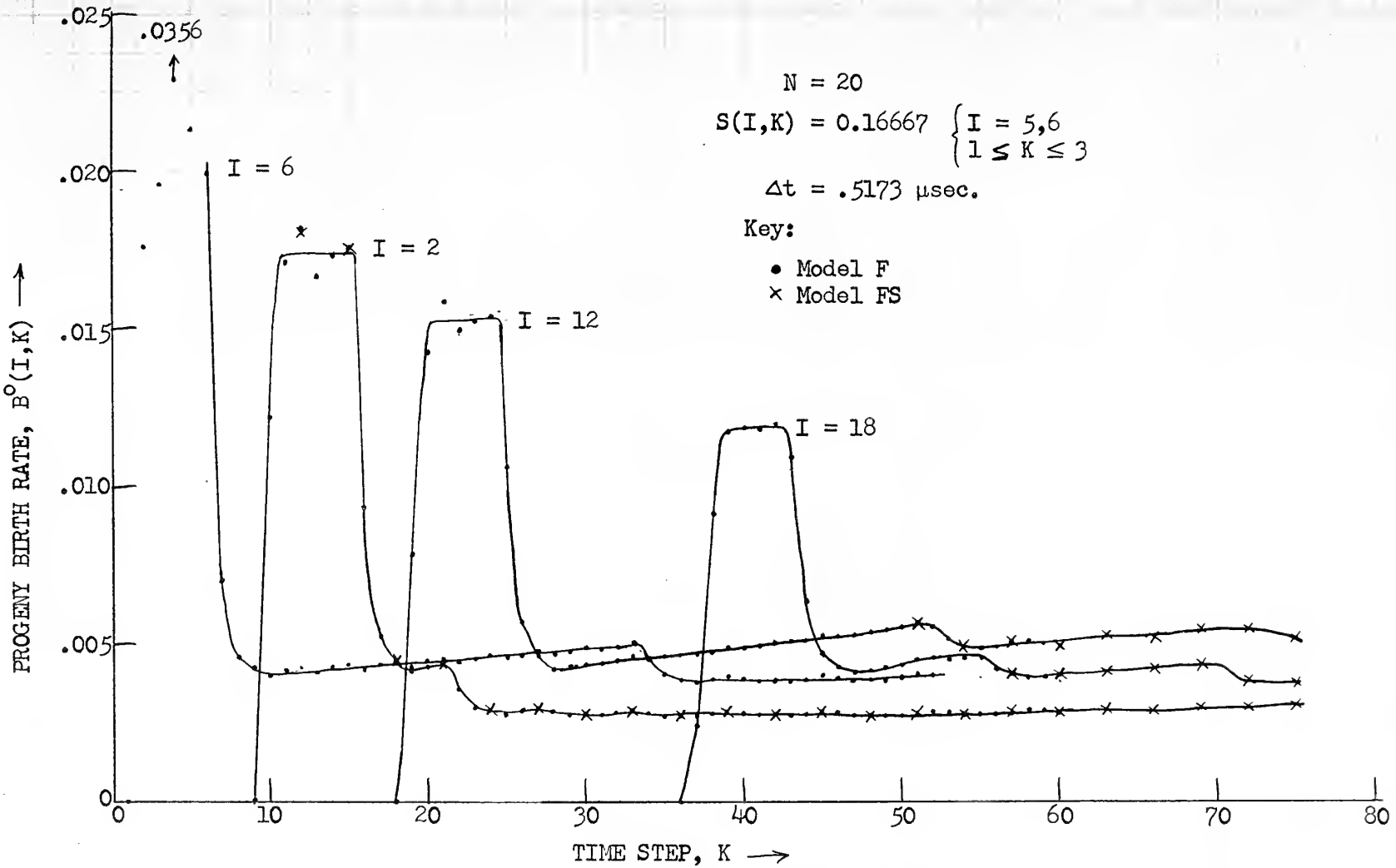

Figure 2F.2 Transient Response to Localized Source in 6.375 cm. System Computed with Models F and FS. $B^{\circ}(I,K)$ vs. K for Regions 2, 6, 12, 18.

attenuation of the waves with time and distance. The attenuation occurs because $c = 1.4 < 2$; for n collisions of particles in the wave, only 0.7n particles are emitted in the direction of the wave motion. Neglecting the ~~undetstood~~ understood numerical fluctuations, note that after the source wave has passed a given region I, the birth rate varies smoothly for a time and then decreases rapidly for a few time steps. The dip in the curve is the reflected result of the leakage of one of the two source waves from the finite system. The change is fairly large and sudden because the contribution to the flux in region I of particles born earlier due to collisions of parent particles belonging to the source wave is lost as the wave leaves the system.

For computing the response to a localized external source in a small system such as this, a large value of N is desirable to show the detail of the response and to minimize numerical oscillations by satisfying Eq. (2F.1a) with the largest possible integer. Comparing Models F and FS, Model F is preferable since the Model F solution is almost identical to the Model FS solution and computing time and storage requirements are less for Model F. Comparing Models F and M, Model F will yield better solutions because the non-integer $\tau_k(I,J)$ will serve to damped out numerical oscillations caused by discontinuities or steep ramps in the τ-dependence of $B(J,t-\tau)$. Since Model M is more than twice as fast as Model F, however, the question of which model is better for a particular problem is left unresolved.

In the next subsection, we study a large system in which the source is spread out over several mean free paths and has a much longer duration than the source in the 6.375 cm system.

2F.3 Transient Response in Large, Supercritical System

In this subsection we treat a 100 cm homogeneous system with $\Sigma = 0.5\ cm^{-1}$, $c = 1.05$ and $v = 2 \times 10^5$ cm/sec. Models F and FS were used to compute the transient response to an external source located in the interval $10 < x < 20$ cm and lasting for 32.97 microseconds. Runs were made for N=20 and N=30.

For the runs with N=20, the source was located in regions 3 and 4 and lasted for six time steps, $6\Delta t$, where $\Delta t = 5.49577 \mu sec$. The birth rates were computed for 100 time steps.

The runs with N=30 were made in order to test the convergence with N of the transient responses computed with each model. The source is located in regions 4, 5 and 6, which cover the same portion of the system as regions 3 and 4 in the twenty-region problem. The unit time step, Δt, was arbitrarily set equal to $3.66345 \mu sec$, which is two-thirds that of the 20-region runs and is less than the $\tau(I,I)$. Therefore, the external source lasted for nine time steps and the birth rates were computed for 150 time steps.

For the appropriate values of I and K, the external source rate S(I,K) was set equal to unity for both the 20- and 30-region problems; it is here interpreted as the mean source rate density, $cm^{-1}sec^{-1}$, in region I at time step K. Since the computed values of $B^{\circ}(I,K)$ or B(I,K) must be assigned the same units as S(I,K), the transient results printed out for the 20- and 30-region runs may be compared directly.

The solid curves in Fig. 2F.3 show the 30-region, Model FS birth rate distributions at time steps 15, 45, 90 and 150. It is obvious that the system is very supercritical. Note the gradual shift of the peak birth rate density towards the right. Compared with the transient responses reported for small systems in the previous subsection, the lack of a source wave separation may be somewhat startling at first. The reason for it is that the source in the 100 cm system is spread out over five mean free paths while that in the 6.375 cm system is localized to a region only 0.319 mean free path wide. The great majority of external source particles in the large system collide in the regions containing the source, as do their progeny. Furthermore, the source duration in the 100 cm system is 21.2 times longer than that in the system of the preceding subsection.

The dashed-line curve in Fig. 2F.3 shows the birth rate distribution at time step 150 which was generated by the 30-region, Model F run. Note that the propagation rate is greater, the distribution is flatter, and the total population is smaller than predicted by Model FS. All of these effects are consequences of the excessive leakage away from the peak of the distribution, an error which is characteristic of the flat approximation.

The points circumscribed by circles are the 20-region, Model FS results. The points surrounded by squares are the 20-region, Model F results. Each set of data is for time step 100 of the 20-region problem, which corresponds to time step 150 of the 30-region problem. Note that the degree of convergence of the Model F results is poor but that the direction of convergence is towards the Model FS results.

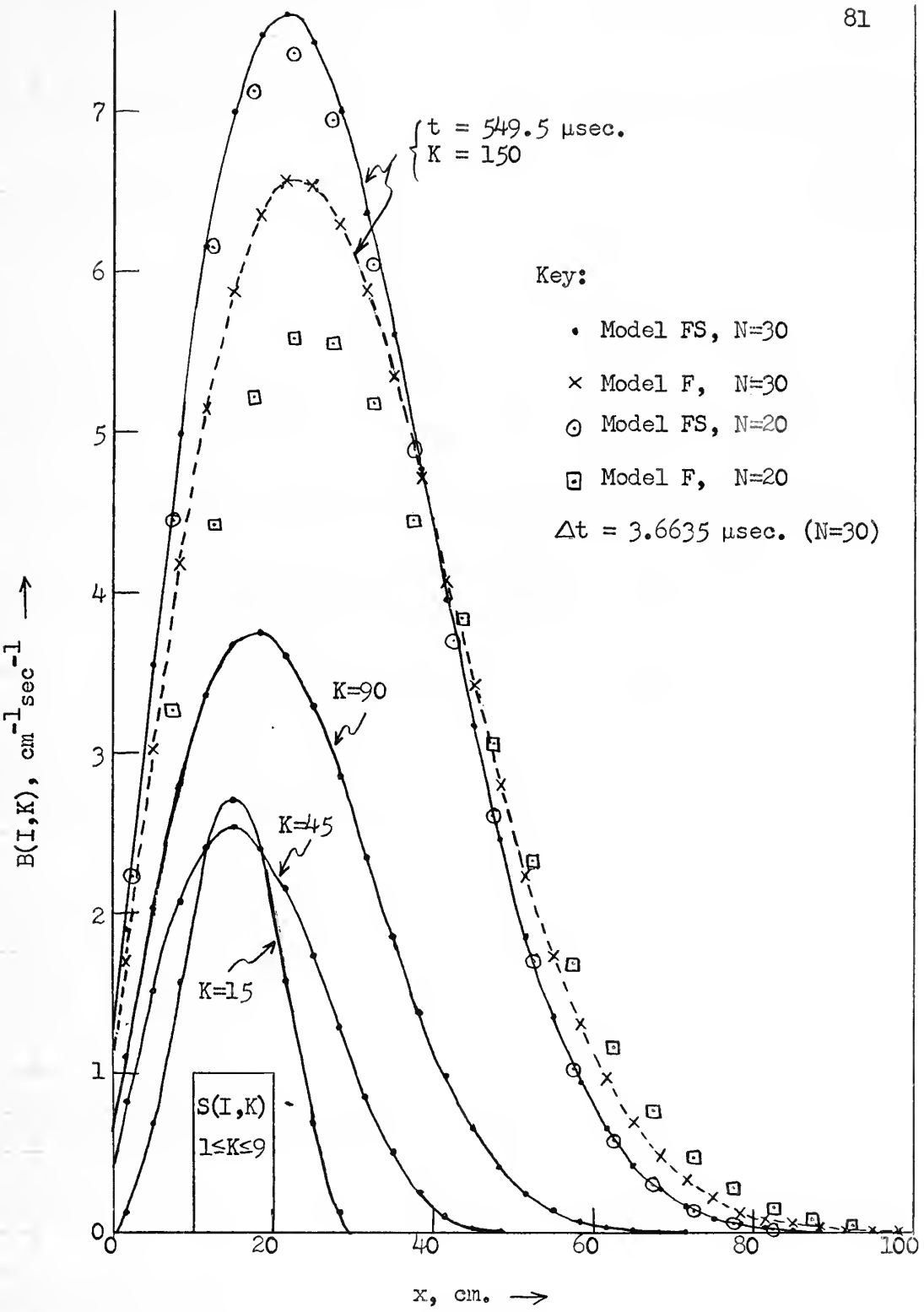

Figure 2F.3 Response to Localized Source in 100 cm. Reactor. B(I,K) vs. I for K = 15, 45, 90, 150 for 30-Region Model FS Run. Comparison of Birth Rate Distributions at t = 549.5 μsec Computed with Models F and FS, N = 20 and 30.

The convergence of the Model FS results is rather good, indicating that the Model FS curves closely approximate the correct solution. An important conclusion supported by the data is that the errors of the 30-region, Model F results are several times greater than those of the 20-region, Model FS results. Furthermore, the 20-region run was completed in less than two-thirds of the computing time required for the thirty-region run.

The direction of convergence of the Model FS results makes sense. First of all, the slightly greater population in the 30-region problem is consistent with the increasing λ vs N convergence curves reported for supercritical systems in Section 2E. Second, note that the greatest errors occur near the peak of the curve where the shape is convex. A curvature correction would reduce the leakage out of those sub-regions where the curvature is convex, thereby increasing the magnitude of the peak.

Figure 2F.4 shows the birth rate distribution shapes assumed by Models F and FS at time steps 10 and 150 for the purpose of computing the transfers $(J,10)\rightarrow(I,10+\tau_k(I,J))$ and $(J,150)\rightarrow(I,150+\tau_k(I,J))$. The superiority of the Model FS fit is obvious. Note that the slope-correction modes are dynamic modes in that their shapes vary with time to match the changing population distribution.

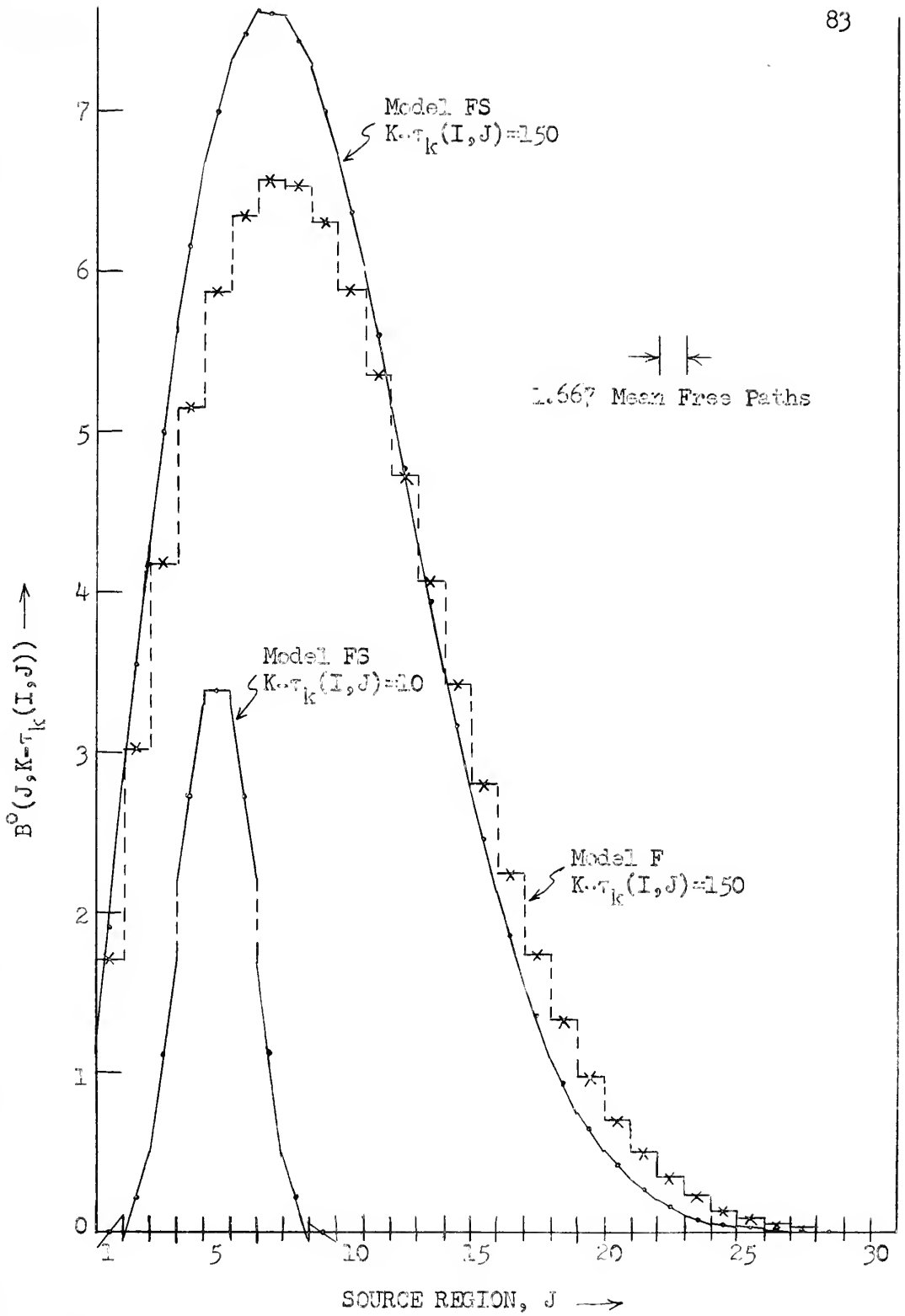

Figure 2F.4 Transient Response in 100 cm. System. Distributions Assumed in Source Regions J by Models F and FS for Source Time-steps 10 and 150.

2G. COMPUTATION OF AN IMPORTANCE DISTRIBUTION

The capability of our numerical models to handle external sources localized in space and time permits the "brute-force" computation of importance distributions for systems of the type studied in Section 2E. For these systems, the asymptotic flux distribution, the asymptotic adjoint flux distribution and the x-dependence of the importance of an isotropic external source are identical. Thus we have another method to test the validity of our numerical models; the computed importance distribution should agree with the computed asymptotic flux distribution.

In this section, we describe the method and report the results obtained with Model FS for the 6.375 cm homogeneous system of Subsection 2E.2. The system was subdivided into 13 regions. Seven transients were computed, each of which is the system response to a unit external source in a different region L, where L ranges from 1 to 7. In each run, the source in region L was set to last for 10 time steps and the transient was computed for 300 time steps. By time step 300, the higher natural modes in the response had substantially decayed, leaving only the slowly growing asymptotic distribution. The total birth rate in the system at time step 300,

$$\sum_{I=1}^{N} B(I,300),$$

is a measure of the importance of the external source that was located in region L. Since Model FS treats S(L) as uniformly

distributed over region L, the sum is proportional to the mean importance in region L. By computing the sum of the B(I,300) for each of the seven runs and by taking advantage of symmetry, we obtained the relative importance distribution for the system. The normalized importance distribution, $\phi_o^+(I)$, is compared with the asymptotic flux distribution, $\phi_o(I)$, in Table 2G.1. The agreement is excellent.

Table 2G.1

Comparison of Computed Importance and Flux Distribution in 6.375 cm System

Region, I	Asymptotic Flux, $\phi_o(I)$	Importance, $\phi_o^+(I)$
1,13	.7117	.7114
2	.8505	.8505
3	.9689	.9688
4	1.0640	1.0642
5	1.1336	1.1336
6,8	1.1761	1.1763
7	1.1904	1.1903

2H. COMPUTED RESPONSE TO AN EXTERNAL SOURCE VARYING SINUSOIDALLY WITH TIME

Systems with time-varying sources or secondary emission coefficients are easily handled with the finite-integral method. Example problems are now discussed.

A Model F run was made for the twenty-region, 6.375 cm homogeneous system with a sinusoidally-varying source in region 3:

$$S(3,K) = \sin \frac{\pi(K-1)}{12} \quad . \qquad (2H.1)$$

The source period is 24 time steps or 12.415 microseconds. The program was run for 400 time steps.

For this run, a special version of subroutine SOURCE was needed to control the time dependence of S(3). By setting the OVRR4 control variable NSRC equal to 4, subroutine SOURCE is called at each time step and the source distribution is altered according to Eq. (2H.1).

The birth rates in regions 5 and 18 are plotted versus time step in Fig. (2H.1). The response settles out after a few periods, with peaks separated by 24 time steps. Note that the mean birth rate is greater than zero, due to having started with a positive source contribution. The response in region 5 lags the source in region 3 by 6.8 time steps and the response in region 18 lags the source by 47.5 time steps. The corresponding flight times from the center of region 3 to the centers of regions 5 and 18 are 6.162 and 46.215 time steps, respectively. Note the attenuation in the peak-to-peak amplitude with increasing distance from the source. This effect is also evident in Table 2H.2, which gives the regional birth rates at time step 385, at which time the external source rate is zero. The spatial oscillations reflect the fact that the period of the source is less than the time required to cross the system.

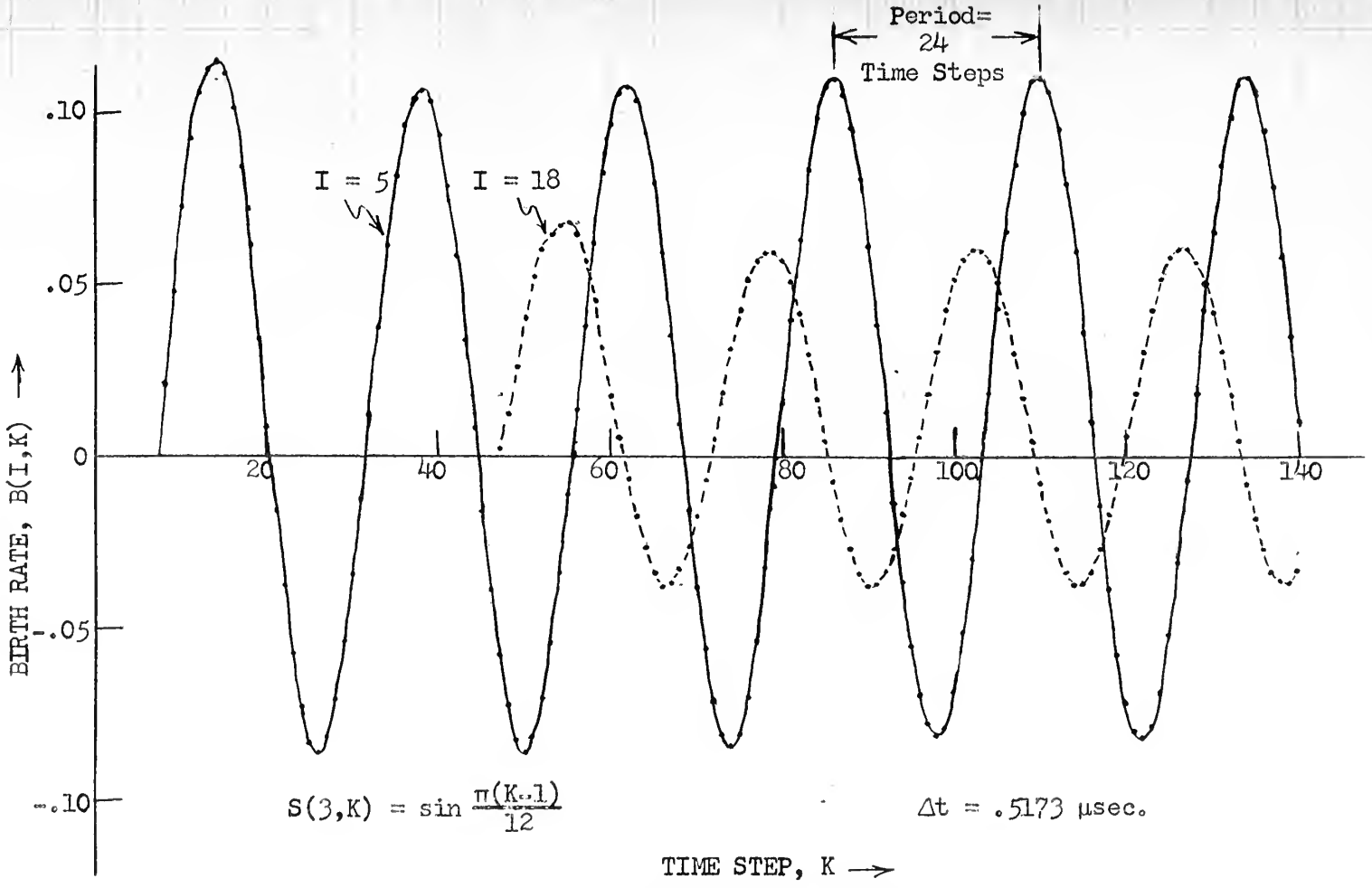

Figure 2H.1 Response to Sinusoidally-varying Source in Region 3 of 20-Region, 6.375 cm. System. B(I,K) vs. K for Regions 5 and 18.

Table 2H.1

Response to Sinusoidally-Varying Source:
B(I,385)

Region, I	B(I,385)	Region, I	B(I,385)
1	-.0952	11	-.0142
2	-.0834	12	-.0498
3	-.0380	13	-.0427
4	-.0734	14	-.0011
5	-.0802	15	.0467
6	-.0300	16	.0707
7	.0424	17	.0580
8	.0917	18	.0190
9	.0908	19	-.0212
10	.0449	20	-.0388

2I. COMPUTED RESPONSE TO A TIME-DEPENDENT SECONDARY EMISSION COEFFICIENT

For this problem we start with the 20-region, 6.375 cm homogeneous system having $\Sigma = 0.5$ cm^{-1} and $c = 1.4$. By setting the OVRR4 control variable NMEM equal to 3, the known asymptotic distribution and inverse period (see Table 2E.1) are read in by the program; the program then fills the storage locations reserved for the initial memory with the asymptotic solution. At time step 1, the secondary emission coefficient c is set equal to 2.0 in regions 1 through 6; at each subsequent time step it is reduced by 0.012 until the value reaches 0.812 at time step 100. At time step 101, the secondary emission coefficient in regions 1 through 6 is restored to its

original value of 1.4 and is not changed thereafter. The program is run for 150 time steps. Model F was used for the computations.

This problem illustrates the use of the subroutine TDEP. A special, but very simple, version was written in order to control the time variation of c(I). By setting the OVRR4 control variable KTDEP equal to 2, subroutine TDEP is called from subroutine CALC4 at each time step.

Figure 2I.1 shows the time response of the flux in regions 3, 8 and 15. Recalling that the original system is nearly critical, note the delays in the propagation to regions 8 and 15 of the effects of the discontinuous increase in c at time step 1. Similar delays are evident in the propagation of the effects of the discontinuous increase at time step 101. Slight numerical oscillations result from the large discontinuous changes in c. These appear to have a period of approximately three time steps; 3.08 time steps are required for a particle to cross one subregion.

Figure 2I.2 shows the asymptotic birth rate distribution at time step 0 and the subsequent distributions at time steps 24, 75 and 120. The discontinuities at time steps 24 and 75 are due to the spatial discontinuity of c. The K=24 birth rates in regions 14 through 20 are less than .0002 greater than those at K = 0, illustrating again the propagation delay. Similarly, the dip in the distribution at region 13 of the K=120 curve is due to the fact that additional particles born in region 6 at time step 101 have not yet reached region 13.

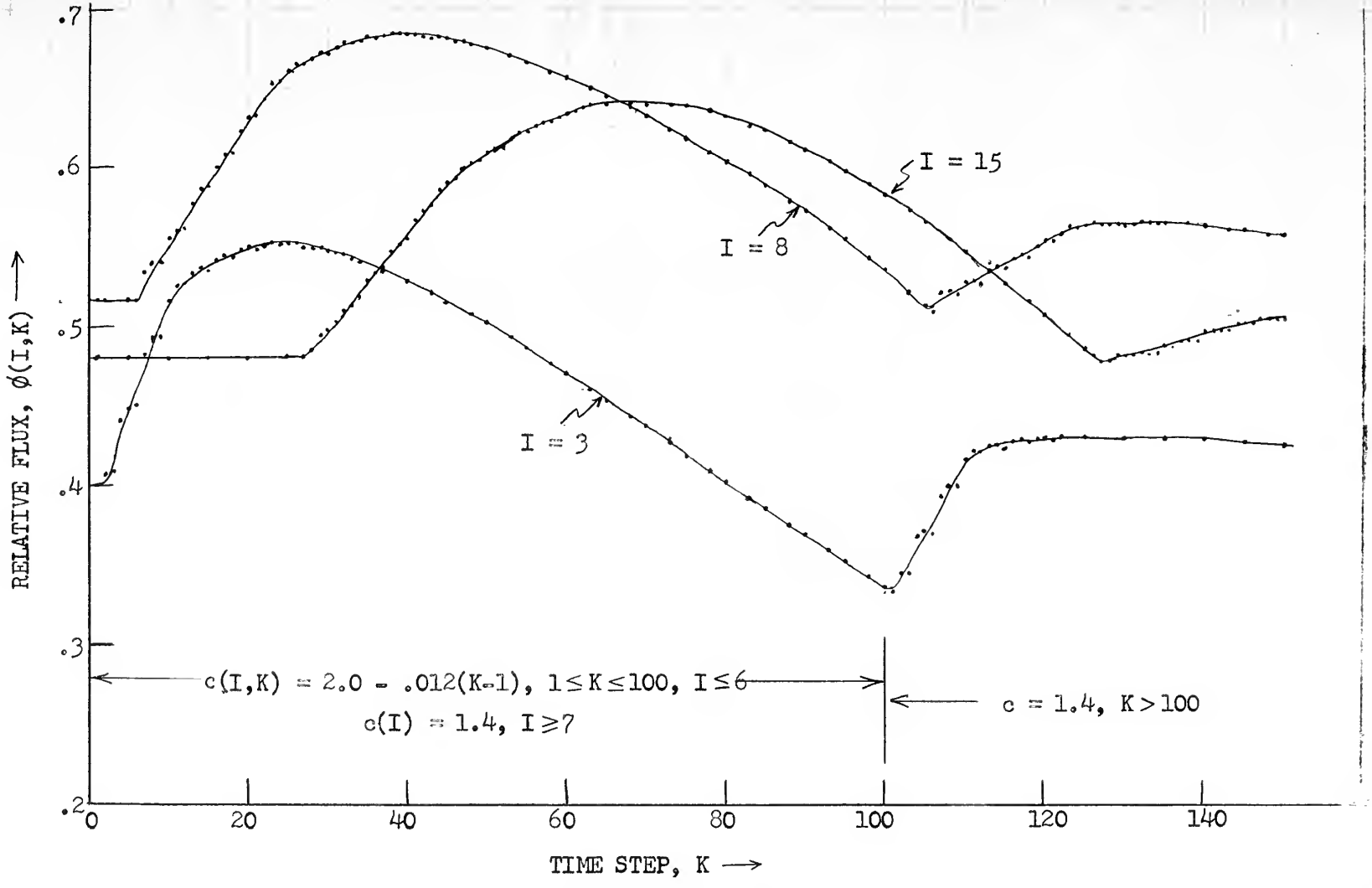

Figure 2I.1 Transient Response to Linear Reduction of c with Time in Regions 1 to 6 of 20-Region 6.375 cm. System. $\phi(I,K)$ vs. K for Regions 3, 8 and 15.

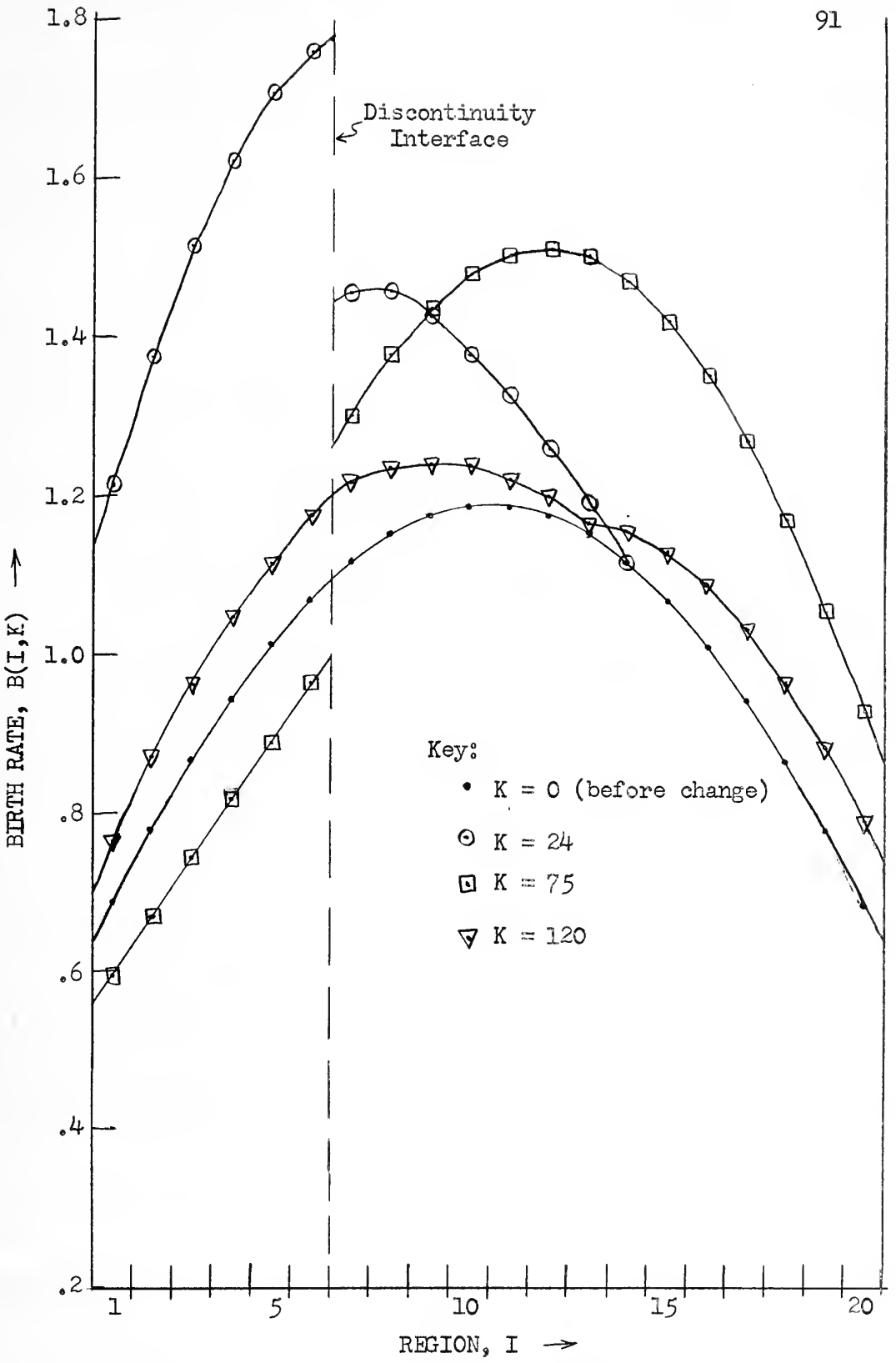

Figure 2I.2 Transient Response to Time-dependent c.
B(I,K) vs. I for Time Steps 0, 24, 75 and 120.

Summary of Chapter 2

The results presented in this chapter clearly demonstrate that that finite-integral approximation is an effective tool for computing time-dependent transport solutions. The discrete-delay-time approximation is seen to be satisfactory for line geometry. All models developed and tested have the desirable computational characteristics of explicitness and convergence.

Due to the small unit time step, the method is best suited for computing fast space-time transients of short duration. Due both to the growth of errors with increasing P(I) and to limitations imposed on N by limited storage capacity, the method is best suited for treating relatively small systems. Space- and time-dependent external sources and secondary emission coefficients are easily handled with the finite integral approximation.

Detailed comparisons of the various models were made at appropriate points in the chapter. To summarize, the unit computing time per [(J→I)] transfer computation is .0002 sec for Model M, .0005 sec for Model F and .0009 sec for Model FS. The usefulness of the fixed distribution models is limited to relatively small systems with optically-thin regions [$P(I) < 0.5$]. Where a large N is desirable for a detailed solution, such as the fast transient computed for the small 6.375 cm system in Subsection 2F.2, the fixed-distribution models are sufficiently accurate and have an advantage over Model FS with respect to both storage requirements and computing time. For problems in

which there is no compelling reason for limiting the region size, however, we have found Model FS to be more efficient in all cases studied.

Concerning the further improvement of the numerical models, the addition of a slope correction to account for the growth rate in source region J would be helpful. One simple way to incorporate this correction into Model FS is to use the progeny birth rates $B^{o}(J+1,\ K-\tau_k(I,J+1))$ and $B^{o}(J-1,K-\tau_k(I,J-1))$ in lieu of $B^{o}(J+1,K-\tau_k(I,J))$ and $B^{o}(J-1,K-\tau_k(I,J))$ in Eqs. (2C.5,7) for computing $C_1(J,K-\tau_k(I,J))$. The value of adding a curvature correction mode will be investigated for slab geometry in the next two chapters.

Understanding the physical significance of the approximations involved in the various models, one can readily see that the models developed have analogues for multi-dimensional geometries and even for treating energy dependence. These analogues will be discussed in Chapter 5.

CHAPTER 3

THE TIME-DEPENDENT, MONOENERGETIC SLAB REACTOR

Introduction to Chapter 3

In this chapter we develop, test and evaluate numerical models for Eq. (1A.1), the integral-transport equations for slab geometry. The basic methodology illustrated in Chapter 2 is adapted to accomplish these purposes. The integral equation for the progeny birth rate, $B^{o}(I,t)$, is derived from Eq. (1A.1) in Section 3A.

Three numerical models for solving the integral transport equation, Models F, FS and FSC, are developed in Section 3B. Models F and FS are extensions of the analogous models developed for line geometry. A curvature-correction is included in Model FSC. The final expressions for the transfer parameters are linear combinations of exponential integral functions. The procedure used to compute numbers from these expressions is described in Section 3C. Some features of the applicable computer program, TOVSR, are discussed briefly in Section 3D.

Asymptotic solutions computed with the numerical models are studied in Section 3E. As demonstrated in Chapter 2, these solutions are useful for isolating and evaluating the various approximations incorporated in the models. The accuracy of the models for nearly-critical systems is established by the asymptotic solutions computed for systems reported to be critical in the literature. The technique of solving auxiliary problems to determine errors in the asymptotic solutions for very supercritical and very subcritical systems is used

to evaluate the discrete-delay-time approximation. In order to test the accuracy of computed distributions, the classical Milne problem for a pure scattering medium is solved; the results are compared with published data in Section 3F. The transient response computed for a system with an initial, localized external source is studied in Section 3G. Finally, importance distributions computed for homogeneous and inhomogeneous systems are reported in Section 3H.

Since the slab regions are unbounded in the (y,z)-plane, the discrete-delay-time approximation is found to be inadequate for treating systems with rapidly growing or decaying populations. In Section 5J, we formulate a multiple-delay-time model by subdividing angular space into N_μ angular intervals; this model is characterized by improved sampling of the time-dependence of the birth rate in source region J.

3A. THE INTEGRAL EQUATION FOR THE PROGENY BIRTH RATE, $B^o(I)$

As with Model FS for the line reactor, the progeny birth rate, $B^o(I,t)$, is used as the fundamental dependent variable in the slab models. This permits discontinuities in the external source distribution at interfaces between regions, while retaining the capability to superimpose flat, slope-correction, and curvature-correction modes to approximate the spatial distribution of the progeny birth rate in source region J.

To obtain the integral equation for $B^o(I,t)$, we first substitute

$$b(x,t) = b^o(x,t) + s(x,t) \qquad (3A.1)$$

into Eq. (1A.1) and subtract s(x,t) from each side. Then following the procedure of Section 1B, we obtain:

$$B^{o}(I,t) = c(I,t) \sum_{J=1}^{N} \left\{ \frac{1}{2} \int_{o}^{1} d\mu \int_{(\Delta x)_I} dx \Sigma(I) \cdot \right.$$

$$\left. \cdot \int_{(\Delta x)_J} \frac{dx'}{\mu} \, b(x', t - \frac{|x-x^{o}|}{\mu v}) \cdot \exp\left(- \frac{[x-x^{o}]}{|x-x^{o}|} \int_{x^{o}}^{x} \frac{dx''}{\mu} \Sigma(x'') \right) \right\} . \qquad (3A.2)$$

3B. FORMULATION OF THE NUMERICAL MODELS

3B.1 The Discrete-Delay-Time Approximation

For the discrete-delay-time approximation, we make the following substitution in the integrand of Eq. (3A.2):

$$b(x^{o}, t - \frac{|x-x^{o}|}{\mu v}) = b(x^{o}, t - \tau(I,J)) \quad . \qquad (3B.1)$$

As for Models F and FS for line geometry, $\tau(I,J)$ is the mean delay time between birth and collision of neutrons from a uniformly-distributed source in region J that collide in region I.

Because the regions are unbounded and the transfer parameters account for neutrons emitted at all μ in the interval $0 < \mu \leq 1$, the errors introduced with these approximations are greater than for line geometry. Referring to Fig. 2A.3 , the hatched area in the figure applies only for neutrons emitted at $\mu = 1$; in an analogous diagram for slab geometry, the hatched area would extend back to

$-\infty$ along the time ordinate. Slab geometry thus offers an extreme test for the discrete-delay-time approximation.

3B.2 Approximation of the Birth Rate Distribution in Region J

Here we derive expressions for the terms in the three-mode approximation for $b(x',t-\tau(I,J))$, Eq. (1B.1). An external source in region J is assumed to be distributed uniformly over region J; i.e.,

$$s(x',t-\tau) = \frac{S(J,t-\tau)}{\Delta x} \quad , \qquad (3B.2)$$

where τ is understood to mean $\tau(I,J)$. The x'-dependence of the progeny birth rate density, $b^{o}(x',t-\tau)$, in source region J is approximated by superimposing flat, slope-correction and curvature-correction modes. In deriving the three-mode expression for $b^{o}(x',t-\tau)$, we require that the properties c and Σ be homogeneous across three successive regions which include region J. The progeny birth rate density is then continuous across the three regions and is, in most cases, a smoothly-varying function. In contrast with Model FS for line geometry, production cross-sections are not needed in the expression for $b^{o}(x,t-\tau)$; computing time is thereby reduced and the secondary emission coefficient is permitted to vary with time.

In the computer program TOVSR, the value of the input variable KTRL(J) is used to identify the relative position of region J with respect to a property-discontinuity interface. KTRL(J) is set equal to 1 if there is a discontinuity at the left boundary of region J; $B^{o}(J,t-\tau)$, $B^{o}(J+1,t-\tau)$ and $B^{o}(J+2,t-\tau)$ are then used to compute the modal coefficients for region J. KTRL(J) is set equal to -1 if there

is a discontinuity at the right boundary of region J; the progeny birth rates in regions J, J-1 and J-2 are then used to compute the modal coefficients. If there are no discontinuities at the boundaries of region J, KTRL(J) is set equal to zero and the progeny birth rates in regions J-1, J and J+1 are used to compute the modal coefficients.

Consider the case for KTRL(J) = 1. We define

$$B^{o}(x',t-\tau) = b^{o}(x',t-\tau)\Delta x, \qquad (3B.3)$$

where $B^{o}(x,t-\tau)$ has the units $[(cm)^{-2}(\Delta x)^{-1}sec^{-1}]$. We next introduce the coordinate variable

$$w = \frac{x' - x_j}{\Delta x}, \qquad (3B.4)$$

which has its origin at x_j, the center of region J. We next assume that the progeny birth rate distribution in regions J, J+1 and J+2 can be fit by the following quadratic expression:*

$$B^{o}(w,t-\tau) = a_o + a_1 w + a_2 w^2 \quad . \qquad (3B.5)$$

The computed progeny birth rates in regions J, J+1, and J+2 are then given by

$$B^{o}(J,t-\tau) = \int_{-1/2}^{1/2} dw[a_o + a_1 w + a_2 w^2] \, , \qquad (3B.6a)$$

---

*Note: After the expressions for a_o, a_1 and a_2 in Eq. (3B.5) have been derived, Eq. (3B.5) is used to describe the birth rate distribution in region J only. $B^{o}(w,t-\tau)$ may then be assumed equal to zero for $|w| > 1/2$.

$$B^{o}(J+1,t-\tau) = \int_{1/2}^{3/2} dw[a_o + a_1 w + a_2 w^2] , \qquad (3B.6b)$$

and

$$B^{o}(J+2,t-\tau) = \int_{3/2}^{5/2} dw[a_o + a_1 w + a_2 w^2] . \qquad (3B.6c)$$

Equations (3B.6) are solved algebraically for a_o, a_1 and a_2 in terms of the three progeny birth rates. Substituting the resulting expressions into Eq. (3B.5) and rearranging some of the terms, we obtain the following expression for the progeny birth rate distribution in region J:

$$B^{o}(w,t-\tau) = B^{o}(J,t-\tau) +$$

$$+ \left[4B^{o}(J+1,t-\tau) - 3B^{o}(J,t-\tau) - B^{o}(J+2,t-\tau)\right] \frac{w}{2} +$$

$$+ \left[\frac{B^{o}(J+2,t-\tau) + B^{o}(J,t-\tau)}{2} - B^{o}(J+1,t-\tau)\right]\left[w^2 - \frac{1}{12}\right] . \qquad (3B.7)$$

Substituting Eqs. (3B.3,4) into Eq. (3B.7), dividing by Δx, adding the source rate density to each side, and applying Eq. (3B.2), we obtain

$$b(x',t-\tau) = b^{o}(x',t-\tau) + S(J,t-\tau)/\Delta x$$

$$= B(J,t-\tau)\left[\frac{1}{\Delta x}\right] + C_1(J,t-\tau)\left[\frac{x'-x_j}{2[\Delta x]^2}\right] +$$

$$+ C_2(J,t-\tau)\left[\frac{[x'-x_j]^2}{[\Delta x]^3} - \frac{1}{12\Delta x}\right], \qquad (3B.8)$$

where the expressions in the three brackets define the unit flat, slope-correction and curvature-correction modes, respectively;* the modal coefficients are given by

$$B(J,t-\tau) = B^{o}(J,t-\tau) + S(J,t-\tau) \ , \qquad (3B.9a)$$

$$C_1(J,t-\tau) = 4B^{o}(J+1,t-\tau) - 3B^{o}(J,t-\tau) - B^{o}(J+2,t-\tau) \ , \qquad (3B.9b)$$

and

$$C_2(J,t-\tau) = \frac{B^{o}(J+2,t-\tau) + B^{o}(J,t-\tau)}{2} - B^{o}(J+1,t-\tau) \ . \qquad (3B.9c)$$

Only the expression (3B.9a) is independent of the value of KTRL(J). For KTRL(J) = -1, we obtain

$$C_1(J,t-\tau) = -4B^{o}(J-1,t-\tau) + 3B^{o}(J,t-\tau) + B^{o}(J-2,t-\tau) \qquad (3B.10a)$$

and

$$C_2(J,t-\tau) = \frac{B^{o}(J-2,t-\tau) + B^{o}(J,t-\tau)}{2} - B^{o}(J-1,t-\tau) \ . \qquad (3B.10b)$$

For KTRL(J) = 0, we obtain

$$C_1(J,t-\tau) = B^{o}(J+1,t-\tau) - B^{o}(J-1,t-\tau) \qquad (3B.11a)$$

and

$$C_2(J,t-\tau) = \frac{B^{o}(J+1,t-\tau) + B^{o}(J-1,t-\tau)}{2} - B^{o}(J,t-\tau) \ . \qquad (3B.11b)$$

Note that C_1 is positive when the birth rate density increases with x and that C_2 is positive when the curvature is concave. The integrals

---

* Note: $u_o(x')$, $u_1(x')$ and $u_2(x')$, respectively, of Eq. (1B.1)

over region J of the unit slope-correction and curvature-correction modes are equal to zero.

3B.3 Derivation of Expressions for the Transfer Parameters

Substituting Eqs. (3B.1) and (3B.8) into Eq. (3A.2), we obtain

$$B^{o}(I,t) = c(I,t) \sum_{J=1}^{N} \Big[G(I,J)B(J,t-\tau(I,J)) +$$

$$+ G_{slp}(I,J)C_1(J,t-\tau(I,J)) + G_{crv}(I,J)C_2(J,t-\tau(I,J)) \Big] ; \qquad (3B.12)$$

The expressions for the transfer coefficients are given by

$$\begin{Bmatrix} G(I,J) \\ G_{slp}(I,J) \\ G_{crv}(I,J) \end{Bmatrix} = \frac{1}{2} \int_{o}^{1} d\mu \int_{(\Delta x)_I} \frac{dx \Sigma(I)}{\mu} \int_{(\Delta x)_J} dx' \left[\frac{1}{\Delta x}\right] \begin{Bmatrix} 1 \\ \left[\frac{x'-x_j}{2\Delta x}\right] \\ \left[\frac{x'-x_j}{\Delta x}\right]^2 - \frac{1}{12} \end{Bmatrix}$$

$$\cdot \exp\left(- \frac{[x-x']}{|x-x'|} \int_{x'}^{x} \frac{dx''}{\mu} \Sigma(x'') \right) . \qquad (3B.13)$$

Based on a uniformly distributed source in region J, the delay time is given by

$$\tau(I,J) = \frac{1}{2vG(I,J)} \int_{o}^{1} d\mu \int_{(\Delta x)_I} \frac{dx}{\mu} \Sigma(I) \int_{(\Delta x)_J} dx' \frac{|x-x'|}{\mu} \frac{1}{\Delta x} \cdot$$

$$\cdot \exp\left(- \frac{[x-x']}{|x-x'|} \int_{x'}^{x} \frac{dx''}{\mu} \Sigma(x'') \right) . \qquad (3B.14)$$

Eqs. (3B.13) and (3B.14) may be integrated rigorously, yielding closed-form expressions in terms of exponential integral functions.

The exponential integral function of order n is defined as follows:

$$E_n(p) = \int_1^\infty dy\, y^{-n}\, e^{-py} = \int_0^1 d\mu\, \mu^{n-2} e^{-p/\mu} \quad , \qquad (3B.15)$$

where $y = 1/\mu$, $n \geq 0$, and p is a dimensionless parameter equal, for our purposes, to an optical width in mean free paths parallel to the x-axis. The limiting value of $E_n(p)$ as p approaches zero is $1/[n-1]$ for $n \geq 1$.

We elected to follow the more physical approach, by analogy with the line reactor, of integrating first over x' and x and then expressing the integrals over μ as exponential integral functions. Figure 3B.1 shows the physical model corresponding to the kernal in the integrals over the spatial coordinates for neutrons emitted towards the right at the angle $\cos^{-1}\mu$.

In order to check the derived expressions, we replaced the integrals over μ in Eqs. (3B.13) with appropriate $E_1(p)$ kernals and then carried out the integrations over regions J and I. For this procedure, the following two relations, given in the "Handbook of Mathematical Functions"[16], were needed:

$$\frac{dE_{n+1}(p)}{dp} = E_n(p) \quad , \qquad n \geq 0 \; ; \qquad (3B.16)$$

$$nE_{n+1}(p) = e^{-p} - pE_n(p) \quad , \qquad n \geq 1 \quad . \qquad (3B.17)$$

After considerable algebra, the same expressions were obtained for the transfer coefficients.

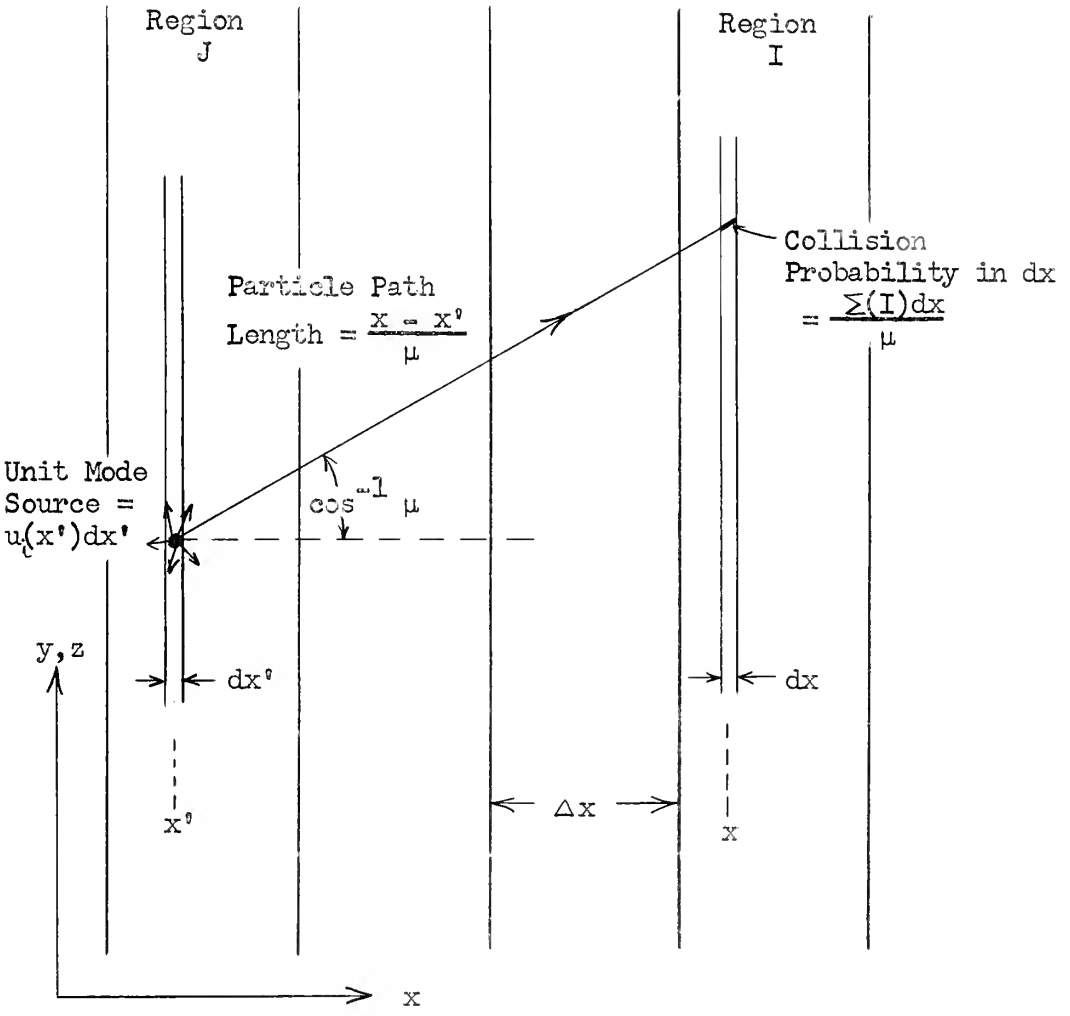

Figure 3B.1 Physical Interpretation of Transfer Kernel

As in Chapter 2, P(I) is the optical width of region I, $\Sigma(I)\Delta x$, in mean free paths parallel to the x-axis; $P_b(I,J)$ is the sum of the optical widths of all regions lying between I and J. The expressions derived for the transfer parameters are then given by Eqs. (3B.18-19); for purposes of brevity, P_i is subsituted for P(I), P_j for P(J) and P_b for $P_b(I,J)$. For I=J:

$$G(I,I) = 1 - \frac{1}{P_i}\left[0.5 - E_3(P_i)\right] ; \qquad (3B.18a)$$

$$G_{slp}(I,I) = 0 ; \qquad (3B.18b)$$

$$G_{crv}(I,I) = \frac{1}{6P_i}\left[-0.5 + E_3(P_i)\right] + \frac{1}{3P_i}\left[1 + 3E_4(P_i)\right] +$$

$$+ \frac{1}{P_i}\left[-0.5 + 2E_5(P_i)\right] ; \qquad (3B.18c)$$

$$\tau(I,J) = \left[\frac{1 + E_2(P_i) - \frac{1}{P_i}\left[1 - 2E_3(P_i)\right]}{P_i G(I,I)}\right]\frac{\Delta x}{v} . \qquad (3B.18d)$$

The expressions for I≠J are as follows:

$$G(I,J) = \frac{1}{2P_j}\left[E_3(P_b) - E_3(P_b + P_j) + E_3(P_b + P_j + P_i) - E_3(P_b + P_i)\right]; \qquad (3B.19a)$$

$$G_{slp}(I,J) = \frac{[I-J]}{8P_j|I-J|}\left(\left[E_3(P_b) + E_3(P_b+P_j) - E_3(P_b+P_j+P_i) - E_3(P_b+P_i)\right]\right.$$

$$\left. + \frac{2}{P_j}\left[- E_4(P_b) + E_4(P_b+P_j) - E_4(P_b+P_j+P_i) + E_4(P_b+P_i)\right]\right) ; \qquad (3B.19b)$$

$$G_{crv}(I,J) = \frac{1}{12P_j}\left[E_3(P_b) - E_3(P_b+P_j) + E_3(P_b+P_j+P_i) - E_3(P_b+P_i)\right] +$$

$$+ \frac{1}{2P_j^2}\left[- E_4(P_b) - E_4(P_b+P_j) + E_4(P_b+P_j+P_i) + E_4(P_b+P_i)\right] +$$

$$+ \frac{1}{P_j^3}\left[E_5(P_b) - E_5(P_b+P_j) + E_5(P_b+P_j+P_i) - E_5(P_b+P_i)\right] ; \quad (3B.19c)$$

$$\tau(I,J) = \frac{1}{2P_jG(I,J)}\left(\left[\frac{1}{P_i} + \frac{1}{P_j}\right]\left[E_3(P_b) - E_3(P_b+P_j) + E_3(P_b+P_j+P_i) - E_3(P_b+P_i)\right] + \left[|I-J| - 1\right]\left[E_2(P_b) - E_2(P_b+P_j) + E_2(P_b+P_j+P_i) - E_2(P_b+P_i)\right] + \left[-E_2(P_b+P_j) + 2E_2(P_b+P_j+P_i) - E_2(P_b+P_i)\right]\right)\frac{\Delta x}{v} . \quad (3B.19d)$$

3B.4 The Numerical Equation

As in the line models, the unit time step, Δt, is set equal to, or less than, the smallest of the $\tau(I,I)$. The delay times expressed as numbers of unit time steps are then given by

$$\tau_k(I,J) = \frac{\tau(I,J)}{\Delta t} \quad (3B.20)$$

Associating time step K with time t in Eqs. (3B.12), we obtain

$$B^o(I,K) = c(I,K)\sum_{J=1}^{N}\Big[G(I,J)B(J,K-\tau_k(I,J)) + G_{slp}(I,J)C_1(J,K-\tau_k(I,J)) + G_{crv}(I,J)C_2(J,K-\tau_k(I,J))\Big] , \quad (3B.21)$$

where B, C_1 and C_2 are computed according to the relations (3B.9-11) and the transfer parameters, according to the relations (3B.18-20).

In program TOVSR, the transfer parameters are computed once and then stored. B, C_1 and C_2 are recomputed each time they are used, i.e., for each $J \rightarrow I$ transfer computation; memory storage is provided only for the arrays B^o and S. The argument K is dropped from the array c and the c(I) are altered at time steps for which changes are scheduled.

3C. COMPUTATION AND ANALYSIS OF TRANSFER COEFFICIENTS

To compute accurate values for the transfer parameters requires accurate values of the exponential integrals in Eqs. (3B.18-19). In order to obtain these values, two 250-element tables of $E_3(p)$ data are read into the computer. The one table includes the values of $E_3(p)$ for arguments in the range $0.01 \leq p \leq 2.50$, with a spacing of 0.01; the second covers the range of arguments $0.1 \leq p \leq 25.0$, with a spacing of 0.1. The $E_3(p)$ data for $p \leq 2.0$ were obtained from the "Handbook of Mathematical Functions"[16]. The values for $p > 2.0$ were computed with a program written by the author, which uses a 401-point Simpsons' Rule formula to numerically integrate the second form of Eq. (3B.15). The computed integrals are accurate to six digits.

The value of $E_3(p)$ for an argument lying between the tabulated arguments is obtained by third-order polynomial interpolation, using the tabulated values for the argument just less than the desired

argument and for the three successively larger arguments. Test calculations showed that the third-order interpolation scheme yields results consistent with the six-digit accuracy of the tabulated data. Having found the value of $E_3(p)$ by interpolation, the values of $E_2(p)$, $E_4(p)$ and $E_5(p)$ are computed according to the recursion relation, Eq. (3B.17). The operations described in this paragraph are performed in subroutine TABLE of the program TOVSR. The values of the exponential integrals are then used in subroutine TPARAM to compute the transfer parameters.

Note that the expressions for G, G_{slp}, G_{crv} and $\tau v/\Delta x$ in Eqs. (3B.18-19) are dimensionless functions of various optical widths only. Table 3C.1 contains some sample values obtained for the (I=J) transfer parameters. The numbers in the second column, $\tau v/\Delta x$, are the mean flight paths, in units of Δx, of neutrons which are born in region I and collide in region I. In contrast to the line reactor, for which $\tau v/\Delta x$ approaches 1/3 as P(I) approaches zero, the parameter assumes very large values for small P(I) in the slab reactor. In optically-thin regions, the great majority of the emitted neutrons that collide in the same region were emitted at large angles with respect to the x-axis. One consequence of the longer mean flight paths is a unit time step which is much larger than that for a line reactor of equivalent width and number of regions. The third and fourth columns contain the flat-mode collision and leakage probabilities. The fifth column gives the net increase in the collision rate in region I due to a birth rate distribution described by the unit

Table 3C.1

Slab Parameters in Region I vs. Optical Width of Region I

P(I)	$\frac{\tau(I,I)v}{\Delta x}$	G(I,I)	Leakage 1-G(I,I)	$G_{crv}(I,I)$	Leakage $-G_{crv}(I,I)$	$\frac{-G_{crv}(I,I)}{1-G(I,I)}$
.005	30.6	.01631	.98369	-.01587		
.010	18.0	.02766	.97234	-.00384		
.020	10.3	.04841	.95159	-.00031		
.030	7.44	.06659	.93341	-.00020		
.075	3.68	.13267	.86733	-.00052	.00052	0.0006
.100	2.97	.16292	.83708	-.00067	.00067	.0008
.125	2.52	.19020	.80980	-.00083	.00083	.0010
.20	1.80	.25973	.74027	-.00128	.00128	.0017
.25	1.54	.29874	.70126	-.00157	.00157	.0022
.50	.962	.44321	.55679	-.00286	.00286	.0051
1.0	.602	.60969	.39031	-.00475	.00475	.0122
2.0	.371	.76507	.23493	-.00674	.00674	.0287
4.0	.215	.87569	.12431	-.00748	.00748	.0602
7.0	.132	.92858	.07142	-.00656	.00656	.0918

curvature-correction mode. Since the net birth rate in the curvature-correction mode is equal to zero, $-G_{crv}(I,J)$ in column 6 describes the net increase in the leakage rate from the region. The ratio given in column 7 clearly shows the increasing importance of the curvature correction with increasing P(I).

The computed values of $G_{crv}(I,I)$ for $P(I) < 0.1$ are incorrect. Consider the third term on the right-hand side of Eq. (3B.18c). Errors in the value of $E_5(P_i)$ are magnified by the factor $2/P_i^3$, which is very large for small P_i. The tabulated exponential integral data and interpolated values do not have a sufficient number of digits of accuracy to yield accurate values of $G_{crv}(I,I)$. The same

difficulty is evident in Eq. (3B.19c) for $G_{crv}(I,J)$. Consequently the curvature correction should not be applied for source regions less than 0.1 mfp thick; the analogous lower limit for the slope correction is 0.02 mfp.

The transfer parameters computed for source region 9 and receiver regions I in a 15-region inhomogeneous system are given in Table 3C.2.

3D. THE COMPUTER PROGRAM TOVSR

The FORTRAN II program TOVSR is described in Appendix B. This program is very similar to the line reactor program OVRR4 as regards both general format and flexibility features.

Either Model F, Model FS or Model FSC can be selected for a particular calculation. These models correspond to the use of one, two or three modes, respectively, in Eq. (3B.21). An option is available for specifying the level of approximation separately for each source region J. Computing times per time step are given by Eq. (2B.12), where α_t is 0.0005 sec for Model F, 0.0006 sec for FS, and 0.0007 sec for FSC.

As in OVRR4, an option is included to permit more efficient computation of steady-state distributions and to compute time-independent generation-to-generation transients. With this option, all $\tau_k(I,J)$ in Eq. (3B.21) are set equal to unity. This option was used to compute the solution of the Milne problem reported in Section 3F. All other solutions reported in this chapter have been computed using the time-dependent option.

Table 3C.2

Transfer Coefficients for an Inhomogeneous Slab System

$W = 3.75$ cm. $N = 15$ $\Delta x = 0.25$ cm.

$\Sigma(I) = 0.5$, $P(I) = 0.125$, $I = 1\text{-}10$;

$\Sigma(I) = 1.0$, $P(I) = 0.25$, $I = 11\text{-}15$.

$t = 1.7529$ μsec. $v = 2.2 \times 10^5$ cm/sec.

$\frac{\Delta x}{v\Delta t} = 0.648$ = No. of time steps to cross Δx

Transfer Coefficients for J = 9

I	P(I)	G(I,9)	$G_{slp}(I,9)$	$G_{crv}(I,9)$	$\tau_k(I,9)$
1	.125	.013772	-.000120	.000003	8.6701
2	.125	.017070	-.000156	.000003	7.9260
3	.125	.021392	-.000207	.000003	7.1670
4	.125	.027199	-.000282	.000006	6.3873
5	.125	.035286	-.000400	.000010	5.5789
6	.125	.047198	-.000610	.000019	4.7263
7	.125	.066607	-.001061	.000048	3.7949
8	.125	.108533	-.002890	.000316	2.6391
9(I=J)	.125	.190203	0	-.000829	1.6353
10 (Interface)	.125	.108533	.002890	.000316	2.6391
11	.25	.113805	.001671	.000066	3.4297
12	.25	.062485	.000682	.000016	3.9669
13	.25	.038462	.000363	.000006	4.6198
14	.25	.024978	.000214	-.000001	5.2919
15	.25	.016756	.000136	.000011	5.9672

3E. COMPUTATION OF ASYMPTOTIC SOLUTIONS

As with the line models, we begin the testing of the slab models by using them to generate asymptotic solutions for source-free systems with time-independent properties. The procedure used to generate asymptotic solutions was described in Section 2E.

3E.1 Tests of Reported Critical Thicknesses

In an early paper on the S_N Method, Carlson and Bell[17] reported "exact" critical slab half-thicknesses in mean free paths (mfp) for several values of the secondary emission coefficient, c. These values are best estimates based on error analyses and convergence trends of several methods used to compute the critical half-thicknesses. Carlson and Bell conclude that the "exact" values are accurate to within one or two places in the fourth decimal place. We have tested TOVSR on the "exactly" critical systems having $c = 1.4$ and $c = 1.02$, treating each problem as an (x,t)-dependent problem and generating the approximate asymptotic solution.

Table 3E.1 gives the asymptotic inverse periods computed for the $c = 1.4$ case, for which the "exact" critical thickness, P_c, is 1.4732 mfp. The first six runs listed demonstrate the convergence of the computed values of λ with increasing N for Model FSC. The next two runs permit comparison of Model FSC with Models FS and F. Note that the results of Models FSC and FS for $N = 26$ differ only slightly, whereas Model FSC with $N = 5$ predicts a more accurate inverse period than Model F with $N = 26$.

Table 3E.1

Tests of Critical Slab Thickness for c = 1.4

c = 1.4	$\Sigma = 0.5$ cm^{-1}			v = 2.2×10^5 cm/sec	
Tested P_c = 1.4732 mean free paths					
W, cm	$\Sigma W/P_c$	Model	N	Computed Inverse Period, λ, sec^{-1}	Predicted P_c
(critical					
2.9464	1	FSC	5	- 28.7	1.4740
2.9464	1	FSC	7	- 15.3	1.4736
2.9464	1	FSC	10	- 6.8	1.4734
2.9464	1	FSC	13	- 3.6	1.4733
2.9464	1	FSC	16	- 2.2	1.4733
2.9464	1	FSC	26	- 0.7	1.4732
2.9464	1	FS	26	- 0.9	1.4732
2.9464	1	F	26	- 40.1	1.4743
(Off-Critical)					
2.9170	.990	FSC	26	-550.	
2.9317	.995	FSC	26	-274.	
2.9464	1.000	FSC	26	- 0.7	
2.9611	1.005	FSC	26	270.	
2.9758	1.010	FSC	26	537.	

The last group of runs are for systems with thicknesses slightly greater or less than the "exact" critical thickness. Note the approximately linear relation between the inverse period and W for nearly critical systems. Using the results of the 26-region, Model FSC runs for $\Sigma W/P_c = 0.995$ and 1.005 to estimate the coefficient of linearity, $\delta W/\delta\lambda$, we may calculate the critical thickness which we would predict from the values of W and λ for any particular run. For example, for the 5-region, Model FSC run we obtain

$$\text{Predicted } P_c = 0.5\left[2.9464 + 28.7\left(\frac{2.9611 - 2.9317}{270 + 274}\right)\right] = 1.4740 \text{ mfp}$$

The predicted critical thicknesses are tabulated for the first eight runs listed in Table 3E.1. The closeness of the predicted P_c and the "exact" P_c is a good measure of the accuracy of the asymptotic solution computed in a particular run. Note that the results for the 26-region runs with Models FS and FSC are in complete agreement with the "exact" critical thickness.

The normalized asymptotic birth rate (or flux) distributions computed with Model FSC for N=13 and N=26 are given in Table 3E.2. The equivalence of the distributions to within one part in 10,000 both illustrates the fact that $B_o(I)$ is an integral over region I and demonstrates the high degree of convergence of the computed distributions.

Table 3E.2

Birth Rate Distribution in Critical Slab having c = 1.4

N = 26			N = 13	
I	$B_o(I)$	$\frac{B_o(I)+B_o(I+1)}{2}$	$B_o(I)$	I
1,26	.64591	.69327	.69322	1,13
2	.74064			
3	.81910	.85349	.85343	2
4	.88788			
5	.94876	.97561	.97562	3
6	1.00246			
7	1.04933	1.06941	1.06943	4
8	1.08949			
9	1.12299	1.13641	1.13644	5
10	1.14983			
11	1.16999	1.17672	1.17676	6,8
12,15	1.18345			
13	1.19018	1.19018	1.19022	7
14	1.19018			

Results for the critical system having c = 1.02 are given in Table 3E.3; the "exact" critical thickness for this system is 11.3310 mfp. Again, the results of Models FS and FSC agree closely and are considerably better than the results of the flat approximation. In order to find the predicted critical thicknesses, one additional Model FSC run was made with N = 25 and W = 11.38766 cm, 0.5 percent greater than the "exact" critical thickness. The inverse period computed for this system is 37.4 sec^{-1}. Using the two 25-region, Model FSC results to estimate $\delta W/\delta\lambda$, we obtain

Table 3E.3

Tests of Critical Slab Thickness for c = 1.02

c = 1.02 Σ = 1.0 cm^{-1} v = 2.2x10^5 cm/sec W = 11.3310 cm Tested P_c = 11.3310 mfp			
Model	N	λ, sec^{-1}	Predicted P_c.
F	10	-938.	-----
FS	10	- 11.7	11.348
FSC	10	- 9.6	11.345
FSC	25	- 1.6	11.333

$$\text{Predicted } P_c = 11.3310 + 11.7\left[\frac{11.38766 - 11.3310}{37.4 + 1.6}\right] = 11.348 \text{ mfp}$$

for the 10-region Model FS run.

The critical thicknesses predicted by our models are compared with the published results of other methods in Table 3E.4. Note that the number of dependent variables in the finite-integral models is considerably less than the number required for equivalent accuracy in P_L and S_L Models.

The results obtained for the two critical systems demonstrate the effectiveness of the slope- and curvature-correction models in treating the spatial distribution of the birth rate in region J. With confidence in the accuracy of solutions computed for nearly critical systems, we will next study a very supercritical system. With the aid of accurate auxiliary system solutions, we can isolate and evaluate errors introduced with the discrete-delay-time approximation and find the limitations on the growth rate for solutions of acceptable accuracy.

Table 3E.4

Comparison with Critical Thicknesses
Predicted by Other Methods

Method	Reference	No. of Dependent Variables	P_c for c=1.4	No. of Dependent Variables	P_c for c=1.02
"Exact"	(17)	----	1.4732	----	11.3310
Model FSC	----	26	1.4732	25	11.333
" "	----	5	1.4740	10	11.345
Model FS	----	26	1.4732	10	11.348
EP	(17)	----	1.4768	----	11.3310
Pomraning	18	----	1.4768	----	11.3318
S_{16}	17	272	1.4744	272	11.3388
S_8	17	144	1.4766	144	11.3404
P_5	17	112	1.5036	112	11.3446
P_3	17	64	1.5586	64	11.3656

Notes: (1) EP is the "Extrapolated End-Point Method."

(2) The half-thickness was subdivided into 16 regions for the P_L and S_L computations.[17] No. of variables = 16(L+1).

3E.2 Small, Supercritical, Homogeneous Slab

In this subsection we report the results obtained for a 10 cm system with c=1.4 and Σ=0.4. As was shown in the previous subsection, the critical system having these properties is only 2.9464 cm thick. The data in the top half of Table 3E.5 are the asymptotic inverse periods computed by Models F, FS and FSC for several values of N. Note that, in contrast with results obtained for line systems and for the critical slab system, the data for $N \leq 25$ do not converge rapidly with increasing N towards a particular asymptotic value.

Table 3E.5

Computed Inverse Periods for 10 cm Supercritical Reactor

W = 10 cm c = 1.4 Σ = 0.5

v = 2×10^5 cm/sec

N	Model F λ, sec^{-1}	Model FS λ, sec^{-1}	Model FSC λ, sec^{-1}
7	30004	30618	30693
10	30593	30952	30973
13	30856	31088	31096
16	31035	31196	31200
19	31146	31264	---
25	---	---	31321 (-6.35)

Auxiliary Problems: W = 10 cm v = 2.10^5 cm/sec

Model FSC N = 25

	First Auxiliary Problem	Second Auxiliary Problem
λ_{est}, sec^{-1}	31300	33450
c^*	1.06626	1.04908
Σ^*, cm^{-1}	.65650	.66725
λ^*, sec^{-1}	2135 (-0.4)	-7.4
Corrected $\lambda = \lambda_{est} + \lambda^*$	33435 (-0.02)	33443 (~ 0)

Note: Numbers in parentheses are percentage errors based on the assumed accuracy of the results of the second auxiliary problem.

In order to check the accuracy of the results, we first observe that, for source-free systems with time-independent properties, the same operations may be applied to the slab integral equation, Eq. (1A.1), as were applied to the line integral equation in Subsection 2E.4. Auxiliary systems defined by Eqs. (2E.11), which have the same asymptotic spatial distribution as the reference system, may be studied. If the auxiliary system is nearly critical, its asymptotic solution can be found very accurately, based on the results of the previous subsection. In this way, the correct asymptotic solution for the reference system may be determined and the errors resulting from the combination of the discrete-delay-time approximation, the uniform source assumed in deriving the expression for $\tau(I,J)$, and the population growth rate may be evaluated. For the 10 cm system, two successive auxiliary problems were solved, each using the best information available for selecting λ_{est}. As can be seen from Table 3E.5, the second auxiliary system is sufficiently close to critical that we may be confident in the accuracy of its solution. We conclude that the inverse period of the reference system is 33443 sec^{-1}, from which we calculate a 6.35 percent error in the inverse period predicted by the best reference system run. This is considered unsatisfactory.

To obtain some useful conclusions from the above result, we first note that the 6.35 percent error is due to our having neglected the growth rates in the individual source regions J in formulating the model. For the asymptotic solution ,the computed contribution to B(I,t) from parent neutrons born in region J has an unacceptable

error when $\dot{B}(J,t')/B(J,t') = \lambda = 33443 \text{ sec}^{-1}$ for $t' < [t - [|I-J| - 1]\Delta x/v]$, where $\dot{B}$ is the rate of growth of B. For a growing space-time transient in a system having the same Σ, W and v as the reference system but space-time dependent c and S, we can conclude that the computed contribution to B(I,t) from parent neutrons born in region J would have an error at least as large as for the asymptotic solution if $\lambda(J,t') = \dot{B}(J,t')/B(J,t') \geq 33443 \text{ sec}^{-1}$ for <u>all</u> $t' < [t - [|I-J| - 1]\Delta x/v]$; conversely, if $\dot{B}(J,t')/B(J,t') < 33443 \text{ sec}^{-1}$, the error would be smaller. The actual error depends on the history of $\lambda(J,t')$, with greater weight assigned to more recent history. The error in B(I,t) depends of course on the errors in the contributions from all J.

The conclusions of the preceding paragraph may be generalized to a still broader class of systems by noting that the transfer parameters G(I,J), $G_{slp}(I,J)$, $G_{crv}(I,J)$ and $\tau_k(I,J)$ in Eq. (3B.21) are functions of optical distances only and are not explicitly dependent on Δx or v. For any homogeneous system which has the same $[\Sigma W]$ and c as the reference system, it can be shown that Model FSC with N=25 will yield an asymptotic inverse period which is low by 6.35 percent. Further, the dimensionless parameter $\lambda/[v\Sigma]$ will have the same value as for the reference system, 0.3344, although Σ, v and λ may be different from the reference system values. This parameter is therefore helpful for correlating errors due to the neglect of growth rate in the discrete-delay-time models.

From Table 3E.5, the inverse period computed for the less supercritical first auxiliary system, 2135 sec^{-1}, has an error of only 0.4 percent. From the normalized asymptotic birth rate distributions given in Table 3E.6, it is evident that errors due to growth rate are negligible in the spatial distribution computed for the first auxiliary system. The solution of the first auxiliary problem is therefore considered to be quite satisfactory. The values of parameters of interest are $\Sigma W = 6.565$, $c = 1.06626$ and $\lambda/[v\Sigma] = .0163$.

Similar studies for subcritical systems indicate that spatial distributions having negligible error due to growth rate, and inverse periods with less than one percent error due to growth rate, can be computed for systems with $|\lambda|/[v\Sigma] \leq 0.02$, As discussed previously, we can have confidence in the reasonable accuracy of computed space-time transients if

$$|\lambda(J,t')|/[v\Sigma] \leq 0.02 \text{ for } t' < t \text{ and } 1 \leq J \leq N .$$

Note that the unsatisfactory convergence of the reference system inverse periods with increasing N is in marked contrast with the excellent results obtained for the 10 cm supercritical line reactor of Subsection 2E.5. In the line models, the neutrons born in region J that collide in region I at time t were born during a finite time interval; this interval shrinks to zero with Δx. In the slab models, on the other hand, the time interval of parent births in region J remains unbounded as the width of region J shrinks to zero. To adequately sample the time-dependence of the birth rate in a source region in which the birth rate varies rapidly with time requires use of a multiple-delay-time model. Such a model is formulated in Section 3I.

Table 3E.6

Computed Asymptotic Birth Rate Distributions in 10 cm Reactor

Model FSC		N = 25	
Region I	Reference Problem $B_o(I)$	First Auxiliary Problem $B_o(I)$	Second Auxiliary Problem $B_o(I)$
1,25	.38798	.38534	.38529
2	.54064	.53853	.53850
3	.67486	.67325	.67322
4	.79762	.79652	.79650
5	.90981	.90924	.90923
6	1.01113	1.01105	1.01105
7	1.10087	1.10126	1.10127
8	1.17832	1.17912	1.17914
9	1.24276	1.24391	1.24393
10	1.29355	1.29499	1.29502
11	1.33021	1.33186	1.33188
12,14	1.35235	1.35413	1.35416
13	1.35976	1.36158	1.36161

3E.3 Inhomogeneous System

In Table 3E.7, we report the results obtained for a 3.75 cm inhomogeneous system consisting of a 2.5 cm multiplying region and a 1.25 cm absorbing region. The slight errors are consistent with those obtained for homogeneous systems. The parameter $\lambda/[v\Sigma]$ is .0278 in the multiplying region and .0139 in the absorbing region. The spatially-averaged value is .0232.

Table 3E.7

Tests of Supercritical, Inhomogeneous System

W = 3.75 cm N = 15 $v = 2.2 \times 10^5$ cm/sec

Model FSC

Reference Problem	Auxiliary Problem
$\Sigma(I) = 0.5$, $c(I) = 1.4$; $1 \le I \le 10$	$\lambda_{est} = 3032.8 \text{ sec}^{-1}$
	$\Sigma^*(I) = .51379$, $c^*(I) = 1.36244$; $1 \le I \le 10$
$\Sigma(I) = 1.0$, $c(I) = 0.9$; $11 \le I \le 15$	$\Sigma^*(I) = 1.01379$, $c^*(I) = .88776$; $11 \le I \le 15$
$\lambda = 3032.8 \text{ sec}^{-1}$	$\lambda^* = 22.1 \text{ sec}^{-1}$
Error = - 0.7 percent	Corrected $\lambda = 3055 \text{ sec}^{-1}$

Computed Flux Distributions, $\phi_o(I)$

Region, I		Reference Problem	Auxiliary Problem
1		.79489	.79386
2		.99206	.99208
3		1.14137	1.14142
4		1.25398	1.25404
5		1.33129	1.33137
6	c > 1	1.37299	1.37307
7		1.37838	1.37846
8		1.34656	1.34662
9		1.27563	1.27567
10		1.15765	1.15765
11		.92408	.92402
12		.72154	.72145
13	c < 1	.56730	.56720
14		.43443	.43434
15		.30784	.30775

3F. APPROXIMATE SOLUTION OF THE MILNE PROBLEM FOR c = 1.0

In order to evaluate the accuracy of flux distributions computed by the program TOVSR, we applied the program to the Milne problem for a pure scattering medium. Weinberg and Wigner[9] tabulate the relative fluxes at various optical distances from the interface which were obtained by the exact Wiener-Hopf method and by various order P_L approximations. We therefore have a basis for comparison.

The Milne problem treats a semi-infinite, homogeneous medium having an interface with a vacuum at x = 0 and an external source at $x = \infty$. The interesting part of the solution is the steady-state flux distribution near the interface, where the flux falls below the extrapolated values of the linearly-varying (for c = 1.0) interior distribution.

In formulating the Milne problem for TOVSR, which treats only finite slabs and has a limit of thirty regions of equal Δx, the optical distance between the source and the vacuum interface must be sufficiently large that effects of the isotropic source and the right-hand boundary on the spatial and angular flux shapes in the interior are small. Furthermore, considerable detail concerning the spatial shape within two mean free paths of the interface is desired. Since this problem is a steady-state problem and since all of the expressions for the transfer coefficients involve optical thicknesses only, the above requirements are met by stretching the medium in the vicinity of the interface and then treating the system as inhomogeneous. In a thirty-region run, the twelve regions near the interface cover 0.6 mfp,

the next six regions cover 3.0 mfp and the final 12 regions cover 24 mfp. The external source was placed in region 30.

The distributions computed by the program are given in Table 3F.1. Since the rate of convergence towards the steady state solution was very slow, several successive runs were made with improved estimates of the solution read in as the initial distribution.* The data given in Table 3F.1 are not a fully converged solution but are close enough to permit meaningful analysis. The ratios B(I,K)/B(I,K-1) for regions 1, 3, 11, 16, 25 and 30 are .9999760, .9999761, .9999762, .9999772, .9999918, and .9999984, respectively. The shape is fairly well stabilized in regions 1 through 16, which cover the interval $0 < p < 2.7$, where p is the optical distance from the interface.

In order to compare the computed distribution with the numbers quoted by Weinberg and Wigner, it was necessary to convert the mean flux values, $\phi_o(I)$, to a smooth distribution and then to compute the flux at discrete optical distances from the interface. The unfolding method used in Subsection 3B.2 to derive expressions for the modal coefficients was adapted for this purpose. Treating the data in each of regions 1 through 12 as the integral of the distribution in the particular region, a program was written to fit the distribution with an 11th order polynomial and to compute the relative flux at various optical distances from the interface. The ~~rleative~~ relative flux values were then normalized such that $\phi(0.1)$ is equal to 1.2608. In Table 3F.2 we compare our results with those of the Wiener-Hopf Method and the

---

* Note: With the program SLBCEL, written at a later date and described in Chapter 4, a fully converged solution can be obtained in a few seconds.

Table 3F.1

Distributions Computed by TOVSR for the Milne Problem

Model FSC	W = 30 cm	c = 1.0	
N = 30	External Source in Region 30		
Region, I	$\Sigma(I)$ P(I)	Normalized Birth Rate $B_o(I)$	Normalized Mean Flux $\phi_o(I)$
1	.05	.00236478	.084410
2	.05	.00264078	.094262
3	.05	.00288541	.102994
4	.05	.00311616	.111231
5	.05	.00333824	.119158
6	.05	.00355439	.126873
7	.05	.00376617	.134432
8	.05	.00397461	.141873
9	.05	.00418041	.149219
10	.05	.00438410	.156490
11	.05	.00458606	.163698
12	.05	.00478663	.170858
13	.50	.0586824	.209465
14	.50	.0780282	.278520
15	.50	.0971683	.346840
16	.50	.1162269	.414869
17	.50	.1352503	.482773
18	.50	.1542561	.550614
19	2.00	.806928	.720077
20	2.00	1.110568	.991037
21	2.00	1.413972	1.261785
22	2.00	1.717133	1.532317
23	2.00	2.020046	1.802627
24	2.00	2.322707	2.072713
25	2.00	2.625121	2.342578
26	2.00	2.927321	2.612252
27	2.00	3.229604	2.881200
28	2.00	3.584196	3.153808
29	2.00	3.853561	3.438800
30	2.00	3.755654	3.351430

Table 3F.2

Results of Milne Problem - Comparison with Other Methods

Optical Distance from Interface, p	Relative Flux Normalized to $\phi(.10) = 1.2608$			
	Our Results	Wiener-Hopf (Exact)	P_{15}	P_5
0	1.0047(47)	1.0000	1.0064(64)	1.0281(281)
.05	1.1444			
.10	1.2608	1.2608	1.2608	1.2608
.15	1.3682			
.20	1.4711(-3)	1.4714	1.4774(60)	1.4794(80)
.25	1.5708			
.30	1.6682(-3)	1.6685	1.6770(85)	1.6876(191)
.35	1.7639			
.40	1.8583(-4)	1.8587	1.8683(96)	1.8882(295)
.45	1.9516			
.50	2.0439(-4)	2.0443	2.0547(104)	2.0831(388)
.55	2.1356			
.60	2.2267(-4)	2.2271	2.2383(112)	2.2739(468)
.70	2.4084(7)	2.4077	2.4199(122)	2.4618(541)
.80	2.5860(-8)	2.5868	2.5999(131)	2.6473(605)
.90	2.7633(-19)	2.7652	2.7789(137)	2.8312(660)
1.00	2.9402(-17)	2.9419	2.9607(188)	3.0137(718)
2.00	4.6890(-12)	4.6902	4.7152(250)	4.8108(1206)

Note: Numbers in parenthesis are equal to $[\phi_{approx.} - \phi_{exact}] \times 10^4$.

P_5 and P_{15} approximations. The relative fluxes for $p > 0.6$ were obtained by fitting the local distribution by a quadratic, in the manner of Subsection 3B.2. Basing comparisons on the exactness of the Wiener-Hopf Method results, note that the small errors in our results are considerably less than the errors in the P_5 and P_{15} results.

The results obtained for the Milne problem demonstrate that integral regional birth rates $B_o(I)$ can be computed very accurately by our method and can be successfully unfolded to yield a continuous distribution, and that the finite-integral method is competitive with the P_N method.

3G. FAST TRANSIENT RESPONSE TO A LOCALIZED INITIAL SOURCE

In this section we present results obtained for the space-time transient response to an external source localized in space and time. The system studied is a 4 cm homogeneous slab having $\Sigma = 0.5$ cm^{-1} and $c = 1.4$. The particle velocity is 2×10^5 cm/sec. The system is subdivided into 15 regions and a unit external source rate is maintained in region 4 for one time step. The problem studied here for slab geometry is analogous to the first problem studied for line geometry in Section 2F, in that we compute the transient response to an external source rate localized to only one region and lasting for only one time step.

The birth rate distributions computed at time steps 2, 4, 6, 8, 12 and 30 are tabulated in Table 3G.1. Features to note in the data are the existence of a propagation front, the smoothing out of the predicted distribution by time step 8 and the onset of asymptoticity by time step 30. Note that the computed response does not have the violent numerical oscillations obtained for the analogous line problem and shown in the dashed-line curve of Fig. 2F.1. This difference is due to the following factors. First, in the slab reactor, the x-dependence of the neutron distribution, including the original external source neutrons, smears out with time because the neutrons are emitted at various angles with respect to the x-axis. In the line reactor, on the other hand, smoothing results from successive collisions only. Second, as can be seen from the parameter $v\Delta t/\Delta x$, the unit time step is approximately eight times larger than it would be in a line reactor having the same width and properties. Third,

Table 3G.1

Transient Response to Localized Initial Source

W = 4.0 cm N = 15 $v = 2 \times 10^5$ cm/sec

$\Sigma = 0.5$ cm^{-1} c = 1.4

$\Delta t = 3.209$ μsec $\frac{v\Delta t}{\Delta x} = 2.407$

Unit external source rate in region 4 for 1 time step.

I	$\tau_k(1,I)$	B(I,2)	B(I,4)	B(I,6)	B(I,8)	B(I,12)	B(I,30)
1	1.000	---	.0713	.0479	.0356	.0321	.0609
2	1.626	---	.0816	.0555	.0440	.0405	.0776
3	2.353	.0586	.0766	.0538	.0499	.0468	.0909
4	2.941	.2783	.0523	.0529	.0534	.0517	.1017
5	3.480	.0586	.0767	.0539	.0547	.0553	.1102
6	3.992	---	.0817	.0573	.0545	.0576	.1163
7	4.487	---	.0713	.0541	.0530	.0584	.1200
8	4.969	---	.0258	.0534	.0496	.0579	.1213
9	5.442	---	.0003	.0420	.0473	.0563	.1200
10	5.908	---	---	.0306	.0438	.0537	.1163
11	6.368	---	---	.0245	.0360	.0500	.1102
12	6.823	---	---	.0103	.0293	.0456	.1018
13	7.274	---	---	.0014	.0201	.0402	.0909
14	7.722	---	---	---	.0131	.0341	.0776
15	8.167	---	---	---	.0102	.0265	.0610

the mean angle of emission with respect to the x-axis of the particles which are born in J and collide in I decreases as $|I-J|$ increases; this is evident in the decreasing value of the ratio $\tau_k(I,J)/|I-J|$ with increasing $|I-J|$. All of the above factors contribute to the rapid propagation and smoothing with increasing K.

It can be shown that the spatial oscillations in the computed distributions at time steps 4 and 6 are physically impossible for the slab system studied here. These oscillations are numerical conse-

quences of the discrete-delay-time approximation and the discontinuities in the (x,t)-dependence of the external source rate. To compute a solution having more accurate detail, a multiple-delay-time model should be used.

The importance distributions reported in the next section demonstrate that the relative contributions to the total population at a later time from initial sources located in different regions of the system may be obtained reasonably accurately from the computed transient responses to the individual sources.

3H. COMPUTATION OF IMPORTANCE DISTRIBUTIONS

In this section we report the importance distributions computed with Model FSC for a critical homogeneous reactor and a supercritical, inhomogeneous system. As outlined in Chapter 2, the computation of an importance distribution involves solving several localized-source problems of the type reported in the previous section.

In Table 3H.1, we report the results obtained for the 2.9464 cm critical slab which was studied in Subsection 3E.1. The importance distribution is compared with the asymptotic flux distribution; percent deviations are tabulated. In Table 3H.2, we report the results obtained for the inhomogeneous system studied in Subsection 3E.3.

Note that for both systems the percent deviation of the importance from the flux is negligible for all regions except those which are adjacent and next-adjacent to a boundary or an interface. Even for the latter regions, however, the percent deviations are very small.

Table 3H.1

Importance Distribution in Critical Slab having c = 1.4

W = 2.9464 cm $\Sigma = 0.5\ cm^{-1}$ c = 1.4

Model FSC N = 13

Source Life = 3 time steps Δt = 2.791 μsec

Importance computed from populations at time step 40.

Region, I	Normalized Asymptotic Flux, $\phi_o(I)$	Normalized Importance, $\phi_o^+(I)$	Percent Deviation, $100\left[\frac{\phi^+ - \phi}{\phi}\right]$
1,13	.69108	.69320	-.306
2	.85564	.85343	+.259
3	.97558	.97563	-.005
4	1.06933	1.06944	-.010
5	1.13645	1.13644	+.001
6,8	1.17679	1.17676	+.003
7	1.19026	1.19022	+.003

Table 3H.2

Importance Distribution in Supercritical Inhomogeneous System

W = 3.75 cm	N = 15	Model FSC
$\Sigma(I) = 0.5$ cm^{-1}	c(I) = 1.4,	$1 \leq I \leq 10$;
$\Sigma(I) = 1.0$ cm^{-1},	c(I) = 0.9,	$11 \leq I \leq 15$.
Source Life = 3 time steps.		$\Delta t = 1.753$ μsec.

Importance distribution computed from populations at time step 60.

Region, I	Normalized Asymptotic Flux, $\phi_o(I)$	Normalized Importance, $\phi_o^+(I)$	Percent Deviation $100\,\frac{\phi^+ - \phi}{\phi}$
1	.79489	.79211	-.350
2	.99206	.99511	+.304
3	1.14137	1.14140	+.003
4	1.25398	1.25392	-.005
5	1.33129	1.33138	+.007
6	1.37299	1.37310	+.008
7	1.37838	1.37840	+.002
8	1.34656	1.34662	+.004
9	1.27563	1.27758	+.153
10 (interface)	1.15765	1.15542	-.193
11	.92408	.92788	+.412
12	.72154	.71719	-.603
13	.56730	.56728	-.004
14	.43443	.43675	+.535
15	.30784	.30585	-.648

3I. FORMULATION OF A MULTIPLE-DELAY-TIME MODEL

From the results obtained for the first auxiliary system of Subsection 3E.2, for the inhomogeneous system of Subsection 3E.3 and for several subcritical systems, we have concluded that the slab models can generate very accurate asymptotic distributions, and inverse periods accurate to within one percent, for systems in which the dimensionless parameter $|\lambda|/[v\Sigma] < .02$. This conclusion was extended to space-time transient solutions by use of the local parameter $\lambda(J,t')$. For slab systems with much larger growth or decay rates, however, the discrete-delay-time approximation is not satisfactory. Recall that, with this approximation, the mean flight-time of neutrons which are born in region J and collide in region I is a weighted average for neutrons emitted over the entire angular range, $0 < \mu \leq 1$.

In this section we propose a multiple-delay-time model which can better sample the time dependence of the birth rate in source region J. The model is formulated by subdividing the angular range into N_μ intervals of width $\Delta\mu = 1/N_\mu$. Sets of transfer parameters having the arguments (I,J,I_μ) are then computed for neutrons emitted in each angular interval, identified by the integer I_μ. For isotropic emission, it is not necessary to introduce angular-dependent birth rates since the angular dependence of the birth rate is separable and is accounted for in the transfer parameters.

In deriving the expressions (3B.18-19) for the transfer parameters used in TOVSR, we integrated first over the spatial variables

for neutrons emitted at a fixed angle $\cos^{-1}\mu$. We then weighted this expression by the angular dependence of the birth rate distribution and wrote down by inspection the final expressions for the integrals over μ in terms of exponential integral functions. We could have just as easily expressed integrals over the limited angular interval identified by I_μ in terms of what we shall call "partial-range exponential integral functions," defined by

$$E_n(p,I_\mu) = \int_{(\Delta\mu)_{I_\mu}} d\mu\, \mu^{n-2} e^{-p/\mu} \quad . \tag{3I.1}$$

Each of the expressions (3B.19), for $I \neq J$, is valid for neutrons emitted in the angular interval identified by I_μ if we merely add I_μ to the arguments of G, G_{slp}, G_{crv}, τ and the exponential integral functions. The appropriate expressions for I=J are the following:

$$G(I,I,I_\mu) = E_2(0,I_\mu) - \frac{1}{P_i}\left[E_3(0,I_\mu) - E_3(P_i,I_\mu)\right]; \tag{3I.2a}$$

$$G_{slp}(I,I,I_\mu) = 0 \; ; \tag{3I.2b}$$

$$G_{crv}(I,I,I_\mu) = -\frac{1}{6P_i}\left[E_3(0,I_\mu) - E_3(P_i,I_\mu)\right] +$$

$$+\frac{1}{P_i^2}\left[E_4(0,I_\mu) + E_4(P_i,I_\mu)\right] - \frac{2}{P_i^3}\left[E_5(0,I_\mu) - E_5(P_i,I_\mu)\right] \; ; \tag{3I.2c}$$

$$\tau(I,I,I_\mu) = \left[\frac{E_2(0,I_\mu) + E_2(P_i,I_\mu) - \frac{2}{P_i}\left[E_3(0,I_\mu) - E_3(P_i,I_\mu)\right]}{P_i\, G(I,I,I_\mu)}\right]\frac{\Delta x}{v} \quad . \tag{3I.2d}$$

Equations (3I.2) reduce to Eqs. (3B.18) for $N_\mu = 1$.

The finite-integral approximation for the multiple-delay-time model is given by the following extension of Eq. (3B.21):

$$B^o(I,K) = c(I,K) \sum_{J=1}^{N} \sum_{I_\mu=1}^{N_\mu} \Big[G(I,J,I_\mu)B(J,K-\tau_k(I,J,I_\mu)) + G_{slp}(I,J,I_\mu)C_1(J,K-\tau_k(I,J,I_\mu)) + G_{crv}(I,J,I_\mu)C_2(J,K-\tau_k(I,J,I_\mu))\Big] \quad . \tag{3I.3}$$

It may be readily seen by comparing Eqs. (3I.3) and (3B.21) that both computing time per time step and transfer-parameter storage requirements are greater by a factor of N_μ in the multiple-delay-time model. Much greater accuracy is expected for time-dependent problems, however, with this more complex model.

In order to evaluate the convergence properties, we recommend that the multiple-delay-time model having flat and slope-correction modes be coded and that this model be tested for various N_μ on such simple problems as the computation of the asymptotic solution for the very supercritical system in Subsection 3E.2 and the transient response problem of Section 3G. We also recommend testing the growth-rate slope-correction proposed in the summary of Chapter 2. With this correction, the expression for $C_1(J,K-\tau_k(I,J,I_\mu))$ for KTRL(J) = 0 is

$$C_1(J,K-\tau_k(I,J,I_\mu)) = B^o(J+1,t-\tau_k(I,J+1,I_\mu)) - B^o(J-1,t-\tau_k(I,J-1,I_\mu)) \quad . \tag{3I.4}$$

Equations (3B.9b) for KTRL(J) = 1 and (3B.10a) for KTRL(J) = -1 are similarly modified.

Table 3I.1 gives some representative values of the $E_n(p,I_\mu)$ for $N_\mu = 6$, which were obtained by numerical integration with a 201-point Simpson's formula. Whether simple recursion relations exist for these functions is not known; we did not attempt to find them.

Table 3I.1

Partial-Range Exponential Integrals, $E_n(p,I_\mu)$,
for $N_\mu = 6$

I_μ	$(\Delta\mu)_{I_\mu}$	$E_2(.01,I_\mu)$	$E_3(.01,I_\mu)$	$E_4(.01,I_\mu)$	$E_5(.01,I_\mu)$
1	0 → 1/6	.1340077(0)	.1241001(-1)	.1411972(-2)	.1781372(-3)
2	1/6 → 2/6	.1598829(0)	.4003413(-1)	.1039401(-1)	.2787545(-2)
3	2/6 → 3/6	.1626615(0)	.6779784(-1)	.2863478(-1)	.1224880(-1)
4	3/6 → 4/6	.1638146(0)	.9556979(-1)	.5613478(-1)	.3319153(-1)
5	4/6 → 5/6	.1644501(0)	.1233444(0)	.9289403(-1)	.7024536(-1)
6	5/6 → 1	.1648533(0)	.1511201(0)	.1389125(0)	.1280399(0)
I_μ		$E_2(.1,I_\mu)$	$E_3(.1,I_\mu)$	$E_4(.1,I_\mu)$	$E_5(.1I_\mu)$
1		.4603062(-1)	.5320844(-2)	.6695686(-3)	.8912697(-4)
2	Same	.1103410(0)	.2801710(-1)	.7365059(-2)	.1996480(-2)
3	as	.1307285(0)	.5464831(-1)	.2314624(-1)	.9927524(-2)
4	above	.1402588(0)	.8191410(-1)	.4816390(-1)	.2850730(-1)
5		.1457870(0)	.1094006(0)	.8243310(-1)	.6236505(-1)
6		.1493988(0)	.1369902(0)	.1259480(0)	.1161303(0)
I_μ		$E_2(1.0,I_\mu)$	$E_3(1.0,I_\mu)$	$E_4(1.0,I_\mu)$	$E_5(1.0,I_\mu)$
1		.5304267(-4)	.7905618(-5)	.1190009(-5)	.1806494(-6)
2	Same	.3494260(-2)	.9843863(-3)	.2826998(-3)	.8251028(-4)
3	as	.1521981(-1)	.6541043(-2)	.2843961(-2)	.1249957(-2)
4	above	.2996671(-1)	.1768419(-1)	.1050383(-1)	.6278192(-2)
5		.4385285(-1)	.3307038(-1)	.2503970(-1)	.1903424(-1)
6		.5590873(-1)	.5140397(-1)	.4739104(-1)	.4380909(-1)

Note: Numbers should be multiplied by 10^{α}, where α is given in the parentheses.

Summary of Chapter 3

In this chapter we have described the development and testing of time-dependent finite-integral models for computing transport solutions in slab geometry. The results for the Milne Problem and for nearly critical systems demonstrate the effectiveness of the variable-distribution models. Although the problems studied have regions less than two mean free paths thick, the effective optical widths are much larger for neutrons emitted at large angles with respect to the x-axis. Where model comparisons have been made, the slope-correction model was found to be far superior to the flat approximation, whereas the curvature correction added little additional accuracy. Where solution accuracy was compared with that of other approximate methods, the finite-integral method was found to be competitive.

The discrete-delay-time approximation is satisfactory for systems in which the local population growth or decay rates are relatively small, i.e., where $|\lambda(J,t')|/[v\Sigma] < 0.02$ for $t' < t$ and $1 \leq J \leq N$. For such systems, it has an advantage over the proposed multiple-delay-time approximation in that less storage is required, computing time per time step is much smaller and the unit time step is larger.

The multiple-delay-time model formulated in Section 3I both improves the sampling of the time dependence of the parent birth rate and bounds the time intervals of eligible parent births in in region J for all $I_\mu > 1$. As this model is a more detailed

approximation of Eq. (1A.1), we expect that the model will be effective for treating faster space-time transients with reasonable accuracy.

CHAPTER 4

APPLICATION OF SLAB MODELS FOR STEADY-STATE CELL CALCULATIONS

Introduction to Chapter 4

In this chapter we extend the slab models to treat infinite systems consisting of repeated, symmetric unit cells. The steady-state neutron population in one of these basically absorbing systems is supported by an external source distribution, which may represent a slowing-down source in a thermal-speed problem or a fission source in a fast-speed problem. Because the unit cell is symmetric, we focus attention on the half-cell and subdivide it into N regions. The boundaries of the half-cell are planes of symmetry for both the properties and the source distribution and, consequently, for the flux distribution also. Since the angular flux $\phi(x_b,\mu) = \phi(x_b,-\mu)$ at each boundary, the boundary planes are treated as perfectly reflecting surfaces.

Our purpose in treating these systems is to study further the worth of the slope-correction and curvature-correction models introduced in Chapter 3. Recently published papers report and compare certain integral parameters obtained for certain two-region slab cells using a wide variety of transport methods, both differential and integral. We have, therefore, a basis for comparison. Furthermore, finite-integral models developed and coded in the past have for the

---

Note: In the statement above, $\phi(x_b,\mu)$ refers to neutrons moving towards the right and $\phi(x_b,-\mu)$ refers to particles moving towards the left, consistent with the interval previously defined for μ, $0 < \mu \leq 1$.

most part dealt with the cell problem. The slab formulations of Honeck[3], Judge[4] and Church[6] are characterized by the flat approximation and iterative solution schemes. By making comparisons with Model F for given limitations on computer time and storage, we show that Models FS and FSC, coupled with an efficient non-iterative solution procedure, extend the usefulness of the integral approach to larger cells and significantly improve the accuracy of distributions computed for half-cells thicker than one mean free path.

In Section 4A, we describe how the expressions (3B.18-19) for the spatial transfer coefficients in an isolated slab reactor are used to compute the spatial transfer coefficients in the half-cell. In Section 4B, we describe the two optional procedures used in program SLBCEL to compute birth rate distributions; these procedures take advantage of the unique simplicity of the time-independent equations. In Section 4C, we describe briefly some features of the program SLBCEL.

In Section 4D, we test the models on cells of various sizes and compare the results with those reported for other methods. From the birth rate and flux distributions computed by the program, such integral parameters as source multiplication, disadvantage factor and thermal utilization are readily obtained. In Section 4E, we report the steady-state distributions computed for a large, isolated, subcritical slab reactor containing an external source. To obtain these results, a special version of Subroutine PARAM1 was written for the case of non-reflecting boundaries; we were then able to

exploit the greatly improved computational efficiency of SLBCEL over that of TOVSR for this class of problems.

4A. COMPUTATION OF THE SPATIAL TRANSFER COEFFICIENTS

The isolated half-cell shown in Fig. 4A.1, with its perfectly reflecting boundaries, is equivalent to the infinite system of repeated symmetric cells. The hypothetical reflections at the cell boundaries account for parent neutrons born in image source regions J. Focussing attention on the isolated half-cell, note that there are two groups of particles which we must consider separately; those emitted towards the right follow the path 1-3-5-, and those emitted towards the left follow the path 2-4-.

A spatial transfer coefficient for the half-cell is then given by the sum of all of the collision contributions 1, 2, 3, 4, etc. from a unit modal source distribution in region J. Each of these angle-integrated contributions can be computed directly from Eqs. (3B.19) for $I \neq J$ provided that P_b is redefined as the sum of the optical widths of all regions traversed by the particles after escaping source region J and before entering region I on the pass in which they collide in I. A modification is required in Eq. (3B.19b) for $G_{slp}(I,J)$; regardless of the relative positions of I and J, the expression $[I-J]/|I-J|$ is replaced by +1 for particles emitted towards the right and by -1 for those emitted towards the left. For I=J, Eqs. (3B.18a,c) are used to compute the contributions to G(I,I) and $G_{crv}(I,I)$ of collisions occurring before the particles can escape the source region. These numbers are then stored. For collision

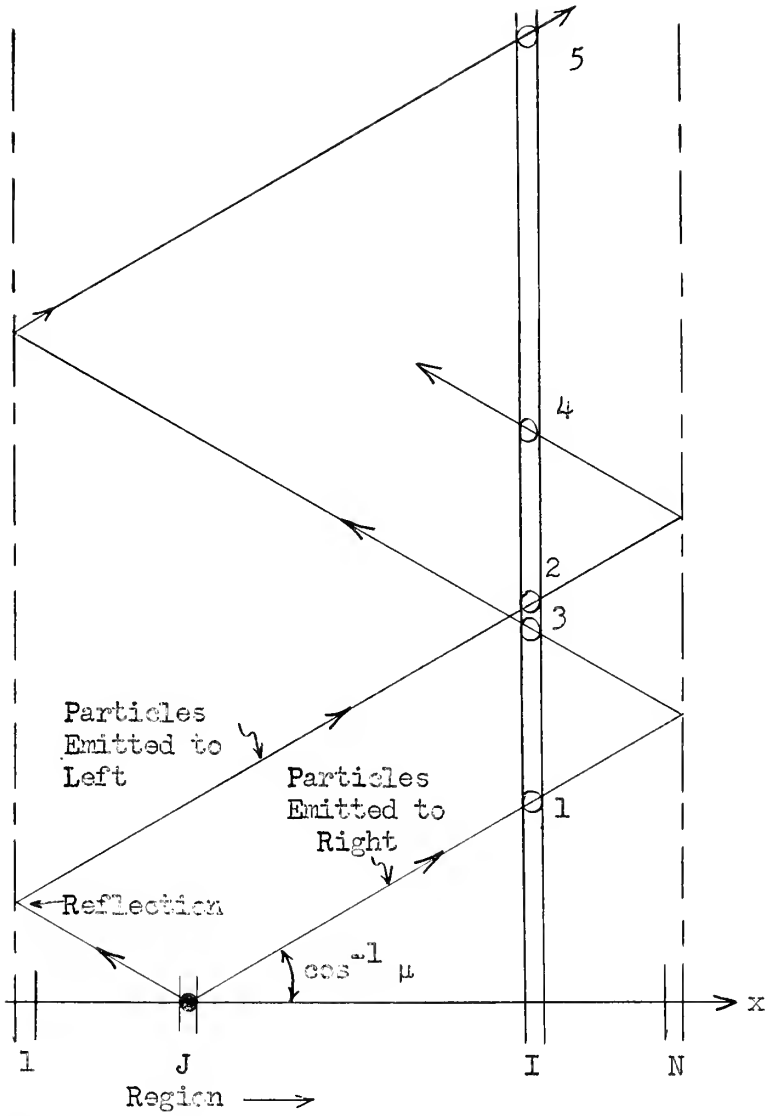

Figure 4A.1 Isolated Half-cell with Reflecting Boundaries.

contributions in subsequent passes through region I, Eqs. (3B.19) are applicable. Note that $G_{slp}(I,I)$ is not normally equal to zero in the cell formulation.

In computing the transfer coefficients with Eqs. (3B.19a-c) we take advantage of the linearity of the expressions in the $E_n(p)$. Note that Eq. (3B.19c) contains all twelve $E_n(p)$ terms required for a particular collision contribution. These twelve terms are identified successivly by the elements F(1) through F(12) of array F for particles emitted towards the right and by the elements F(13) through F(24) for particles emitted towards the left. Consider the case of the particles emitted towards the right in Fig. (4A.1) and their contribution to the transfer coefficients for J→I. P_i and P_j are fixed for all contributions 1, 3, 5, etc. For the collision contribution denoted by 1,

$$P_b = \sum_{J+1}^{I-1} P(L) \quad . \tag{4A.1}$$

The value of each of the 12 $E_n(p)$ is found and is stored in the appropriate element of F. Then P_b is increased by

$$\Delta P_{b1} = P_i + 2 \sum_{I+1}^{N} P(L) \; ; \tag{4A.2}$$

The corresponding $E_n(p)$ values for collision contribution 3 are found and added to the appropriate elements of F. For collision contribution 5, P_b is increased by

$$\Delta P_{b2} = P_1 + 2 \sum_{1}^{I-1} P(L) \quad , \qquad (4A.3)$$

and the corresponding values of the $E_n(p)$ added to the elements of F. The steps described in Eqs. (4A.2 and 3) are repeated (NRFL-1) times, where NRFL is a program control variable giving the number of successive double reflections which are to be considered before attenuation renders further contributions negligible. The analogous procedure is then carried out for the particles emitted towards the left, yielding the elements 13 to 24 of array F. The Eqs. (3B.19a-c) are then reformulated in terms of the F(L) and the cell transfer coefficients are computed. $G_{slp}(I,J)$, for example, is given by the following set of expressions:

$$\alpha = [F(1) + F(2) - F(3) - F(4)] - [F(13) + F(14) - F(15) - F(16)]; \qquad (4A.4a)$$

$$\beta = [-F(5) + F(6) - F(7) + F(8)] - [-F(17) + F(18) - F(19) + F(20)]; \qquad (4A.4b)$$

$$G_{slp}(I,J) = \frac{1}{SP_J}\left[\alpha + \frac{2\beta}{P_J}\right] \quad . \qquad (4A.4c)$$

4B. ITERATIVE AND NON-ITERATIVE PROCEDURES FOR SOLVING THE NUMERICAL EQUATIONS

4B.1 Simplification of the Iterative Equations for Time-Independent Problems

In formulating the variable-distribution models we assume, as in Chapter 3, that c and Σ are homogeneous across at least three regions

which include region J. Because the external sources normally represent fission or slowing-down sources, we treat the external source distribution as continuous and smooth across the same regions. B(I,K) is used as the fundamental variable in program SLBCEL; slope and curvature corrections are applied to the external source as well as to the progeny birth rate. The generation-to-generation finite-integral approximation is then given by the following set of equations:

$$B(I,K) = c(I) \sum_{J=1}^{N} [G(I,J)C_o(J,K-1) + G_{slp}(I,J)C_1(J,K-1) + G_{crv}(I,J)C_2(J,K-1)] + S(I) \; ; \qquad (4B.1a)$$

$$C_o(J,K-1) = B(J,K-1) \; ; \qquad (4B.1b)$$

for KTRL(J) = + 1,

$$C_1(J,K-1) = 4B(J+1,K-1) - 3B(J,K-1) - B(J+2,K-1) \; , \qquad (4B.1c)$$

and

$$C_2(J,K-1) = \frac{B(J+2,K-1) + B(J,K-1)}{2} - B(J+1,K-1) \; ; \qquad (4B.1d)$$

for KTRL(J) = -1

$$C_1(J,K-1) = -4B(J-1,K-1) + 3B(J,K-1) + B(J-2,K-1) \; , \qquad (4B.1e)$$

and

$$C_2(J,K-1) = \frac{B(J-2,K-1) + B(J,K-1)}{2} - B(J-1,K-1) \; ; \qquad (4B.1f)$$

finally, for KTRL(J) = 0,

$$C_1(J,K-1) = B(J+1,K-1) - B(J-1,K-1) \quad , \tag{4B.1g}$$

and

$$C_2(J,K-1) = \frac{B(J+1,K-1) + B(J-1,K-1)}{2} - B(J,K-1) \quad . \tag{4B.1h}$$

Since the generation agrument is the same for all terms in Eqs. (4B.1b-h), we can directly substitute these expressions into Eq. (4B.1a) and generate the following matrix equation:

$$\underline{B}(K) = \underline{c}T\underline{B}(K-1) + \underline{S} \quad , \tag{4B.2}$$

where $\underline{B}$ and $\underline{S}$ are column vectors, $\underline{c}$ is a row vector and T is square matrix N elements on a side. If we now compute the matrix,

$$H = \underline{c}T, \tag{4B.3}$$

we obtain the simple iterative operational form

$$\underline{B}(K) = H\underline{B}(K-1) + \underline{S} \quad , \tag{4B.4a}$$

or

$$B(I,K) = \sum_{J=1}^{N} H(I,J)B(J,K-1) + S(I) \quad . \tag{4B.4b}$$

In SLBCEL, the transfer coefficients are computed in Subroutine PARAM1, the arrays T and H are computed in Subroutine PARAM2, and an option is available for computing the solution by iteration (4B.4) in Subroutine CLCITN. Our purpose for including the iteration option into SLBCEL was to check the solutions computed by the more efficient non-iterative scheme described below.

4B.2 Non-Iterative Computational Procedure

If $\underline{B}(K-1)$ in Eq. (4B.4a) is the correct solution vector, the computed $\underline{B}(K)$ will equal $\underline{B}(K-1)$. The converged steady-state solution $\underline{B}$ for $K\to\infty$ is then given by

$$[I-H]\underline{B} = \underline{S} \ , \qquad (4B.5)$$

where I is the identity matrix, with elements on the principal diagonal equal to unity and all other elements equal to zero. The vector $\underline{B}$ is the only unknown in Eq. (4B.5). The equation therefore represents a set of N linear, inhomogeneous, algebraic equations.

In order to solve these equations, the M.I.T. Computation Center Library function XSIMEQF[19] was used in Subroutine CLCMEQ. XSIMEQF uses a reduction procedure to solve the set of N equations. For all problems in which the XSIMEQF-computed solutions were tested by iteration, the iterated solutions agreed to within 3 units in the seventh digit. The non-iterative solutions are therefore as accurate as can be desired, considering the approximations in our method.

4C. THE COMPUTER PROGRAM SLBCEL

The FORTRAN II program SLBCEL is listed in Appendix C. The program may be used with $N \leq 40$. Inputs are P(I), c(I), and S(I).* The locations of property-discontinuity interfaces are specified by KTRL(J), as in TOVSR. The model to be used for approximating the birth rate distribution in region J is specified by KMDC(J), as in

---

* Note: There is no need to specify Δx or W for time-independent problems.

TOVSR. The use of either the iterative or the non-iterative solution procedure is optional. With Model F, all N regions may be assigned different properties. With Model FS or FSC, properties must be homogeneous over intervals of at least three regions.

Program output includes the unnormalized birth rate distribution, the normalized flux distribution, and the cell multiplication. The relative flux distribution (mean flux in region I) is computed according to

$$\phi(I) = \frac{B(I) - S(I)}{c(I)\ P(I)} \ ; \qquad (4C.1)$$

it is then normalized such that

$$\sum_{I=1}^{N} \phi(I) = N \ . \qquad (4C.2)$$

The cell multiplication is given by

$$\text{Multiplication} = \sum_{I=1}^{N} B(I) \Big/ \sum_{I=1}^{N} S(I) \qquad (4C.3)$$

The major portion of the required computing time is used for computing the transfer coefficient arrays G, G_{slp} and G_{crv}, particularly in the case of optically-thin cells for which NRFL must be large. Note that the transfer coefficients depend only on the set of N optical region widths P(I). Once a set is computed, it can be used for efficient parametric studies or problems with varying property-discontinuity interfaces (consistent with discontinuities in P(I), of course), models (F, FS or FSC in a particular region J),

secondary emission coefficients, and source distributions. This flexibility has been incorporated into the program. To solve successive problems having identical arrays G, G_{slp} and G_{crv} but different sets of KTRL(J) and KMDC(J), the program recomputes the elements of array T according to the new discontinuity-interface locations and model assignments for the various regions. Further, the program logic permits the successive solution of problems having the same array T but different arrays c and S and different solution procedures. In addition, options are included for punched-card output of the coefficient arrays and for reading the arrays back in on a later job, in lieu of recomputing them.

4D. RESULTS OF CELL CALCULATIONS

In this section we report the results obtained in test calculations on simple, fuel-moderator type cells reported in the literature. Optical thicknesses of the tested half-cells range from 0.2208 to 12.22 mean free paths.

4D.1 Very Small Half-Cell .2208 Mean Free Path Thick

In this subsection we report the results obtained for a very small cell. The half-cell properties and input data are given in Fig. (4D.1). This cell was studied by Meneghetti[20] using the DSN, P_L and double-P_L methods and by Church[6] using his HGI method--an approximate integral formulation useful for half-cells less than one mean free path thick.

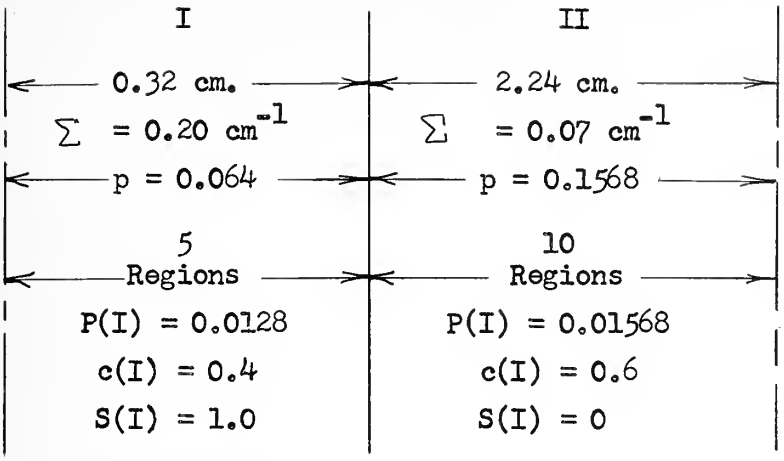

Figure 4D.1 Parameters for Small Half-Cell Problem

The distributions computed by SLBCEL using Models F, FS and FSC are given in Table 4D.1. The advantage factor, equal to the mean flux in cell section I divided by the mean flux in cell section II, is computed from the output distribution. The source in cell section I represents a fission source; the cross-sections are those of a fast group. Note that the results of Models F and FS are nearly identical; the small deviations of the Model FS results have the correct directions for a slope correction. The comparative results demonstrate that the flat approximation is quite satisfactory for small cells with fairly flat distributions and regions with very small P(I). Based on the similarity of the Model F and Model FS results, there should not be a detectable difference between the Model FS and Model FSC results. The Model FSC results demonstrate the effects of errors in the computed elements of the array G_{crv} for very thin source regions J. We refer the reader to the comments in Section 3C.

Table 4D.1

Results of Small Cell Problem

	Model F		Model FS	Model FSC	
Mult.	2.16079		2.16079	2.16067	
Advantage Factor	1.1210		1.1210	1.1211	
I	B(I)	Normalized ϕ(I)	Normalized ϕ(I)	Normalized ϕ(I)	Direction of Error
1	1.27524	1.09311	1.09313	1.09288	-
2	1.27438	1.08968	1.08970	1.08997	+
3	1.27259	1.08260	1.08262	1.08274	+
4	1.26963	1.07083	1.07085	1.07092	+
5 (interface)	1.26473	1.05137	1.05140	1.05147	+
6	.47014	1.01614	1.01615	1.01627	+
7	.45928	.99267	.99266	.99247	-
8	.45199	.97691	.97689	.97683	-
9	.44651	.96507	.96506	.96520	+
10	.44231	.95598	.95597	.95602	+
11	.43904	.94892	.94891	.94883	-
12	.43659	.94362	.94361	.94361	0
13	.43481	.93978	.93977	.93973	-
14	.43365	.93727	.93725	.93709	-
15	.43309	.93605	.93604	.93599	-

In Table 4D.2, we compare the SLBCEL advantage factor with those reported for other methods. Meneghetti analyzes the DSN, P_L and double-P_L results. Our result agrees with the HGI and double-P_5 values to within 0.5 percent.

Of all systems solved using SLBCEL, this small cell required the longest computing time, 2.89 minutes. All but a small fraction of

Table 4D.2

Advantage Factors for Small Cell by Various Calculations

L	DSN	L	P_L	L	double-P_L	HGI	SLBCEL
		1	1.014				
2	1.015						
		3	1.028				
4	1.038	5	1.042				
		7	1.053	1	1.054		
		9	1.065				
8	1.074	11	1.076				
		13	1.085	2	1.091		
16	1.108			3	1.115		
						1.119	1.1210
				4	1.124		
				5	1.126		

Notes: a) DSN, P_L, double-P_L from Meneghetti[20]
b) HGI from Church[6]
c) Numbers given above were estimated from published graphs.

this time was used in computing the transfer coefficients. Fifty-six double reflections were treated; this value of NRFL is equivalent to following those particles emitted parallel to the x-axis for 25 mean free paths. NRFL and the computing time could therefore have been reduced by one-half without noticeable changes in the computed distributions. In addition, the closeness of the Model F and Model FS solutions shows that a much smaller N would be satisfactory with either Model F or Model FS. (Computing time for computing the transfer parameters for any particular model is proportional to N^2.)

This problem requires the use of $N \geq 6$ for Model FS, at least three regions for the fuel section and three for the moderator section. We suspect, based on the N = 15 results and the relative flatness of the overall flux distribution that the Model F and Model FS solutions for N = 6 would agree closely. In this case, Model F would be preferable for this problem since it would require computing only the coefficients G(I,J) and may yield satisfactory solutions for $N < 6$. For very small cells, then, we claim no advantage for Models FS and FSC over the flat approximation.

Ten solutions were computed during the 2.89 minute job. The three non-iterative solutions given in Table 4D.1 were checked by the iterative method; in addition, non-iterative and iterative, Model F and Model FS solutions were computed for an altered source distribution in which $S(I) = 0$ for $I \leq 5$ and $S(I) = 1.0$ for $I \geq 6$. These latter solutions yielded a disadvantage factor of 1.0741, which is the ratio of the mean flux in cell section II to that in cell section I. The fact that these ten successive solutions were computed illustrates the program flexibility.

4D.2 Intermediate Cells

In this subsection we study a group of four fuel-moderator cells having the properties given in Fig. (4D.2). Half-cell optical widths range from 0.8872 to 3.5488 mfp. Disadvantage factors for these cells have been reported by a number of authors.

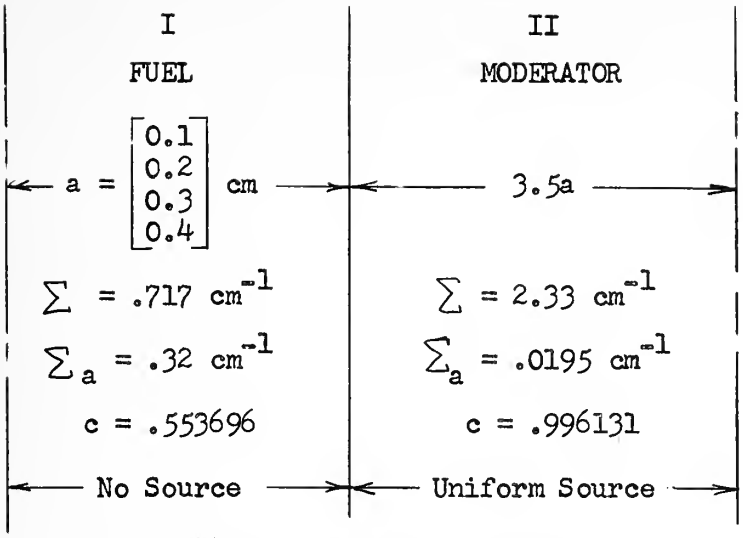

Figure 4D.2 Physical Parameters of Intermediate-Size Half-Cells

The input data, computed multiplications, and computed disadvantage factors for eight runs are tabulated in Table 4D.3. In runs 1, 5 and 7, different approximation models are used in the fuel and moderator regions. Comparing runs 4, 5 and 6, note that the curvature correction has negligible effect on the solutions for the largest cell of this group. Comparing runs 7 and 8, note that the use of the slope correction in the moderator regions gives a small but significant improvement over the values obtained with the flat approximation.

The relative flux distributions for runs 1, 2, 3, 4 and 8 and the birth rate distribution for run 4 are given in Table 4D.4. Comparing runs 4 and 8, note the tendency of the flat approximation to produce a distribution which is too flat; this effect is general. The increasing spread between high and low flux values with increasing cell size is evident in both the distributions and the disadvantage

Table 4D.3

SLBCEL Runs for Intermediate Cells

Run No.	a, cm.	N	Fuel:S(I)=0			Moderator:S(I)=1.0			Multi-plication	Dis-advantage Factor
			Model	No. of rgns.	P(I)	Model	No. of rgns.	P(I)		
1	0.1	18	F	4	.017925	FS	14	.05825	24.484	1.0979
2	0.2	18	FS	4	.03585	FS	14	.1165	26.633	1.2317
3	0.3	20	FS	6	.03585	FS	14	.17475	29.311	1.4075
4	0.4	27	FSC	6	.0478	FSC	21	.155333	32.463	1.6283
5	↓	↓	FS	↓	↓	FSC	↓	↓	32.463	1.6283
6			FS			FS			32.463	1.6283
7			F			FS			32.464	1.6284
8	↓	↓	F	↓	↓	F	↓	↓	32.406	1.6241

factors. Fig. 4D.3 shows the flux distribution in the half-cell with the 0.4 cm fuel region.

The calculated values of the disadvantage factors for the four cells are compared with values reported in the literature in Table 4D.5. Note the scatter in the results obtained by different workers. The SLBCEL values fall within the range of the results of the more rigorous of the other methods--the S_8 calculations and the methods of Weiss and Ferziger/Robinson.

In order to check the SLBCEL value of 1.628 for the 1.8 cm half-cell, further Model FSC tests were made with varying numbers of sub-regions in the fuel and moderator sections. These tests were expected to point out any inconsistencies in our cell formulation or to establish the degree of convergence of the solutions with respect to the number and disposition of subregions. The results, given in Table 4D.6, strongly support the value quoted in Table 4D.5.

Table 4D.4

Computed Distributions for Intermediate Cells

I	Normalized Mean Flux in Region I					B(I)
	Run 1 a = 0.1	Run 2 a = 0.2	Run 3 a = 0.3	Run 8 a = 0.4 Model F	Run 4 a = 0.4 Model FSC	Run 4 a = 0.4 Model FSC
1	.92246	.83498	.75927	.6499	.64863	3.11204
2	.92553	.83938	.76211	.6534	.65213	3.12884
3	.93015	.84885	.76795	.6607	.65933	3.16339
4	.93895	.86606	.77719	.6721	.67070	3.21795
5	.96241	.91583	.79070	.6889	.68729	3.29753
6	.98433	.95766	.81114	.7142	.71229	3.41748
7	.99709	.98610	.87952	.7815	.78016	22.7845
8	1.00677	1.00856	.94519	.8460	.84540	24.6064
9	1.01456	1.02719	.99217	.8952	.89491	25.9886
10	1.02088	1.04295	1.03049	.9371	.93704	27.1651
11	1.02627	1.05637	1.06305	.9743	.97434	28.2067
12	1.03069	1.06774	1.09110	1.0078	1.00797	29.1456
13	1.03434	1.07725	1.11531	1.0383	1.03854	29.9992
14	1.03733	1.08504	1.13604	1.0660	1.06643	30.7780
15	1.03960	1.09119	1.15354	1.0914	1.09188	31.4887
16	1.04135	1.09576	1.16795	1.1145	1.11506	32.1359
17	1.04241	1.09879	1.17939	1.1355	1.13608	32.7229
18	1.04306	1.10030	1.18792	1.1543	1.15502	33.2519
19			1.19358	1.1712	1.17196	33.7247
20			1.19640	1.1861	1.18692	34.1425
21				1.1991	1.19995	34.5064
22				1.2102	1.21108	34.8172
23				1.2194	1.22032	35.0753
24				1.2268	1.22770	35.2814
25				1.2323	1.23323	35.4356
26				1.2360	1.23691	35.5383
27				1.2378	1.23874	35.5896

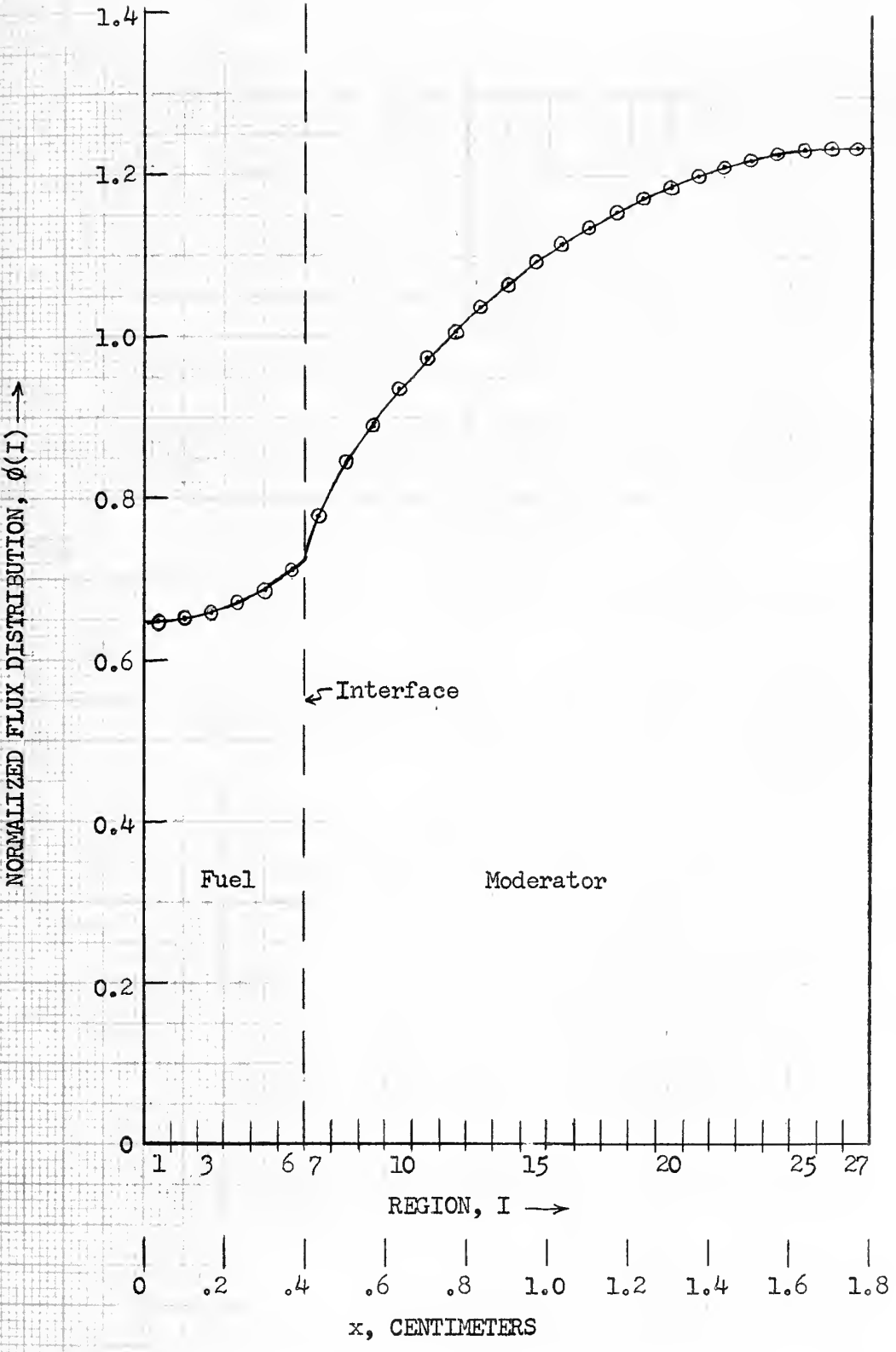

Figure 4D.3 Flux Distribution in 1.8 cm. Half-cell.

Table 4D.5

Disadvantage Factors for Intermediate Cells by Various Calculations *

Method	Reference	Disadvantage Factor			
		a=0.1	a=0.2	a=0.3	a=0.4 cm
P_1	21	1.02	1.11	1.24	1.45
Pomraning and Clark	23	1.06	1.18	1.34	1.56
Theys	24	1.08	1.20	1.37	1.59
S_8 (Perkins)	22	1.069	1.203	1.382	1.605
Weiss	21	1.097	1.215	1.382	1.601
SLBCEL	--	1.098	1.232	1.408	1.628
Ferziger and Robinson	22	1.099	1.239	1.422	1.650
S_8 (Theys)	24	1.09	1.23	1.42	1.65
Pomraning	18	1.24	1.34	1.48	1.68

The footnote referenced by Table 4D.5 indicates discrepancies in the exact values of c used by different workers. In order to check the variation of the disadvantage factor with different combinations of c in the fuel and moderator, four additional runs were made using the transfer coefficient arrays previously computed and punched out on cards. The results are given in Table 4D.7,

* Note: In Table 4D.5, all references use $\Sigma = .717$ cm^{-1} in the fuel and $\Sigma = 2.33$ cm^{-1} in the moderator. It seems that there are some discrepencies, however, in the values used for c in the various calculations. Reference 22 specifies $\Sigma_a = .32$ cm^{-1} in the fuel and $\Sigma_a = .0195$ cm^{-1} in the moderator, where Σ_a is the absorption cross section. From these values we calculated our values of c. References 18, 21 and 23 specify c = 0.554 in the fuel and c = 1 or 1.000 in the moderator. With the latter values of c, SLBCEL solutions yield somewhat larger disadvantage factors than those given in Table 4D.5. (See Table 4D.7) The earliest of the references, 24, specifies $\Sigma_a = .320$ cm^{-1} in the fuel but does not specify either c or Σ_a for the moderator, which is water.

Table 4D.6

Disadvantage Factors for the 1.8 cm Half-Cell with Various Arrangements of Regions

Optical Width of Fuel = .2868 mean free path Optical Width of Moderator = 3.262 mean free paths			
N	No. of Fuel Regions	No. of Moderator Regions	Disadvantage Factor
11	4	7	1.627
22	8	14	1.6280
27	6	21	1.6283
30	3	27	1.6283
28	8	20 { 9 covering .699 mfp nearest interface 11 covering the remaining 2.563 mfp	1.6284

Table 4D.7

Variation of Computed Parameters with c in the 1.8 cm Half-Cell

Model FS		N = 27 (6-21)	
Fuel c	Moderator c	Multiplication	Disadvantage Factor
.553696	0.991631	32.463	1.6283
.553696	1.0	43.968	1.6374
.554	1.0	43.987	1.6370
.554	0.99	30.898	1.6262

from which it is clear that the disadvantage factor does not vary greatly with c. Note, however, the sensitivity of the cell multiplication.

The job time for the four runs of Table 4D.7 was only 0.59 minutes, of which only 17 seconds were used for executing the

program. Since the arrays, G, G_{slp} are G_{crv} had been computed previously, we can conclude that the time required to solve a twenty-seven region problem by the non-iterative method is approximately four seconds. The usefulness of the SLBCEL for parametric studies is evident. Once the value of N and the values of the P(I) are specified, the arrays G, G_{slp}, and G_{crv} are determined. These arrays can then be used for successive problems with varying numbers and locations of discontinuity interfaces, varying c(I) and varying source distributions.

For the intermediate-size cells, in particular for the 1.8 cm half-cell, we conclude that Model FS is the more satisfactory Model. First, note that the 27-region, Model F result in Table 4D.3 is not as accurate as the 11-region, Model FSC result in Table 4D.6. Model F with N = 27 requires more computing time and storage than Model FSC with N = 11. Second, note that the integral parameters in Table 4D.3 obtained with Models FS and FSC for N = 27 are identical. From results presented in Chapter 3 and in the next section, it is not likely that Model FS and Model FSC results would differ by much for smaller values of N.

4D.3 Very Large Half-Cell 12.22 Mean Free Paths Thick

In this subsection we study a representative, very thick half-cell consisting of a small fuel region and a large moderator region. The half-cell data are given in Fig. (4D.4). Note that we have split the moderator region into two sections and have used thinner regions in

the section adjacent to the fuel. This cell has been studied by Weinberg and Wigner[9] and by Pomraning[18].

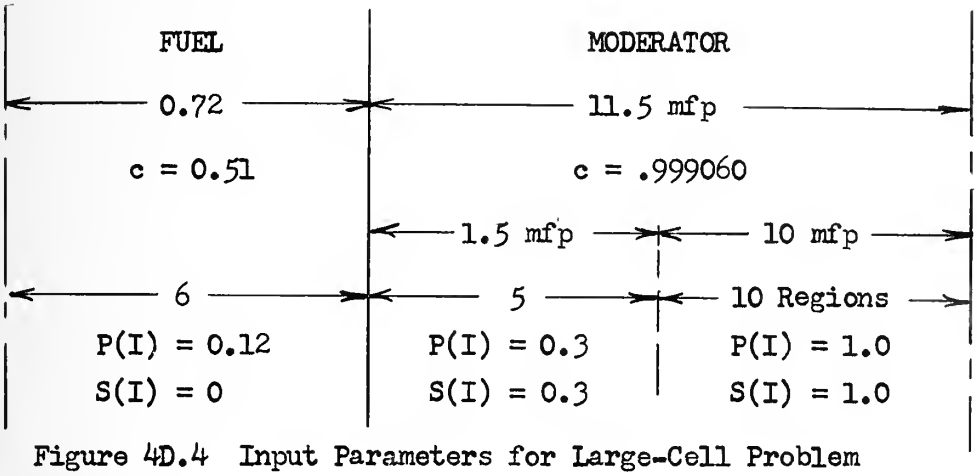

Figure 4D.4 Input Parameters for Large-Cell Problem

Calculated parameters of interest for purposes of comparison are the disadvantage factor,

$$\frac{\bar{\phi}_{mod.}}{\bar{\phi}_{fuel}} = \frac{\sum_{I=7}^{21}\left[B(I) - S(I)\right]}{[.99906][11.5]} \cdot \frac{[.51][.72]}{\sum_{I=1}^{6}\left[B(I) - S(I)\right]}, \qquad (4D.1)$$

and the thermal utilization,

$$f = \frac{\left[\frac{1 - .51}{.51}\right]\sum_{I=1}^{6}[B(I) - S(I)]}{\sum_{I=1}^{21} S(I)}. \qquad (4D.2)$$

These parameters, plus the computed multiplications and distributions, are given in Table 4D.8 for runs made with Models F, FS, and FSC. The effect of the curvature correction is noticeable but still small.

Note that the largest region is one mean free path thick. The flat approximation, Model F, is totally inadequate for this system, as can be seen from the flattened birth rate distribution in Table 4D.8 and in the comparison of our results with published data in Table 4D.9. The integral parameters computed with Models FS and FSC agree with the exact values, whereas the flat approximation yields poorer results than diffusion theory. For the Model FS calculation reported at the bottom of Table 4D.9, eight regions were used for the fuel section and 32 for the moderator section; of the latter, fifteen were 0.2 mfp thick and seventeen 0.5 mfp thick.

An interesting feature of the variable-distribution models in SLBCEL is the capability to treat smoothly-varying source distributions with the same ease as uniform source distributions. For example, external source distributions having a quadratic shape between two discontinuity interfaces are rigorously represented by Model FSC; those having higher-order shapes are approximated by a sequence of quadratic shapes. An additional run was made with Model FSC to compute the distribution resulting from a source which decreases linearly with optical distance from the fuel interface:

$$S(p) = 1.575 - 0.1[p - 0.72] \frac{\text{neutrons}}{\text{cm}^2(\text{mfp})\text{sec}} \quad . \qquad (4D.3)$$

The computed integral parameters and birth rate distributions are given in Table 4D.10, where they are compared with the results for the uniform source distribution.

Table 4D.8

Results for Very Large Half-Cell

	Model F	Model FS	Model FSC	
Disadvantage Factor	5.0238	5.4900	5.4903	
Thermal Utilization	.8666	.85600	.85599+	
Multiplication	143.68	154.93	154.94	
I	B(I)	B(I)	B(I)	Relative Flux
1	1.50577	1.48962	1.48962	.237925
2	1.53902	1.52229	1.52229	.243142
3	1.60773	1.58973	1.58973	.253914
4	1.71714	1.69695	1.69695	.271039
5	1.87844	1.85456	1.85454	.296210
6	2.12456	2.09266	2.09259	.334232
(interface)				
7	13.5664	13.4331	13.4334	.428331
8	16.6450	16.5643	16.5645	.530447
9	19.3590	19.2919	19.2918	.619393
10	21.9142	21.8323	21.8318	.702233
11	24.4165	24.2473	24.2457	.780959
(pseudo-interface)				
12	95.3673	97.0047	97.0161	.939435
13	114.1602	119.6497	119.6591	1.16098
14	130.8847	139.5569	139.5652	1.35574
15	145.4443	156.8359	156.8438	1.52480
16	157.8626	171.5524	171.5599	1.66878
17	168.1673	183.7522	183.7594	1.78814
18	176.3823	193.4706	193.4776	1.88323
19	182.5269	200.7355	200.7424	1.95431
20	186.6154	205.5674	205.5742	2.00158
21	188.6572	207.9795	207.9863	2.02518

Table 4D.9

Large Cell Integral Parameters by Various Calculations

Method	Reference	Disadvantage Factor	Thermal Utilization
Model F (6-5-10)	--	5.024	0.8666
Diffusion Theory	18	5.108	0.8647
P_1	18	5.201	0.8625
Pomraning	18	5.429	0.8574
P_3	18	5.459	0.8567
P_5	18	5.481	0.8562
Exact	18,9	5.490	0.8560
Models FS and FSC (6-5-10)	--	5.490	0.8560
Model FS (8-15-17)	--	5.4908	0.85599

Table 4D.10

Comparison of Solutions for Flat and Linearly Decreasing Source Distributions in the Moderator Region of the Large Half-Cell

		Uniform Source		Linearly Decreasing Source	
Disadvantage Factor		5.4903		4.8416	
Thermal Utilization		.8560		.8708	
Multiplication		159.94		139.21	
I	P(I)	S(I)	B(I)	S(I)	B(I)
1	.12	0	1.48962	0	1.51376
2	.12	0	1.52229	0	1.54717
3	.12	0	1.58973	0	1.61620
4	.12	0	1.69695	0	1.72598
5	.12	0	1.85454	0	1.88755
6	.12	0	2.09259	0	2.13233
(interface)					
7	.3	.3	13.4334	.468	13.8740
8	.3	.3	16.5645	.459	17.0212
9	.3	.3	19.2918	.450	19.7039
10	.3	.3	21.8318	.441	22.1526
11	.3	.3	24.2457	.432	24.4347
(pseudo-interface)					
12	1.0	1.0	97.0161	1.375	96.2209
13	1.0	1.0	119.6591	1.275	115.8524
14	1.0	1.0	139.5652	1.175	131.9220
15	1.0	1.0	156.8438	1.075	144.8158
16	1.0	1.0	171.5599	.975	154.8878
17	1.0	1.0	183.7594	.875	162.4710
18	1.0	1.0	193.4776	.775	167.8880
19	1.0	1.0	200.7424	.675	171.4549
20	1.0	1.0	205.5742	.575	173.4835
21	1.0	1.0	209.9863	.475	174.2688
		SUM: 11.5		SUM: 11.500	

4E. RESULTS OF ISOLATED REACTOR CALCULATIONS

In this subsection we report the steady-state distributions computed by SLBCEL for a very large, three-section, isolated reactor. The special version of Subroutine PARAM1 for non-reflecting boundaries was used for these computations. The system studied is shown in Fig. (4E.1). Runs were made with Models F, FS and FSC for both N = 18 and N = 36. Total job time was 0.94 minutes.

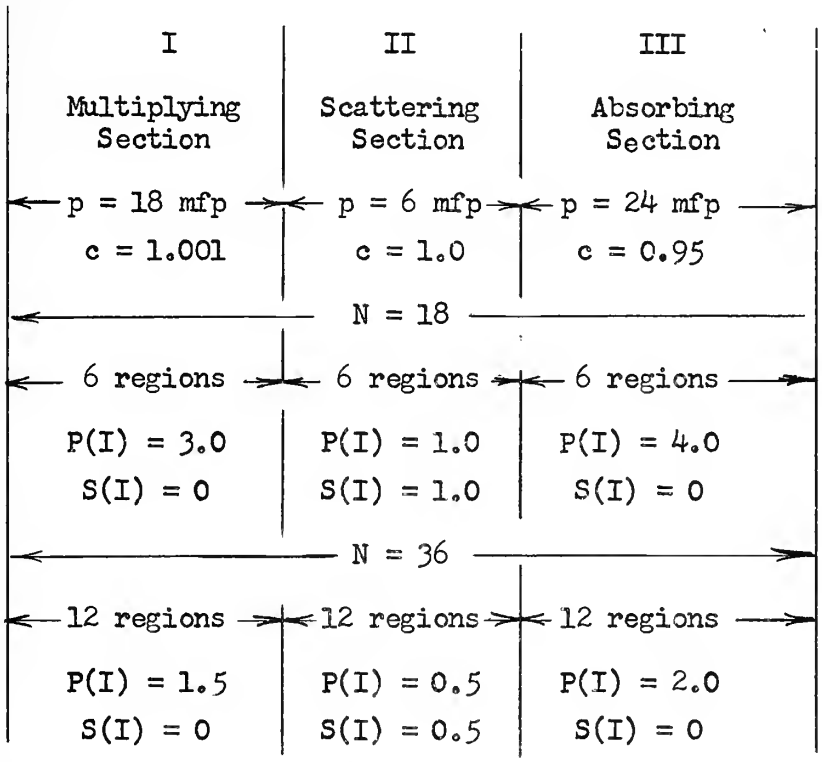

Figure 4E.1 Input Parameters for Three-Region Reactor

The regions in this reactor are sufficiently large, considering the wide variation in the flux distribution, to illustrate the limitations of our models. The computed values of the multiplication are given in Table 4E.1. The closeness of the Model FS and FSC results is somewhat surprising for such a large system, particularly in con-

Table 4E.1

Computed Values of the Multiplication
in Large Isolated System

N	Model F	Model FS	Model FSC
18	131.7	210.7	210.9
36	175.4	219.2	219.4

trast with the relatively large difference between the 18- and 36-region results. The computed flux distributions, given in Tables 4E.2 and 4E.3, show that eighteen regions are inadequate for generating a correct flux distribution. The quadratic approximations for the parent birth rate distribution are incapable of fitting a distribution which decreases by two orders of magnitude across three regions in the absorbing section. By contrast, the 36-region flux distributions computed with Models FS and FSC decrease by only one order of magnitude across three regions and appear to be reasonably good solutions. Using the 36-region, Model FSC distribution as the basis for comparison, it is clear from Table 4E.3 that, in spite of the negative fluxes, the 18-region distributions computed with Models FS and FSC are superior to the 36-region distribution computed with Model F.

The 36-region, Model FSC distribution is shown in Fig. (4E.2). An expanded view of the relative flux in the regions near the scatterer-absorber interface, as approximated by the superimposed modes of Model FSC, is shown in Fig. (4E.3). Note that the discontinity at the interface is relatively slight for such a wide variation in level over a few-region interval.

Table 4E.2

Relative Mean Fluxes Computed for Large System with N = 36

	Model F		Model FS	Model FSC	
I	$\phi(I)$	$\frac{\phi(I)+\phi(I+1)}{2}$	$\phi(I)$	$\phi(I)$	$\frac{\phi(I)+\phi(I+1)}{2}$
1	.2017	.2908	.1818	.1818	.2788
2	.3798		.3757	.3757	
3	.5550	.6413	.5644	.5643	.6565
4	.7275		.7488	.7487	
5	.8966	.9790	.9281	.9280	1.0146
6	1.0614		1.1011	1.1011	
7	1.2212	1.2982	1.2668	1.2667	1.3452
8	1.3752		1.4238	1.4237	
9	1.5227	1.5929	1.5713	1.5712	1.6397
10	1.6631		1.7082	1.7081	
11	1.7957	1.8582	1.8339	1.8337	1.8913
12	1.9206		1.9489	1.9488	
(interface)-					
13	2.0129	2.0303	2.0253	2.0251	2.0337
14	2.0477		2.0426	2.0423	
15	2.0558	2.0480	2.0385	2.0383	2.0264
16	2.0401		2.0146	2.0144	
17	2.0013	1.9655	1.9712	1.9711	1.9398
18	1.9396		1.9085	1.9085	
19	1.8549	1.8011	1.8265	1.8266	1.7760
20	1.7473		1.7252	1.7253	
21	1.6164	1.5391	1.6043	1.6046	1.5343
22	1.4617		1.4635	1.4639	
23	1.3811	1.1736	1.3013	1.3021	1.2078
24	1.0661		1.1122	1.1135	
(interface)-					
25	.6951	.5400	.7031	.7019	.5171
26	.3849		.3334	.3322	
27	.2129	.1654	.1521	.1520	.1106
28	.1178		.0688	.0691	
29	.0651	.0506	.0310	.0314	.0228
30	.0360		.0140	.0142	
31	.0199	.0155	.0063	.0065	.0047
32	.0110		.0028	.0029	
33	.0060	.0047	.0013	.0013	.0010
34	.0033		.0006	.0006	
35	.0017	.0012	.0002	.0002	.0002
36	.0007		.0001	.0001	

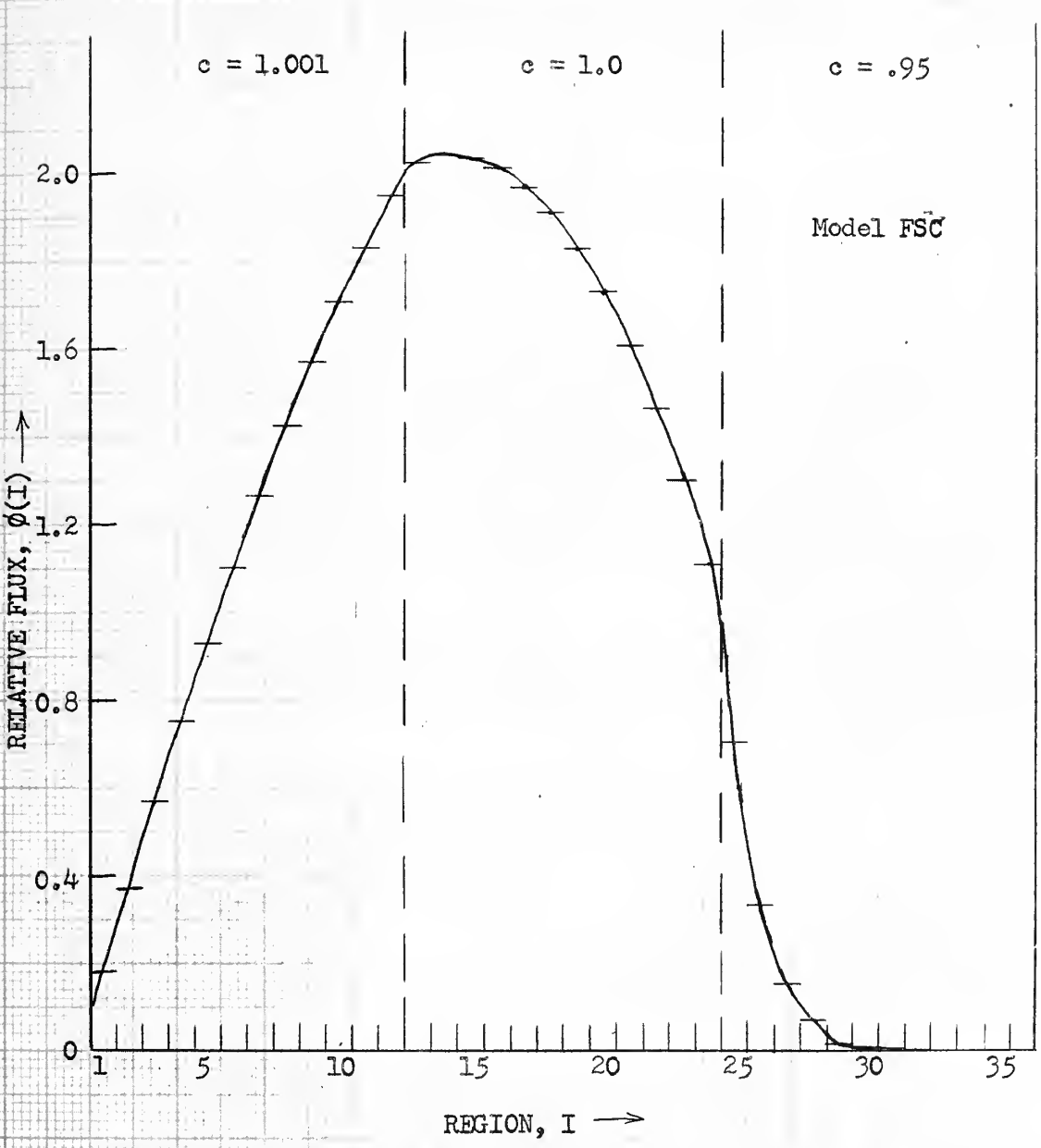

Figure 4E.2 Flux Distribution in Large Isolated System with Uniform Source in Central Section.

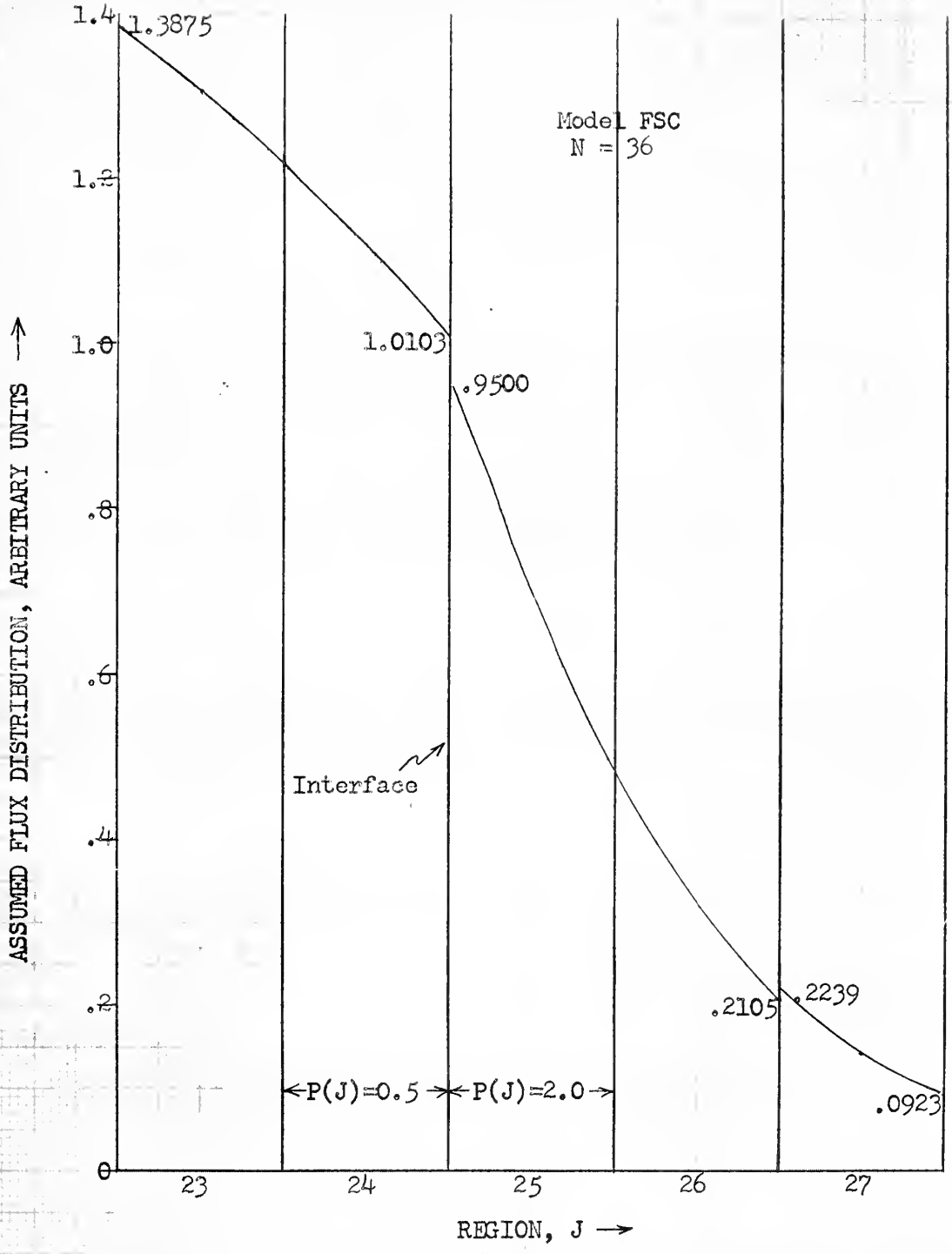

Figure 4E.3 Flux Distribution Assumed by Model FSC for Computing J→I Transfer.

Table 4E.3

Relative Mean Fluxes Computed for Large System with N = 18

	Model F		Model FS	Model FSC	
I	N=18 Run	Two-Region Averages of N=36 Run	N=18 Run	N=18 Run	Two-Region Averages of N=36 Run
1	.3239	.2908	.2803	.2806	.2788
2	.6382	.6513	.6605	.6604	.6565
3	.9451	.9790	1.0195	1.0194	1.0146
4	1.2411	1.2982	1.3506	1.3505	1.3452
5	1.5227	1.5929	1.6459	1.6458	1.6397
6	1.7868	1.8582	1.8996	1.8992	1.8913
(interface)	- - - - -	- - - - -	- - - - -	- - - - -	- - - - -
7	1.9898	2.0303	2.0438	2.0426	2.0337
8	2.0458	2.0480	2.0333	2.0324	2.0264
9	1.9905	1.9655	1.9400	1.9396	1.9398
10	1.8275	1.8011	1.7653	1.7658	1.7760
11	1.5562	1.5391	1.5080	1.5099	1.5343
12	1.1681	1.1736	1.1600	1.1640	1.2078
(interface)	- - - - -	- - - - -	- - - - -	- - - - -	- - - - -
13	.5688	.5400	.5354	.5323	.5171
14	.2356	.1654	.1430	.1397	.1106
15	.0975	.0506	.0208	.0215	.0228
16	.0402	.0155	-.0023	-.0008	.0047
17	.0163	.0047	-.0029	-.0020	.0010
18	.0058	.0012	-.0009	-.0007	.0002

Summary of Chapter 4

In this chapter, an efficient steady-state code, SLBCEL, was developed in order to evaluate more thoroughly the worth of the flat approximation and the variable-distribution models. SLBCEL treats both half-cells with perfectly reflecting boundaries and isolated systems with non-reflecting boundaries.

In Section 4D, the models were tested on cell systems having widely varying dimensions. For all systems, computed integral parameters agree closely with the best published results. For the very small cell having regions less than 0.016 mean free path thick, the flat approximation is satisfactory; the slope correction does not alter the results significatnly, and use of the curvature correction introduces errors due to large numerical errors in the coefficients $G_{crv}(I,J)$. For the 1.8 cm intermediate call having 0.155 mfp regions in the moderator section, Models FS and FSC yield nearly identical results; the flat approximation is less satisfactory. For the large cell having regions 0.3 and 1.0 mfp thick in the moderator, the Model FSC result is only slightly better than the excellent Model FSC result; the flat approximation, on the other hand, is totally inadequate. Only in the very large system studied in Section 4E do we encounter upper limits on the applicability of the variable-distribution models as regards permissible regions widths.

For all of the larger systems, the curvature correction has little effect on the solution. This characteristic is consistent with the results reported in Chapter 3. Computing time and, more significantly, storage requirements can be reduced by neglecting the curvature correction.

It is clear that the use of the slope-correction adds greatly to the power of the finite-integral method. First, for a given problem, the required number of regions is considerably reduced, as can be seen from the comparison of Run 8 of Table 4D.3 and the

eleven-region run given in Table 4D.6. Computing time for a given model is proportional to N^2; for a given N, Model FS computing time is less than twice that of Model F. Second, for a given maximum number of regions, our method extends the usefulness of the integral approach to much larger cells and isolated systems. Coupled with the non-iterative solution procedure, accurate solutions for such systems can be generated very efficiently.

We recommend the use of Model FS for half-cells and isolated systems which are greater than one mfp thick. For all such systems tested in this chapter, as well as in Chapter 3, a significant advantage over the flat approximation has been noted.

The accuracy of the integral parameters reported in this chapter, coupled with the evidence of accurate cosine solutions for homogeneous line systems in Section 2E and the accurate results obtained for the Milne problem in Section 3F, gives cause for confidence in the reasonable accuracy of the computed B(I). This confidence is reinforced by several examples in which the closeness of distributions computed for different values of N indicates a high degree of convergence towards the correct solution. From a set of integral regional birth rates B(I), for I in a particular homogeneous section of the system, a smoothly-varying solution distribution may be obtained by approximating the distribution by a polynomial with unknown coefficients and using the B(I) to determine the values of the coefficients. With accurate B(I), the polynomial solution cannot be very far from the correct solution of the transport equation, as the

integral of the polynomial over each region in the homogeneous section will be accurate. Recall that the technique just described was used successfully for the Milne problem in Section 3F.

Extension of the SLBCEL methodology to treat systems of repeated, non-symmetric cells is fairly simple. In this case, particles leaving the cell across the right cell-broundary in Fig. (4A.1) are replaced by particles entering the cell across the left boundary. The two formulas (4A.2 and 3) for ΔP_b are replaced by one simple formula:

$$\Delta P_b = \sum_{L=1}^{N} P(L) \quad . \qquad (4S.1)$$

CHAPTER 5

SUMMARY

5A. REVIEW

In this thesis we have developed, tested and evaluated numerical models for solving the (x,t)-dependent integral transport equations for line and slab geometries, Eqs. (1A.1) and (1A.3) respectively. The methodology used to formulate these models was outlined in Chapter 1.

In Chapter 2, we developed and tested a number of models for Eq. (1A.3), the integral-transport equation for line geometry. We found that, for a given degree of accuracy, the slope-correction model requires only a fraction of the regions needed with the fixed-distribution models for systems with relatively smooth flux distributions, and is in most cases more efficient with respect to computing time. The discrete-delay-time approximation proved to be quite satisfactory in the line models; this makes possible the computation of accurate, fast space-time transients, subject only to slight restrictions on external source localization and rates of property changes. The results presented in Chapter 2 demonstrate that the finite-integral method is an effective tool for space-time studies. The method is best suited for space-time transients of short duration in relatively small systems.

In Chapter 3, the flat approximation and slope-correction models developed for line geometry were extended to treat slab geometry. A curvature-correction mode was added to the formulation.

Tests made to calculate critical thicknesses and to solve the Milne problem yielded results which compare quite well with the best published data. Studies of asymptotic solutions generated by the slab models indicate that errors due to the discrete-delay-time approximation and to the neglect of growth rate informulating the models are very small for problems in which $|\lambda(J,t')|/[v\Sigma] < 0.02$, where $\lambda(J,t') = \dot{B}(J,t')/B(J,t')$, $t' < t$ and $1 \leq J \leq N$. For systems in which the $|\lambda(J,t')|/[v\Sigma]$ are very large, on the other hand, the discrete-delay-time approximation is inadequate for coupling the unbounded slab regions. We have shown how our models can be extended to a multiple-delay-time formulation which will yield more accurate results for (x,t)-dependent problems in such systems.

In Chapter 4, we extended the "bare" slab formulation to treat infinite systems of repeated, symmetric unit cells. An efficient program, SLBCEL, was developed which can compute very accurate flux distributions over the entire range of cell sizes of interest. In the results obtained with SLBCEL, the value of the slope-correction model is clearly demonstrated. The curvature correction, on the other hand, does not significantly improve the accuracy.

5B. RECOMMENDATIONS FOR FURTHER WORK

5B.1 Improvement of Slab Formulation for Time-dependent Problems

In any further work with the time-dependent slab models, we recommend that the curvature correction be dropped from the formulation and greater attention be given to accounting for the time dependence

of the parent birth rate distribution. To this end, the multiple delay-time model, minus the curvature correction, should be helpful. In addition, the application of a slope-correction for the time dependence in computing $C_1(J,t-\tau)$ should yield a considerably improved model.

5B.2 Extension to Multidimensional Geometries

A more interesting problem involves the development of finite-integral models for systems which are finite in two or three dimensions. With Models F and FS, the transfer parameters are given by double integrals in the line system and by triple integrals in the slab; in a two-dimensional plane system, however, the transfer parameters are given by quadruple integrals. The expressions are even more complex for three-dimensional systems.

Consider the two-dimensional plane system. From the analysis of time-dependent results for the rod and the slab, the discrete-delay-time approximation should be satisfactory for space-time transients provided that the regions are bounded and have a fairly regular shape. The use of regular shapes, i.e., squares or hexagons, will also simplfy the computation of transfer coefficients by minimizing the required number of formulas. The distribution of parent births in a source region J must be specified; as in the line system, the distribution may be approximated in several ways. The analogy with the line models is fairly obvious, and we would expect that the same characteristics found for the line models would apply for analogous multidimensional models. With Model M, for example,

we treated all parent births as if they occured at the center of region J; we found that particles tend to be trapped in region J, increasingly so as the optical distance from the center to the edge increases. With the flat approximation, we found both by analysis and from numerical results that the computed distributions tend to be flatter than the true solutions. Limitations on region sizes for a particular approximation in the multidimensional geometry are expected to be quite similar to those found for the line systems. A procedure for incorporating a slope correction, for use with square-shaped regions, is to superimpose two slope correction modes to account for gradients with respect to coordinates x and y.

Once the birth distribution or unit modal distribution is specified for region J, the number of neutrons colliding in region I must be computed. Since the multiple integrals are very complex, a type of numerical integration is recommended. Dividing regions J and I into a number of very small subregions, a simple model, such as that analogous to line Model I, can be used to compute the subregion-to-subregion transfer. For a given source subregion in J, the total deposition in I is computed by simple addition over the subregions of I. The J $\rightarrow$ I transfer coefficient may then be computed by weighting the transfers from the various subregions of J with the unit modal distribution and adding. An alternative procedure, which may be more efficient, involves the use of multidimensional integration formulas, such as those given in the "Handbook of Mathematical Functions."[16]

5B.3 Extension to Multispeed Systems

Analogies may also be drawn between the line models and three possible approaches for treating energy space.

First, by analogy with Models I and M, the neutrons born in each of Q energy groups are assigned a particular average speed and, for each spatial region, a particular collision cross-section. Group-to-group transfer parameters are also specified. The system then consists of Q monoenergetic systems coupled by collision events. Extension of the monoenergetic programs is fairly trivial for this case, since the monoenergetic expressions for the delay times and spatial transfer coefficients apply for the neutrons in a particular parent group.

Second, by analogy with Model F, a fixed, continuous energy distribution is assumed for the neutrons born in a particular group and region. By analogy with the numerical integration procedure proposed for multidimensional systems, spatial transfer coefficients and delay times are computed for a representative number of discrete energies in the group according to the speeds and cross sections at those energies. By appropriately weighting these parameters with the assumed distribution and adding, one may obtain the space-time transfer parameters for the group.

Third, because the energy-transfer distribution functions are fairly smooth for most types of neutron-target interactions, the energy dependence of the birth rate will be smoother than that of the collision rate in a finite system in which the collision cross

section, and therefore the leakage probability, varies within an energy group. This suggests that superposition of flat and variable slope-correction modes for the energy dependence of the birth rate in a particular group and region may be feasible. An analogy may be drawn with line Model FS.

APPENDIX A

THE PROGRAM OVRR4 (LINE GEOMETRY)

The program OVRR4 is written in FORTRAN II language for the IBM-7094 computer. Six subroutines are required for the program: SOURCE, TDEP, RREAD, RCNTRL, PARAM4 and CALC4. The functions of each subroutine are described by comment statements in the listings. The short MAIN program and the six subroutines occupy 5021 (decimal) core locations. COMMON storage occupies 16139 locations.

An input form is given in Section A1. The input variables are defined in Section A2; the output variables are defined in Section A3. The program output for a simple example problem is given in Section A4. Finally, the FORTRAN listings are given in Section A5.

A1. OVRR4 INPUT FORM

Notes: (a) Input data cards should be arranged in the order shown.

(b) Numbered cards are mandatory for each problem; inclusion of alphabetically designated sets of cards is conditional.

(c) FORTRAN II format is given in the brackets.

Card No.	Condition	Variables to be Read	Format
0	--	NPROB	[I5]
	For each problem to be solved, read the following:		
1	--	NTYP,N,NT,NSTP,MHOM,MODC,NMEM,NCOT,NSRC	[9I5]
2	--	MODR,MITN,NDET,LIS,JSC,KPARA,KPARB,NSP,NSPD	[9I5]
3	--	KSRC,MLIM,KTSS,KTDEP,KXXA,KXXB,KXXC,KXXD,KXXE	[9I5]
4	--	WD,SPD,CONV,EIGA,TSRC,TMITN	[6E12.5]
A	MHOM=1	SIGD(1),C(1)	[2E12.5]
B	MHOM=2	(SIGD(I),C(I),I=1,N)	[6E12.5]
C	NDET>0	(LID(ID),ID=1,NDET)	[3I5]
D	MODR=2	SIGDM	[E12.5]
E	NMEM=2,3	(B(I,1),I=1,N)	[6E12.5]
F	NSRC=1,2,	(S(I),I=1,N)	[6E12.5]
G	NTYP=1, NT>1	Add new set of cards 1 through F for each additional run.	
H	NTYP=3	(KEXA(I),I=1,NT)	[14I5]
I	NTYP=4, NT>1	Add the following cards for each additional pass:	
		TMITN	[E12.5]
		(SIGD(I),C(I),I=1,N)	[6E12.5]

A2. DESCRIPTION OF OVRR4 INPUT VARIABLES

Notes: (a) Assignable values are enclosed in brackets. Where different values alter the program logic, the meanings are defined.

(b) The variables are arranged in the order in which they are read into the program.

INTEGERS

NPROB = No. of independent problems to be solved [≥ 1]

NTYP = Problem Type (See Subroutine RCNTRL).

[
1 - General Problem. NT Runs with same PARAM4-computed properties.
2 - Homogeneous reactor. Computations for NT different values of N.
3 - Initial localized source problem. NT successive runs with source in different regions.
4 - Time-dependent properties which are read in at time of each change. NT sets of properties.
5 - Time-dependent properties controlled or computed by user-written subroutine TDEP. TDEP called NT times.
]

N = No. of subregions [$4 \leq N \leq 30$]

NT = No. of successive runs or passes as described under NTYP. [≥ 1]

NSTP = Increase in N for each successive run of NTYP = 2 Problem. [≥ 1, if NTYP = 2]

MHOM = [
1 - For homogeneous reactor.
2 - For homogeneous reactor.
]

MODC = [
1 - Model F (Flat approximation)
2 - Model FS (Slope correction)
]

OVRR4 INPUT VARIABLES (cont'd)

NMEM = Control variable for setting the LIM time steps of initial memory.

- 1 - Sets B(I,K) = 1.0, I = 1, N; K = 1, LIM.
- 2 - Reads in B(I,1), I = 1, N; Sets B(I,K) = B(I,1), I = 1, N; K = 2, LIM.
- 3 - Reads in B(I,1), I = 1, N; Sets B(I,K) in accordance with inverse period EIGA for I = 1, N; K = 2, LIM.
- 4 - Sets B(I,K) = 10^{-25}, I = 1, N; K = 1, LIM.

NCOT = Control variable for asymptoticity testing and transient print out.

- 1 - Tests for asymptoticity at each time step. Does not print transient results.
- 2 - No asymptoticity convergence test. Prints transient results with a spacing of NSP time steps.
- 3 - Both tests for asymptoticity and prints transient.

NSRC = Source rate control variable.

- 1 - Reads in S(I), I = 1, N; source constant in time.
- 2 - Reads in S(I), I = 1, N; source lasts JSC time steps.
- 3 - Sets S(I) = 0, I = 1, N.
- 4 - Calls user written subroutine SOURCE at each time step.

MODR =

- 1 - One pass into subroutine CALC4 for a given problem or run.
- 2 - NT passes through CALC4 for same problem or run, where property changes are made before each pass. Run continues with new properties. Always use this value with NTYP = 4 or 5.

MITN = Maximum number of time steps [≥ 1]. For NTYP = 4 or 5, MITN = TMITN/unit time step.

NDET = No. of detectors [$0 \leq$ NDET ≤ 3].
Detectors located in regions LID(ID), ID=1,3.
NDET > 0 causes printout of S(LIS) and detector responses, with a spacing of NSPD time steps.

OVRR4 INPUT VARIABLES (cont'd)

LIS = Region for which source rate S(LIS) is to be printed out if NDET > 0. [1 ≤ LIS ≤ N, if NDET > 0].

JSC = Duration in time steps of initial source distribution. [0 ≤ JSC, if NSRC = 2]. If JSC = 0, JSC is set equal to TSRC/unit time step.

KPARA = Print control variable in subroutine PARAM4.

- 1 - Prints calculated parameters.
- 2 - Does not print.

KPARB = Print control variable in PARAM4.

- 1 - Prints array G(I,J).
- 2 - Does not print.

NSP = Time step spacing in transient print out. [≥ 1, if NCOT = 2,3]

NSPD = Time step spacing in detector response print out. [≥ 1, if NDET > 0]

KSRC = (Dummy, not used in listed program). [any]

MLIM = Control variable for LIM, the number of memory time steps

- 0 - LIM computed by program.
- >0 - LIM is set equal to MLIM. Useful to reduce computation time in large reactors. Sometimes needed to get suitably large LIM when MODR = 2.

KTSS =

- 1 - Time-dependent problem.
- 2 - Steady state or generation-to-generation problem.

KTDEP =

- 1 - Subroutine TDEP not called from CALC4.
- 2 - TDEP called from CALC4 at each time step if KTSS = 1.

KXXA, KXXB, KXXC, KXXD, KXXE = Dummy variables included in READ statement and Program COMMON for user convenience in selective reprogramming. [any]

FLOATING POINT VARIABLES

WD = Reactor length, cm.

SPD = Particle speed, cm./sec.

CONV = Asymptoticity convergence criterion.

EIGA = Inverse period, sec^{-1}, for setting initial memory if NMEM = 3.

TSRC = Duration in seconds of the initial source distribution if NSRC = 2. (See JSC)

TMITN = Time in seconds, after start of problem, until which the current set of properties are to apply, if NTYP = 4 or 5. (See MITN)

SIGDM = Maximum collision cross-section expected in a problem with time dependent properties, if MODR = 2. Fixes a unit time step which remains constant and is less than or equal to every expected time delay $\tau(I,J)$.

ARRAYS

SIGD(I) = Collision cross section, cm^{-1}, in region I.

C(I) = Mean number of secondaries per collision in region I.

LID(ID) = Region in which detector No. ID is located.

B(I,1) = Birth rate in region I to be used in setting up the initial memory. (Note that B(I,K) in this program does not include external source rates. These are stored in B(I,K+200)).

S(I) = Source rate in nodal region I.

KEXA(L) = Region for initial source in run L of an NTYP = 3 problem.

A3. DESCRIPTION OF OVRR4 OUTPUT VARIABLES

Note: Variables listed in order of appearance. Those described in the previous section are not included here.

SIGP(I) = Production cross-section, cm^{-1}, in region I.

Printed if KPARA = 1:

DLTX = Length of subregion, cm^{-1}.

TS = Unit time step, sec.

TSMALL = Distance particle travels during unit time step, units of DLTX.

LIM = No. of time steps reserved for memory.

E(I) = Non-attenuation factor for particles crossing region I.

FLT(I) = No. of particles born in region I per unit flat mode which escape region I in each direction

SLP(I) = No. of particles born in region I per unit slope-correction mode which escape region I in the direction of increasing birth rate.

TOUT(I) = Mean distance travelled in region I, in units of DLTX, by those particles from a uniformly distributed source in region I that escape from region I.

GI(I) = Factor proportional to the fraction of particles born in region I which collide in region I.

Printed if KPARA = 1 and KPARB = 1:

G(I,J) for $J > I$ = Fraction surviving flight path across regions between I and J.

G(I,J) for $J \leq I$ = Mean number of time steps delay, $\tau_k(I,J)$, between births in region J (or I) and collisions in region I (or J).

OVRR4 OUTPUT VARIABLES (cont'd)

Printed if NCOT = 1 or 3.

NCN = [1 - asymptotic solution.
2 - Solution not asymptotic. CONV not satisfied.]

CONVB = Level of asymptoticity convergence attained.

NSC = Number of time steps or iterations completed.

EIGB = Inverse period, sec^{-1}, of the asymptotic solution.

BIRTH RATE = Normalized asymptotic birth rate, including the external source rate, in region I

FLUX = Normalized flux distribution in region I

Printed if NCOT = 2 or 3

B(I,K) = Progeny birth rate in region I at time step K, excluding contributions from external sources. The values for I = N+1, N+2, N+3 are the ratios $R_1(K)$, $R_2(K)$ and $R_3(K)$ of equations (2E.2).

A4. EXAMPLE OF PRINTED OUTPUT FROM OVRR4

OVRR4 PROBLEM 1 RUN 1 PASS 1 PAGE 1

INITIAL INPUT DATA

NTYP = 1	N = 6	NT = 1	NSTP = 0	MHOM = 2
MODC = 2	NMEM = 4	NCOT = 3	NSRC = 2	MODR = 1
MITN = 200	NDET = 3	LIS = 2	JSC = 10	KPARA = 1
KPARB = 1	NSP = 10	NSPD = 4	KSRC = 0	MLIM = 0
KTSS = 1	KTDEP = 1	KXXA = 0	KXXB = 0	
KXXC = 0	KXXD = 0	KXXE = 0		

WD = .50000E 01 CENTIMETERS. SPD = .20000E 06 CM./SEC.

CONV = 1.00000E-06 EIGA = .00000E 00 INVERSE SEC.

TSRC = .00000E 00 SECONDS. TMITN = .00000E 00 SECONDS.

RGN.	B(I,1)	S(I)	SIGD(I)	C(I)	SIGP(I)
1	.00000E 00	.00000E 00	1.000000	1.400000	1.400000
2	.00000E 00	.10000E 01	1.000000	1.400000	1.400000
3	.00000E 00	.00000E 00	1.000000	1.400000	1.400000
4	.00000E 00	.00000E 00	.500000	.900000	.450000
5	.00000E 00	.00000E 00	.500000	.900000	.450000
6	.00000E 00	.00000E 00	.500000	.900000	.450000

EXAMPLE PROBLEM (cont'd)

OVRR4 PROB. TYPE 1 RUN NUMBER 1 PASS NUMBER 1 PAGE 2

CALCULATED INPUT PARAMETERS FOLLOW.

N = 6 MITN = 200

DLTX = .8333333E 00 TS = .1207303E-05

TSMALL = .2897528E 00 UNITS OF DLTX. LIM = 20

SIGDM = .00000E 00 JSC = 10

RGN	SIGD(I)	C(I)	SIGP(I)	E(I)	GI(I)	FLT(I)	SLP(I)	TOUT(I)
1	1.000000	1.400000	1.400000	.434598	.568654	.339241	.011645	.431346
2	1.000000	1.400000	1.400000	.434598	.568654	.339241	.011645	.431346
3	1.000000	1.400000	1.400000	.434598	.568654	.339241	.011645	.431346
4	.500000	.900000	.450000	.659241	.534622	.408911	.007079	.465378
5	.500000	.900000	.450000	.659241	.534622	.408911	.007079	.465378
6	.500000	.900000	.450000	.659241	.534622	.408911	.007079	.465378

OVRR4 PROB. TYPE 1 RUN NUMBER 1 PASS NUMBER 1 PAGE 3

MATRIX G(I,J) FOLLOWS.

MATRIX ELEMENTS

I						
1	1.0000000	1.0000000	.4345982	.1888756	.1245145	.0820850
2	2.9773397	1.0000000	1.0000000	.4345982	.2865048	.1888756
3	6.4285575	2.9773397	1.0000000	1.0000000	.6592406	.4345982
4	9.9972258	6.5460079	3.0947901	1.0728039	1.0000000	.6592406
5	13.4484435	9.9972258	6.5460079	3.2122405	1.0728039	1.0000000
6	16.8996613	13.4484435	9.9972258	6.6634583	3.2122405	1.0728039

EXAMPLE PROBLEM (cont'd)

OVRR4 PROBLEM 1 RUN 1 PASS 1 PAGE 4

TRANSIENT RESULTS B(I,NSC) = BIRTH RATE - EXTERNAL SOURCE.

Time Step / Region	10	20	30	40	50
1	.9490277E 00	.8739997E 00	.6908735E 00	.6901077E 00	.6256174E 00
2	.1489863E 01	.9626003E 00	.9679487E 00	.8706196E 00	.8177185E 00
3	.9662511E 00	.1073411E 01	.8755780E 00	.8509327E 00	.7740931E 00
4	.1776079E 00	.2285542E 00	.2480716E 00	.2094180E 00	.1999343E 00
5	.1062234E-01	.2665763E 00	.1773733E 00	.1745403E 00	.1565949E 00
6	-.1323335E-03	.1437537E 00	.1579833E 00	.1239979E 00	.1197438E 00
7	.1090249E 01	.1006063E 01	.9707021E 00	.1008692E 01	.9845400E 00
8	.1105481E 01	.1011428E 01	.9718456E 00	.1007472E 01	.9845984E 00
9	.1105481E 01	.1011428E 01	.9718456E 00	.1007472E 01	.9845984E 00

Time Step / Region	60	70	80	90	100
1	.5800014E 00	.5365613E 00	.4955838E 00	.4586511E 00	.4238753E 00
2	.7530713E 00	.6960864E 00	.6443524E 00	.5953029E 00	.5507134E 00
3	.7183094E 00	.6644356E 00	.6136771E 00	.5679445E 00	.5248811E 00
4	.1832766E 00	.1696509E 00	.1569928E 00	.1450281E 00	.1341858E 00
5	.1465356E 00	.1352425E 00	.1249368E 00	.1156511E 00	.1068586E 00
6	.1095810E 00	.1014863E 00	.9392837E-01	.8673827E-01	.8027630E-01
7	.9954461E 00	.9910203E 00	.9925177E 00	.9921773E 00	.9921458E 00
8	.9955614E 00	.9909657E 00	.9925387E 00	.9921696E 00	.9921484E 00
9	.9955614E 00	.9909657E 00	.9925387E 00	.9921696E 00	.9921484E 00

OVRR4 PROBLEM 1 RUN 1 PASS 1 PAGE 5

TRANSIENT RESULTS B(I,NSC) = BIRTH RATE - EXTERNAL SOURCE.

Time Step / Region	110	120	130	140	150
1	.3920354E 00	.3624606E 00	.3351622E 00	.3099069E 00	.2865566E 00
2	.5091019E 00	.4707882E 00	.4353026E 00	.4025073E 00	.3721806E 00
3	.4854555E 00	.4488321E 00	.4150292E 00	.3837556E 00	.3548411E 00
4	.1240336E 00	.1147058E 00	.1060570E 00	.9806781E-01	.9067863E-01
5	.9884628E-01	.9138217E-01	.8450283E-01	.7813429E-01	.7224745E-01
6	.7419107E-01	.6861671E-01	.6344114E-01	.5866273E-01	.5424253E-01
7	.9922450E 00	.9921673E 00	.9922123E 00	.9921905E 00	.9921995E 00
8	.9922443E 00	.9921672E 00	.9922125E 00	.9921903E 00	.9921996E 00
9	.9922443E 00	.9921672E 00	.9922125E 00	.9921903E 00	.9921996E 00

EXAMPLE PROBLEM (cont'd)

OVRR4 PROBLEM 1 RUN 1 PASS 1 PAGE 6

CONVERGENCE RESULTS

NCOT = 3 NCN = 1 NSC = 158

CONVB = .72270632E-06 EIGB = -.64870129E 04

ASYMPTOTIC DISTRIBUTIONS

REG. NO.	BIRTH RATE	FLUX
1	1.39699146	1.01783647
2	1.81440863	1.32196318
3	1.72988527	1.26038015
4	.4420650 4	1.00204204
5	.35221361	.79837311
6	.26443609	.59940519

OVRR 4 PROBLEM 1 RUN 1 PASS 1 PAGE 7

CONVERGENCE RESULTS

RESULTS OF LAST FIVE TIME STEPS

1	.2777171E 00	.2755496E 00	.2733995E 00	.2712666E 00	.2691504E 00
2	.3606992E 00	.3578853E 00	.3550927E 00	.3523215E 00	.3495718E 00
3	.3438952E 00	.3412112E 00	.3385488E 00	.3359076E 00	.3332872E 00
4	.8788142E-01	.8719585E-01	.8651542E-01	.8584015E-01	.8517016E-01
5	.7001868E-01	.6947218E-01	.6893015E-01	.6839248E-01	.6785899E-01
6	.5256932E-01	.5215927E-01	.5175222E-01	.5134822E-01	.5094740E-01
7	.9921948E 00	.9921953E 00	.9921971E 00	.9921985E 00	.9921988E 00
8	.9921948E 00	.9921953E 00	.9921971E 00	.9921986E 00	.9921988E 00
9	.9921948E 00	.9921953E 00	.9921971E 00	.9921986E 00	.9921988E 00

EXAMPLE PROBLEM (cont'd)

OVRR4 PROBLEM 1 RUN 1 PASS 1 PAGE 8

DETECTOR RESPONSE RESULTS NDET = 3

LOCATION TIME STEP	SOURCE 2	DETECTOR 1 1	DETECTOR 2 3	DETECTOR 3 5
4	.10000000E 01	.19572037E 00	.19572037E 00	.76003810E-25
8	.10000000E 01	.59420481E 00	.59541364E 00	-.21580986E-02
12	.00000000E 00	.84884194E 00	.89684200E 00	.24293809E 00
16	.00000000E 00	.58167829E 00	.67086925E 00	.37480523E 00
20	.00000000E 00	.62785693E 00	.76672231E 00	.59239183E 00
24	.00000000E 00	.51331267E 00	.63798831E 00	.42849359E 00
28	.00000000E 00	.52992656E 00	.67068320E 00	.44582165E 00
32	.00000000E 00	.50297674E 00	.63731425E 00	.40998826E 00
36	.00000000E 00	.49235677E 00	.61290647E 00	.38347941E 00
40	.00000000E 00	.49293405E 00	.60780910E 00	.38786743E 00
44	.00000000E 00	.46442316E 00	.57382783E 00	.35901010E 00
48	.00000000E 00	.46001838E 00	.56917858E 00	.36116089E 00
52	.00000000E 00	.43876885E 00	.54315834E 00	.34346013E 00
56	.00000000E 00	.42843870E 00	.53042549E 00	.33592805E 00
60	.00000000E 00	.41428671E 00	.51307812E 00	.32563477E 00
64	.00000000E 00	.40087601E 00	.49641993E 00	.31397025E 00
68	.00000000E 00	.38972744E 00	.48265921E 00	.30616978E 00
72	.00000000E 00	.37651087E 00	.46622930E 00	.29506172E 00
76	.00000000E 00	.36584054E 00	.45301386E 00	.28707210E 00
80	.00000000E 00	.35398841E 00	.43834078E 00	.27763730E 00
84	.00000000E 00	.34331395E 00	.42511710E 00	.26924586E 00
88	.00000000E 00	.33269590E 00	.41197893E 00	.26101890E 00
92	.00000000E 00	.32234119E 00	.39914940E 00	.25278385E 00
96	.00000000E 00	.31252598E 00	.38700087E 00	.24517967E 00
100	.00000000E 00	.30276809E 00	.37491510E 00	.23746348E 00
104	.00000000E 00	.29351145E 00	.36345339E 00	.23023356E 00
108	.00000000E 00	.28441099E 00	.35218464E 00	.22308737E 00
112	.00000000E 00	.27565400E 00	.34134001E 00	.21621280E 00
116	.00000000E 00	.26715297E 00	.33081416E 00	.20955595E 00
120	.00000000E 00	.25890040E 00	.32059433E 00	.20307149E 00
124	.00000000E 00	.25092700E 00	.31072137E 00	.19682597E 00
128	.00000000E 00	.24317537E 00	.30112238E 00	.19074048E 00
132	.00000000E 00	.23568108E 00	.29184229E 00	.18486439E 00
136	.00000000E 00	.22840713E 00	.28283507E 00	.17915860E 00
140	.00000000E 00	.22136211E 00	.27411117E 00	.17363176E 00
144	.00000000E 00	.21453414E 00	.26565623E 00	.16827722E 00
148	.00000000E 00	.20791485E 00	.25745955E 00	.16308409E 00
152	.00000000E 00	.20150237E 00	.24951904E 00	.15805503E 00
156	.00000000E 00	.19528538E 00	.24182058E 00	.15317811E 00

```
*      LIST8
*      LABEL
COVRR4
       DIMENSION SIGD(30),SIGP(30),LID(3),B(33,400),S(30),
      1G(30,30),C(30),GI(30),E(30),TOUT(30),FLT(30),
      2SLP(30),D(3,200),NTS(200),SRCI(200),NXX(200),BEQ(30),
      3FLX(30),KEXA(30),EXB(30),EXC(200),EXD(200)
       COMMON NTYP,N,NT,NSTP,MHOM,MODC,NMEM,NCOT,NSRC,
      1MODR,MITN,NDET,LIS,JSC,KPARA,KPARB,NSP,NSPD,
      2KSRC,MLIM,KTSS,KTDEP,KXXA,KXXB,KXXC,KXXD,KXXE,
      3MA,NPAG,INDX,IPASS,NSC,NSD,LIM,KFL,SIGDM,
      4WD,SPD,CONV,EIGA,TSRC,TMITN,EIGB,QUAN,TS,DLTX,
      5SIGD,SIGP,LID,B,S,G,C,GI,E,TOUT,FLT,SLP,D,NTS,SRCI,
      6NXX,BEQ,FLX,KEXA,EXB,EXC,EXD
    1  FORMAT(I5)
       READ 1,NPROB
   50  CALL RREAD
       CALL RCNTRL
       NPROB=NPROB-1
       IF (NPROB) 100,100,50
  100  CALL EXIT
       END




*      LIST8
*      LABEL
       SUBROUTINE TDEP
C
C     DUMMY SUBROUTINE  --  TIME-DEPENDENT PROPERTIES.
C
       RETURN
       END




*      LIST8
*      LABEL
       SUBROUTINE SOURCE
C
C     DUMMY SUBROUTINE  --  TIME DEPENDENT SOURCES.
C
       RETURN
       END
```

```
*      LIST8
*      LABEL
       SUBROUTINE RREAD
C
C     SUBROUTINE READS IN AND PRINTS OUT INPUT DATA FOR
C     A PARTICULAR PROBLEM.
C
       DIMENSION SIGD(30),SIGP(30),LID(3),B(33,400),S(30),
      1G(30,30),C(30),GI(30),E(30),TOUT(30),FLT(30),
      2SLP(30),D(3,200),NTS(200),SRCI(200),NXX(200),BEQ(30),
      3FLX(30),KEXA(30),EXB(30),EXC(200),EXD(200)
       COMMON NTYP,N,NT,NSTP,MHOM,MODC,NMEM,NCOT,NSRC,
      1MODR,MITN,NDET,LIS,JSC,KPARA,KPARB,NSP,NSPD,
      2KSRC,MLIM,KTSS,KTDEP,KXXA,KXXB,KXXC,KXXD,KXXE,
      3MA,NPAG,INDX,IPASS,NSC,NSD,LIM,KFL,SIGDM,
      4WD,SPD,CONV,EIGA,TSRC,TMITN,EIGB,QUAN,TS,DLTX,
      5SIGD,SIGP,LID,B,S,G,C,GI,E,TOUT,FLT,SLP,D,NTS,SRCI,
      6NXX,BEQ,FLX,KEXA,EXB,EXC,EXD
    1 FORMAT(9I5)
    2 FORMAT(6E12.5)
    3 FORMAT(2E12.5)
    5 FORMAT(3I5)
    7 FORMAT(1H1,5X6H OVRR4,3X8H PROBLEM I3,
     13X4H RUN I3,3X5H PASS I3,5X5H PAGE I4)
    8 FORMAT(1H0,20X,19H INITIAL INPUT DATA/)
    9 FORMAT(1H0,4X7H NTYP =I3,7X4H N =I3,6X5H NT =I3,
     14X7H NSTP =I3,4X7H MHOM =I3//5X7H MODC =I3,
     24X7H NMEM =I3,4X7H NCOT =I3,4X7H NSRC =I3,
     34X7H MODR =I3//5X7H MITN =I5,2X7H NDET =I3,
     45X6H LIS =I3,5X6H JSC =I5,3X8H KPARA =I3//
     54X8H KPARB =I3,5X6H NSP =I4,3X7H NSPD =I4,
     63X7H KSRC =I4,3X7H MLIM =I4//5X7H KTSS =I4,
     72X8H KTDEP =I4,3X7H KXXA =I4,3X7H KXXB =I4//
     85X7H KXXC =I4,3X7H KXXD =I4,3X7H KXXE =I4)
   10 FORMAT(1H0,5X5H WD =E12.5,13H CENTIMETERS.,
     19X6H SPD =E12.5,9H CM./SEC.//10X7H CONV =E12.5,
     210X7H EIGA =E12.5,13H INVERSE SEC.//5X7H TSRC =E12.5,
     39H SECONDS.,7X8H TMITN =E12.5,9H SECONDS.)
   11 FORMAT(1H0,4HRGN.,4X7H B(I,1),7X5H S(I),5X8H SIGD(I),
     13X5H C(I),2X8H SIGP(I))
   12 FORMAT(I4,2X,2E13.5,3F10.6)
   17 FORMAT(E12.5)
      MA=1
      NPAG=1
      INDX=1
      IPASS=1
      READ 1,NTYP,N,NT,NSTP,MHOM,MODC,NMEM,NCOT,NSRC,
     1MODR,MITN,NDET,LIS,JSC,KPARA,KPARB,NSP,NSPD,
     2KSRC,MLIM,KTSS,KTDEP,KXXA,KXXB,KXXC,KXXD,KXXE
      READ 2,WD,SPD,CONV,EIGA,TSRC,TMITN
      QUAN=N
      GO TO (101,102),MHOM
C
C     HOMOGENEOUS REACTOR
```

```
  101 READ 3,SIGD(1),C(1)
      DO 20 I=2,N
      SIGD(I)=SIGD(1)
   20 C(I)=C(1)
      GO TO 106
C
C     INHOMOGENEOUS REACTOR.
C
  102 READ 2,(SIGD(I),C(I),I=1,N)
  106 DO 107 I=1,N
  107 SIGP(I)=C(I)*SIGD(I)
      IF (NDET) 110,110,104
C
C     DETECTOR LOCATIONS WHEN DETECTORS ARE USED.
C
  104 READ 5,(LID(ID),ID=1,NDET)
  110 GO TO (60,50),MODR
C
C     MAXIMUM COLLISION CROSS SECTION EXPECTED FOR CASE OF
C     TIME-DEPENDENT COLLISION CROSS-SECTION, SIGD(I).
C
   50 READ 17,SIGDM
   60 GO TO (120,111,111,120),NMEM
C
C     INITIAL MEMORY INPUT.
C
  111 READ 2,(B(I,1),I=1,N)
  120 GO TO  (125,125,130,130),NSRC
C
C     SOURCE DISTRIBUTION.
C
  125 READ 2,(S(I),I=1,N)
C
C     PRINT OUT INPUT DATA.
C
  130 PRINT 7, NTYP,INDX,IPASS,NPAG
      NPAG=NPAG+1
      PRINT 8
      PRINT 9,NTYP,N,NT,NSTP,MHOM,MODC,NMEM,NCOT,NSRC,
     1MODR,MITN,NDET,LIS,JSC,KPARA,KPARB,NSP,NSPD,
     2KSRC,MLIM,KTSS,KTDEP,KXXA,KXXB,KXXC,KXXD,KXXE
      PRINT 10,WD,SPD,CONV,EIGA,TSRC,TMITN
      PRINT 11
      PRINT 12,(I,B(I,1),S(I),SIGD(I),C(I),SIGP(I),I=1,N)
      RETURN
      END



*     LIST8
*     LABEL
      SUBROUTINE RCNTRL
C
```

```
C     THIS SUBROUTINE CONTROLS PROGRAM FLOW FOR FIVE BASIC
C     PROBLEM TYPES, IDENTIFIED BY THE VALUE OF NTYP.
C
      DIMENSION SIGD(30),SIGP(30),LID(3),B(33,400),S(30),
     1G(30,30),C(30),GI(30),E(30),TOUT(30),FLT(30),
     2SLP(30),D(3,200),NTS(200),SRCI(200),NXX(200),BEQ(30),
     3FLX(30),KEXA(30),EXB(30),EXC(200),EXD(200)
      COMMON NTYP,N,NT,NSTP,MHOM,MODC,NMEM,NCOT,NSRC,
     1MODR,MITN,NDET,LIS,JSC,KPARA,KPARB,NSP,NSPD,
     2KSRC,MLIM,KTSS,KTDEP,KXXA,KXXB,KXXC,KXXD,KXXE,
     3MA,NPAG,INDX,IPASS,NSC,NSD,LIM,KFL,SIGDM,
     4WD,SPD,CONV,EIGA,TSRC,TMITN,EIGB,QUAN,TS,DLTX,
     5SIGD,SIGP,LID,B,S,G,C,GI,E,TOUT,FLT,SLP,D,NTS,SRCI,
     6NXX,BEQ,FLX,KEXA,EXB,EXC,EXD
   13 FORMAT(1415)
   16 FORMAT(E12.5/(6E12.5))
      GO TO (100,200,300,400,500),NTYP
C
C     GENERAL PROBLEM.   FOR NT GREATER THAN 1, THE
C     TRANSFER PARAMETERS REMAIN VALID FOR ADDITIONAL
C     PROBLEMS WITH CHANGING SOURCES,C(I), REACTOR SIZES,ETC.
C
  100 CALL PARAM4
      INDEX=1
  102 CALL CALC4
      INDEX=INDEX+1
      IF (NT-INDEX) 100),101,101
  101 CALL RREAD
      GO TO 102
C
C     HOMOGENEOUS REACTOR, COMPUTATIONS FOR NT DIFFERENT
C     VALUES OF N.
C
  200 CALL PARAM4
      CALL CALC4
      INDX=INDX+1
      IF(NT-INDX) 1000,201,201
  201 N=N+NSTP
      GO TO 200
C
C     SUCCESSIVE INITIAL SOURCE PROBLEMS, WHERE SOURCE IS
C     LOCALIZED TO ONE REGION AND LASTS FOR JSC TIME
C     STEPS.  NTYP=3 IS USEFUL FOR IMPORTANCE DISTRIBUTIONS
C     AND FAST TRANSIENTS.  THE KEXA(I) ARE THE
C     SPECIFIED SOURCE REGIONS FOR SUCCESSIVE RUNS.
C
  300 READ 13, (KEXA(I),I=1,NT)
      CALL PARAM4
      KZA=NSRC
  301 DO 302 I=1,N
  302 S(I)=0.0
      L=KEXA(INDX)
      LIS=L
      S(L)=1.0
```

```
      CALL CALC4
      NSRC=KZA
      INDX=INDX+1
      IF (NT-INDX) 1000,301,301
C
C     PROBLEM WITH TIME-DEPENDENT PROPERTIES WHICH ARE READ
C     IN AT TIME OF EACH CHANGE.  NT IS THE NUMBER OF
C     SUCCESSIVE SETS OF PROPERTIES TO BE READ IN. EACH
C     SET WILL LAST UNTIL TMITN SECONDS.
C
  400 CALL PARAM4
      MITN=TMITN/TS
      CALL CALC4
      IPASS=IPASS+1
      IF (NT-IPASS) 1000,401,401
  401 READ 16,TMITN,(SIGD(I),C(I),I=1,N)
      DO 402 I=1,N
  402 SIGP(I)=C(I)*SIGD(I)
      GO TO 400
C
C     TIME-DEPENDENT PROPERTIES ARE CONTROLLED OR COMPUTED BY
C     A USER-WRITTEN SUBROUTINE,TDEP. (SIMPLE FUNCTIONS
C     OF TIME,FEEDBACK,ETC.)
C
  500 CALL TDEP
      CALL PARAM4
      MITN=TMITN/TS
      CALL CALC4
      IPASS=IPASS+1
      IF(NT-IPASS) 1000,500,500
 1000 RETURN
      END




*     LIST8
*     LABEL
      SUBROUTINE PARAM4
C
C     THIS SUBROUTINE CONVERTS THE INPUT DATA TO THE
C     PARAMETERS WHICH WILL BE NEEDED IN THE BIRTH RATE
C     COMPUTATIONS IN SUBROUTINE CALC4.
C
      DIMENSION SIGD(30),SIGP(30),LID(3),B(33,400),S(30),
     1G(30,30),C(30),GI(30),E(30),TOUT(30),FLT(30),
     2SLP(30),D(3,200),NTS(200),SRCI(200),NXX(200),BEQ(30),
     3FLX(30),KEXA(30),EXB(30),EXC(200),EXD(200)
      COMMON NTYP,N,NT,NSTP,MHOM,MODC,NMEM,NCOT,NSRC,
     1MODR,MITN,NDET,LIS,JSC,KPARA,KPARB,NSP,NSPD,
     2KSRC,MLIM,KTSS,KTDEP,KXXA,KXXB,KXXC,KXXD,KXXE,
     3MA,NPAG,INDX,IPASS,NSC,NSD,LIM,KFL,SIGDM,
     4WD,SPD,CONV,EIGA,TSRC,TMITN,EIGB,QUAN,TS,DLTX,
```

```
     5SIGD,SIGP,LID,B,S,G,C,GI,E,TOUT,FLT,SLP,D,NTS,SRCI,
     6NXX,BEQ,FLX,KEXA,EXB,EXC,EXD
    1 FORMAT(1H1,3X6H OVRR4,3X10H PROB.TYPE I3,
     13X11H RUN NUMBER I3,3X12H PASS NUMBER I3,3X5H PAGE I3)
    2 FORMAT(1H0,15X36H CALCULATED INPUT PARAMETERS FOLLOW./
     1//10X,4H N =I3,15X7H MITN =I6//10X7H DLTX =E14.7,
     210X5H TS =E14.7///5X9H TSMALL =E14.7,2X,
     315H UNITS OF DLTX.,5X6H LIM =I5///10X7H SIGDM =E12.5,
     45X6H JSC =I5///1X3HRGN,8H SIGD(I),3X5H C(I),
     52X8H SIGP(I),3X5H E(I),3X6H GI(I),3X7H FLT(I),
     62X7H SLP(I),2X8H TOUT(I)//(I3,1X,3F10.6,5F9.6))
    3 FORMAT(1H0,20X23H MATRIX G(I,J) FOLLOWS.//2H I,20X,
     116H MATRIX ELEMENTS )
   10 FORMAT(I3,6F11.7/5X6F11.7/7X6F11.7/9X6F11.7/11X6F11.7)
      QUAN=N
      DLTX=WD/QUAN
      NM2=N-2
      NM=N-1
      DO 22 I=1,N
      ARGU=SIGD(I)*DLTX
      E(I)=EXPF(-ARGU)
      FLT(I)=(1.0-E(I))/(2.0*ARGU)
      SLP(I)=(1.0+E(I)-2.0*(1.0-E(I))/ARGU)/(8.0*ARGU)
      GI(I)=(1.0-2.0*FLT(I))/(1.0-E(I))
      TOUT(I)=1.0/ARGU-E(I)/(1.0-E(I))
      G(I,I)=(ARGU-2.0+(ARGU+2.0)*E(I))/(ARGU*(ARGU-
     11.0+E(I)))
      GO TO (15,22),MHOM
   22 CONTINUE
      GO TO 210
C
C     HOMOGENEOUS REACTOR.
C
   15 DO 200 I=2,N
      E(I)=E(1)
      FLT(I)=FLT(1)
      SLP(I)=SLP(1)
      GI(I)=GI(1)
      TOUT(I)=TOUT(1)
  200 G(I,I)=G(1,1)
C
C     G(I,J), FOR J GREATER THAN I, CONTAINS THE
C     ATTENUATION FACTOR OVER THE REGIONS BETWEEN I AND J.
C
  210 DO 211 I=1,NM
  211 G(I,I+1)=1.0
      DO 212 I=1,NM2
      IP2=I+2
      DO 212 J=IP2,N
  212 G(I,J)=G(I,J-1)*E(J-1)
C
C     G(I,J), FOR J LESS THAN OR EQUAL TO I, CONTAINS
C     THE MEAN TIME DELAY BETWEEN BIRTHS IN J (OR I) AND
C     COLLISIONS IN I (OR J).
```

```
C
      DO 213 I=2,N
      IM=I-1
      DO 213 J=1,IM
      Q=I-J-1
  213 G(I,J)=Q+TOUT(I)+TOUT(J)
C
C     COMPUTATION OF UNIT TIME STEP, TS SECONDS.
C
      GO TO (309,430),MODR
  430 ARGU=SIGDM*DLTX
      F=EXPF(-ARGU)
      TSMALL=(ARGU-2.0+(ARGU+2.0)*F)/(ARGU*(ARGU-1.0+F))
      GO TO 325
  309 K=1
      DO 320 L=2,N
      IF(G(L,L)-G(K,K)) 310,320,320
  310 K=L
  320 CONTINUE
      TSMALL=G(K,K)
  325 DO 330 I=1,N
  330 G(I,I)=G(I,I)/TSMALL + 1.0E-08
      DO 340 I=2,N
      IM=I-1
      DO 340 J=1,IM
  340 G(I,J)=G(I,J)/TSMALL
      TS=TSMALL*DLTX/SPD
C
C     COMPUTATION OF LIM, AN INTEGER GREATER THAN OR EQUAL
C     TO THE NUMBER OF TIME STEPS FOR WHICH MEMORY IS
C     REQUIRED.
C
      LIM=QUAN/TSMALL
      IF (MLIM) 344,344,343
  343 LIM=MLIM
  344 IF (JSC) 350,350,360
  350 JSC=TSRC/TS
  360 GO TO (51,60),KPARA
C
C     PRINT OUT CALCULATED PARAMETERS.
C
   51 PRINT 1,NTYP,INDX,IPASS,NPAG
      NPAG=NPAG+1
      PRINT 2,N,MITN,DLTX,TS,TSMALL,LIM,SIGDM,JSC,(I,
     1SIGD(I),C(I),SIGP(I),E(I),GI(I),FLT(I),SLP(I),
     2TOUT(I),I=1,N)
      GO TO (52,60),KPARB
   52 PRINT 1,NTYP,INDX,IPASS,NPAG
      NPAG=NPAG+1
      PRINT 3
      DO 53 I=1,N
   53 PRINT 10, I,(G(I,J),J=1,N)
   60 RETURN
      END
```

```
*      LIST8
*      LABEL
       SUBROUTINE CALC4
C
C     THIS SUBROUTINE SOLVES THE PROBLEM POSED AND PRINTS
C     OUT THE RESULTS.
C
       DIMENSION SIGD(30),SIGP(30),LID(3),B(33,400),S(30),
      1G(30,30),C(30),GI(30),E(30),TOUT(30),FLT(30),
      2SLP(30),D(3,200),NTS(200),SRCI(200),NXX(200),BEQ(30),
      3FLX(30),KEXA(30),EXB(30),EXC(200),EXD(200)
       COMMON NTYP,N,NT,NSTP,MHOM,MODC,NMEM,NCOT,NSRC,
      1MODR,MITN,NDET,LIS,JSC,KPARA,KPARB,NSP,NSPD,
      2KSRC,MLIM,KTSS,KTDEP,KXXA,KXXB,KXXC,KXXD,KXXE,
      3MA,NPAG,INDX,IPASS,NSC,NSD,LIM,KFL,SIGDM,
      4WD,SPD,CONV,EIGA,TSRC,TMITN,EIGB,QUAN,TS,DLTX,
      5SIGD,SIGP,LID,B,S,G,C,GI,E,TOUT,FLT,SLP,D,NTS,SRCI,
      6NXX,BEQ,FLX,KEXA,EXB,EXC,EXD
     1 FORMAT(1H1,5X6H OVRR4,3X8H PROBLEM I3,
      13X4H RUN I3,3X5H PASS I3,5X5H PAGE I4)
     2 FORMAT(1H0,5X18H TRANSIENT RESULTS,
      15X41H B(I,NSC) = BIRTH RATE - EXTERNAL SOURCE.)
     3 FORMAT(1H0,9HTIME STEP,I5,4I13/7H REGION/
      1(I3,4X,5E13.7))
     4 FORMAT(1H0,20X20H CONVERGENCE RESULTS)
     5 FORMAT(1H0,5X7H NCOT =I2,10X6H NCN =I2,10X6H NSC =I5//
      110X8H CONVB =E14.8,10X7H EIGB =E14.8)
     6 FORMAT(1H0/20X25H ASYMPTOTIC DISTRIBUTIONS//9H REG. NO.,
      15X11H BIRTH RATE,11X5H FLUX/(I6,7XF11.8,F20.8))
     7 FORMAT(1H0,20X31HRESULTS OF LAST FIVE TIME STEPS//
      1(I5,2X,5E13.7))
     8 FORMAT(1H0,20X26H DETECTOR RESPONSE RESULTS,
      110X7H NDET =I2//13X7H SOURCE,8X11H DETECTOR 1,
      25X11H DETECTOR 2,5X11H DETECTOR 3/9H LOCATION I8,
      33I16/10H TIME STEP)
     9 FORMAT(I6,4E16.8)
    11 FORMAT(1H0,9HTIME STEP,I5,4I13/)
    12 FORMAT(I3,4X,5E13.7)
       GO TO (100,300),MA
   300 GO TO (285,151),MODR
   100 GO TO (2000,2010),KTSS
C
C     FOR STEADY STATE PROBLEM.
C
  2010 LIM=4
C
C     SET UP PROBLEM CONSTANTS.
C
  2000 LIMK=200-LIM
       LIMT=LIM+200
       LIMTP=LIMT+1
```

```
      LIMP=LIM+1
      NM=N-1
      NNN=LIM+NSP
      N1=N+1
      N2=N+2
      N3=N+3
      NM3=N-3
      NHALF=N/2
      NNB=0
      NSD=1
      NSC=0
C
C     SET INITIAL MEMORY IN B(I,K).
C
      GO TO (110,120,130,140),NMEM
  110 DO 111 I=1,N
  111 B(I,1)=1.0
  120 DO 121 J=2,LIM
      DO 121 I=1,N
  121 B(I,J)=B(I,1)
      GO TO 150
  130 ARGO=EIGA*TS
      R=EXPF(ARGO)
      DO 131 J=2,LIM
      K1=J-1
      DO 131 I=1,N
  131 B(I,J)=R*B(I,K1)
      GO TO 150
  140 DO 141 I=1,N
  141 B(I,1)=1.0E-25
      GO TO 120
C
C     CLEAR REMAINDER OF B(I,K) ARRAY.
C
  150 DO 119 J=LIMP,400
      DO 119 I=1,N3
  119 B(I,J)=0.0
  151 K=LIM
C
C     COMPUTE BIRTH RATE DISTRIBUTION AT TIME STEP NSC.
C
  152 NSC=NSC+1
      KFL=K
      K1=K
      K=K+1
      KTWO=K+200
C
C     SOURCE DISTRIBUTION AT TIME STEP NSC.
C
      GO TO (160,154,155,157),NSRC
  154 IF(JSC-NSC) 155,160,160
  155 DO 156 I=1,N
  156 S(I)=0.0
      NSRC=1
```

```
      GO TO 160
  157 CALL SOURCE
  160 GO TO (166,966),MODC
C
C     FLAT APPROXIMATION.
C
  166 GO TO (2020,2030),KTSS
C
C     TIME-DEPENDENT PROBLEM.
C
 2020 GO TO (2021,2022),KTDEP
 2022 CALL TDEP
 2021 DO 161 I=1,N
      SUM=0.0
      DO 162 J=1,N
      IF (J-I) 163,164,165
  163 KT=G(I,J)
      IF (KT-LIM) 301,162,162
  301 TT=KT
      W=G(I,J)-TT
      MK=K-KT
      SUM=SUM+FLT(J)*G(J,I)*((1.0-W)*(B(J,MK)+B(J,MK+200))+
     1W*(B(J,MK-1)+B(J,MK+199)))
      GO TO 162
  164 KT=G(I,I)
      IF (KT-LIM) 302,162,162
  302 TT=KT
      W=G(I,I)-TT
      MK=K-KT
      SUM=SUM+GI(I)*((1.0-W)*(B(J,MK)+B(J,MK+200))+
     1W*(B(J,MK-1)+B(J,MK+199)))
      GO TO 162
  165 KT=G(J,I)
      IF (KT-LIM) 303,162,162
  303 TT=KT
      W=G(J,I)-TT
      MK=K-KT
      SUM=SUM+FLT(J)*G(I,J)*((1.0-W)*(B(J,MK)+B(J,MK+200))+
     1W*(B(J,MK-1)+B(J,MK+199)))
  162 CONTINUE
      B(I,KTWO)=S(I)
  161 B(I,K)=C(I)*(1.0-E(I))*SUM
      GO TO 175
C
C     STEADY STATE PROBLEM  --  GENERATION STEP NSC.
C
 2030 DO 2161 I=1,N
      SUM=0.0
      DO 2162 J=1,N
      IF (J-I) 2163,2164,2165
 2163 SUM=SUM+FLT(J)*G(J,I)*(B(J,K1)+S(J))
      GO TO 2162
 2164 SUM=SUM+GI(I)*(B(I,K1)+S(I))
      GO TO 2162
```

```
 2165 SUM=SUM+FLT(J)*G(I,J)*(B(J,K1)+S(J))
 2162 CONTINUE
 2161 B(I,K)=C(I)*(1.0-E(I))*SUM
      GO TO 175
C
C     SLOPE CORRECTION.
C
  966 GO TO (2220,2230),KTSS
C
C     TIME-DEPENDENT PROBLEM.
C
 2220 GO TO (2221,2222),KTDEP
 2222 CALL TDEP
 2221 DO 961 I=1,N
      SUM=0.0
      IF (I-1) 972,972,971
  971 KT=G(I,1)
      IF (KT-LIM) 304,972,972
  304 TT=KT
      W=G(I,1)-TT
      MK=K-KT
      MKM=MK-1
      GAM=2.0*(B(2,MK)*SIGP(1)/SIGP(2)-B(1,MK))
      HAM=2.0*(B(2,MKM)*SIGP(1)/SIGP(2)-B(1,MKM))
      SUM=SUM+G(1,I)*(FLT(1)*((1.0-W)*(B(1,MK)+B(1,MK+200))+
     1W*(B(1,MKM)+B(1,MKM+200)))+SLP(1)*((1.0-W)*GAM+W*HAM))
  972 DO 973 J=2,NM
      IF (J-I) 974,973,975
  974 KT=G(I,J)
      IF (KT-LIM) 305,973,973
  305 TT=KT
      W=G(I,J)-TT
      MK=K-KT
      MKM=MK-1
      JP=J+1
      JM=J-1
      GAM=SIGP(J)*(B(JP,MK)/SIGP(JP)-B(JM,MK)/SIGP(JM))
      HAM=SIGP(J)*(B(JP,MKM)/SIGP(JP)-B(JM,MKM)/SIGP(JM))
      SUM=SUM+G(J,I)*(FLT(J)*((1.0-W)*(B(J,MK)+B(J,MK+200))+
     1W*(B(J,MKM)+B(J,MKM+200)))+SLP(J)*((1.0-W)*GAM+W*HAM))
      GO TO 973
  975 KT=G(J,I)
      IF (KT-LIM) 306,973,973
  306 TT=KT
      W=G(J,I)-TT
      MK=K-KT
      MKM=MK-1
      JP=J+1
      JM=J-1
      GAM=SIGP(J)*(B(JM,MK)/SIGP(JM)-B(JP,MK)/SIGP(JP))
      HAM=SIGP(J)*(B(JM,MKM)/SIGP(JM)-B(JP,MKM)/SIGP(JP))
      SUM=SUM+G(I,J)*(FLT(J)*((1.0-W)*(B(J,MK)+B(J,MK+200))+
     1W*(B(J,MKM)+B(J,MKM+200)))+SLP(J)*((1.0-W)*GAM+W*HAM))
  973 CONTINUE
```

```
      IF (N-I) 977,977,976
  976 KT=G(N,I)
      IF (KT-LIM) 307,977,977
  307 TT=KT
      W=G(N,I)-TT
      MK=K-KT
      MKM=MK-1
      GAM=2.0*(B(NM,MK)*SIGP(N)/SIGP(NM)-B(N,MK))
      HAM=2.0*(B(NM,MKM)*SIGP(N)/SIGP(NM)-B(N,MKM))
      SUM=SUM+G(I,N)*(FLT(N)*((1.0-W)*(B(N,MK)+B(N,MK+200))+
     1W*(B(N,MKM)+B(N,MKM+200)))+SLP(N)*((1.0-W)*GAM+W*HAM))
  977 KT=G(I,I)
      TT=KT
      W=G(I,I)-TT
      MK=K-KT
      MKM=MK-1
      SUM=SUM+GI(I)*((1.0-W)*(B(I,MK)+B(I,MK+200))+
     1W*(B(I,MKM)+B(I,MKM+200)))
      B(I,KTWO)=S(I)
  961 B(I,K)=C(I)*(1.0-E(I))*SUM
      GO TO 175
C
C     STEADY STATE PROBLEM  --  GENERATION STEP NSC.
C
 2230 DO 2961 I=1,N
      SUM=0.0
      IF (I-1) 2972,2972,2971
 2971 GAM=2.0*(B(2,K1)*SIGP(1)/SIGP(2)-B(1,K1))
      SUM=SUM+G(1,I)*(FLT(1)*(B(1,K1)+S(1))+SLP(1)*GAM)
 2972 DO 2973 J=2,NM
      IF (J-I) 2974,2973,2975
 2974 GAM =SIGP(J)*(B(J+1,K1)/SIGP(J+1)-B(J-1,K1)/SIGP(J-1))
      SUM=SUM+G(J,I)*(FLT(J)*(B(J,K1)+S(J))+SLP(J)*GAM)
      GO TO 2973
 2975 GAM=SIGP(J)*(B(J-1,K1)/SIGP(J-1)-B(J+1,K1)/SIGP(J+1))
      SUM=SUM+G(I,J)*(FLT(J)*(B(J,K1)+S(J))+SLP(J)*GAM)
 2973 CONTINUE
      IF (N-I) 2977,2977,2976
 2976 GAM=2.0*(B(NM,K1)*SIGP(N)/SIGP(NM)-B(N,K1))
      SUM=SUM+G(I,N)*(FLT(N)*(B(N,K1)+S(N))+SLP(N)*GAM)
 2977 SUM=SUM+GI(I)*(B(I,K1)+S(I))
 2961 B(I,K)=C(I)*(1.0-E(I))*SUM
  175 IF (NDET) 177,177,171
C
C     RECORD DETECTOR RESPONSES IF NDET GREATER THAN ZERO.
C
  171 NNA=NNB
      NNB=NSC/NSPD
      IF(NNB-NNA)177,177,145
  145 ID=0
  147 IF (NDET-ID) 176,176,146
  146 ID=ID+1
      LOC=LID(ID)
      D(ID,NSD)=B(LOC,K)/SIGP(LOC)
```

```
      GO TO 147
  176 NTS(NSD)=NSC
      SRCI(NSD)=S(LIS)
      NSD=NSD+1
      IF (NSD-200) 177,177,399
  399 NSDM=200
      JAD=1
      GO TO 400
  405 NSD=1
  177 GO TO (180,178,180),NCOT
C
C     DISTRIBUTION SPACE-TIME CONVERGENCE TESTS.
C
  180 B(N1,K)=B(1,K)/B(1,K1)
      B(N2,K)=B(NHALF,K)/B(NHALF,K1)
      B(N3,K)=B(NM3,K)/B(NM3,K1)
      IF(NSC-LIM)178,178,181
  181 V1=ABSF(B(N2,K)-B(N1,K))
      CONVB=V1
      IF(V1-CONV) 182,178,178
  182 V2=ABSF(B(N3,K)-B(N1,K))
      V3=ABSF(B(N1,K)-B(N1,K1))
      V4=ABSF(B(N2,K)-B(N2,K1))
      V5=ABSF(B(N3,K)-B(N3,K1))
      CONVB=V1+V2+V3+V4+V5
      IF (CONVB-CONV) 250,250,178
C
C     COMPLETION CHECKS.
C
  178 IF(MITN-NSC) 200,200,179
  179 IF (200-K) 183,183,152
  183 GO TO (185,184,184),NCOT
  184 KFL=200
      JAT=1
C
C     PRINT OUT TRANSIENT RESULTS.
C
   60 NAF=NSC-KFL
      IF(KFL-NNN) 59,52,52
   52 DO 108 J=NNN,KFL,NSP
  108 NXX(J)=J+NAF
      LLL=NNN
   53 III=0
      PRINT 1, NTYP,INDX,IPASS,NPAG
      NPAG=NPAG+1
      PRINT 2
   54 JJJ=LLL+4*NSP
      MMM=KFL+NSP-1-JJJ
      IF(MMM) 56,56,50
   50 PRINT 3,(NXX(J),J=LLL,JJJ,NSP),
     1(I,(B(I,J),J=LLL,JJJ,NSP),I=1,N3)
      LLL=JJJ+NSP
      IF(N-20) 51,51,53
   51 IF(III) 55,55,53
```

```
   55 III=1
      GO TO 54
   56 IF(KFL-LLL) 59,58,58
   58 PRINT 11,(NXX(J),J=LLL,KFL,NSP)
      DO 57 I=1,N3
   57 PRINT 12,I,(B(I,J),J=LLL,KFL,NSP)
   59 NAA=NSC/NSP
      NAB=NSP*NAA
      NAC=NSC - NAB
      NNN=LIM + NSP - NAC
      GO TO (185,265),JAT
  185 JAR=1
      KSL=LIMK
C
C     B(I,K) ARRAY FILLED, RESET FOR NEXT PASS.
C
  277 DO 186 J=1,LIM
      L=KSL+J
      DO 186 I=1,N3
  186 B(I,J)=B(I,L)
      DO 118 J=LIMP,200
      DO 118 I=1,N3
  118 B(I,J)=0.0
      DO 101 J=201,LIMT
      L=KSL+J
      DO 101 I=1,N
  101 B(I,J)=B(I,L)
      DO 102 J=LIMTP,400
      DO 102 I=1,N
  102 B(I,J)=0.0
      GO TO (151,285),JAR
C
C     THE SPECIFIED NUMBER OF TIME STEPS HAS BEEN REACHED.
C
  200 KFL=K
      NCN=2
      GO TO 260
C
C     THE DISTRIBUTION HAS CONVERGED.
C
  250 KFL=K
      NCN=1
  260 GO TO (265,261,261),NCOT
  261 JAT=2
      GO TO 60
  265 GO TO (266,270,266),NCOT
C
C     COMPUTE AND PRINT OUT CONVERGENCE RESULTS.
C
  266 EIGB=LOGF(B(N2,KFL))/TS
      KFLT=KFL+200
      SUM=0.0
      SUMT=0.0
      DO 132 I=1,N
```

```
      FLX(I)=B(I,KFL)/SIGP(I)
      GO TO (66,65),KTSS
   65 B(I,KFLT)=S(I)
   66 BEQ(I)=B(I,KFL)+B(I,KFLT)
      SUM=SUM+BEQ(I)
  132 SUMT=SUMT+FLX(I)
      SUM=SUM/QUAN
      SUMT=SUMT/QUAN
      DO 133 I=1,N
      BEQ(I)=BEQ(I)/SUM
  133 FLX(I)=FLX(I)/SUMT
      KM7=KFL-4
      PRINT 1, NTYP,INDX,IPASS,NPAG
      NPAG=NPAG+1
      PRINT 4
      PRINT 5, NCOT,NCN,NSC,CONVB,EIGB
      PRINT 6,(I,BEQ(I),FLX(I),I=1,N)
      PRINT 1, NTYP,INDX,IPASS,NPAG
      NPAG=NPAG+1
      PRINT 4
      PRINT 7,(I,(B(I,J),J=KM7,KFL),I=1,N3)
  270 IF(NDET)275,275,271
  271 NSDM=NSD-1
      JAD=2
C
C     PRINT OUT DETECTOR RESPONSE READINGS.
C
  400 JAAA=1
      JBBB=45
   85 PRINT 1, NTYP,INDX,IPASS,NPAG
      NPAG=NPAG+1
      PRINT 8,NDET,LIS,(LID(I),I=1,NDET)
      IF(NSDM-JBBB)81,81,82
   81 JBBB=NSDM
   82 DO 83 J=JAAA,JBBB
   83 PRINT 9,NTS(J),SRCI(J),(D(I,J),I=1,NDET)
      IF(NSDM-JBBB) 401,401,84
   84 JAAA=JAAA+45
      JBBB=JBBB+45
      GO TO 85
  401 GO TO (405,275),JAD
  275 GO TO (285,276),MODR
C
C     RESET INDICES AND MEMORY IN PREPARATION FOR ALTERED
C     PROPERTIES ON THE NEXT PASS.
C
  276 MA=2
      NSD=1
      JAR=2
      KSL=KFL-LIM
      GO TO 277
  285 RETURN
      END
```

APPENDIX B

THE PROGRAM TOVSR (SLAB GEOMETRY)

The program TOVSR, for the time-dependent monoenergetic slab reactor, is written in FORTRAN II language for the IBM-7094 computer. In addition to the short MAIN program, the following seven subroutines are required: SOURCE, TDEP, READ2, CONTRL, TPARAM, TABLE and TCALC. The functions of each subroutine are described by comment statements in the listings. The program occupies 4435 (decimal) core locations. COMMON storage occupies 15775 locations.

An input form is given in Section B1. The input variables are defined in Section B2 and the output variables are defined in Section B3. The program output for a simple example problem, the 5-region, Model FSC run of Table 3E.1, is given in Section B4. Finally, the FORTRAN listings are given in Section B5.

B1. TOVSR INPUT FORM

Notes: (a) 126 $E_3(p)$ data cards are read-in before card No. 0.

(b) Input data cards should be arranged in the order shown.

(c) Numbered cards are mandatory for each problem; inclusion of alphabetically designated sets of cards is conditional.

(d) FORTRAN II format is given in the brackets.

Card No.	Condition	Variables to be Read	FORMAT
0	--	NPROB	[I5]
	Read the following for each problem to be solved:		
1	--	NTYP,N,NT,NSTP,MHOM,MODC,NMEM,NCOT,NSRC	[9I5]
2	--	MODR,MITN,NDET,LIS,JSC,KPARA,KPARB,NSP,NSPD	[9I5]
3	--	KSRC,MLIM,KTSS,KTDEP,KMIX,KXXA,KXXB,KXXC,KXXD	[9I5]
4	--	WD,SPD,CONV,EIGA,TSRC,TMITN	[6E12.5]
A	MHOM=1	SIGD(1),C(1)	[2E12.5]
B	MHOM=2	(SIGD(I),C(I),I=1,N)	[6E12.5]
C	MHOM=2	(KTRL(I),I=1,N)	[14I5]
D	KMIX>0	(KMDC(I),I=1,N)	[14I5]
E	NDET>0	(LID(ID),ID=1,NDET)	[3I5]
F	MODR=2	SIGDM	[E12.5]
G	NMEM=2,3	(B(I,1),I=1,N)	[6E12.5]
H	NSRC=1,2	(S(I),I=1,N)	[6E12.5]
I	NTYP=1, NT>1	Add new set of cards 1 through F for each additional run	
J	NTYP=3	(KEXA(I),I=1,NT)	[14I5]
K	NTYP=4, NT>1	Add the following cards for each additional pass:	
		TMITN	[E12.5]
		(SIGD(I),C(I),I=1,N)	[6E12.5]
		(KTRL(I),I=1,N)	[14I5]

B2. DESCRIPTION OF TOVSR INPUT VARIABLES

Notes: (a) Assignable values are enclosed in brackets. Where different values alter the logical flow of the program, the meaning of each value is defined.

(b) The variables are arranged in the order in which they are are read by the program.

INTEGERS

NPROB = No. of independent problems to be solved [≥ 1]

NTYP = Problem Type (See Subroutine CONTRL).

[1 - General problem. NT runs with same TPARAM-computed properties.
2 - Homogeneous reactor. Computations for NT different values of N.
3 - Initial, localized source problem. NT successive runs with sources in different regions.
4 - Time-dependent properties are read-in at time of each change. NT sets of properties.
5 - Time-dependent properties controlled or computed by user-written subroutine TDEP.]

N = No. of regions. [$4 \leq N \leq 30$]

NT = No. of successive runs or passes, as described under NTYP. [≥ 1]

NSTP = Increase in N for each successive run of an NTYP = 2 problem. [≥ 1, if NTYP=2]

MHOM = [1 - Homogeneous reactor.
2 - Inhomogeneous reactor.]

MODC = [1 - Model F (Flat approximation).
2 - Model FS (Slope Correction).
3 - Model FSC (Slope and curvature corrections).]

TOVSR INPUT VARIABLES (cont'd)

NMEM = Control variable for setting the LIM time steps of initial memory.

1 - Sets B(I,K) = 1.0 for I=1, N and K=1, LIM.
2 - Reads B(I,1) for I=1, N; sets B(I,K) = B(I,1) for I = 1, N and K = 2, LIM.
3 - Reads B(I,1) for I = 1, N; sets B(I,K) in accordance with inverse period EIGA for I = 1, N and K = 2, LIM.
4 - Sets B(I,K) = 10^{-25} for I = 1, N and K = 1, LIM.

NCOT = Control variable for asymptoticity testing and transient print out.

1 - Tests for asymptoticity at each time step. Does not print transient results.
2 - No asymptoticity convergence test. Prints transient results with a spacing of NSP time steps.
3 - Both tests for asymptoticity and prints transient.

NSRC = Source rate control variable.

1 - Reads S(I) for I = 1, N; source constant in time.
2 - Reads S(I) for I = 1, N; source lasts JSC time steps.
3 - Sets S(I) = 0 for I = 1, N.
4 - Calls user-written Subroutine SOURCE at each time step.

MODR =

1 - One pass into Subroutine TCALC.
2 - NT passes through TCALC, where property changes are made before each pass. Run continues with new properties. Always use this value with NTYP = 4 or 5.

MITN = Maximum number of time steps [≥ 1]. For NTYP = 4 or 5, MITN = TMITN/unit time step.

NDET = No. of detectors [$0 \leq$ NDET ≤ 3]. Detectors are located in regions LID(ID), ID = 1,3. NDET > 0 causes printout of S(LIS) and detector responses with a spacing of NSPD time steps.

LIS = Region for which source rate S(LIS) is to be printed out if NDET > 0. [$1 \leq$ LIS $\leq$ N, if NDET > 0].

TOVSR INPUT VARIABLES (cont'd)

JSC = Duration in time steps of initial source distribution. [≥ 0, if NSRC = 2]. If JSC = 0, program computes new value equal to TSRC/unit time step.

KPARA = Print control variable in Subroutine TPARAM.
- 1 - Prints calculated parameters.
- 2 - Does not print.

KPARB = Print control variables in TPARAM.
- 1 - Prints arrays G(I,J), GSLP(I,J), GCRV(I,J) and GTAU(I,J).
- 2 - Does not print.

NSP = Time step spacing in transient print out. [≥ 1, if NCOT = 2,3]

NSPD = Time step spacing in detector-response print out. [≥ 1, if NDET > 0]

KSRC = (Dummy variable not used in listed program). [any]

MLIM = Control variable for LIM, the number of memory time steps.
- 0 - LIM computed by program.
- >0 - LIM is set equal to MLIM.

KTSS =
- 1 - Time-dependent problem.
- 2 - Steady-state or generation-to-generation problem.

KTDEP =
- 1 - Subroutine TDEP not called from TCALC.
- 2 - TDEP called from TCALC at each time step if KTSS = 1.

KMIX =
- 0 - Sets KMDC(I) = MODC for I = 1, N.
- >0 - Reads KMDC(I) for I = 1, N.

KXXA, KXXB, KXXC, KXXD = Dummy variables included in READ statement and program COMMON for user convenience in selective reprogramming. [any]

FLOATING POINT VARIABLES

WD = Reactor Width, cm.

SPD = Neutron speed, cm./sec.

CONV = Asymptoticity convergence criterion.

TOVSR INPUT VARIABLES (cont'd)

EIGA = Inverse period, sec^{-1}, for setting initial memory if NMEM = 3.

TSRC = Duration in seconds of the initial source distribution if NSRC = 2. (See JSC).

TMITN = Time in seconds, after start of transient, until which the current set of properties is to apply, if NTYP = 4 or 5. (See MITN).

SIGDM = Maximum collision cross-section expected in a problem with time-dependent properties, for MODR = 2. Fixes a unit time step which remains constant and is less than or equal to every expected time delay $\tau(I,J)$.

ARRAYS

SIGD(I) = Collision cross-section, cm^{-1}, in region I.

C(I) = Mean number of secondaries per collision in region I.

KTRL(I) = [1 - Property discontinuity at left edge of region I.
0 - No property discontinuities at edges of region I.
-1 - Property discontinuity at right edge of region I.]

KMDC(I) = [1 - Flat approximation for parent neutrons born in region I.
2 - Slope correction.
3 - Slope and curvature corrections.]

LID(ID) = Region in which detector No. ID is located.

B(I,1) = Progeny birth rate in region I to be used in setting up the initial memory. (Note that B(I,K) in this program does not include external source rates. These are stored in B(I,K + 150).)

S(I) = External source rate in region I.

KEXA(I) = Region for initial source in run I of an NTYP = 3 problem.

B3. DESCRIPTION OF TOVSR OUTPUT VARIABLES

Note: Variables are listed in order of appearance. Those described in the previous section are not included here.

Printed if KPARA = 1:

DLTX = Width of subregion, cm.

TS = Unit time step, sec.

TSMALL = Distance particle travels during unit time step divided by DLTX.

LIM = No. of time steps reserved for memory.

KSMALL = Integer computed in TPARAM. LIM is set equal to the product of N and KSMALL if MLIM = 0.

PATH(I) = Optical width of region I in mean free paths parallel to the x-axis.

Printed if KPARA = 1 and KPARB = 1:

G(I,J) = Spatial transfer coefficient for the flat mode.

GSLP(I,J) = Spatial transfer coefficient for the slope-correction mode.

GCRV(I,J) = Spatial transfer coefficient for the curvature-correction mode.

GTAU(I,J) = Mean delay, in unit time steps, between births in J and collisions in I.

Printed if NCOT = 1 or 3:

NCN = [1 - Asymptotic solution.
2 - Solution not asymptotic. CONV not satisfied.]

NSC = Number of time steps or iterations completed.

CONVB = Degree of asymptoticity convergence attained.

EIGB = Inverse period, sec^{-1}, of the asymptotic solution.

BIRTH RATE = Normalized asymptotic birth rate distribution, including the external source rate.

FLUX = Normalized flux distribution.

Printed if NCOT = 2 or 3:

B(I,K) = Progeny birth rate in region I at time step K; it does not include contributions from external sources. The values for I = N + 1, N + 2, and N + 3 are the ratios $R_1(I)$, $R_2(K)$ and $R_3(K)$ of equations (2E.2).

B.4 EXAMPLE OF PRINTED OUTPUT FROM TOVSR

TOVSR PROBLEM 1 RUN 1 PASS 1 PAGE 1

INITIAL INPUT DATA

NTYP = 1	N = 5	NT = 1	NSTP = 0	MHOM = 1
MODC = 3	NMEM = 1	NCOT = 1	NSRC = 3	MODR = 1
MITN = 50	NDET = 0	LIS = 0	JSC = 0	KPARA = 1
KPARB = 1	NSP = 0	NSPD = 0	KSRC = 0	MLIM = 0
KTSS = 1	KTDEP = 1	KMIX = 0	KXXA = 0	
KXXB = 0	KXXC = 0	KXXD = 0		

WD = .29464E 01 CENTIMETERS. SPD = .22000E 06 CM./SEC.

CONV = 1.00000E-07 EIGA = .00000E 00 INVERSE SEC.

TSRC = .00000E 00 SECONDS. TMITN = .00000E 00 SECONDS.

RGN.	B(I,1)	S(I)	SIGD(I)	C(I)	KMDC(I)	KTRL(I)
1	.00000E 00	.00000E 00	.500000	1.400000	3	1
2	.00000E 00	.00000E 00	.500000	1.400000	3	0
3	.00000E 00	.00000E 00	.500000	1.400000	3	0
4	.00000E 00	.00000E 00	.500000	1.400000	3	0
5	.00000E 00	.00000E 00	.500000	1.400000	3	-1

EXAMPLE PROBLEM (cont'd)

TOVSR PROB. TYPE 1 RUN NUMBER 1 PASS NUMBER 1 PAGE 2

CALCULATED INPUT PARAMETERS FOLLOW.

N = 5 MITN = 50

DLTX = .5892800E 00 TS = .3688355E-05

TSMALL = .1376999E 01 UNITS OF DLTX. LIM = 5

SIGDM = .00000E 00 JSC = 0 KSMALL = 1

RGN.	PATH(I)
1	.294640
2	.294640
3	.294640
4	.294640
5	.294640

TOVSR PROB. TYPE 1 RUN NUMBER 1 PASS NUMBER 1 PAGE 3

MATRIX G(I,J) FOLLOWS.

MATRIX ELEMENTS

I					
1	.3299258	.1517087	.0712791	.0405118	.0246691
2	.1517087	.3299258	.1517087	.0712791	.0405118
3	.0712791	.1517087	.3299258	.1517087	.0712791
4	.0405118	.0712791	.1517087	.3299258	.1517087
5	.0246691	.0405118	.0712791	.1517087	.3299258

TOVSR PROB. TYPE 1 RUN NUMBER 1 PASS NUMBER 1 PAGE 4

MATRIX GSLP(I,J) FOLLOWS.

MATRIX ELEMENTS

I					
1	0.	-.0059650	-.0018119	-.008750	-.0004837
2	.0059650	0.	-.0059650	-.0018119	-.0008750
3	.0018119	.0059650	0.	-.0059650	-.0018119
4	.0008750	.0018119	.0059650	0.	-.0059650
5	.0004837	.0008750	.0018119	.0059650	0.

EXAMPLE PROBLEM (cont'd)

TOVSR PROB. TYPE 1 RUN NUMBER 1 PASS NUMBER 1 PAGE 5

MATRIX GCRV(I,J) FOLLOWS.

MATRIX ELEMENTS

I_1					
1	-.0018220	.0007313	.0001005	.0000374	.0000172
2	.0007313	-.0018220	.0007313	.0001005	.0000374
3	.0001005	.0007313	-.0018220	.0007313	.0001005
4	.0000374	.0001005	.0007313	-.0018220	.0007313
5	.0000172	.0000374	.0001005	.0007313	-.0018220

TOVSR PROB. TYPE 1 RUN NUMBER 1 PASS NUMBER 1 PAGE 6

MATRIX GTAU(I,J) FOLLOWS.

MATRIX ELEMENTS

I_1					
1	1.0000000	1.7955801	2.8463779	3.7300318	4.5622697
2	1.7955801	1.0000000	1.7955801	2.8463779	3.7300318
3	2.8463779	1.7955801	1.0000000	1.7955801	2.8463779
4	3.7300318	2.8463779	1.7955801	1.0000000	1.7955801
5	4.5622697	3.7300318	2.8463779	1.7955801	1.0000000

TOVSR PROBLEM 1 RUN 1 PASS 1 PAGE 7

CONVERGENCE RESULTS

NCOT = 1 NCN = 1 NSC = 24

CONVB = .81956387E-07 EIGB = -.28672820E 02

ASYMPTOTIC DISTRIBUTIONS

REG. NO.	BIRTH RATE	FLUX
1	.81504759	.81504758
2	1.09297632	1.09297632
3	1.18395206	1.18395206
4	1.09297638	1.09297638
5	.81504769	.81504768

CONVERGENCE RESULTS

RESULTS OF LAST FIVE TIME STEPS

1	.7960513E 00	.7959673E 00	.7958832E 00	.7957990E 00	.7957149E 00
2	.1067503E 01	.1067390E 01	.1067277E 01	.1067164E 01	.1067051E 01
3	.1156358E 01	.1156236E 01	.1156114E 01	.1155991E 01	.1155869E 01
4	.1067503E 01	.1067390E 01	.1067277E 01	.1067164E 01	.1067051E 01
5	.7960514E 00	.7959674E 00	.7958833E 00	.7957991E 00	.7957150E 00
6	.9998945E 00	.9998945E 00	.9998943E 00	.9998943E 00	.9998942E 00
7	.9998943E 00	.9998942E 00	.9998942E 00	.9998942E 00	.9998943E 00
8	.9998943E 00	.9998942E 00	.9998942E 00	.9998942E 00	.9998943E 00

```
*      LIST8
*      LABEL
CTOVSR
       DIMENSION SIGD(30),C(30),KTRL(30),KMDC(30),PATH(30),
      1G(30,30),GSLP(30,30),GCRV(30,30),GTAU(30,30),
      2B(33,300),NXX(150),LID(3),D(3,200),NTS(200),S(30),
      3SRCI(200),BEQ(30),FLX(30),KEXA(30),EXB(30),EXC(150),
      4EXD(150),E3A(250),E3B(250)
       COMMON NTYP,N,NT,NSTP,MHOM,MODC,NMEM,NCOT,NSRC,
      1MODR,MITN,NDET,LIS,JSC,KPARA,KPARB,NSP,NSPD,
      2KSRC,MLIM,KTSS,KTDEP,KMIX,KXXA,KXXB,KXXC,KXXD,
      3KXXE,MA,NPAG,INDX,IPASS,NSC,NSD,LIM,KFL,ARGU,AF,BF,
      4CF,DF,WD,SPD,CONV,EIGA,TSRC,TMITN,EIGB,QUAN,TS,DLTX,
      5SIGDM,SIGD,C,KTRL,KMDC,G,GSLP,GCRV,GTAU,B,NXX,LID,D,
      6NTS,S,SRCI,BEQ,FLX,KEXA,EXB,EXC,EXD,E3A,E3B
     1 FORMAT(I5)
     2 FORMAT(4E16.9)
       READ 2, (E3A(I),I=1,250)
       READ 2, (E3B(I),I=1,250)
       READ 1,NPROB
    50 CALL READ2
       CALL CONTRL
       NPROB=NPROB-1
       IF (NPROB) 100,100,50
   100 CALL EXIT
       END




*      LIST8
*      LABEL
       SUBROUTINE SOURCE
C
C     DUMMY SUBROUTINE  --  TIME DEPENDENT SOURCES.
C
       RETURN
       END




*      LIST8
*      LABEL
       SUBROUTINE TDEP
C
C     DUMMY SUBROUTINE  --  TIME-DEPENDENT PROPERTIES.
C
       RETURN
       END
```

```
*      LIST8
*      LABEL
       SUBROUTINE READ2
C
C     SUBROUTINE READS IN AND PRINTS OUT INPUT DATA FOR
C     A PARTICULAR PROBLEM.
C
       DIMENSION SIGD(30),C(30),KTRL(30),KMDC(30),PATH(30),
      1G(30,30),GSLP(30,30),GCRV(30,30),GTAU(30,30),
      2B(33,300),NXX(150),LID(3),D(3,200),NTS(200),S(30),
      3SRCI(200),BEQ(30),FLX(30),KEXA(30),EXB(30),EXC(150),
      4EXD(150),E3A(250),E3B(250)
       COMMON NTYP,N,NT,NSTP,MHOM,MODC,NMEM,NCOT,NSRC,
      1MODR,MITN,NDET,LIS,JSC,KPARA,KPARB,NSP,NSPD,
      2KSRC,MLIM,KTSS,KTDEP,KMIX,KXXA,KXXB,KXXC,KXXD,
      3KXXE,MA,NPAG,INDX,IPASS,NSC,NSD,LIM,KFL,ARGU,AF,BF,
      4CF,DF,WD,SPD,CONV,EIGA,TSRC,TMITN,EIGB,QUAN,TS,DLTX,
      5SIGDM,SIGD,C,KTRL,KMDC,G,GSLP,GCRV,GTAU,B,NXX,LID,D,
      6NTS,S,SRCI,BEQ,FLX,KEXA,EXB,EXC,EXD,E3A,E3B
     1 FORMAT(9I5)
     2 FORMAT(6E12.5)
     3 FORMAT(2E12.5)
     5 FORMAT(3I5)
     7 FORMAT(1H1,5X6H TOVSR,3X8H PROBLEM I3,
      13X4H RUN I3,3X5H PASS I3,5X5H PAGE I4)
     8 FORMAT(1H0,20X,19H INITIAL INPUT DATA/)
     9 FORMAT(1H0,4X7H NTYP =I3,7X4H N =I3,6X5H NT =I3,
      14X7H NSTP =I3,4X7H MHOM =I3//5X7H MODC =I3,
      24X7H NMEM =I3,4X7H NCOT =I3,4X7H NSRC =I3,
      34X7H MODR =I3//5X7H MITN =I5,2X7H NDET =I3,
      45X6H LIS =I3,5X6H JSC =I5,3X8H KPARA =I3//
      54X8H KPARB =I3,5X6H NSP =I4,3X7H NSPD =I4,
      63X7H KSRC =I4,3X7H MLIM =I4//5X7H KTSS =I4,
      72X8H KTDEP =I4,3X7H KMIX =I4,3X7H KXXA =I4//
      85X7H KXXB =I4,3X7H KXXC =I4,3X7H KXXD =I4)
    10 FORMAT(1H0,5X5H WD =E12.5,13H CENTIMETERS.,
      19X6H SPD =E12.5,9H CM./SEC.//10X7H CONV =E12.5,
      210X7H EIGA =E12.5,13H INVERSE SEC.//5X7H TSRC =E12.5,
      39H SECONDS.,7X8H TMITN =E12.5,9H SECONDS.)
    11 FORMAT(1H0,4HRGN.,4X7H B(I,1),7X5H S(I),5X8H SIGD(I),
      13X5H C(I),2X8H KMDC(I),9H  KTRL(I))
    12 FORMAT(I4,2X,2E13.5,2F10.6,I4,2XI5)
    13 FORMAT(14I5)
    17 FORMAT(E12.5)
       MA=1
       NPAG=1
       INDX=1
       IPASS=1
       READ 1,NTYP,N,NT,NSTP,MHOM,MODC,NMEM,NCOT,NSRC,
      1MODR,MITN,NDET,LIS,JSC,KPARA,KPARB,NSP,NSPD,
      2KSRC,MLIM,KTSS,KTDEP,KMIX,KXXA,KXXB,KXXC,KXXD
       READ 2,WD,SPD,CONV,EIGA,TSRC,TMITN
       QUAN=N
       NM=N-1
```

```
      GO TO (101,102),MHOM
C
C     HOMOGENEOUS REACTOR
C
  101 READ 3,SIGD(1),C(1)
      DO 20 I=2,N
      KTRL(I)=0
      SIGD(I)=SIGD(1)
   20 C(I)=C(1)
      KTRL(1)=1
      KTRL(N)=-1
      GO TO 106
C
C     INHOMOGENEOUS REACTOR.
C
  102 READ 2,(SIGD(I),C(I),I=1,N)
      READ 13, (KTRL(I),I=1,N)
  106 IF (KMIX) 108,108,107
C
C     KMDC(J) SPECIFIES WHAT APPROXIMATION IS TO BE USED IN
C     THE SOURCE REGION, J.  FLAT APPROXIMATION FOR KMDC(J)
C     =1, SLOPE CORRECTION FOR KMDC(J)=2, SLOPE AND
C     CURVATURE CORRECTIONS FOR KMDC(J)=3.
C
  107 READ 13, (KMDC(I),I=1,N)
      GO TO 103
  108 DO 21 I=1,N
   21 KMDC(I)=MODC
  103 IF(NDET) 110,110,104
C
C     DETECTOR LOCATIONS WHEN DETECTORS ARE USED.
C
  104 READ 5,(LID(ID),ID=1,NDET)
  110 GO TO (60,50),MODR
C
C     MAXIMUM COLLISION CROSS SECTION EXPECTED FOR CASE OF
C     TIME-DEPENDENT COLLISION CROSS-SECTION, SIGD(I).
C
   50 READ 17,SIGDM
   60 GO TO (120,111,111,120),NMEM
C
C     INITIAL MEMORY INPUT.
C
  111 READ 2,(B(I,1),I=1,N)
  120 GO TO  (125,125,130,130),NSRC
C
C     SOURCE DISTRIBUTION.
C
  125 READ 2,(S(I),I=1,N)
C
C     PRINT OUT INPUT DATA.
  130 PRINT 7, NTYP,INDX,IPASS,NPAG
      NPAG=NPAG+1
      PRINT 8
```

```
      PRINT 9,NTYP,N,NT,NSTP,MHOM,MODC,NMEM,NCOT,NSRC,
     1MODR,MITN,NDET,LIS,JSC,KPARA,KPARB,NSP,NSPD,
     2KSRC,MLIM,KTSS,KTDEP,KMIX,KXXA,KXXB,KXXC,KXXD
      PRINT 10,WD,SPD,CONV,EIGA,TSRC,TMITN
      PRINT 11
      PRINT 12,(I,B(I,1),S(I),SIGD(I),C(I),KMDC(I),
     1KTRL(I),I=1,N)
      RETURN
      END



*     LIST8
*     LABEL
      SUBROUTINE CONTRL
C
C     THIS SUBROUTINE CONTROLS PROGRAM FLOW FOR FIVE BASIC
C     PROBLEM TYPES, IDENTIFIED BY THE VALUE OF NTYP.
C
      DIMENSION SIGD(30),C(30),KTRL(30),KMDC(30),PATH(30),
     1G(30,30),GSLP(30,30),GCRV(30,30),GTAU(30,30),
     2B(33,300),NXX(150),LID(3),D(3,200),NTS(200),S(30),
     3SRCI(200),BEQ(30),FLX(30),KEXA(30),EXB(30),EXC(150),
     4EXD(150),E3A(250),E3B(250)
      COMMON NTYP,N,NT,NSTP,MHOM,MODC,NMEM,NCOT,NSRC,
     1MODR,MITN,NDET,LIS,JSC,KPARA,KPARB,NSP,NSPD,
     2KSRC,MLIM,KTSS,KTDEP,KMIX,KXXA,KXXB,KXXC,KXXD,
     3KXXE,MA,NPAG,INDX,IPASS,NSC,NSD,LIM,KFL,ARGU,AF,BF,
     4CF,DF,WD,SPD,CONV,EIGA,TSRC,TMITN,EIGB,QUAN,TS,DLTX,
     5SIGDM,SIGD,C,KTRL,KMDC,G,GSLP,GCRV,GTAU,B,NXX,LID,D,
     6NTS,S,SRCI,BEQ,FLX,KEXA,EXB,EXC,EXD,E3A,E3B
   13 FORMAT(14I5)
   16 FORMAT(E12.5/(6E12.5))
      GO TO (100,200,300,400,500),NTYP
C
C     GENERAL PROBLEM.   FOR NT GREATER THAN 1, THE
C     TRANSFER PARAMETERS REMAIN VALID FOR ADDITIONAL
C     PROBLEMS WITH CHANGING SOURCES,C(I),REACTOR SIZE, ETC.
C
  100 CALL TPARAM
      INDEX=1
  102 CALL TCALC
      INDEX=INDEX+1
      IF (NT-INDEX) 1000,101,101
  101 CALL READ2
      GO TO 102
C
C     HOMOGENEOUS REACTOR, COMPUTATIONS FOR NT DIFFERENT
C     VALUES OF N.
C
  200 CALL TPARAM
      CALL TCALC
      INDX=INDX+1
```

```
      IF(NT-INDX) 1000,201,201
  201 N=N+NSTP
      GO TO 200
C
C     SUCCESSIVE INITIAL SOURCE PROBLEMS, WHERE SOURCE IS
C     LOCALIZED TO ONE REGION AND LASTS FOR JSC TIME
C     STEPS.  NTYP=3 IS USEFUL FOR IMPORTANCE DISTRIBUTIONS
C     AND FAST TRANSIENTS.  THE KEXA(I) ARE THE
C     SPECIFIED SOURCE REGIONS FOR SUCCESSIVE RUNS.
C
  300 READ 13, (KEXA(I),I=1,NT)
      CALL TPARAM
      KZA=NSRC
  301 DO 302 I=1,N
  302 S(I)=0.0
      L=KEXA(INDX)
      LIS=L
      S(L)=1.0
      CALL TCALC
      NSRC=KZA
      INDX=INDX+1
      IF (NT-INDX) 1000,301,301
C
C     PROBLEM WITH TIME-DEPENDENT PROPERTIES WHICH ARE READ
C     IN AT TIME OF EACH CHANGE.  NT IS THE NUMBER OF
C     SUCCESSIVE SETS OF PROPERTIES TO BE READ IN. EACH
C     SET WILL LAST UNTIL TMITN SECONDS.
C
  400 CALL TPARAM
      MITN=TMITN/TS
      CALL TCALC
      IPASS=IPASS+1
      IF (NT-IPASS) 1000,401,401
  401 READ 16,TMITN,(SIGD(I),C(I),I=1,N)
      READ 13, (KTRL(I),I=1,N)
      GO TO 400
C
C     TIME-DEPENDENT PROPERTIES ARE CONTROLLED OR COMPUTED BY
C     A USER-WRITTEN SUBROUTINE,TDEP. (SIMPLE FUNCTIONS
C     OF TIME,FEEDBACK,ETC.)
C
  500 CALL TDEP
      CALL TPARAM
      MITN=TMITN/TS
      CALL TCALC
      IPASS=IPASS+1
      IF(NT-IPASS) 1000,500,500
 1000 RETURN
      END
```

```
*      LIST8
*      LABEL
       SUBROUTINE TPARAM
C
C     THIS SUBROUTINE CONVERTS THE INPUT DATA TO THE
C     TRANSFER PARAMETERS WHICH WILL BE NEEDED IN THE
C     BIRTH RATE COMPUTATIONS IN SUBROUTINE TCALC.
C
       DIMENSION SIGD(30),C(30),KTRL(30),KMDC(30),PATH(30),
      1G(30,30),GSLP(30,30),GCRV(30,30),GTAU(30,30),
      2B(33,300),NXX(150),LID(3),D(3,200),NTS(200),S(30),
      3SRCI(200),BEQ(30),FLX(30),KEXA(30),EXB(30),EXC(150),
      4EXD(150),E3A(250),E3B(250)
       COMMON NTYP,N,NT,NSTP,MHOM,MODC,NMEM,NCOT,NSRC,
      1MODR,MITN,NDET,LIS,JSC,KPARA,KPARB,NSP,NSPD,
      2KSRC,MLIM,KTSS,KTDEP,KMIX,KXXA,KXXB,KXXC,KXXD,
      3KXXE,MA,NPAG,INDX,IPASS,NSC,NSD,LIM,KFL,ARGU,AF,BF,
      4CF,DF,WD,SPD,CONV,EIGA,TSRC,TMITN,EIGB,QUAN,TS,DLTX,
      5SIGDM,SIGD,C,KTRL,KMDC,G,GSLP,GCRV,GTAU,B,NXX,LID,D,
      6NTS,S,SRCI,BEQ,FLX,KEXA,EXB,EXC,EXD,E3A,E3B
     1 FORMAT(1H1,3X6H TOVSR,3X10H PROB.TYPE I3,
      13X11H RUN NUMBER I3,3X12H PASS NUMBER I3,3X5H PAGE I3)
     2 FORMAT(1H0,15X36H CALCULATED INPUT PARAMETERS FOLLOW./
      1//10X,4H N =I3,15X7H MITN =I6//10X7H DLTX =E14.7,
      210X5H TS =E14.7///5X9H TSMALL =E14.7,2X,
      215H UNITS OF DLTX.,5X6H LIM =I5///10X8H SIGDM =E12.5,
      45X6H JSC =I5,10X9H KSMALL =I3///5X4HRGN.,5X8H PATH(I)//
      5(4X,I3,3X,F12.6))
     3 FORMAT(1H0,20X23H MATRIX G(I,J) FOLLOWS.//2H I,20X,
      116H MATRIX ELEMENTS )
     5 FORMAT(1H0,20X26H MATRIX GSLP(I,J) FOLLOWS. //
      12H I,20X,16H MATRIX ELEMENTS )
     6 FORMAT(1H0,20X26H MATRIX GCRV(I,J) FOLLOWS. //
      12H I,20X,16H MATRIX ELEMENTS )
     7 FORMAT(1H0,20X26H MATRIX GTAU(I,J) FOLLOWS.  //
      12H I,20X,16H MATRIX ELEMENTS )
    10 FORMAT(I3,6F12.7/5X6F12.7/7X6F12.7/9X6F12.7/11X6F12.7)
       QUAN=N
       DLTX=WD/QUAN
       NM=N-1
       NM2=N-2
C
C     MEAN FREE PATHS ACROSS REGION I.
C
       DO 22 I=1,N
       PATH(I)=SIGD(I)*DLTX
       GO TO (15,22),MHOM
    22 CONTINUE
       GO TO 210
C
C     HOMOGENEOUS REACTOR.
C
    15 DO 200 I=2,N
   200 PATH(I)=PATH(1)
```

```
C     STORE NUMBER OF MEAN FREE PATHS BETWEEN REGIONS I AND J.
C
  210 DO 211 I=1,NM
  211 G(I,I+1)=0.0
      DO 212 I=1,NM2
      IP2=I+2
      DO 212 J=IP2,N
  212 G(I,J)=G(I,J-1)+PATH(J-1)
      IA=0
C
C     START AND REENTRY POINT FOR RECEIVER REGIONS, IA.
C
  750 IA=IA+1
      PI=PATH(IA)
      ARGU=PI
      CALL TABLE
      F5=AF
      F10=BF
      F15=CF
      F20=DF
      G(IA,IA)=1.0-(0.5-F10)/PI
      GTAU(IA,IA)=(1.0+F5+(2.0*F10-1.0)/PI)/(PI*G(IA,IA))
      GCRV(IA,IA)=(-0.5+F10)/(6.0*PI)+(1.0+3.0*F15)/
     1(3.0*PI**2)+(-0.5+2.0*F20)/(PI**3)
C
C     START OF LOOP FOR SOURCE REGIONS, JA.
C
      JA=IA+1
      PJ=PATH(JA)
      ARGU=0.0
      F1=1.0
      F6=0.5
      F11=1.0/3.0
      F16=0.25
      GO TO 820
  800 JA=JA+1
      PJ=PATH(JA)
      ARGU=G(IA,JA)
      CALL TABLE
      F1=AF
      F6=BF
      F11=CF
      F16=DF
  820 ARGU=ARGU+PJ
      CALL TABLE
      F2=AF
      F7=BF
      F12=CF
      F17=DF
      ARGU=ARGU+PI
      CALL TABLE
      F3=AF
      F8=BF
      F13=CF
```

```
      F18=DF
      ARGU=ARGU-PJ
      CALL TABLE
      F4=AF
      F9=BF
      F14=CF
      F19=DF
      X=F6-F7+F8-F9
      G(IA,JA)=X/(2.0*PJ)
      G(JA,IA)=X/(2.0*PI)
      P=JA-IA-1
      GTAU(IA,JA)=(2.0*F3-F2-F4+P*(F1-F2+F3-F4))/X+1.0/PI+
     1 1.0/PJ
      GTAU(JA,IA)=GTAU(IA,JA)
      Y=F16-F17+F18-F19
      GCRV(IA,JA)=X/(12.0*PJ)-(F11+F12-F13-F14)/(2.0*PJ**2)+
     1Y/(PJ**3)
      GCRV(JA,IA)=X/(12.0*PI)-(F11-F12-F13+F14)/(2.0*PI**2)+
     1Y/(PI**3)
      GSLP(IA,JA)=-(F6+F7-F8-F9+(2.0/PJ)*(-F11+F12-F13+F14))/
     1(8.0*PJ)
      GSLP(JA,IA)=(F6-F7-F8+F9+(2.0/PATH(IA))*(-F11+F12-F13
     1+F14))/(8.0*PI)
      IF (N-JA) 821,821,800
C
C     COMPLETION OF JA LOOP.
C
  821 GO TO (900,822),MHOM
  822 IF (N-IA-1) 823,823,750
  823 IA=N
      PI=PATH(N)
      ARGU=PI
      CALL TABLE
      F5=AF
      F10=BF
      F15=CF
      F20=DF
      G(IA,IA)=1.0-(0.5-F10)/PI
      GTAU(IA,IA)=(1.0+F5+(2.0*F10-1.0)/PI)/(PI*G(IA,IA))
      GCRV(IA,IA)=(-0.5+F10)/(6.0*PI)+(1.0+3.0*F15)/
     1(3.0*PI**2)+(-0.5+2.0*F20)/(PI**3)
      GO TO 600
C
C     COMPLETION OF IA LOOP.
C
C     HOMOGENEOUS REACTOR.
C
  900 DO 910 I=2,NM
      G(I,I)=G(1,1)
      GTAU(I,I)=GTAU(1,1)
      GCRV(I,I)=GCRV(1,1)
      IP=I+1
      DO 910 J=IP,N
      L=J-I+1
```

```
      G(I,J)=G(1,L)
      G(J,I)=G(L,1)
      GTAU(I,J)=GTAU(1,L)
      GTAU(J,I)=GTAU(L,1)
      GCRV(I,J)=GCRV(1,L)
      GCRV(J,I)=GCRV(L,1)
      GSLP(I,J)=GSLP(1,L)
  910 GSLP(J,I)=GSLP(L,1)
      G(N,N)=G(1,1)
      GTAU(N,N)=GTAU(1,1)
      GCRV(N,N)=GCRV(1,1)
C
C     COMPUTATION OF UNIT TIME STEP, TS SECONDS.
C
  600 GO TO (309,430),MODR
  430 ARGU=SIGDM*DLTX
      CALL TABLE
      F5=AF
      F10=BF
      X=1.0-(0.5-F10)/ARGU
      P=(1.0+F5+(2.0*F10-1.0)/ARGU)/(ARGU*X)
      KSMALL=1.0/P + 1.0
      X=KSMALL
      TSMALL=1.0/X
      GO TO 325
  309 K=1
      DO 320 L=2,N
      IF (GTAU(L,L)-GTAU(K,K)) 310,320,320
  310 K=L
  320 CONTINUE
      TSMALL=GTAU(K,K)
      KSMALL=1.0/TSMALL + 1.0
  325 DO 330 I=1,N
      DO 330 J=1,N
  330 GTAU(I,J)=GTAU(I,J)/TSMALL
      DO 340 I=1,N
  340 GTAU(I,I)=GTAU(I,I)+1.0E-08
      TS=TSMALL*DLTX/SPD
C
C     COMPUTATION OF LIM, AN INTEGER GREATER THAN OR EQUAL
C     TO THE NUMBER OF TIME STEPS FOR WHICH MEMORY IS
C     REQUIRED.
C
      LIM=N*KSMALL
      IF (MLIM) 344,344,343
  343 LIM=MLIM
  344 IF(JSC) 350,350,360
  350 JSC=TSRC/TS
C
C     PRINT OUT PARAMETERS.
C
  360 GO TO (51,60),KPARA
   51 PRINT 1,NTYP,INDX,IPASS,NPAG
      NPAG=NPAG+1
```

```
      PRINT 2,N,MITN,DLTX,TS,TSMALL,LIM,SIGDM,JSC,KSMALL,
     1(I,PATH(I),I=1,N)
      GO TO (52,60),KPARB
   52 PRINT 1,NTYP,INDX,IPASS,NPAG
      NPAG=NPAG+1
      PRINT 3
      DO 53 I=1,N
   53 PRINT 10, I,(G(I,J),J=1,N)
      PRINT 1,NTYP,INDX,IPASS,NPAG
      NPAG=NPAG+1
      PRINT 5
      DO 54 I=1,N
   54 PRINT 10, I,(GSLP(I,J),J=1,N)
      PRINT 1,NTYP,INDX,IPASS,NPAG
      NPAG=NPAG+1
      PRINT 6
      DO 55 I=1,N
   55 PRINT 10,I,(GCRV(I,J),J=1,N)
      PRINT 1,NTYP,INDX,IPASS,NPAG
      NPAG=NPAG+1
      PRINT 7
      DO 56 I=1,N
   56 PRINT 10, I,(GTAU(I,J),J=1,N)
   60 RETURN
      END




*     LIST8
*     LABEL
      SUBROUTINE TABLE
C
C     THIS SUBROUTINE USES THIRD-ORDER POLYNOMIAL INTER-
C     POLATION TO DETERMINE THE VALUE OF THE THIRD ORDER
C     EXPONENTIAL INTEGRAL, BF=E3(ARGU), WHERE THE
C     ARGUMENT LIES BETWEEN TABULAR VALUES.  RECURSION
C     RELATIONS ARE THEN USED TO DETERMINE E2(ARGU),
C     E4(ARGU) AND E5(ARGU).
C
      DIMENSION SIGD(30),C(30),KTRL(30),KMDC(30),PATH(30),
     1G(30,30),GSLP(30,30),GCRV(30,30),GTAU(30,30),
     2B(33,300),NXX(150),LID(3),D(3,200),NTS(200),S(30),
     3SRCI(200),BEQ(30),FLX(30),KEXA(30),EXB(30),EXC(150),
     4EXD(150),E3A(250),E3B(250)
      COMMON NTYP,N,NT,NSTP,MHOM,MODC,NMEM,NCOT,NSRC,
     1MODR,MITN,NDET,LIS,JSC,KPARA,KPARB,NSP,NSPD,
     2KSRC,MLIM,KTSS,KTDEP,KMIX,KXXA,KXXB,KXXC,KXXD,
     3KXXE,MA,NPAG,INDX,IPASS,NSC,NSD,LIM,KFL,ARGU,AF,BF,
     4CF,DF,WD,SPD,CONV,EIGA,TSRC,TMITN,EIGB,QUAN,TS,DLTX,
     5SIGDM,SIGD,C,KTRL,KMDC,G,GSLP,GCRV,GTAU,B,NXX,LID,D,
     6NTS,S,SRCI,BEQ,FLX,KEXA,EXB,EXC,EXD,E3A,E3B
      IF (ARGU-20.1) 20,10,10
```

```
C     ARGU GREATER THAN 20.1, INTEGRALS ASSUMED EQUAL
C     TO ZERO.
C
   10 AF=0.0
      BF=0.0
      CF=0.0
      DF=0.0
      GO TO 1000
   20 Q=EXPF(-ARGU)
      IF (ARGU-2.4799) 30,30,60
   30 IF (ARGU- 0.0100) 40,40,50
C
C     ARGU LESS THAN 0.01 .
   40 X=ARGU/0.01
      LESS=0
      BY=0.5
      GO TO 55
C
C     ARGU BETWEEN 0.01 AND 2.4799.
   50 P=ARGU/0.01
      LESS=P
      A=LESS
      X=P-A
      BY=E3A(LESS)
   55 BZ1=E3A(LESS+1)-BY
      BZ2=(E3A(LESS+2)-BY)/2.0
      BZ3=(E3A(LESS+3)-BY)/3.0
      GO TO 70
C
C     ARGU BETWEEN 2.4799 AND 20.1 .
   60 P=ARGU/0.10
      LESS=P
      A=LESS
      X=P-A
      BY=E3B(LESS)
      BZ1=E3B(LESS+1)-BY
      BZ2=(E3B(LESS+2)-BY)/2.0
      BZ3=(E3B(LESS+3)-BY)/3.0
C
C     COMPUTATION OF POLYNOMIAL COEFFICIENTS.
   70 BC3=(BZ3+BZ1)/2.0 - BZ2
      BC2=BZ2-BZ1-3.0*BC3
      BC1=BZ1-BC2-BC3
      BF=BY+X*(BC1+X*(BC2+X*(BC3)))
C
C     RECURSION RELATIONS FOR EXPONENTIAL INTEGRALS OF
C     ORDERS 2, 4, AND 5.
C
      AF=(Q-2.0*BF)/ARGU
      CF=(Q-ARGU*BF)/3.0
      DF=(Q*(1.0-ARGU/3.0)+BF*ARGU**2/3.0)/4.0
 1000 RETURN
      END
```

```
*      LIST8
*      LABEL
       SUBROUTINE TCALC
C
C     THIS SUBROUTINE SOLVES THE PROBLEM POSED AND PRINTS
C     OUT THE RESULTS.
C
       DIMENSION SIGD(30),C(30),KTRL(30),KMDC(30),PATH(30),
      1G(30,30),GSLP(30,30),GCRV(30,30),GTAU(30,30),
      2B(33,300),NXX(150),LID(3),D(3,200),NTS(200),S(30),
      3SRCI(200),BEQ(30),FLX(30),KEXA(30),EXB(30),EXC(150),
      4EXD(150),E3A(250),E3B(250)
       COMMON NTYP,N,NT,NSTP,MHOM,MODC,NMEM,NCOT,NSRC,
      1MODR,MITN,NDET,LIS,JSC,KPARA,KPARB,NSP,NSPD,
      2KSRC,MLIM,KTSS,KTDEP,KMIX,KXXA,KXXB,KXXC,KXXD,
      3KXXE,MA,NPAG,INDX,IPASS,NSC,NSD,LIM,KFL,ARGU,AF,BF,
      4CF,DF,WD,SPD,CONV,EIGA,TSRC,TMITN,EIGB,QUAN,TS,DLTX,
      5SIGDM,SIGD,C,KTRL,KMDC,G,GSLP,GCRV,GTAU,B,NXX,LID,D,
      6NTS,S,SRCI,BEQ,FLX,KEXA,EXB,EXC,EXD,E3A,E3B
     1 FORMAT(1H1,5X6H TOVSR,3X8H PROBLEM I3,
      13X4H RUN I3,3X5H PASS I3,5X5H PAGE I4)
     2 FORMAT(1H0,20X18H TRANSIENT RESULTS)
     3 FORMAT(1H0,9HTIME STEP,I5,4I13/7H REGION/
      1(I3,4X,5E13.7))
     4 FORMAT(1H0,20X20H CONVERGENCE RESULTS)
     5 FORMAT(1H0,5X7H NCOT =I2,10X6H NCN =I2,10X6H NSC =I5//
      110X8H CONVB =E14.8,10X7H EIGB =E14.8)
     6 FORMAT(1H0/20X25H ASYMPTOTIC DISTRIBUTIONS//9H REG. NO.,
      15X11H BIRTH RATE,11X5H FLUX/(I6,7XF11.8,F20.8))
     7 FORMAT(1H0,20X31HRESULTS OF LAST FIVE TIME STEPS//
      1(I5,2X,5E13.7))
     8 FORMAT(1H0,20X26H DETECTOR RESPONSE RESULTS,
      110X7H NDET =I2//13X7H SOURCE,8X11H DETECTOR 1,
      25X11H DETECTOR 2,5X11H DETECTOR 3/9H LOCATION I8,
      33I16/10H TIME STEP)
     9 FORMAT(I6,4E16.8)
    11 FORMAT(1H0,9HTIME INDX,I5,4I13/)
    12 FORMAT(I3,4X,5E13.7)
       GO TO (100,300),MA
   300 GO TO (285,151),MODR
   100 GO TO (2000,2010),KTSS
C
C     FOR STEADY STATE PROBLEM.
C
  2010 LIM=4
C
C     SET UP PROBLEM CONSTANTS.
C
  2000 LIMK=150-LIM
       LIMT=LIM+150
       LIMTP=LIMT+1
```

```
      LIMP=LIM+1
      NM=N-1
      NNN=LIM+NSP
      N1=N+1
      N2=N+2
      N3=N+3
      NM3=N-3
      NHALF=N/2
      NNB=0
      NSD=1
      NSC=0
C
C     SET INITIAL MEMORY IN B(I,K).
C
      GO TO (110,120,130,140),NMEM
  110 DO 111 I=1,N
  111 B(I,1)=1.0
  120 DO 121 J=2,LIM
      DO 121 I=1,N
  121 B(I,J)=B(I,1)
      GO TO 150
  130 X=EIGA*TS
      R=1.0+X*(1.0+X*(0.5+X*(1.0/6.0+X*(1.0/24.0+
     1X*(1.0/120.0+X*(1.0/720.0+X/5040.0))))))
      DO 131 J=2,LIM
      K1=J-1
      DO 131 I=1,N
  131 B(I,J)=R*B(I,K1)
      GO TO 150
  140 DO 141 I=1,N
  141 B(I,1)=1.0E-25
      GO TO 120
C
C     CLEAR REMAINDER OF B(I,K) ARRAY.
C
  150 DO 119 J=LIMP,300
      DO 119 I=1,N3
  119 B(I,J)=0.0
  151 K=LIM
C
C     COMPUTE BIRTH RATE DISTRIBUTION AT TIME STEP NSC.
C
  152 NSC=NSC+1
      KFL=K
      K1=K
      K=K+1
      KTWO=K+150
C
C     SOURCE DISTRIBUTION AT TIME STEP NSC.
C
      GO TO (160,154,155,157),NSRC
  154 IF(JSC-NSC) 155,160,160
  155 DO 156 I=1,N
  156 S(I)=0.0
```

```
      NSRC=1
      GO TO 160
  157 CALL SOURCE
  160 GO TO (2220,2230),KTSS
C
C     TIME-DEPENDENT PROBLEM.
C
 2220 GO TO (2221,2222),KTDEP
 2222 CALL TDEP
 2221 DO 961 I=1,N
      SUM=0.0
      DO 962 J=1,N
      TT=GTAU(I,J)
      KT=TT
      IF (KT-LIM) 970,962,962
  970 TK=KT
      W=TT-TK
      WM=1.0-W
      MK=K-KT
      MKM=MK-1
      C0=WM*B(J,MK)+W*B(J,MKM)
      KAK=KMDC(J)-2
      IF (KAK) 977,971,971
  971 IF (KTRL(J)) 973,975,974
  973 A2=WM*B(J-1,MK)+W*B(J-1,MKM)
      A3=WM*B(J-2,MK) + W*B(J-2,MKM)
      Q=-1.0
      GO TO 976
  974 A2=WM*B(J+1,MK) + W*B(J+1,MKM)
      A3=WM*B(J+2,MK) + W*B(J+2,MKM)
      Q=1.0
  976 C1=Q*(4.0*A2-3.0*C0-A3)
      C2=(A3+C0)/2.0-A2
      GO TO 977
  975 A2=WM*B(J-1,MK) + W*B(J-1,MKM)
      A3=WM*B(J+1,MK) + W*B(J+1,MKM)
      C1=A3-A2
      C2=(A3+A2)/2.0-C0
  977 C0=C0+WM*B(J,MK+150)+W*B(J,MKM+150)
      IF (KAK) 978,979,980
  978 SUM=SUM+G(I,J)*C0
      GO TO 962
  979 SUM=SUM+G(I,J)*C0 + GSLP(I,J)*C1
      GO TO 962
  980 SUM=SUM+G(I,J)*C0 + GSLP(I,J)*C1 + GCRV(I,J)*C2
  962 CONTINUE
      B(I,KTWO)=S(I)
  961 B(I,K)=C(I)*SUM
      GO TO 175
C
C     STEADY STATE PROBLEM  --  GENERATION STEP NSC.
C
 2230 DO 2961 I=1,N
      SUM=0.0
```

```
      DO 2962 J=1,N
      C0=B(J,K1)
      KAK=KMDC(J)-2
      IF(KAK) 2977,2971,2971
 2971 IF (KTRL(J)) 2973,2975,2974
 2973 A2=B(J-1,K1)
      A3=B(J-2,K1)
      Q=-1.0
      GO TO 2976
 2974 A2=B(J+1,K1)
      A3=B(J+2,K1)
      Q=1.0
 2976 C1=Q*(4.0*A2-3.0*C0-A3)
      C2=(A3+C0)/2.0-A2
      GO TO 2977
 2975 A2=B(J-1,K1)
      A3=B(J+1,K1)
      C1=A3-A2
      C2=(A3+A2)/2.0-C0
 2977 C0=C0+S(J)
      IF (KAK) 2978,2979,2980
 2978 SUM=SUM+G(I,J)*C0
      GO TO 2962
 2979 SUM=SUM + G(I,J)*C0 + GSLP(I,J)*C1
      GO TO 2962
 2980 SUM=SUM+G(I,J)*C0 + GSLP(I,J)*C1 + GCRV(I,J)*C2
 2962 CONTINUE
 2961 B(I,K)=C(I)*SUM
  175 IF (NDET) 177,177,171
C
C     RECORD DETECTOR RESPONSES IF NDET GREATER THAN ZERO.
C
  171 NNA=NNR
      NNB=NSC/NSPD
      IF(NNB-NNA)177,177,145
  145 ID=0
  147 IF (NDET-ID) 176,176,146
  146 ID=ID+1
      LOC=LID(ID)
      D(ID,NSD)=B(LOC,K)/(C(LOC)*SIGD(LOC))
      GO TO 147
  176 NTS(NSD)=NSC
      SRCI(NSD)=S(LIS)
      NSD=NSD+1
      IF (NSD-200) 177,177,399
  399 NSDM=200
      JAD=1
      GO TO 400
  405 NSD=1
  177 GO TO (180,178,180),NCOT
C
C     DISTRIBUTION SPACE-TIME CONVERGENCE TESTS.
C
  180 R(N1,K)=B(1,K)/B(1,K1)
```

```
      B(N2,K)=B(NHALF,K)/B(NHALF,K1)
      B(N3,K)=B(NM3,K)/B(NM3,K1)
      IF(NSC-LIM)178,178,181
  181 V1=ABSF(B(N2,K)-B(N1,K))
      CONVB=V1
      IF(V1-CONV) 182,178,178
  182 V2=ABSF(B(N3,K)-B(N1,K))
      V3=ABSF(B(N1,K)-B(N1,K1))
      V4=ABSF(B(N2,K)-B(N2,K1))
      V5=ABSF(B(N3,K)-B(N3,K1))
      CONVB=V1+V2+V3+V4+V5
      IF (CONVB-CONV) 250,250,178
C
C     COMPLETION CHECKS.
C
  178 IF(MITN-NSC) 200,200,179
  179 IF (150-K) 183,183,152
  183 GO TO (185,184,184),NCOT
  184 KFL=150
      JAT=1
C
C     PRINT OUT TRANSIENT RESULTS.
C
   60 NAF=NSC-KFL
      IF(KFL-NNN) 59,52,52
   52 DO 108 J=NNN,KFL,NSP
  108 NXX(J)=J+NAF
      LLL=NNN
   53 III=0
      PRINT 1, NTYP,INDX,IPASS,NPAG
      NPAG=NPAG+1
      PRINT 2
   54 JJJ=LLL+4*NSP
      MMM=KFL+NSP-1-JJJ
      IF(MMM) 56,56,50
   50 PRINT 3,(NXX(J),J=LLL,JJJ,NSP),
     1(I,(B(I,J),J=LLL,JJJ,NSP),I=1,N3)
      LLL=JJJ+NSP
      IF(N-20) 51,51,53
   51 IF(III) 55,55,53
   55 III=1
      GO TO 54
   56 IF(KFL-LLL) 59,58,58
   58 PRINT 11,(NXX(J),J=LLL,KFL,NSP)
      DO 57 I=1,N3
   57 PRINT 12,I,(B(I,J),J=LLL,KFL,NSP)
   59 NAA=NSC/NSP
      NAB=NSP*NAA
      NAC=NSC - NAB
      NNN=LIM + NSP - NAC
      GO TO (185,265),JAT
  185 JAR=1
      KSL=LIMK
```

```
C
C     B(I,K) ARRAY FILLED, RESET FOR THE NEXT PASS.
C
  277 DO 186 J=1,LIM
      L=KSL+J
      DO 186 I=1,N3
  186 B(I,J)=B(I,L)
      DO 118 J=LIMP,150
      DO 118 I=1,N3
  118 B(I,J)=0.0
      DO 101 J=151,LIMT
      L=KSL+J
      DO 101 I=1,N
  101 B(I,J)=B(I,L)
      DO 102 J=LIMTP,300
      DO 102 I=1,N
  102 B(I,J)=0.0
      GO TO (151,285),JAT
C
C     THE SPECIFIED NUMBER OF TIME STEPS HAS BEEN REACHED.
C
  200 KFL=K
      NCN=2
      GO TO 260
C
C     THE DISTRIBUTION HAS CONVERGED.
C
  250 KFL=K
      NCN=1
  260 GO TO (265,261,261),NCOT
  261 JAT=2
      GO TO 60
  265 GO TO (266,270,266),NCOT
C
C     COMPUTE AND PRINT OUT CONVERGENCE RESULTS.
C
  266 EIGB=LOGF(B(N2,KFL))/TS
      KFLT=KFL+150
      SUM=0.0
      SUMT=0.0
      DO 132 I=1,N
      FLX(I)=B(I,KFL)/(C(I)*SIGD(I))
      GO TO (66,65),KTSS
   65 B(I,KFLT)=S(I)
   66 BEQ(I)=B(I,KFL)+B(I,KFLT)
      SUM=SUM+BEQ(I)
  132 SUMT=SUMT+FLX(I)
      SUM=SUM/QUAN
      SUMT=SUMT/QUAN
      DO 133 I=1,N
      BEQ(I)=BEQ(I)/SUM
  133 FLX(I)=FLX(I)/SUMT
      KM7=KFL-4
      PRINT 1, NTYP,INDX,IPASS,IPAG
```

```
      NPAG=NPAG+1
      PRINT 4
      PRINT 5, NCOT,NCN,NSC,CONVB,EIGB
      PRINT 6,(I,BEQ(I),FLX(I),I=1,N)
      PRINT 1, NTYP,INDX,IPASS,NPAG
      NPAG=NPAG+1
      PRINT 4
      PRINT 7,(I,(B(I,J),J=KM7,KFL),I=1,N3)
  270 IF(NDET)275,275,271
  271 NSDM=NSD-1
      JAD=2
C
C     PRINT OUT DETECTOR RESPONSE READINGS.
C
  400 JAAA=1
      JBBB=45
   85 PRINT 1, NTYP,INDX,IPASS,NPAG
      NPAG=NPAG+1
      PRINT 8,NDET,LIS,(LID(I),I=1,NDET)
      IF(NSDM-JBBB)81,81,82
   81 JBBB=NSDM
   82 DO 83 J=JAAA,JBBB
   83 PRINT 9,NTS(J),SRCI(J),(D(I,J),I=1,NDET)
      IF(NSDM-JBBB) 401,401,84
   84 JAAA=JAAA+45
      JBBB=JBBB+45
      GO TO 85
  401 GO TO (405,275),JAD
  275 GO TO (285,276),MODR
C
C     RESET INDICES AND MEMORY IN PREPARATION FOR ALTERED
C     PROPERTIES ON THE NEXT PASS.
C
  276 MA=2
      NSD=1
      JAR=2
      KSL=KFL-LIM
      GO TO 277
  285 RETURN
      END
```

APPENDIX C

THE PROGRAM SLBCEL

The program SLBCEL is written in FORTRAN-II language for the IBM-7094 computer. Along with the MAIN program, nine subroutines are required: READ1, READ2, READ3, CONTRL, PARAM1, PARAM2, TABLE1, CLCMEQ and CLCITN. The functions of each subroutine are described by comment statements in the program listings. The short MAIN program and the nine subroutines occupy 3865 (decimal) core locations. COMMON storage occupies 10849 locations.

An input form is given in Section C1. The input variables are defined in Section C2. The program output for a simple example problem is given in Section C3. Finally, the FORTRAN listings of the program are given in Section C4. Two versions of Subroutine PARAM1 are included. The first is the cell version which treats the boundary planes as perfectly reflecting surfaces; the second is the isolated reactor version which treats the boundary planes as non-reflecting surfaces. Only one of these versions should be included in the binary deck for a particular job.

C1. SLBCEL INPUT FORM

Notes: (a) 126 $E_3(p)$ data cards are read in before card No. 0.

(b) Input cards should be arranged in the order shown.

(c) Numbered cards or sets of cards are mandatory for each problem; inclusion of alphabetically-designated sets of cards is conditional.

(d) FORTRAN II format is given in the brackets.

Card No.	Condition	Variables to be Read	Format
0	--	NPROB	[I5]
	Read the following for each problem to be solved on this job:		
1	--	N,NREAD,NT,NSUC,MODC,KMIX,NRFL,NCLC,NMEM	[9I5]
2	--	MITN,KPRNT1,KPRNT2,KPRNT3,KPNCH1,KPNCH2,KXXA, KXXB,KXXC	[9I5]
3	--	TMULT,CONV	[2E12.5]
4	--	(PATH(I),I=1,N)	[6E12.5]
5	--	(C(I),I=1,N)	[6E12.5]
6	--	(S(I),I=1,N)	[6E12.5]
7	--	(KTRL(I),I=1,N)	[14I5]
A	KMIX>0	(KMDC(I),I=1,N)	[14I5]
B	NMEM=2	(B(I,1),I=1,N)	[6E12.5]
C	NREAD=2	((G(I,J),J=1,N),I=1,N),	[6F11.7]
		((GSLP(I,J),J=1,N),I=1,N),	[6F11.7]
		((GCRV(I,J),J=1,N),I=1,N).	[6F11.7]
D	NREAD=3	((T(I,J),J=1,N),I=1,N)	[6F11.7]
(X)	NT>1 and	Add the following cards for each additional run of this problem:	
1X	--	NCLC,NEWSRC,NMEM,KPRNT3	[4I5]
AX	NSUC=1	(C(I),I=1,N)	[6E12.5]
BX	NEWSRC=1	(S(I),I=1,N)	[6E12.5]
CX	NMEM=2	(B(I,1),I=1,N)	[6E12.5]

C2. DESCRIPTION OF SLBCEL INPUT VARIABLES

Notes: (a) Assignable values are enclosed in brackets. Where different values alter the logical flow of the program, the meanings are defined.

(b) The variables are arranged in the order in which they are read into the computer by the program.

INTEGERS

NPROB = No. of independent problems to be solved on this job. [≥ 1]

N = No. of subregions . [$4 \leq N \leq 40$]

NREAD = Control variable for transfer coefficients.

[1 - Computes G, GSLP and GCRV in subroutine PARAM1.
2 - Reads arrays G, GSLP and GCRV from input data.
3 - Reads array T from input data cards.
4 - Uses G, GSLP and GCRV from previous problem.]

NT = No. of runs for this problem. [≥ 1]

NSUC = Control variable for secondary emission coefficients in successive runs.

[1 - Reads new values of the C(I) for each additional run, if NT > 1. No changes allowed in approximation model or in locations of discontinuities (except for Model 4).
2 - Uses the values of the C(I) used in the previous run.]

MODC = [1 - Model F (Flat approximation).
2 - Model FS (Slope correction).
3 - Model FSC (Slope and Curvature Corrections).]

KMIX = [≤ 0 - Sets KMDC(J) = MODC for all J.
> 0 - Reads KMDC(J) for J=1, N.]

SLBCEL INPUT VARIABLES (cont'd)

NRFL = Number of double reflections to consider in computing the transfer coefficients G,GSLP and GCRV, if NREAD = 1.

- ≤0 - Program sets NRFL = 12.5/TPATH, where TPATH is the computed optical width of the half-cell.
- >0 - Program uses the assigned value.

NCLC = Control variable for solution method.

- 1 - Uses Subroutine CLCITN to get iterative solution.
- 2 - Uses Subroutine CLCMEQ to get non-iterative solution.

NMEM = Control variable for setting initial trial distribution if NCLC = 1.

- 1 - Sets B(I,1) = TMULT for all I.
- 2 - Reads B(I,1) for I = 1, N.
- 3 - Uses B(I,1) from previous run. Note that the solution distribution from CLCMEQ is stored in B(I,1). This solution can then be checked by iteration in CLCITN.

MITN = Maximum number of iterations if NCLC = 1.

KPRNT1 =

- 1 - Prints arrays G, GSLP and GCRV if they are computed in this problem.
- 2 - Does not print.

KPRNT2 =

- 1 - Prints array T if computed.
- 2 - Does not print.

KPRNT3 =

- 1 - Prints array H in CLCITN or array A = [I-H] in CLCMEQ.
- 2 - Does not print.

KPNCH1 =

- 1 - Punched-card output of arrays G, GSLP and GCRV, if computed. (Format: 6F11.7)
- 2 - Does not punch.

SLBCEL INPUT VARIABLES (cont'd)

KPNCH2 = [1 - Punched-card output of array T if computed.
(Format: 6F11.7)
2 - Does not punch.]

KXXA
KXXB
KXXC } = Dummary variables included in READ statement and program COMMON for user convenience in selective reprogramming. [any]

NEWSRC = Control variable for source distribution in successive runs.
[1 - Reads new values of the S(I) for each additional run, if NT > 1. Source must be continuous between assigned interfaces.
2 - Uses the source distribution from the previous run.]

FLOATING POINT VARIABLES

TMULT = Estimated value of cell multiplication used in Subroutine CLCITN if NMEM = 1.

CONV = Asymptoticity convergence criterion used in CLCITN. (Normally set equal to 10^{-6} or 10^{-7}).

ARRAYS

PATH(I) = Optical width of subregion I in mean free paths parallel to the x-axis.

C(I) = Mean number of secondaries per collision in region I.

S(I) = External source rate in region I.

KTRL(I) = [1 - Property or source discontinuity at left edge of region I.
0 - No discontinuities at edges of region I.
-1 - Discontinuity at right edge of region I.]

SLBCEL INPUT VARIABLES (cont'd)

KMDC(J) = [1 - Flat approximation for parent neutrons born in region J. (Model F).
2 - Slope correction. (Model FS).
3 - Slope and curvature corrections. (Model FSC).]

B(I,1) = Initial, trial birth rate in region I. The birth rate includes the external source rate.

G(I,J) = Transfer coefficient for the unit flat mode.

GSLP(I,J) = Transfer coefficient for the unit slope-correction mode.

GCRV(I,J) = Transfer coefficient for the unit curvature-correction mode.

T(I,J) = Combination of elements of arrays G, GSLP and GCRV formed according to the values of the elements of KTRL and KMDC.

$\underline{B}(K) = \underline{CTB}(K-1) + \underline{S}$.

C3. PRINTED OUTPUT FROM EXAMPLE PROBLEM

Four runs were made in the example problem for which the printed output is given below. The input arrays PATH, KMDC and KTRL and the computed arrays G, GSLP, GCRV and T are identical for each run. In Run 1, the non-iterative solution was found for the six subregion system with the specified arrays C and S. In Run 2, the solution of Run 1 was checked by iteration. In Run 3, the value of the secondary emission coefficient in the fuel was reduced from 0.8 to 0.6. In Run 4, the source distribution in the moderator was altered. Total job time was 0.38 minute, of which only 6 seconds were used in the execution of this problem.

SLBCEL INPUT DATA RUN 1 PAGE 1

N = 6	NREAD = 1	NT = 4	NSUC = 1
MODC = 3	KMIX = 0	NRFL = 0	NCLC = 2
NMEM = 3	MITN = 10	KPRNT1 = 1	KPRNT2 = 1
KPRNT3 = 1	KPNCH1 = 2	KPNCH2 = 2	KXXA = 0
KXXB = 0	KXXC = 0		

ESTIMATED MULTIPLICATION = 0.

CONVERGENCE CRITERION = 1.00000E-07

I	KMDC(I)	KTRL(I)
1	3	1
2	3	0
3	3	-1
4	3	1
5	3	0
6	3	-1

NRFL = 3 TPATH = 3.90000

EXAMPLE OUTPUT (cont'd)

SLBCEL TRANSFER COEFFICIENT ARRAYS RUN 1 PAGE 2

MATRIX G(I,J) FOLLOWS.

MATRIX ELEMENTS

I						
1	.485947	.223550	.111245	.040692	.009731	.003354
2	.223550	.373641	.176778	.052481	.011481	.003847
3	.111245	.176778	.348813	.088563	.015463	.004923
4	.135641	.174938	.295210	.620146	.160347	.037770
5	.032436	.038269	.051545	.160347	.618080	.184898
6	.011181	.012823	.016410	.037770	.184898	.765208

SLBCEL TRANSFER COEFFICIENT ARRAYS RUN 1 PAGE 3

MATRIX GSLP(I,J) FOLLOWS.

MATRIX ELEMENTS

I						
1	-.006048	-.007875	-.002703	-.002545	-.000505	-.000095
2	.004222	-.000877	-.006530	-.003583	-.000613	-.000111
3	.000949	.005566	-.000284	-.007543	-.000867	-.000148
4	.000728	.002701	.008571	-.000486	-.012203	-.001310
5	.000116	.000379	.000749	.012141	.000353	-.010509
6	.000033	.000105	.000197	.002016	.013835	.012172

SLBCEL TRANSFER COEFFICIENT ARRAYS RUN 1 PAGE 4

MATRIX GCRV(I,J) FOLLOWS.

MATRIX ELEMENTS

I						
1	-.001107	.000846	.000139	.000300	.000050	.000014
2	.000846	-.001814	.000761	.000490	.000062	.000017
3	.000140	.000761	-.001842	.001521	.000094	.000023
4	.000101	.000181	.000903	-.004697	.002175	.000211
5	.000017	.000020	.000029	.002175	-.004709	.002327
6	.000004	.000005	.000008	.000211	.002327	-.002592

EXAMPLE OUTPUT (cont'd)

SLBCEL PARAMETERS RUN 1 PAGE 5

ARRAY T(I,J) FOLLOWS.

I						
1	.509203	.210290	.101249	.048920	-.000436	.005293
2	.205127	.416858	.151985	.064018	-.002978	.006769
3	.102076	.182651	.352108	.112731	-.015757	.011975
4	.139920	.142381	.323488	.631341	.165955	.020967
5	.032492	.035671	.054087	.112957	.708889	.141479
6	.011182	.012149	.017082	.030032	.144327	.813517

SLBCEL MATRIX EQUATION SOLUTION RUN 1 PAGE 6

COEFFICIENT MATRIX A(I,J), FOR A*B=S, FOLLOWS.

I						
1	.592638	-.168232	-.080999	-.039136	.000348	-.004234
2	-.164102	.666514	-.121588	-.051214	.002383	-.005416
3	-.081661	-.146121	.718314	-.090185	.012606	-.009580
4	-.139920	-.142381	-.323488	.368659	-.165955	-.020967
5	-.032492	-.035671	-.054087	-.112957	.291111	-.141479
6	-.011182	-.012149	-.017082	-.030032	-.144327	.186483

SLBCEL MATRIX EQUATION SOLUTION RUN 1 PAGE 7

DETERMINANT OF COEFFICIENT MATRIX = .925321E-03

CELL MULTIPLICATION = .35605E 02

I	PATH(I)	C(I)	S(I)	BIRTH RATE	REL. FLUX
1	.30000E 00	.80000E 00	.00000E 00	.3682532E 01	.6491763E 00
2	.30000E 00	.80000E 00	.00000E 00	.3903945E 00	.6882081E 00
3	.30000E 00	.80000E 00	.00000E 00	.4413504E 01	.7780361E 00
4	.10000E 01	.10000E 01	.10000E 01	.2626546E 02	.1068943E 01
5	.10000E 01	.10000E 01	.10000E 01	.3273977E 02	.1342861E 01
6	.10000E 01	.10000E 01	.10000E 01	.3581040E 02	.1472775E 01

EXAMPLE OUTPUT (cont'd)

SLBCEL INPUT FROM READ3 RUN 2 PAGE 8

NCLC = 1 NEWSRC = 2

NMEM = 3 KPRNT3 = 1

SLBCEL ITERATED SOLUTION RUN 2 PAGE 9

ITERATION MATRIX H(I,J) FOR B=HB+S.

I						
1	.407362	.168232	.080999	.039136	-.000348	.004234
2	.164102	.333486	.121588	.051214	-.002383	.005416
3	.081661	.146121	.281686	.090185	-.012606	.009580
4	.139920	.142381	.323488	.631341	.165955	.020967
5	.032492	.035671	.054087	.112957	.708889	.141479
6	.011182	.012149	.017082	.030032	.144327	.813517

SLBCEL ITERATED SOLUTION RUN 2 PAGE 10

RESULTS

THE DISTRIBUTION HAS CONVERGED.

CONVERGENCE LEVEL ATTAINED = .37253E-07

NO. OF ITERATIONS COMPLETED = 5

CELL MULTIPLICATION = 35.60520

I	PATH(I)	C(I)	S(I)	BIRTH RATE	REL. FLUX
1	.30000E 00	.80000E 00	.00000E 00	.3682532E 01	.6491763E 00
2	.30000E 00	.80000E 00	.00000E 00	.3903944E 01	.6882081E 00
3	.30000E 00	.80000E 00	.00000E 00	.4413504E 01	.7780360E 00
4	.10000E 01	.10000E 01	.10000E 01	.2626546E 02	.1068943E 01
5	.10000E 01	.10000E 01	.10000E 01	.3273976E 02	.1342861E 01
6	.10000E 01	.10000E 01	.10000E 01	.3581040E 02	.1472775E 01

EXAMPLE OUTPUT (cont'd)

SLBCEL ITERATED SOLUTION RUN 2 PAGE 11

RESULTS OF LAST FIVE ITERATIONS

I					
1	.3682532E 01	.3682532E 01	.3682532E 01	.3682532E 01	.3682532E 01
2	.3903944E 01	.3903944E 01	.3903944E 01	.3903944E 01	.3903944E 01
3	.4413504E 01	.4413504E 01	.4413504E 01	.4413504E 01	.4413504E 01
4	.2626546E 02	.2626546E 02	.2626546E 02	.2626546E 02	.2626546E 02
5	.3273977E 02	.3273976E 02	.3273976E 02	.3273976E 02	.3273976E 02
6	.3581040E 02	.3581040E 02	.3581040E 02	.3581040E 02	.3581040E 02
7	1.0000000E 00	1.0000000E 00	1.0000000E 00	1.0000000E 00	1.0000000E 00
8	.1000000E 01	1.0000000E 00	1.0000000E 00	1.0000000E 00	1.0000000E 00
9	.1000000E 01	1.0000000E 00	1.0000000E 00	1.0000000E 00	1.0000000E 00

SLBCEL INPUT FROM READ3 RUN 3 PAGE 12

NCLC = 2 NEWSRC = 2

NMEM = 3 KPRNT3 = 1

SLBCEL MATRIX EQUATION SOLUTION RUN 3 PAGE 13

COEFFICIENT MATRIX A(I,J), FOR A*B=S, FOLLOWS.

I						
1	.694478	-.126174	-.060749	-.029352	.000261	-.003176
2	-.123076	.749885	-.091191	-.038411	.001787	-.004062
3	-.061246	-.109591	.788735	-.067639	.009454	-.007185
4	-.139920	-.142381	-.323488	.368659	-.165955	-.020967
5	-.032492	-.035671	-.054087	-.112957	.291111	-.141479
6	-.011182	-.012149	-.017082	-.030032	-.144327	.186483

EXAMPLE OUTPUT (cont'd)

SLBCEL MATRIX EQUATION SOLUTION RUN 3 PAGE 14

DETERMINANT OF COEFFICIENT MATRIX = .213634E-02

CELL MULTIPLICATION = .24662E 02

I	PATH(I)	C(I)	S(I)	BIRTH RATE	REL. FLUX
1	.30000E 00	.60000E 00	.00000E 00	.1284958E 01	.4681764E 00
2	.30000E 00	.60000E 00	.00000E 00	.1430717E 01	.5212840E 00
3	.30000E 00	.60000E 00	.00000E 00	.1784321E 01	.6501201E 00
4	.10000E 01	.10000E 01	.10000E 01	.1781428E 02	.1102736E 01
5	.10000E 01	.10000E 01	.10000E 01	.2430039E 02	.1528116E 01
6	.10000E 01	.10000E 01	.10000E 01	.2737208E 02	.1729568E 01

SLBCEL INPUT FROM READ 3 RUN 4 PAGE 15

NCLC = 2 NEWSRC = 1

NMEM = 3 KPRNT3 = 2

SLBCEL MATRIX EQUATION SOLUTION RUN 4 PAGE 16

DETERMINANT OF COEFFICIENT MATRIX = .213634E-02

CELL MULTIPLICATION = .23851E 02

I					
1	.30000E 00	.60000E 00	.00000E 00	.1283145E 01	.4802877E 00
2	.30000E 00	.60000E 00	.00000E 00	.1429824E 01	.5351905E 00
3	.30000E 00	.60000E 00	.00000E 00	.1787026E 01	.6688932E 00
4	.10000E 01	.10000E 01	.12000E 01	.1798377E 02	.1130805E 01
5	.10000E 01	.10000E 01	.11000E 01	.2372486E 02	.1524348E 01
6	.10000E 01	.10000E 01	.70000E 00	.2534530E 02	.1660475E 01

```
*      LIST8
*      LABEL
CSLBCEL
       DIMENSION PATH(40),C(40),KTRL(40),KMDC(40),S(40),
      1G(40,40),GSLP(40,40),GCRV(40,40),T(40,40),H(40,40),
      2B(43,43),FLX(40),F(24),E3A(250),E3B(250),
      3SA(43,2),ERASE(43),EXTRA(40),EXTRB(40)
       COMMON N,NREAD,NT,NSUC,MODC,KMIX,NREL,NCLC,NMEM,
      1MITN,MA,NPAG,INDX,KPRNT1,KPRNT2,KPRNT3,KPNCH1,KPNCH2,
      2KXXA,KXXB,KXXC,TMULT,CONV,ARGU,BF,CF,DF,
      3PATH,C,KTRL,KMDC,S,G,GSLP,GCRV,T,H,
      4B,FLX,F,E3A,E3B,SA,ERASE,EXTRA,EXTRB
     1 FORMAT(I5)
     2 FORMAT(4E16.9)
       READ 2, (E3A(I),I=1,250)
       READ 2, (E3B(I),I=1,250)
       READ 1, NPROB
    50 CALL READ1
       CALL CONTRL
       NPROB=NPROB-1
       IF (NPROB) 100,100,50
   100 CALL EXIT
       END
```

```
*      LIST8
*      LABEL
       SUBROUTINE READ1
C
C     SUBROUTINE READS IN PROGRAM CONTROL CONSTANTS AND
C     INITIAL INPUT DATA FOR A PARTICULAR PROBLEM.
C
       DIMENSION PATH(40),C(40),KTRL(40),KMDC(40),S(40),
      1G(40,40),GSLP(40,40),GCRV(40,40),T(40,40),H(40,40),
      2B(43,43),FLX(40),F(24),E3A(250),E3B(250),
      3SA(43,2),ERASE(43),EXTRA(40),EXTRB(40)
       COMMON N,NREAD,NT,NSUC,MODC,KMIX,NREL,NCLC,NMEM,
      1MITN,MA,NPAG,INDX,KPRNT1,KPRNT2,KPRNT3,KPNCH1,KPNCH2,
      2KXXA,KXXB,KXXC,TMULT,CONV,ARGU,BF,CF,DF,
      3PATH,C,KTRL,KMDC,S,G,GSLP,GCRV,T,H,
      4B,FLX,F,E3A,E3B,SA,ERASE,EXTRA,EXTRB
     1 FORMAT(9I5)
     2 FORMAT(2E12.5)
     3 FORMAT(6E12.5)
     4 FORMAT(14I5)
     5 FORMAT(1H1,5X18H SLBCEL INPUT DATA ,10X4H RUN I3,
      110X5H PAGE I3)
     6 FORMAT(1H0,8X4H N =I3,4X8H NREAD =I3,7X5H NT =I3,
      15X7H NSUC =I3//6X7H MODC =I3,5X7H KMIX =I3,
      25X7H NREL =I3,5X7H NCLC =I3//6X7H NMEM =I3,
      34X7H MITN =I4,3X9H KPRNT1 =I3,3X9H KPRNT2 =I3//
```

```
     44X9H KPRNT3 =I3,3X9H KPNCH1 =I3,3X9H KPNCH2 =I3,
     55X7H KXXA =I3//6X7H KXXB =I3,5X7H KXXC =I3)
    7 FORMAT(1H0,5X27H ESTIMATED MULTIPLICATION = F10.5//
     16X24H CONVERGENCE CRITERION = E12.5)
    8 FORMAT(1H0,2X2H I,1X8H KMDC(I),2X8H KTRL(I)/
     1(I5,I6,5XI5))
      MA=1
      NPAG=1
      INDX=1
      READ 1,N,NREAD,NT,NSUC,MODC,KMIX,NREL,NCLC,NMEM,
     1MITN,KPRNT1,KPRNT2,KPRNT3,KPNCH1,KPNCH2,KXXA,KXXB,KXXC
      READ 2,TMULT,CONV
      READ 3, (PATH(I),I=1,N)
      READ 3, (C(I),I=1,N)
      READ 3, (S(I),I=1,N)
      READ 4, (KTRL(I),I=1,N)
      IF (KMIX) 20,20,10
   10 READ 4, (KMDC(I),I=1,N)
      GO TO 30
   20 DO 21 I=1,N
   21 KMDC(I)=MODC
   30 GO TO (50,40,50),NMEM
   40 READ 3, (B(I,1),I=1,N)
C
C     PRINT OUT INPUT DATA.
C
   50 PRINT 5,INDX,NPAG
      NPAG=NPAG+1
      PRINT 6,N,NREAD,NT,NSUC,MODC,KMIX,NREL,NCLC,
     1NMEM,MITN,KPRNT1,KPRNT2,KPRNT3,KPNCH1,KPNCH2,
     2KXXA,KXXB,KXXC
      PRINT 7,TMULT,CONV
      PRINT 8, (I,KMDC(I),KTRL(I),I=1,N)
      RETURN
      END



*     LIST8
*     LABEL
      SUBROUTINE READ2
C
C     SUBROUTINE READS TRANSFER COEFFICIENT ARRAYS G, GSLP,
C     AND GCRV WHEN NREAD EQUALS 2, OR THE ARRAY T WHEN
C     NREAD EQUALS 3.
C
      DIMENSION PATH(40),C(40),KTRL(40),KMDC(40),S(40),
     1G(40,40),GSLP(40,40),GCRV(40,40),T(40,40),H(40,40),
     2B(43,43),FLX(40),F(24),E3A(250),E3B(250),
     3SA(43,2),ERASE(43),EXTRA(40),EXTRB(40)
      COMMON N,NREAD,NT,NSUC,MODC,KMIX,NREL,NCLC,NMEM,
     1MITN,MA,NPAG,INDX,KPRNT1,KPRNT2,KPRNT3,KPNCH1,KPNCH2,
     2KXXA,KXXB,KXXC,TMULT,CONV,ARGU,BF,CF,DF,
```

```
     3PATH,C,KTRL,KMDC,S,G,GSLP,GCRV,T,H,
     4B,FLX,F,E3A,E3B,SA,ERASE,EXTRA,EXTRB
    1 FORMAT(6F11.7)
    2 FORMAT(1H0,10X37H ARRAYS G, GSLP, GCRV HAVE BEEN READ.)
    3 FORMAT(1H0,10X23H ARRAY T HAS BEEN READ.)
      GO TO (100,10,20,100),NREAD
   10 READ 1, ((G(I,J),J=1,N),I=1,N)
      READ 1, ((GSLP(I,J),J=1,N),I=1,N)
      READ 1, ((GCRV(I,J),J=1,N),I=1,N)
      PRINT 2
      GO TO 100
   20 READ 1, ((T(I,J),J=1,N),I=1,N)
      PRINT 3
  100 RETURN
      END



*     LIST8
*     LABEL
      SUBROUTINE READ3
C
C     SUBROUTINE READS DATA FOR ADDITIONAL RUNS IF
C     NT IS GREATER THAN 1.
C
      DIMENSION PATH(40),C(40),KTRL(40),KMDC(40),S(40),
     1G(40,40),GSLP(40,40),GCRV(40,40),T(40,40),H(40,40),
     2B(43,43),FLX(40),F(24),E3A(250),E3B(250),
     3SA(43,2),ERASE(43),EXTRA(40),EXTRB(40)
      COMMON N,NREAD,NT,NSUC,MODC,KMIX,NREL,NCLC,NMEM,
     1MITN,MA,NPAG,INDX,KPRNT1,KPRNT2,KPRNT3,KPNCH1,KPNCH2,
     2KXXA,KXXB,KXXC,TMULT,CONV,ARGU,BE,CE,DE,
     3PATH,C,KTRL,KMDC,S,G,GSLP,GCRV,T,H,
     4B,FLX,F,E3A,E3B,SA,ERASE,EXTRA,EXTRB
    1 FORMAT(1H1,5X24H SLBCEL INPUT FROM READ3,
     110X4H RUN I3,10X5H PAGE I4)
    2 FORMAT(4I5)
    3 FORMAT(1H0,10X7H NCLC =I2,10X9H NEWSRC =I2//
     111X7H NMEM =I2,10X9H KPRNT3 =I2)
    4 FORMAT(6F12.5)
      READ 2, NCLC,NEWSRC,NMEM,KPRNT3
      PRINT 1,INDX,NPAG
      NPAG=NPAG+1
      PRINT 3, NCLC,NEWSRC,NMEM,KPRNT3
      GO TO (10,20),NSUC
   10 READ 4, (C(I),I=1,N)
   20 GO TO (30,40),NEWSRC
   30 READ 4, (S(I),I=1,N)
   40 GO TO (100,50,100),NMEM
   50 READ 4, (B(I,1),I=1,N)
  100 RETURN
      END
```

```
*      LIST8
*      LABEL
       SUBROUTINE CONTRL
C
C     SUBROUTINE DIRECTS PROGRAM FLOW FOR INITIAL AND
C     SUCCESSIVE RUNS OF A GIVEN PROBLEM.
C
       DIMENSION PATH(40),C(40),KTRL(40),KMDC(40),S(40),
      1G(40,40),GSLP(40,40),GCRV(40,40),T(40,40),H(40,40),
      2B(43,43),FLX(40),F(24),E3A(250),E3B(250),
      3SA(43,2),ERASE(43),EXTRA(40),EXTRB(40)
       COMMON N,NREAD,NT,NSUC,MODC,KMIX,NREL,NCLC,NMEM,
      1MITN,MA,NPAG,INDX,KPRNT1,KPRNT2,KPRNT3,KPNCH1,KPNCH2,
      2KXXA,KXXB,KXXC,TMULT,CONV,ARGU,BF,CF,DF,
      3PATH,C,KTRL,KMDC,S,G,GSLP,GCRV,T,H,
      4B,FLX,F,E3A,E3B,SA,ERASE,EXTRA,EXTRB
       GO TO (10,20,30,40),NREAD
   10  CALL PARAM1
       GO TO 40
   20  CALL READ2
       GO TO 40
   30  CALL READ2
       MA=2
   40  CALL PARAM2
   50  GO TO (60,70),NCLC
   60  CALL CLCITN
       GO TO 80
   70  CALL CLCMEQ
   80  INDX=INDX+1
       IF (NT-INDX) 100,90,90
   90  CALL READ3
       NCLC=NCLC
       GO TO (95,50),NSUC
   95  MA=2
       CALL PARAM2
       GO TO 50
  100  RETURN
       END
```

```
*      LIST8
*      LABEL
       SUBROUTINE PARAM1
C
C     GIVEN PATH(I),I=1,N , THIS SUBROUTINE COMPUTES THE
C     TRANSFER COEFFICIENT ARRAYS G, GSLP AND GCRV.
C
       DIMENSION PATH(40),C(40),KTRL(40),KMDC(40),S(40),
      1G(40,40),GSLP(40,40),GCRV(40,40),T(40,40),H(40,40),
      2B(43,43),FLX(40),F(24),E3A(250),E3B(250),
      3SA(43,2),ERASE(43),EXTRA(40),EXTRB(40)
       COMMON N,NREAD,NT,NSUC,MODC,KMIX,NREL,NCLC,NMEM,
      1MITN,MA,NPAG,INDX,KPRNT1,KPRNT2,KPRNT3,KPNCH1,KPNCH2,
      2KXXA,KXXB,KXXC,TMULT,CONV,ARGU,BF,CF,DF,
      3PATH,C,KTRL,KMDC,S,G,GSLP,GCRV,T,H,
      4B,FLX,F,E3A,E3B,SA,ERASE,EXTRA,EXTRB
     1 FORMAT(1H1,5X35H SLBCEL TRANSFER COEFFICIENT ARRAYS,
      15X4H RUN I3,5X5H PAGE I3)
     2 FORMAT(1H0,20X23H MATRIX G(I,J) FOLLOWS. /
      12X2H I,20X16H MATRIX ELEMENTS )
     3 FORMAT(I4,6F10.6/5X6F10.6/6X6F10.6/7X6F10.6/
      18X6F10.6/9X6F10.6/10X6F10.6)
     4 FORMAT(1H0,20X26H MATRIX GSLP(I,J) FOLLOWS. /
      12X2H I,20X16H MATRIX ELEMENTS )
     5 FORMAT(1H0,20X26H MATRIX GCRV(I,J) FOLLOWS. /
      12X2H I,20X16H MATRIX ELEMENTS )
     6 FORMAT(6F11.7)
     7 FORMAT(1H0,5X7H NREL =I3,5X8H TPATH =F10.5)
       TPATH=0.0
       DO 30 I=1,N
       DO 20 J=1,N
       G(I,J)=0.0
    20 GCRV(I,J)=0.0
    30 TPATH=TPATH+PATH(I)
       IF (NREL) 40,40,50
    40 NREL=12.5/TPATH
       PRINT 7,NREL,TPATH
    50 IA=0
C
C     START AND REENTRY POINT FOR RECEIVER REGIONS, IA.
C
   400 IA=IA+1
       IF (N-IA) 800,401,401
   401 PI=PATH(IA)
       BTR=0.0
       BTL=0.0
       DO 402 I=1,IA
   402 BTL=BTL + PATH(I)
       BTL=2.0*(BTL-PI)
       DO 403 I=IA,N
   403 BTR=BTR + PATH(I)
       BTR=2.0*(BTR-PI)
       JA=0
```

```
C     START OF LOOP FOR SOURCE REGIONS, JA.
C
  410 JA=JA+1
      IF (N-JA) 400,411,411
  411 DO 412 I=1,24
  412 F(I)=0.0
      PJ=PATH(JA)
      ARGUR=0.0
      ARGUL=0.0
      ARGU=0.0
      IF (IA-JA) 413,419,416
  413 DO 414 I=JA,N
  414 ARGUR=ARGUR + PATH(I)
      DO 415 I=IA,JA
  415 ARGU=ARGU + PATH(I)
      ARGUR=2.0*(ARGUR-PJ) + ARGU - PI
      ARGUL=ARGU -PI-PJ
      BTA=BTL
      BTB=BTR
      GO TO 420
  416 DO 417 I=1,JA
  417 ARGUL=ARGUL + PATH(I)
      DO 418 I=JA,IA
  418 ARGU=ARGU + PATH(I)
      BTA=BTR
      BTB=BTL
      ARGUL=2.0*(ARGUL-PJ) + ARGU - PI
      ARGUR=ARGU -PI -PJ
      GO TO 420
  419 ARGU=PI
      CALL TABLE1
      G(IA,IA)=1.0-(0.5-BF)/PI
      GCRV(IA,IA)=(-0.5+BF)/(6.0*PI) +
     1(1.0+3.0*CF)/(3.0*PI**2) +(-0.5+2.0*DF)/(PI**3)
      ARGUR=BTR
      ARGUL=BTL
C
C     PARTICLES EMITTED TO THE RIGHT.
C
  420 ARGU=ARGUR
      IF (IA-JA) 422,421,422
  421 BTA=BTL
      BTB=BTR
  422 LINT=1
      GO TO 500
  423 KDX=0
  425 KDX=KDX+1
      ARGU=ARGU+BTA
      LINT=2
      GO TO 500
  426 ARGU=ARGU + BTB
      LINT=3
      GO TO 500
  427 IF (NREL-KDX) 430,430,425
```

```
      F(12)=F(12)+DF
      GO TO (423,426,427),LINT
C
C     PARTICLES EMITTED TO THE LEFT.
C
  600 CALL TABLE1
      F(13)=F(13) + BF
      F(17)=F(17)+CF
      F(21)=F(21)+DF
      ARGU=ARGU+PJ
      CALL TABLE1
      F(14)=F(14) + BF
      F(18)=F(18)+CF
      F(22)=F(22)+DF
      ARGU=ARGU+PI
      CALL TABLE1
      F(15)=F(15) + BF
      F(19)=F(19)+CF
      F(23)=F(23)+DF
      ARGU=ARGU-PJ
      CALL TABLE1
      F(16)=F(16)+BF
      F(20)=F(20)+CF
      F(24)=F(24)+DF
      GO TO (433,436,437),LINT
C
C     IF KPRNT1 = 1, PRINT ARRAYS G, GSLP, AND GCRV.
C
  800 GO TO (810,850),KPRNT1
  810 PRINT 1,INDX,NPAG
      NPAG=NPAG+1
      PRINT 2
      DO 820 I=1,N
  820 PRINT 3, I,(G(I,J),J=1,N)
      PRINT 1,INDX,NPAG
      NPAG=NPAG+1
      PRINT 4
      DO 830 I=1,N
  830 PRINT 3, I,(GSLP(I,J),J=1,N)
      PRINT 1,INDX,NPAG
      NPAG=NPAG+1
      PRINT 5
      DO 840 I=1,N
  840 PRINT 3, I,(GCRV(I,J),J=1,N)
C
C     IF KPNCH1 = 1, PUNCHED-CARD OUTPUT OF ARRAYS G,GSLP
C     AND GCRV.
C
  850 GO TO (860,1000),KPNCH1
  860 PUNCH 6, ((G(I,J),J=1,N),I=1,N)
      PUNCH 6, ((GSLP(I,J),J=1,N),I=1,N)
      PUNCH 6, ((GCRV(I,J),J=1,N),I=1,N)
 1000 RETURN
      END
```

```
*      LIST8
*      LABEL
       SUBROUTINE PARAM1
C
C     GIVEN PATH(I),I=1,N , THIS SUBROUTINE COMPUTES THE
C     TRANSFER COEFFICIENT ARRAYS G, GSLP, AND GCRV FOR
C     A BARE REACTOR.
C
       DIMENSION PATH(40),C(40),KTRL(40),KMDC(40),S(40),
      1G(40,40),GSLP(40,40),GCRV(40,40),T(40,40),H(40,40),
      2B(43,43),FLX(40),F(24),E3A(250),E3B(250),
      3SA(43,2),ERASE(43),EXTRA(40),EXTRB(40)
       COMMON N,NREAD,NT,NSUC,MODC,KMIX,NREL,NCLC,NVEM,
      1MITN,MA,NPAG,INDX,KPRNT1,KPRNT2,KPRNT3,KPNCH1,KPNCH2,
      2KXXA,KXXB,KXXC,TMULT,CONV,ARGU,BE,CE,DE,
      3PATH,C,KTRL,KMDC,S,G,GSLP,GCRV,T,H,
      4B,FLX,F,E3A,E3B,SA,ERASE,EXTRA,EXTRB
     1 FORMAT(1H1,5X35H SLBARE TRANSFER COEFFICIENT ARRAYS,
      15X4H RUN I3,5X5H PAGE I3)
     2 FORMAT(1H0,20X23H MATRIX G(I,J) FOLLOWS. /
      12X2H I,20X16H MATRIX ELEMENTS )
     3 FORMAT(I4,6F10.6/5X6F10.6/6X6F10.6/7X6F10.6/
      18X6F10.6/9X6F10.6/10X6F10.6)
     4 FORMAT(1H0,20X26H MATRIX GSLP(I,J) FOLLOWS. /
      12X2H I,20X16H MATRIX ELEMENTS )
     5 FORMAT(1H0,20X26H MATRIX GCRV(I,J) FOLLOWS. /
      12X2H I,20X16H MATRIX ELEMENTS )
     6 FORMAT(6F11.7)
       NM=N-1
       NM2=N-2
C
C     STORE NUMBER OF MEAN FREE PATHS BETWEEN REGIONS I AND J.
C
       DO 211 I=1,NM
  211  G(I,I+1)=0.0
       DO 212 I=1,NM2
       IP2=I+2
       DO 212 J=IP2,N
  212  G(I,J)=G(I,J-1)+PATH(J-1)
       IA=0
C
C     START AND REENTRY POINT FOR RECEIVER REGIONS, IA.
C
  750  IA=IA+1
       PI=PATH(IA)
       ARGU=PI
       CALL TABLE1
       E10=BE
       E15=CE
       E20=DE
       G(IA,IA)=1.0-(0.5-E10)/PI
       GCRV(IA,IA)=(-0.5+E10)/(6.0*PI)+(1.0+3.0*E15)/
```

```
     1(3.0*PI**2)+(-0.5+2.0*F20)/(PI**3)
C
C    START OF LOOP FOR SOURCE REGIONS, JA.
C
      JA=IA+1
      PJ=PATH(JA)
      ARGU=0.0
      F6=0.5
      F11=1.0/3.0
      F16=0.25
      GO TO 820
  800 JA=JA+1
      PJ=PATH(JA)
      ARGU=G(IA,JA)
      CALL TABLE1
      F6=BF
      F11=CF
      F16=DF
  820 ARGU=ARGU+PJ
      CALL TABLE1
      F7=BF
      F12=CF
      F17=DF
      ARGU=ARGU+PI
      CALL TABLE1
      F8=BF
      F13=CF
      F18=DF
      ARGU=ARGU-PJ
      CALL TABLE1
      F9=BF
      F14=CF
      F19=DF
      X=F6-F7+F8-F9
      G(IA,JA)=X/(2.0*PJ)
      G(JA,IA)=X/(2.0*PI)
      Y=F16-F17+F18-F19
      GCRV(IA,JA)=X/(12.0*PJ)-(F11+F12-F13-F14)/(2.0*PJ**2)+
     1Y/(PJ**3)
      GCRV(JA,IA)=X/(12.0*PI)-(F11-F12-F13+F14)/(2.0*PI**2)+
     1Y/(PI**3)
      GSLP(IA,JA)=-(F6+F7-F8-F9+(2.0/PJ)*(-F11+F12-F13+F14))/
     1(8.0*PJ)
      GSLP(JA,IA)=(F6-F7-F8+F9+(2.0/PATH(IA))*(-F11+F12-F13
     1+F14))/(8.0*PI)
      IF (N-JA) 821,821,800
C
C    COMPLETION OF JA LOOP.
C
  821 IF (N-IA-1) 823,823,750
  823 IA=N
      PI=PATH(N)
      ARGU=PI
      CALL TABLE1
```

```
      F10=BF
      F15=CF
      F20=DF
      G(IA,IA)=1.0-(0.5-F10)/PI
      GCRV(IA,IA)=(-0.5+F10)/(6.0*PI)+(1.0+3.0*F15)/
     1(3.0*PI**2)+(-0.5+2.0*F20)/(PI**3)
C
C     COMPLETION OF IA LOOP.
C
C     IF KPRNT1 = 1, PRINT ARRAYS G, GSLP, AND GCRV.
C
      GO TO (910,950),KPRNT1
  910 PRINT 1,INDX,NPAG
      NPAG=NPAG+1
      PRINT 2
      DO 920 I=1,N
  920 PRINT 3,I,(G(I,J),J=1,N)
      PRINT 1,INDX,NPAG
      NPAG=NPAG+1
      PRINT 4
      DO 930 I=1,N
  930 PRINT 3,I,(GSLP(I,J),J=1,N)
      PRINT 1,INDX,NPAG
      NPAG=NPAG+1
      PRINT 5
      DO 940 I=1,N
  940 PRINT 3,I,(GCRV(I,J),J=1,N)
C
C     IF KPNCH1 = 1, PUNCHED-CARD OUTPUT OF ARRAYS G,GSLP
C     AND GCRV.
C
  950 GO TO (960,1000),KPNCH1
  960 PUNCH 6,((G(I,J),J=1,N),I=1,N)
      PUNCH 6, ((GSLP(I,J),J=1,N),I=1,N)
      PUNCH 6, ((GCRV(I,J),J=1,N),I=1,N)
 1000 RETURN
      END
```

```
*      LIST8
*      LABEL
       SUBROUTINE TABLE1
C
C     THIS SUBROUTINE USES THIRD ORDER POLYNOMIAL
C     INTERPOLATION TO DETERMINE THE VALUE OF THE
C     EXPONENTIAL INTEGRAL OF ORDER THREE,BF=E3(ARGU),
C     WHERE THE ARGUMENT LIES BETWEEN TABULAR VALUES.
C     RECURSION RELATIONS ARE THEN USED TO DETERMINE
C     CF=E4(ARGU) AND DF=E5(ARGU).
C
       DIMENSION PATH(40),C(40),KTRL(40),KMDC(40),S(40),
      1G(40,40),GSLP(40,40),GCRV(40,40),T(40,40),H(40,40),
      2B(43,43),FLX(40),F(24),E3A(250),E3B(250),
      3SA(43,2),ERASE(43),EXTRA(40),EXTRB(40)
       COMMON N,NPEAD,NT,NSUC,MODC,KMIX,NREL,NCLC,NMEM,
      1MITN,MA,NPAG,INDX,KPRNT1,KPRNT2,KPRNT3,KPNCH1,KPNCH2,
      2KXXA,KXXB,KXXC,TMULT,CONV,ARGU,BF,CF,DF,
      3PATH,C,KTRL,KMDC,S,G,GSLP,GCRV,T,H,
      4B,FLX,F,E3A,E3B,SA,ERASE,EXTRA,EXTRB
       IF (ARGU-20.1) 20,10,10
C
C     ARGU GREATER THAN 20.1, INTEGRALS ASSUMED EQUAL
C     TO ZERO.
C
   10  BF=0.0
       CF=0.0
       DF=0.0
       GO TO 1000
   20  Q=EXPF(-ARGU)
       IF (ARGU-2.4799) 30,30,60
   30  IF (ARGU- 0.0100) 40,40,50
C
C     ARGU LESS THAN 0.01 .
C
   40  X=ARGU/0.01
       LESS=0
       BY=0.5
       GO TO 55
C
C     ARGU BETWEEN 0.01 AND 2.4799.
C
   50  P=ARGU/0.01
       LESS=P
       A=LESS
       X=P-A
       BY=E3A(LESS)
   55  BZ1=E3A(LESS+1)-BY
       BZ2=(E3A(LESS+2)-BY)/2.0
       BZ3=(E3A(LESS+3)-BY)/3.0
       GO TO 70
```

```
C
C     ARGU BETWEEN 2.4799 AND 20.1 .
C
   60 P=ARGU/0.10
      LESS=P
      A=LESS
      X=P-A
      BY=E3B(LESS)
      BZ1=E3B(LESS+1)-BY
      BZ2=(E3B(LESS+2)-BY)/2.0
      BZ3=(E3B(LESS+3)-BY)/3.0
C
C     COMPUTATION OF POLYNOMIAL COEFFICIENTS.
C
   70 BC3=(BZ3+BZ1)/2.0 - BZ2
      BC2=BZ2-BZ1-3.0*BC3
      BC1=BZ1-BC2-BC3
      BF=BY+X*(BC1+X*(BC2+X*(BC3)))
C
C     RECURSION RELATIONS FOR THE EXPONENTIAL INTEGRALS
C     OF ORDERS 4 AND 5.
C
      CF=(Q-ARGU*BF)/3.0
      DF=(Q*(1.0-ARGU/3.0)+BF*ARGU**2/3.0)/4.0
 1000 RETURN
      END



*     LIST8
*     LABEL
      SUBROUTINE PARAM2
C
C     THIS SUBROUTINE COMBINES ARRAYS G, GSLP, AND GCRV
C     INTO ONE ARRAY, T(I,J), WHICH SATISFIES THE MATRIX
C     EQUATION B=C*T*B + S.  THE ARRAY H=C*T IS THEN
C     FORMED SUCH THAT B=H*B + S.
C
      DIMENSION PATH(40),C(40),KTRL(40),KMDC(40),S(40),
     1G(40,40),GSLP(40,40),GCRV(40,40),T(40,40),H(40,40),
     2B(43,43),FLX(40),F(24),E3A(250),E3B(250),
     3SA(43,2),ERASE(43),EXTRA(40),EXTRB(40)
      COMMON N,NREAD,NT,NSUC,MODC,KMIX,NREL,NCLC,NMEM,
     1MITN,MA,NPAG,INDX,KPRNT1,KPRNT2,KPRNT3,KPNCH1,KPNCH2,
     2KXXA,KXXB,KXXC,TMULT,CONV,ARGU,BF,CF,DF,
     3PATH,C,KTRL,KMDC,S,G,GSLP,GCRV,T,H,
     4B,FLX,F,E3A,E3B,SA,ERASE,EXTRA,EXTRB
    1 FORMAT(1H1,5X18H SLBCEL PARAMETERS,10X4H RUN I3,
     110X5H PAGE I3)
    2 FORMAT(1H0,20X22H ARRAY T(I,J) FOLLOWS./3X2H I)
    3 FORMAT(2XI3,6F10.6/6X6F10.6/7X6F10.6/8X6F10.6/
     19X6F10.6/10X6F10.6/11X6F10.6)
    4 FORMAT(6F11.7)
```

```
      GO TO (20,80),MA
   20 DO 30 J=1,N
      DO 30 I=1,N
   30 T(I,J)=G(I,J)
      IF (MODC-1) 80,80,31
   31 DO 70 J=1,N
      KA=KMDC(J)-1
      IF (KTRL(J)) 40,50,60
C
C     DISCONTINUITY AT RIGHT INTERFACE OF SOURCE REGION J.
C
   40 GO TO (41,44),KA
C
C     SLOPE CORRECTION
C
   41 DO 42 I=1,N
      T(I,J)=T(I,J)+3.0*GSLP(I,J)
      T(I,J-1)=T(I,J-1)-4.0*GSLP(I,J)
   42 T(I,J-2)=T(I,J-2)+GSLP(I,J)
      GO TO 70
C
C     SLOPE AND CURVATURE CORRECTIONS.
C
   44 DO 45 I=1,N
      T(I,J)=T(I,J)+3.0*GSLP(I,J)+0.5*GCRV(I,J)
      T(I,J-1)=T(I,J-1)-4.0*GSLP(I,J)-GCRV(I,J)
   45 T(I,J-2)=T(I,J-2)+GSLP(I,J)+0.5*GCRV(I,J)
      GO TO 70
C
C     NO DISCONTINUITIES AT INTERFACES OF SOURCE REGION J.
C
   50 GO TO (51,54),KA
C
C     SLOPE CORRECTION.
C
   51 DO 52 I=1,N
      T(I,J-1)=T(I,J-1)-GSLP(I,J)
   52 T(I,J+1)=T(I,J+1)+GSLP(I,J)
      GO TO 70
C
C     SLOPE AND CURVATURE CORRECTIONS.
C
   54 DO 55 I=1,N
      T(I,J)=T(I,J)-GCRV(I,J)
      T(I,J-1)=T(I,J-1)-GSLP(I,J)+0.5*GCRV(I,J)
   55 T(I,J+1)=T(I,J+1)+GSLP(I,J)+0.5*GCRV(I,J)
      GO TO 70
C
C     DISCONTINUITY AT LEFT INTERFACE OF SOURCE REGION J.
C
   60 GO TO (61,64),KA
C
C     SLOPE CORRECTION.
C
```

```
   61 DO 62 I=1,N
      T(I,J)=T(I,J)-3.0*GSLP(I,J)
      T(I,J+1)=T(I,J+1)+4.0*GSLP(I,J)
   62 T(I,J+2)=T(I,J+2)-GSLP(I,J)
      GO TO 70
C
C     SLOPE AND CURVATURE CORRECTIONS.
C
   64 DO 65 I=1,N
      T(I,J)=T(I,J)-3.0*GSLP(I,J)+0.5*GCRV(I,J)
      T(I,J+1)=T(I,J+1)+4.0*GSLP(I,J)-GCRV(I,J)
   65 T(I,J+2)=T(I,J+2)-GSLP(I,J)+0.5*GCRV(I,J)
   70 CONTINUE
C
C     IF KPRNT2 = 1, PRINT COEFFICIENT ARRAY T(I,J).
C
      GO TO (72,75),KPRNT2
   72 PRINT 1,INDX,NPAG
      NPAG=NPAG+1
      PRINT 2
      DO 73 I=1,N
   73 PRINT 3, I,(T(I,J),J=1,N)
C
C     IF KPNCH2 = 1, PUNCHED OUTPUT OF ARRAY T(I,J).
C
   75 GO TO (76,80),KPNCH2
   76 PUNCH 4, ((T(I,J),J=1,N),I=1,N)
C
C     USE CURRENT VALUES OF C(I) TO CONVERT T(I,J) TO H(I,J).
C
   80 DO 81 I=1,N
      CA=C(I)
      DO 81 J=1,N
   81 H(I,J)=CA*T(I,J)
      RETURN
      END
```

```
*      LIST8
*      LABEL
       SUBROUTINE CLCMEQ
C
C     THIS SUBROUTINE SOLVES THE SET OF N LINEAR
C     INHOMOGENEOUS EQUATIONS, (I-H)B=S, USING THE M.I.T.
C     LIBRARY FUNCTION XSIMEQF.  (REFERENCE --  CC-174-5)
C
       DIMENSION PATH(40),C(40),KTRL(40),KMDC(40),S(40),
      1G(40,40),GSLP(40,40),GCRV(40,40),T(40,40),H(40,40),
      2B(43,43),FLX(40),F(24),E3A(250),E3B(250),
      3SA(43,2),ERASE(43),EXTRA(40),EXTRB(40)
       COMMON N,NREAD,NT,NSUC,MODC,KMIX,NREL,NCLC,NMEM,
      1MITN,MA,NPAG,INDX,KPRNT1,KPRNT2,KPRNT3,KPNCH1,KPNCH2,
      2KXXA,KXXB,KXXC,TMULT,CONV,ARGU,BF,CF,DF,
      3PATH,C,KTRL,KMDC,S,G,GSLP,GCRV,T,H,
      4B,FLX,F,E3A,E3B,SA,ERASE,EXTRA,EXTRB
     1 FORMAT(1H1,5X32H SLBCEL MATRIX EQUATION SOLUTION,
      15X4H RUN I3,5X5H PAGE I4)
     2 FORMAT(1H0,6X38H COEFFICIENT MATRIX A(I,J), FOR A*B=S,,
      19H FOLLOWS.//3X2H I)
     3 FORMAT(2XI3,6F10.6/6X6F10.6/7X6F10.6/8X6F10.6/
      19X6F10.6/10X6F10.6/11X6F10.6)
     4 FORMAT(1H0,3X36H DETERMINANT OF COEFFICIENT MATRIX =,
      1F13.6)
     5 FORMAT( 1H0,3X21H OVERFLOW IN XSIMEQF.)
     6 FORMAT(1H0,3X32H COEFFICIENT MATRIX IS SINGULAR.)
     7 FORMAT(1H0,3X22H CELL MULTIPLICATION = F12.5///
      13X2H I,2X8H PATH(I),7X5H C(I),7X5H S(I),
      24X11H BIRTH RATE,2X10H REL. FLUX//(I5,3E13.5,2E14.7))
       DO 30 I=1,N
       DO 20 J=1,N
    20 B(I,J)=-H(I,J)
       SA(I,1)=S(I)
    30 B(I,I)=B(I,I)+1.0
       GO TO (33,40),KPRNT3
    33 PRINT 1,INDX,NPAG
       NPAG=NPAG+1
       PRINT 2
       DO 34 I=1,N
    34 PRINT 3,I,(B(I,J),J=1,N)
    40 DET=1.0
       M=XSIMEQF(43,N,1,B,SA,DET,ERASE)
       PRINT 1,INDX,NPAG
       NPAG=NPAG+1
       GO TO (41,42,43),M
    41 PRINT 4,DET
       GO TO 50
    42 PRINT 5
       GO TO 100
    43 PRINT 6
       GO TO 100
```

```
   50 SUM=0.0
      DO 51 I=1,N
      FLX(I)=(B(I,1)-S(I))/(C(I)*PATH(I))
   51 SUM=SUM+FLX(I)
      QUAN=N
      SUM=SUM/QUAN
      SUMA=0.0
      SUMB=0.0
      DO 52 I=1,N
      FLX(I)=FLX(I)/SUM
      SUMA=SUMA+B(I,1)
   52 SUMB=SUMB+S(I)
      FMULT=SUMA/SUMB
      PRINT 7,FMULT,(I,PATH(I),C(I),S(I),B(I,1),FLX(I),I=1,N)
  100 RETURN
      END



*     LIST8
*     LABEL
      SUBROUTINE CLCITN
C
C     THIS SUBROUTINE SOLVES FOR THE BIRTH RATE BY
C     GENERATION TO GENERATION ITERATION, B=H*B+S , AND
C     PRINTS THE RESULTS.
C
      DIMENSION PATH(40),C(40),KTRL(40),KMDC(40),S(40),
     1G(40,40),GSLP(40,40),GCRV(40,40),T(40,40),H(40,40),
     2B(43,43),FLX(40),F(24),E3A(250),E3B(250),
     3SA(43,2),ERASE(43),EXTRA(40),EXTRB(40)
      COMMON N,NREAD,NT,NSUC,MODC,KMIX,NREL,NCLC,NMEM,
     1MITN,MA,NPAG,INDX,KPRNT1,KPRNT2,KPRNT3,KPNCH1,KPNCH2,
     2KXXA,KXXB,KXXC,TMULT,CONV,ARGU,BF,CF,DF,
     3PATH,C,KTRL,KMDC,S,G,GSLP,GCRV,T,H,
     4B,FLX,F,E3A,E3B,SA,ERASE,EXTRA,EXTRB
    1 FORMAT(1H1,5X25H SLBCEL ITERATED SOLUTION,
     18X4H RUN I3,8X5H PAGE I3)
    2 FORMAT(1H0,10X36H ITERATION MATRIX H(I,J) FOR B=HB+S./
     13X2H I)
    3 FORMAT(2XI3,6F10.6/6X6F10.6/7X6F10.6/8X6F10.6/
     19X6F10.6/10X6F10.6/11X6F10.6)
    4 FORMAT(10X22H B(I,K) RESET FOR PASS I3)
    5 FORMAT( 1H0,25X8H RESULTS)
    6 FORMAT(1H0,10X32H THE DISTRIBUTION HAS CONVERGED.)
    7 FORMAT(1H0,10X35H THE DISTRIBUTION DID NOT CONVERGE.)
    8 FORMAT(10X29H CONVERGENCE LEVEL ATTAINED = F12.5/
     110X30H NO. OF ITERATIONS COMPLETED = I4//
     210X22H CELL MULTIPLICATION = F10.5)
    9 FORMAT(1H0,2X2H I,2X8H PATH(I),7X5H C(I),7X5H S(I),
     14X11H BIRTH RATE,2X10H REL. FLUX//(I5,3E13.5,2E14.7))
   10 FORMAT(1H0,15X32H RESULTS OF LAST FIVE ITERATIONS /
     13X2H I/(I5,2X,5E13.7))
```

```
      N1=N+1
      N2=N+2
      N3=N+3
      NM3=N-3
      NHALF=N/2
      NSC=0
      IPASS=1
      PRINT 1,INDX,NPAG
      NPAG=NPAG+1
      GO TO (15,18),KPRNT3
   15 PRINT 2
      DO 16 I=1,N
   16 PRINT 3, I,(H(I,J),J=1,N)
      PRINT 1,INDX,NPAG
      NPAG=NPAG+1
C
C     SET INITIAL DISTRIBUTION.
C
   18 GO TO (20,30,30),NMFM
   20 DO 21 I=1,N
   21 B(I,1)=TMULT
   30 DO 31 I=1,N
   31 B(I,4)=B(I,1)
      DO 32 I=N1,N3
   32 B(I,4)=0.01
   35 K=4
C
C     COMPUTE BIRTH RATE AT ITERATION STEP NSC.
C
   40 NSC=NSC+1
      K1=K
      K=K+1
      DO 50 I=1,N
      SUM=0.0
      DO 45 J=1,N
   45 SUM=SUM+H(I,J)*B(J,K1)
   50 B(I,K)=SUM+S(I)
C
C     DISTRIBUTION SPACE-ITERATION CONVERGENCE TESTS.
C
      B(N1,K)=B(1,K)/B(1,K1)
      B(N2,K)=B(NHALF,K)/B(NHALF,K1)
      B(N3,K)=B(NM3,K)/B(NM3,K1)
      IF (NSC-4) 60,60,51
   51 V1=ABSF(B(N2,K)-B(N1,K))
      IF (V1-CONV) 53,52,52
   52 CONVB=V1
      GO TO 60
   53 V2=ABSF(B(N3,K)-B(N1,K))
      V3=ABSF(B(N1,K)-B(N1,K1))
      V4=ABSF(B(N2,K)-B(N2,K1))
      V5= ABSF(B(N3,K)-B(N3,K1))
      CONVB=V1+V2+V3+V4+V5
      IF (CONVB-CONV) 70,70,60
```

```
C
C     COMPLETION CHECKS
C
      IF (MOTN.NSC) GO TO 61
      IF (KEY.K) GO TO 71
C
C     BLOCK LOCAL FILLED, RESET FOR NEXT PASS.
C
      DO 60 J=1,
     1   LEJ=0
         DO 60 I=1,
         IF(V(I,J).NE.0) THEN
            IPASS=IPASS+1
            PRINT *,IPASS
            GO TO 68
C
C     THE DISTRIBUTION HAS CONVERGED.
C
   70 KEY=K
      NCYC=1
      GO TO 100
C
C     THE MAXIMUM NUMBER OF ITERATIONS HAS BEEN COMPLETED
C     WITHOUT CONVERGENCE.
C
   80 KEY=K
      NCYC=2
C
C     COMPLETE RELATIVE FULL DISTRIBUTION AND DELL
C     MULTIPLICATION.
C
  100 SUM=0.0
      DO 101 I=1,
      FULL(I)=B(I,KFLAG)*V(I,
  101 SUM=SUM+FULL(I)
      SUM=1.0/SUM
      SUM=SUM*100.0
      SUM=0.0
      DO 102 I=1,
      FULL(I)=FULL(I)*SUM
      SUM=SUM+FULL(I)
  102 SUM=SUM+SUM
      WRITE(6,1) SUM
C
C     PRINT OUT RESULTS.
C
      PRINT 5
      GO TO (103,104,105),
  103 PRINT 6
      GO TO 106
  104 PRINT 7
```

```
105 PRINT 8,CONVB,NSC,FMULT
    PRINT 9,(I,PATH(I),C(I),S(I),B(I,KFL),FLX(I),I=1,N)
    KM4=KFL-4
    PRINT 1,INDX,NPAG
    NPAG=NPAG+1
    PRINT 10,(I,(B(I,J),J=KM4,KFL),I=1,N3)
    DO 106 I=1,N
106 B(I,1)=B(I,KFL)
    RETURN
    END
```

APPENDIX D

SIMPLIFICATION OF THE INTEGRAL-TRANSPORT EQUATION

In stating the integral-transport equation for the neutron distribution in a fairly general nuclear reactor system, it is useful to express it as two coupled equations, each of which relates the directed birth rate density with the directed flux. The directed birth rate density, which is a sum of all production terms in the well-known Boltzmann integro-differential equation, is given by

$$b_d(\underline{r},v,\underline{\Omega},t) = \int_0^{v_{max}} dv' \iint_{4\pi} d\Omega' f_d(\underline{r},v'\rightarrow v,\underline{\Omega}'\rightarrow\underline{\Omega},t)\, c(\underline{r},v',\underline{\Omega}',t)\cdot$$

$$\cdot\, \Sigma(\underline{r},v',\underline{\Omega}',t)\phi_d(\underline{r},v',\underline{\Omega}',t) + s_d(\underline{r},v,\underline{\Omega},t)$$

$$+ \left\{\text{terms for contributions from delayed neutron precursors}\right\}, \tag{D.1}$$

where

$b_d(\underline{r},v,\underline{\Omega},t)$ is the directed birth rate density, $[\text{cm}^3\cdot \frac{\text{cm}}{\text{sec}}\cdot\text{steradian}.\text{sec}]^{-1}$, of neutrons emitted with speed v and direction $\underline{\Omega}$ at position $\underline{r}$ and time t

$\phi_d(\underline{r},v',\underline{\Omega}',t)$ is the directed flux at $(\underline{r},t)$ of neutrons having velocity $v'\underline{\Omega}'$

$\Sigma(\underline{r},v',\underline{\Omega}',t)$ is the macroscopic collision cross section, cm^{-1}, at $(\underline{r},t)$ for neutrons with velocity $v'\underline{\Omega}'$

$c(\underline{r},v',\underline{\Omega}',t)$ is the mean number of prompt secondaries emitted at (r,t) per collision of neutrons with velocity $v'\underline{\Omega}'$

$f_d(\underline{r},v'\to v,\underline{\Omega}'\to\underline{\Omega},t)$ is the secondary neutron distribution function, $[(\text{cm/sec})(\text{steradian})]^{-1}$, and is normalized such that its integral over $dvd\Omega$ is equal to unity

$s_d(\underline{r},v,\underline{\Omega},t)$ is the contribution to $b_d(\underline{r},v,\underline{\Omega},t)$ from an external source located at $(\underline{r},t)$.

We shall neglect the terms which specifically account for delayed neutrons.*

The directed flux is expressed in terms of the directed birth rate density by the following integral relation, which may either be constructed from physical prinicples or be derived from the Boltzmann equation by adapting procedures described in the literature:[9,10,11]

$$\phi_d(\underline{r},v',\underline{\Omega}',t) = \int_0^{R_o(\underline{r},\underline{\Omega}')} dR'\, b_d(\underline{r}-R'\underline{\Omega}',v',\underline{\Omega}',t-\frac{R'}{v'})\cdot$$

$$\cdot\exp\left\{-\int_0^{R'} dR''\,\Sigma(\underline{r}-R''\underline{\Omega}',v',\underline{\Omega}',t-\frac{R''}{v'})\right\} + \phi_d(\underline{r}-R_o(\underline{r},\underline{\Omega}')\underline{\Omega}',v',\underline{\Omega}',t-\frac{R_o(\underline{r},\underline{\Omega}')}{v'})\cdot$$

$$\cdot\exp\left\{-\int_0^{R_o(\underline{r},\underline{\Omega}')} dR''\,\Sigma(\underline{r}-R''\underline{\Omega}',v',\underline{\Omega}',t-\frac{R''}{v'})\right\}, \qquad (D.2)$$

---

*Note: For studying systems at steady-state, delayed neutrons can be included conveniently in the functions c and f_d. For time-dependent problems, the usefulness of numerical models of the type studied here is limited to transients of very short duration. In this case precursor concentrations may either be assumed constant or be corrected periodically; the emission rate of delayed neutrons may be treated as part of the external source rate.

where R' is the distance, cm, from $\underline{r}$ to a source point which lies in the direction $-\underline{\Omega}'$ from $\underline{r}$, and $R_o(\underline{r},\underline{\Omega}')$ is the distance to the boundary. The first term gives the contribution to $\phi_d(\underline{r},v',\underline{\Omega}',t)$ of neutrons born within the defined boundaries of the system, which are assumed to be non-reentrant surfaces;[10] the second term, the boundary term, gives the contribution of neutrons which were born in the surroundings. From this point, we shall consider only systems which are isolated from their surroundings such that the boundary term vanishes.

In contrast with the corresponding differential equation, Eq. (D.2) is a past-hisory formulation which requires detailed knowledge of the past history of both the directed birth rate density and the collision cross section. One consequence is that storage must be provided for the needed memory in computational models based on integral transport equations. A second consequence, for systems with time-varying collision cross sections, is that spatial transfer coefficients analogous to the G(I,J) of Eq. (1B.2) must be recomputed at each time step. Computational effort and storage requirements are greatly reduced by restricting attention to systems with time-independent collision cross sections.*

Whereas Eq. (D.1) involves only neutrons at the point $(\underline{r},t)$, Eq. (D.2) involves only neutrons having the constant velocity $v'\underline{\Omega}'$. Together, Eqs. (D.1) and (D.2) give the integral-transport equation. Either the directed birth rate density or the directed flux can be eliminated from the formulation by substituting one equation into the

*Note: In programs OVRR4 and TOVSR, an option is included for treating time-dependent Σ. The transfer parameters at time t are computed using the Σ at time t, neglecting the past history of Σ. This approximation is suitable only for slowly-varying Σ.

other. Which dependent variable is retained is, in principle, arbitrary. Retention of the birth rate has a practical advantage, however, in that the values of the functions f_d, c and s_d used in the resulting integral-transport equation are the values at time t; the past history of these quantities is not required.

At this point we introduce the simplifications of directional isotropy. For an isotropic medium, the properties Σ and c are independent of the direction $\underline{\Omega}'$ of the colliding neutrons. In addition, we assume that secondary neutrons (e.g., fission neutrons, scattered neutrons) are emitted isotropically in the laboratory frame of reference, in which case

$$f_d(\underline{r},v'\to v,\underline{\Omega}'\to\underline{\Omega},t) = \frac{1}{4\pi} f(\underline{r},v'\to v,t) \ ,$$

where f has the units $[\text{cm/sec}]^{-1}$. With the further simplification that the external source neutrons are emitted isotropically, it is clear from Eq. (D.1) that the directed birth rate density is independent of direction.

With the simplifications of the previous paragraphs, Eqs. (D.1 and 2) reduce to the following:

$$b_d(\underline{r},v,t) = \int_0^{v_{max}} dv' \iint_{4\pi} d\Omega' \, \frac{1}{4\pi} f(\underline{r},v'\to v,t)c(\underline{r},v',t)\cdot$$

$$\cdot\Sigma(\underline{r},v') \quad \phi_d(\underline{r},v',\underline{\Omega}',t) + s_d(\underline{r},v,t) \quad ; \qquad (D.3)$$

$$\phi_d(\underline{r},v',\underline{\Omega}',t) = \int_0^{R_o(\underline{r},\underline{\Omega}')} dR'\; b_d(\underline{r}-R'\underline{\Omega}',v',t-R'/v') \cdot$$

$$\cdot \exp\left\{ - \int_0^{R'} dR''\; \Sigma(\underline{r}-R''\underline{\Omega}',v') \right\} . \qquad (D.4)$$

For slab geometry, the positional argument $\underline{r}$ is replaced by the coordinate x in Eq. (D.3), where $0 \leq x \leq W$. The properties and distributions are constants with respect to the coordinates y and z in the Cortesian reference frame (x,y,z). As regards directional dependence, the argument $\underline{\Omega}'$ is replaced by the coordinate set $(\pm \mu, \Theta)$, where μ is the magnitude of the cosine of the polar angle between the positive direction along the x-axis and $\underline{\Omega}'$, and Θ is the azimuthal angle with the range 2π. The argument μ or $+\mu$ is used for the directed flux of neutrons moving in the direction of increasing x, and $-\mu$ for the directed flux of neutrons moving in the direction of decreasing x, where $0 < \mu \leq 1$. The singular case, $\mu = 0$, is neglected.

Noting that ϕ_d is independent of Θ, we obtain from Eq. (D.4):

$$\phi_a(x,v',\mu,t) = \frac{1}{2} \int_0^x \frac{dx'}{\mu}\; b(x',v',t-\frac{|x-x'|}{\mu v'}) \cdot$$

$$\cdot \exp\left\{ - \int_{x'}^{x} \frac{dx''}{\mu}\; \Sigma(x'',v') \right\} \qquad (D.5a)$$

and

$$\phi_a(x,v',-\mu,t) = \frac{1}{2}\int_x^W \frac{dx'}{\mu}\, b(x',v',t-\frac{|x-x'|}{\mu v'})\cdot$$

$$\cdot\exp\left\{-\int_x^{x'}\frac{dx''}{\mu}\,\Sigma(x'',v')\right\}\quad; \tag{D.5b}$$

where

$$\phi_a(x,v',\pm\mu,t) = \int_0^{2\pi} d\Theta\;\phi_d(x,v',\pm\mu,t) \tag{D.6}$$

is the angular flux, and

$$b(x,v,t) = \iint_{4\pi} d\Omega\, b_d(x,v,t) = 4\pi b_d(x,v,t)\quad . \tag{D.7}$$

Similarly, Eq. (D.3) reduces to

$$b(x,v,t) = \int_0^{v_{max}} dv'\; f(x,v'\to v,t)c(x,v',t)\Sigma(x,v')\cdot$$

$$\cdot\int_0^1 d\mu[\phi_a(x,v',\mu,t) + \phi_a(x,v',-\mu,t)] + s(x,v,t) \tag{D.8}$$

Substituting Eqs. (D.5) into Eq. (D.8), setting $f(x,v'\to v,t)$ equal to the Dirac delta function $\delta(v'-v)$ for monoenergetic neutrons, performing the indicated integration over dv', dropping the argument v from each term and rearranging terms, we obtain the integral-transport equation (1A.1).

APPENDIX E

THE DIFFERENTIAL EQUATIONS FOR LINE GEOMETRY

The following set of two coupled differential equations, with the noted boundary conditions, is equivalent to the integral-transport equation studied for line geometry, Eq . (1A.3):

$$\frac{1}{v}\frac{\partial \phi_R(x,t)}{\partial t} + \frac{\partial \phi_R(x,t)}{\partial x} + \Sigma(x)\phi_R(x,t) =$$

$$= \frac{c(x,t)}{2}\Sigma(x)\,[\phi_R(x,t) + \phi_L(x,t)] + \frac{s(x,t)}{2} \quad ; \quad \text{(E.1a)}$$

$$\frac{1}{v}\frac{\partial \phi_L(x,t)}{\partial t} - \frac{\partial \phi_L(x,t)}{\partial x} + \Sigma(x)\phi_L(x,t) =$$

$$= \frac{c(x,t)}{2}\Sigma(x)\,[\phi_R(x,t) + \phi_L(x,t)] + \frac{s(x,t)}{2} \quad , \quad \text{(E.1b)}$$

where ϕ_R is the directed flux, sec^{-1}, moving towards the right, the direction of increasing x, and ϕ_L is the directed flux moving towards the left. The sum of the identical right-hand sides of the two equations defines the birth rate density, b(x,t), cm^{-1} sec^{-1}. For an isolated system, the boundary fluxes $\phi_R(o,t)$ and $\phi_L(W,t)$, where $0 \leq x \leq W$, are set equal to zero.

E.1 FORMULATION OF A FINITE-DIFFERENCE MODEL, MODEL D

In this section we formulate an implicit, first-order finite-difference approximation for Eqs. (E.1) as simplified by dropping the external source terms, the x-dependence of Σ and the (x,t)-dependence of c. The model is designated Model D. The reason for

formulating and coding Model D is to provide an independent method for checking the asymptotic solutions computed for homogeneous line systems using the finite-integral models developed in Chapter 2.

At this point, we note that for homogeneous line systems the asymptotic birth rate distribution is symmetric with respect to the midpoint of the system* and $\phi_L(x,t) = \phi_R(W-x,t)$. Restricting the applicability of the model to be developed to problems with symmetric birth rate distributions, we make the above substitution for $\phi_L(x,t)$ in the simplified form of Eq. (E.1a). Eq. (E.1b) may then be neglected.

The interval [0,W] corresponding to system width is subdivided into N intervals of width $\Delta x = W/N$. We focus attention on the N+1 discrete points x_i, where $0 \leq i \leq N$, located at the boundaries of the N regions; i.e., $x_o = 0$, $x_1 = \Delta x$, ... , $x_N = N\Delta x = W$. Noting that $\phi_R(x_o,t) = 0$ for the isolated system, we write the simplified form of Eq. (E.1a) for each of the N values of x_i for $i \geq 1$. The equation for a tpyical x_i follows:

$$\frac{1}{v}\frac{\partial \phi_R(x,t)}{\partial t}\Bigg]_{x=x_i} + \frac{\partial \phi_R(x,t)}{\partial x}\Bigg]_{x=x_i} + \Sigma\phi_R(x_i,t) =$$

$$= \frac{c\Sigma}{2}\left[\phi_R(x_i,t) + \phi_R(x_{N-i},t)\right] \quad . \qquad \text{(E.2)}$$

We then approximate each of the N equations by the following finite-difference equation, where $\phi_R(x_i,t)$ is denoted by R_i^{ν} and Δt is the unit time step:

*Note: See Section E.2.

$$\frac{1}{v}\frac{R_i^{\nu} - R_i^{\nu-1}}{\Delta t} + \frac{R_i^{\nu} - R_{i-1}^{\nu}}{\Delta x} + \Sigma R_i^{\nu} = \frac{c\Sigma}{2}[R_i^{\nu} + R_{N-i}^{\nu}] \qquad (E.3)$$

Each of the N equations is then rearranged such that the set of equations is given by the matrix equation,

$$\underline{A}\underline{R}^{\nu} = \underline{R}^{\nu-1} \quad , \qquad (E.4)$$

where A is a square matrix N elements on a side and $\underline{R}^{\nu}$ is a column vector with elements R_i^{ν}. The set of numerical equations for Model D is then given by

$$\underline{R}^{\nu} = A^{-1}\,\underline{R}^{\nu-1} \quad , \qquad (E.5)$$

where the matrix A^{-1} is the inverse of A.

Model D was coded for the IBM-7094 computer. Asymptotic solutions are generated by reading in the system parameters and an arbitrary initial distribution R_i^{o}, and generating the transient from time step to time step using Eq. (E.5). The degree of asymptoticity at a given time step is determined by using the method described in Subsection 2E.1. Some inverse periods computed with Model D are given in Figure 2E.1.

E.2 STATIONARY SOLUTIONS FOR HOMOGENEOUS SYSTEMS

We simplify Eqs. (E.1) by dropping the external source terms, the x-dependence of Σ and the (x,t)-dependence of c. We substitute the following expressions for $\phi_R(x,t)$ and $\phi_L(x,t)$ in the simplified Eqs. (E.1):

$$\phi_R(x,t) = [\phi(x,t) + j(x,t)]/2 \quad ; \tag{E.6a}$$

$$\phi_L(x,t) = [\phi(x,t) - j(x,t)]/2 \ , \tag{E.6b}$$

where $\phi(x,t)$ is the flux, and $j(x,t)$ is the net current in the direction of increasing x. With some rearranging, we obtain the following set of differential equations:

$$\frac{1}{v}\frac{\partial\phi(x,t)}{\partial t} + \frac{\partial j(x,t)}{\partial x} + \Sigma\phi(x,t) = c\Sigma\phi(x,t) \ ; \tag{E.7a}$$

$$\frac{1}{v}\frac{\partial j(x,t)}{\partial t} + \frac{\partial\phi(x,t)}{\partial x} + \Sigma j(x,t) = 0 \ . \tag{E.7b}$$

If the flux distribution in a system described by Eqs. (7) has the asymptotic distribution, we can write

$$\phi(x,t) = \phi_o(x)e^{\lambda t} \tag{E.8a}$$

and

$$j(x,t) = j_o(x)e^{\lambda t} \ . \tag{E.8b}$$

Substituting Eqs. (E.8) into (E.7) and carrying out the indicated operations, we obtain:

$$\frac{d\phi_o(x)}{dx} + [\Sigma + \frac{\lambda}{v}]j_o(x) = 0 \ ; \tag{E.9a}$$

$$\frac{dj_o(x)}{dx} + [\Sigma(1-c) + \frac{\lambda}{v}]\phi_o(x) = 0 \ . \tag{E.9b}$$

Substituting $j_o(x)$, as given by (E.9a), into (E.9b), we obtain

$$\frac{d^2\phi_o(x)}{dx^2} + \alpha^2\phi_o(x) = 0 \ , \tag{E.10}$$

where

$$\alpha^2 = \Sigma^2[c-1] + \frac{\lambda}{v}\Sigma[c-2] - [\frac{\lambda}{v}]^2 \quad . \tag{E.11}$$

Equation (E.10) has the simple form of the steady state diffusion equation for slab or line geometry. In an isolated homogeneous reactor, due to symmetry, the asymptotic flux distribution is given by one of the following expressions, where $y = x-W/2$ and A is an arbitrary normalization constant:

$$\phi_o(y) = A \cos \alpha y, \ \alpha^2 > 0 \ ; \tag{E.12a}$$

$$\phi_o(y) = A \qquad , \ \alpha^2 = 0 \ ; \tag{E.12b}$$

$$\phi_o(y) = A \cosh \alpha_o y, \ \alpha = i\alpha_o, \ \alpha^2 < 0 \ . \tag{E.12c}$$

From Eq. (1A.2),

$$b(x,t) = c\Sigma\phi(x,t) \quad , \tag{E.13}$$

so that the asymptotic birth rate distribution $b_o(x)$ has the same shape as the flux distribution, $\phi_o(x)$.

In Section 2E, we apply the constraint (E.11) and the solution (E.12a) to check the accuracy of asymptotic solutions computed with the finite-integral models.

BIBLIOGRAPHY

1. Honeck, H.C., "The Distribution of Thermal Neutrons in Space and Energy in Reactor Lattices. Part I: Theory," Nucl. Sci. Eng. 8, 193-202 (1960).

2. Honeck, H.C., "The Calculation of Thermal Utilization and Disadvantage Factor in Uranium/Water Lattices," Nucl. Sci. Eng., 18, 49-68 (1964).

3. Honeck, H.C., "THERMOS, A Thermalization Transport Code for Reactor Lattice Calculations," BNL-5826 (1961).

4. Judge, F.D., "Variational Method in the Calculation of Reactor Neutron Flux Density," KAPL-2151, Knolls Atomic Power Laboratory (1961).

5. Radkowsky, A., (editor), "Naval Reactors Physics Handbook, Volume 1, Selected Basic Techniques," TID-7030, Naval Reactors, Division of Reactor Development, United States Atomic Energy Commission, Washington (1964). (page 1496).

6. Church, J.P., "Solving the Transport Equation in Heterogeneous Media using First-Flight Green's Functions for Homogeneous Media," Nucl. Sci. Eng., 21, 49-61 (1965).

7. Judge, F.D., and P.B. Daitch, "Time-Dependent Flux in Small Assemblies," Nucl. Sci. Eng. 20, 428-435 (1964).

8. Richtmyer, R.D., "Difference Methods for Initial-Value Problems," Interscience Publishers, Inc., New York (1957).

9. Weinberg, A.M., and E.P. Wigner, "The Physical Theory of Neutron Chain Reactors," The University of Chicago Press, Chicago (1958).

10. Davison, B., (with J.B. Sykes), "Neutron Transport Theory," Oxford University Press, London (1957).

11. Clark, M. Jr., and K.F. Hansen, "Numerical Methods of Reactor Analysis," Academic Press, New York (1964).

12. Hildebrand, F.B., "Methods of Applied Mathematics," Prentice-Hall, Inc., Englewood Cliffs, N.J. (1952).

13. Wing, G.M., "An Introduction to Transport Theory," John Wiley and Sons, New York (1962).

14. "709/7090 FORTRAN Programming System," IBM Reference Manual, International Business Machines Corporation (1961).

15. Organick, E.I., "A Fortran Primer," Addison-Wesley Publishing Company, Inc., Reading, Mass. (1963).

16. Abramowitz, M., and L.A. Stegun (editors), "Handbook of Mathematical Functions," AMS 55, National Bureau of Standards, Washington (1964).

17. Carlson, B.G., and G.I. Bell, "Solutions of the Transport Equation by the S_N Method," Proc. Second Intern. Conf. Peaceful Uses Atomic Energy 16, 535-549 (1958).

18. Pomraning, G.C., "Transport Effects in Diffusion Theory," Nucl. Sci. Eng. 21, 62-78 (1965).

19. CC-174-5, Bulletin of the M.I.T. Computation Center.

20. Meneghetti, D., "Discrete Ordinate Quadratures for Thin Slab Cells," Nucl. Sci. Eng. 11, 295-303 (1962).

21. Weiss, Z., "About the Generalization of Amouyal-Benoist's Method for Calculating Disadvantage Factors and Flux Distributions in Two-region Cells," Nucl. Sci. Eng. 22, 60-77 (1965).

22. Ferziger, J.H., and A.H. Robinson, "A Transport Theoretic Calculation of Disadvantage Factor," Nucl. Sci. Eng. 21, 382-389 (1965).

23. Pomraning, G.C., and M. Clark, Jr., "A New Asymptotic Diffusion Theory," Nucl. Sci. Eng., 17, 227-233 (1963).

24. Theys, M.H., "Integral Transport Theory of Thermal Utilization Factor in Infinite Slab Geometry," Nucl. Sci. Eng. 7, 58-63 (1960).

BIOGRAPHICAL NOTE

Personal

Born on May 24, 1934 in Dover, New Jersey
Married to Maryanne Rogalski on August 30, 1958 in West Conshohocken, Pennsylvania.
The author and his wife are the proud parents of four children: David John, James Michael, Mary Helen and John Raymond, Jr.

Academic Background

1940-1948	St. Mary's Parochial School, Dover, New Jersey
1948-1952	Seton Hall Preparatory School, South Orange, New Jersey
1952-1957	Villanova University, Villanova, Pennsylvania
1960-1961	U.S. Naval Postgraduate School, Monterey, California
1961-1965	Massachusetts Institute of Technology, Cambridge, Massachusetts

Degrees

1957	Bachelor of Chemical Engineering

Scholarships and Honorary Society Memberships

1948-1952	Tuition Scholarship at Seton Hall Preparatory School
1952-1956	N.R.O.T.C. Scholarship at Villanova University
1962	Society of the Sigma Xi

Professional Society Membership

American Insitute of Chemical Engineers
American Nuclear Society
United States Naval Institute

Professional Experience

1957-1960	Sea Duty aboard USS BORDELON (DDR-881) (Engineer Officer - 19 months)

Lt. Essig is presently assigned to the Division of Naval Reactors, U.S.A.E.C., Washington, D.C.